"LATERAL TYRE FORCES ON OFF-ROAD SURFACES"

by

ARAFA SAYED AHMED EL-RAZAZ

B.Sc. & M.Sc. Mech. Eng.

A Thesis submitted to the University of Leeds

in fulfillment of the requirements for the

Degree of Doctor of Philosophy

Department Of Mechanical Engineering

The University Of Leeds

September 1988

SYNOPSIS

A successful model for off-road tyres must be reliable, efficient and capable of reproducing and predicting the main system phenomena. Mathematical models are proposed for longitudinal, lateral and combined lateral and longitudinal force generation characteristics of off-road tyres.

For a better understanding of off-road tyre behaviour, the study of the interaction between the tyre forces and those generated by the deformed soil is very important. Details of the force system in the contact patch, therefore, are used as a basis for developing models for the prediction of the tractive performance and cornering characteristics of off-road tyres.

Previous work of the relevant literature pertaining to tyre behaviour is reviewed to provide the reader with background information on off-road tyre characteristics.

Various models for off-road tyres of differing degrees of complexity but which all incorporate the key features of off-road tyre problems are then developed.

Previous methods of analysing the combined lateral and longitudinal forces generated by off-road tyres on deformable surfaces are investigated. A modified version of a previous model is then proposed which is based on a different and original method for investigating tyre behaviour in the contact region. An entirely new model is then developed which is based on a modification of the "multi-spoke" tyre model used for road vehicle studies. Predicted results are compared with those obtained from other models and with reported experimental data.

The usefulness of such models is in problems involving the steering, braking and handling behaviour of off-road vehicles. Hence, the models are formulated so that they can be applied to such vehicle problems by enabling lateral and longitudinal forces on the tyre to be predicted from any combined conditions of wheelslip, wheelskid and slip angle.

The proposed models provide an improved qualitative description of behaviour in the contact region. Although slightly more complex than previous models, the computational load is nevertheless sufficiently small that the tyre models can conveniently be incorporated in off-road vehicle handling models.

Suggestions for future recommendations are discussed with particular reference to improving the predictive models and for a possible extension of the study to generate more detailed practical results for tyre forces under controlled experimental conditions.

ACKNOWLEDGEMENTS

I wish to express my deep gratitude to *Dr. CROLLA D.A.* for his invaluable advice and guidance throughout this research. The considerate and thorough way in which he supervised this research work is much appreciated.

I would also like to express my deep gratitude and thanks to the *MISR GOVERNMENT* (*ARAB REPUBLIC OF EGYPT*) who made this scholarship available and financially supported me throughout the period of this study.

The author wishes to acknowledge, with gratitude, all the academic staff of the *Mechanical Engineering Department at Leeds University* who have offered help by any means, in particular *Mr. SHARP R.S.* for his helpful discussion and readiness to offer assistance.

Many thanks to *Mr. Hockley, C.* who assisted in reading the manuscript and making helpful suggestions.

The Author also acknowledges with thanks for discussions with *Dr. SINGH G.* Staff at Civil Engineering Department, University of Leeds.

Finally, I offer my deepest personal thanks to my wife , my sons *Kareem* and *Moamen* and my family for their patience, support of writing this thesis.

TABLE OF CONTENTS

NOMENCLATURE

NOTATION

A	Constant in equation (2.1), m
A_c	Horizontal contact area of patch, m^2
b	Width of tyre contact patch, m
B	Constant in equation (2.1)
c	Soil cohesion, kN/m^2
c_w	Soil cohesion in equation (2.56), kN/m^2
C_a	Soil adhesion, kN/m^2
C	Cone index of the soil, kN/m^2
CAH	Project contact area of patch, m^2
COT	Coefficient of traction (or braking)
$COT_{\max}$	Maximum coefficient of traction
C_s	Initial slope of longitudinal force vs. wheelslip
C_T	Coefficient
C_α	Cornering stiffness at $F_x = 0$
C'_x	Longitudinal tyre stiffness, kN/m^3 *unit slip*
C'_y	Cornering tyre stiffness, kN/m^3 *rad*
d	Undeflected tyre diameter, m
dF_x	The net force on thin strip in X-direction, kN
dF_Y	The net force on thin strip in Y-direction, kN
dt	Small time increment, *Sec*
$d\lambda,\ d\lambda'$	Small longitudinal displacement, m
$d\theta$	Angle between each spokes, Degrees
DR	Radial tyre deflection, m
$EMOB,\ \phi MOB$	Mobility number
f_b	Bending force, kN
f_g	Ground force, kN
f_r	Radial force, kN
f_s	Soil shear force, kN
f_{s_x}	Longitudinal component of soil shear force, kN

f_{s_y}	Lateral component of soil shear force, *kN*
f_t	Elastic resultant spoke force in X-Y Plane, *kN*
f_x	Spoke force in fore and aft direction, *kN*
f_y	Spoke force in lateral direction, *kN*
f_z	Spoke force in vertical direction, *kN*
F	General tyre force, *kN*
F_x	Tyre force in fore and aft direction, *kN*
F_{x_e}	Longitudinal force in equation (2.51)
F_y	Tyre force in lateral direction, *kN*
F_{y_e}	Lateral force in equation (2.52)
F_{ss}	Steady state value of tyre force, *kN*
F_z	Tyre force in vertical direction, *kN*
h	Tyre section height, *m*
j	Soil shear displacement, *m*
j_x	Longitudinal soil shear displacement, *m*
j_y	Lateral soil shear displacement, *m*
J_k	Soil deformation coefficient
K	Soil deformation modulus, *m*
$K_1, K_2, K_4, K_5, K_6, K_7$	Tyre stiffness parameters
K_c	Cohesive soil modulus, kN/m^{n+1}
K_r	Radial tyre stiffness, *kN/m*
K_x	Circumferential tyre stiffness, *kN/m*
K_{x_n}	Longitudinal tyre stiffness, kN/m^3 *unit slip*
K_{y_n}	Cornering tyre stiffness, kN/m^3 *rad*
K_ϕ	Frictional soil modulus, kN/m^{n+2}
l	Length of the tyre contact patch, *m*
l_r	Tyre relaxation length, *m*
LFC	Lateral force coefficient
$LFC_{\max}$	Constant for particular conditions
n	Exponent of soil deformation
N	Number of spokes in the contact region
$N_\gamma, N_c, N_q, N_w, N_{\gamma w}, N_{cw}$	Soil coefficients
P	The resultant force in equation (2.56), *kN*
$P,\ P_g$	Normal ground pressure, kN/m^2

P'	Soil resistance, kN/m
P_e	Soil reaction force against the pseudo interface, kN
q	Surcharge, kN/m^2
R	Undeflected tyre radius, m
s	Wheel slip (or skid), %
S	Laplace operator in equation (2.16)
T	Time constant in equation (2.16)
u	Constant in equation (2.28)
U	Total force in equation (2.30), kN
U	Forward velocity of tyre, m/sec
U_m	Maximum resultant force in equation (2.32), kN
V	Lateral velocity of tyre, m/sec
w	Simply relates to the case in which a wedge is formed
W	Tyre load, kN
x, x'	Distance in longitudinal direction, m
y	Total lateral displacement, m
Z, Z_w	Soil sinkage, m
Z_{max}	Maximum Soil sinkage, m
α	Tyre slip angle, Degrees
α_u	Generalized resultant force
δ	Tyre deflection under load, m
δ_f	Soil-rubber angle of friction, Degrees
δ_s	Tyre steer angle, Degrees
δ_t	Time increment, Sec
δ_x	Longitudinal tyre deflection, m
δ_y	Lateral tyre deformation, m
ε	Entry spoke angle in equation (2.57), Degrees
η	The tyre tread Deformation, m
η_x	Circumferential spoke deflection, m
η_{x_k}	Circumferential spoke deflection in Kinematic position, m
η_y	Lateral spoke deflection, m
η_{y_k}	Lateral spoke deflection in Kinematic position, m
γ	Camber angle, Degrees
γ	Soil specific weight in equation (2.55), kN/m^3

λ	Longitudinal coordinate in the contact region
λ'	Longitudinal displacement, *m*
μ	Coefficient of friction
$\omega,\ \Omega$	Spin velocity of the tyre, *rad/sec*
ϕ	Soil internal angle of friction, Degrees
$\phi(\rho_0)$	Radial force an the spoke tip equation (2.60), *N*
$\rho,\ \rho_0$	Radial spoke deflection in equation (2.57), *N*
σ	Normal ground pressure, kN/m^2
τ	Shear stress, kN/m^2
τ_e	Soil shear density
τ_{e_x}	Longitudinal component of density
τ_{e_y}	Lateral component of density
$\tau_{friction}$	Soil stress due to friction, kN/m^2
τ_k	Stress due to friction in equation (2.48), kN/m^2
τ_{max}	Soil shear strength, kN/m^2
$\tau_s, \tau_{soil}, \tau_{tread}$	Soil shear stress, kN/m^2
τ_x	Component of soil shear stress in X-direction, kN/m^2
τ_y	Component of soil shear stress in Y-direction, kN/m^2
θ	Spoke angle position, Degrees
θ_1	Entry angle, Degrees
θ_2	Rear angle, Degrees
ξ	Angle of the total resultant force, Degrees
$\zeta,\ \zeta_0$	Longitudinal spoke deflection in equation (2.57), *m*

Subscripts

i	Spoke number
max	Maximum
min	Minimum
r	Radial
X, Y, Z	Coordinate system

Abbreviation	
atm	Atmospheric pressure
cm	Centimetres
$f_1(\tan\gamma)$, $f_2(s)$	Functions
Fig.	Figure
in.	inch
kN	Kilonewton
lb, lbs	Pound, Pounds
m	Meter
mm	Millimeters
N	Newton
o	Degrees
rad	Radian
sec	Second
$\underline{s}$	Distance vector
∂	Partial derivative
$\int$	Integration
Σ	Sum
[ ]	References

CHAPTER 1

INTRODUCTION

The background to the growing requirement for off-road tyre models is explained and the overall objectives of the thesis are outlined. Also the main subject matter of each chapter is indicated to summarise the overall structure of the thesis.

One of the important factors that influences the steerability of off-road vehicles is the magnitude of the lateral force developed between the tyre and soil contact area when the plane of the tyre is turned at an angle to the direction of travel. When a tyre operates at a slip angle, tyre distortion occurs and the contact region is displaced laterally relative to the wheel plane.

This study is aimed at an improved understanding of the mechanism of lateral tyre force generation on off-road surfaces. Work to date on the force generated by off-road tyres has been dominated by analyses, measurements and predictions of tractive and rolling resistance behaviour. By comparison, the lateral force characteristics have received little attention, though their importance is becoming more widely recognised, mainly because of the pressure for increased speeds in many agricultural vehicles.

Lateral forces generated at the tyres are responsible for controlling the steering, cornering, and sideslope operation of vehicles. If one reasonably excludes the effects of aerodynamic forces on agricultural vehicles, then the only external forces to make the vehicle move in any direction, longitudinally or laterally, are generated at the tyres.

Traditionally, studies of the steering and handling of agricultural vehicles have taken an emphatic second place to the analysis and prediction of their tractive capabilities. This relative position has reinforced the traditional view of, for example, the tractor as a low speed, draught producer. This view is already changing and the change seems likely to accelerate with trends towards higher speeds for conventional tractors and the development of more specialised vehicles. To support this view, recent studies (Crolla and Horton [1984] and Gohlich [1984]) have pointed to the high percentage of time spent by tractors on transportation and other light duties, operating with the power take off perhaps, for which work rates can be increased simply by increased speed.

The overall picture, therefore, is of a changing emphasis on the requirements of tractors and other agricultural vehicles with one of the design priorities being on safe and stable handling behaviour both on and off the road. Hence, the interest in lateral force characteristics of the tyres fitted to such vehicles.

The main objectives of the study presented in this thesis are :-

1) To analyse the lateral force characteristics of off-road tyres.

2) To develop mathematical models which describe the characteristics of off-road tyres in the above respect.

3) To validate the models by comparison with measured results.

An outline of the contents of the thesis is as follows :

A review of the relevant literature pertaining to tyre behaviour is given in Chapter 2. The object of this is to provide the reader with background information on the subject matter, some of which is essential and some peripheral to the work detailed in this thesis. Previous work is critically reviewed in the context of the objectives above. Documents devoted to methods of theoretical analyses and off-road vehicle dynamics problems are referenced where necessary in the main body of the text.

An approach leading to the off-road tyre force model which is simple but which also incorporates the key features of the problem is given in Chapter 3.

In Chapter 4, this is extended to include the combined lateral and longitudinal tyre force characteristics. Results from a computer model suitable for use in combination with vehicle handling models are presented.

A more detailed model is presented in Chapter 5. This model is called the multi-spoke tyre model and the basis of this model is to use a transfer matrix method to calculate the tyre deflections in the circumferential, lateral and radial directions and to recalculate by an iterative method the tyre forces generated when the tyre moves on an off-road surfaces .

The objective of Chapter 6, is to compare the results obtained from tyre models presented in Chapters 3, 4 and 5 with those results obtained by a range of authors presented in the literature. Comments regarding the accuracy and applicability of each model are made.

Chapter 7 contains a discussion of the main results obtained from models presented in this thesis and concentrates on analysing the relationship between real tyre behaviour and the representation of tyre model behaviour. Conclusions together with a set of recommendations for future work are given in Chapter 8.

CHAPTER 2

REVIEW OF PREVIOUS WORK

A summary of published work to date is presented, concentrating on theoretical and experimental results for off-road tyre forces.

This chapter contains a review of the available work that has been done on the behaviour of off-road tyres in generating lateral and longitudinal forces. Although the behaviour of off-road tyres in generating longitudinal forces in particular tractive forces has received an enormous amount of attention, this work is summarised and not reviewed in detail because it is restricted to the case of the wheel travelling in a straight line. In contrast, studies which include either the generation of lateral forces alone or the combined force generation system are given the most attention because they are central to the theme of the thesis. This work can be categorised into two main basic parts :-

1. BASIC TYRE MECHANICS 2. BASIC SOIL MECHANICS

2.1. BASIC TYRE MECHANICS

The lateral force generated by a tyre, whether on hard or deformable surfaces, depends on the "slip angle" at which the tyre is operating. Slip angle, α, defined in Fig.(2.1), is most conveniently defined as the angle between the direction the tyre is pointing and the direction it is actually going. This definition applies whether or not the wheel is steered. The steer angle, δ_s, is the angle the wheel is pointing relative to a longitudinal axis fixed in the vehicle body.

The forces acting at the tyre and ground interface can be defined in two ways : **"Relative to the direction of travel" or "relative to the plane of the wheel".**

The more convenient of these for vehicle studies is the latter and so throughout this work, tyre forces are defined relative to the plane of the wheel. The forces defined by each of these methods are simply related via the slip angle. Throughout the literature, the terms "side force", "lateral force" and "cornering force" are all used and care must be taken in comparing results to note the definition system used.

Because the effective line of action of the lateral force does not coincide with the centre of the wheel axis, a self-aligning torque is generated. Pneumatic trail is the term used to describe the effective moment arm at which the lateral force acts relative to the

wheel axis centreline.

When a tyre operates at a slip angle, tyre distortion occurs and the contact region is displaced laterally relative to the wheel plane. This is shown in Fig.(2.2), the most important feature being the distortion of the line representing the equatorial line around the circumference of the tyre treadband. This distortion is described in more detail in Fig. (2.3), which shows how the forces are produced by the tyre. These characteristics apply to a hard surface but it will be shown in the next chapters that they can easily be modified for deformable surface conditions.

The literature on the force generated by off-road tyres has been dominated by analyses, measurements and predictions of tractive and rolling resistance behaviour. However, some lateral tyre force investigations have been made with the aim of a better understanding of off-road vehicle handling behaviour. These investigations, theoretical and experimental, have mainly been made on towed, steered pneumatic tyres, although a number of attempts have been made to develop lateral and longitudinal tyre forces on different types of soil.

2.1.1. MEASURED RESULTS

Measurements of soil forces acting on a driven or undriven steered wheel have been made several times in the recent past, and a good summary of results is given by Crolla and Hales [1979] for off-road vehicles. These forces are required for the study of two main aspects of vehicle behaviour :

1) To investigate stability for level ground and side slope operation.

2) To investigate handling characteristics.

Crolla and Horton [1984], have reviewed the available information on the lateral force characteristics of off-road tyres. The main idea of this was to provide a comprehensive summary of existing measurements with a view to using the tyre data in off-road vehicle handling and stability studies.

Phillips [1959] measured and compared reaction forces from a 6.00 x 16 implement tyre with those on a rigid cast iron wheel, on a purpose built experimental rig towed over a grassland surface. With the pneumatic tyre it was found possible to make tests over a fairly wide range from 100 to 1000 *lb* of vertical load, and from 0 to 85° of slip angle. For the cast iron wheel, however, the region within which the apparatus would function properly was considerably reduced. Limits of 400 to 1200 *lb* of vertical load and from 0 to 30° slip angle were made for the cast iron tests.

The results showed that for a given tyre load, the lateral force increased with increased slip angle and reached a maximum value at about 17° of slip angle.

Taylor and Birtwistle [1966] investigated three tread designs for 7.50 x 16 6-ply front tractor tyres in the following operating conditions :

1) A multi-rib or compactor tyre on sandy loam soil.

2) A multi-rib or farm tractor tyre on silty clay soil.

Tests were made under two tyre loads of 1000 and 1500 *lbs.* with a range of slip angle between 0 to 15°. They showed that for a given tyre load, the lateral force coefficient increased with slip angle but the rate of increase reduced after approximately 10° of slip angle.

Schwanghart [1968] using a soil bin made a comprehensive study of a range of tyres, mainly tractor front tyres, and reached several interesting conclusions regarding operation in loose soil. The relationship between lateral force and slip angle was markedly different in loose soil from that on concrete. On concrete the lateral force reached a peak at about 15° slip angle and then decreased, but in loose soil the curve was much flatter and had not reached a peak even at 30° slip angle. For a 5.50 x 16 tyre, the lateral force coefficient decreased slightly as vertical load was increased from 1 to 4 *kN*, and for small variations in vertical load a constant figure could be assumed.

The most comprehensive work of tyres driven on off-road surface was carried out by Krick [1973]. His results are one of the few which include driving, braking, and

lateral forces. The tests were carried out in a soil bin. Two different sets of test were made, the first set was on sandy loam soil with 14% water content and the second set was on plastic slippery soil at 22% water content. Front tractor tyres were used with two different sizes, a 7.50 x 18 AS and 12.50-20 EM at an inflation pressure of 1 *atm.* For each tyre tested, wheelslip was kept constant while variation of slip angle ranged between 0 to 30° and tyre loads of 330, 430 and 530 *kp*.

The results, represented as a set of curves, showed that when the tyre travelled in a straight line (at zero slip angle) there were no changes noticeable from the previous work. As the slip angle increased, the driving force largely dropped. Also with an increased driving force at constant slip angle, the lateral force was considerably reduced.

The tyre characteristics were presented as friction ellipse graphs for a 7.50 x 18 AS tyre. Loads of 430 and 530 *kp* were used in the tests at 1 *atm* inflation pressure. With the variation of slip angle, the negative driving force was a maximum at 55% wheelslip and the positive driving force was maximum at a range of 55 to 100% wheelslip. The tyre characteristic graphs showed a significant relationship between the longitudinal force and lateral force for varying slip angle and wheelslip. As a result, the interaction of the lateral force and driving force significantly affects the motion of a vehicle.

The results obtained by Gilfillan, Spencer and Rowe [1976] for a 7.50 x 16 tractor front tyre were on two types of soil, grass on soft ground and stubble soils with tyre loads of 308, 608, 958 and 1258 *lbs* at 100 lb/in^2 cone index. The results were presented in terms of forces lying in the ground plane and applied by the ground to the wheel, i.e. side force and rolling resistance.

These forces are defined with reference to the direction of travel of the wheel. They defined the steer angle as the angle between the direction of travel and the line of intersection of the wheel vertical plane with the ground plane.

Meyer et al [1978] described measurements of tractor rear tyre performance by measuring the lateral forces generated on sloping ground. Different tyre tread patterns resulted in significantly different lateral forces. The results showed that the influence of sloping ground on the tyre behaviour rather than constraining the tyre to operate at a slip angle.

Work was carried out at N.I.A.E. [1978] to measure lateral tyre forces and involved six different tyre sizes, carefully arranged into three series of experiments to establish the effect of the tread pattern on tyre behaviour. Each of three experiments was carried out on many field surfaces, predominantly stubble and the side force results were analyzed by fitting a curve of the form :

$$LFC = A\,(1-e^{-B\alpha}) \tag{2.1}$$

Equation (2.1) is an empirically obtained result based on fitting curves to measured results. Various forms of equations, including polynominals of different levels, have been tried but the exponential form has the advantage of being reasonably accurate and simple. The constants, A and B, refer of course to a particular set of tyre parameters and ground conditions. Typical examples for three different surfaces are shown in Fig.(2.4) and data such as this is convenient for representing the performance of off-road tyre behaviour in modelling studies.

Del Rosario [1980] has described an investigation of four types of steered pneumatic tyre described below : -

7.50 x 16 8-ply ribless,

7.50 x 16 8-ply traction,

7.50 x 16 8-ply shallow ribbed and

7.50 x 16 6-ply traction

A single wheel tester was designed and developed including ancillary devices to meet the requirements of the tyre behaviour. Results show the significant effect of rib size as a factor on the lateral force. Slip angle was measured from 5 to 25°, and wheelslip from

0 to 50% . A soil tank in the laboratory at Silsoe College was used for the project, with the soil kept at about 8% dry basis.

Gee-Clough and Sommer [1981] measured two tyres, a 4.00 x 8 smooth implement tyre and a 18 x 9.50 8-ply terra-type buffed smooth tyre, in a soil bin. Loam soil was used at four soil strength values, described by cone index values of approximately 150, 300, 550 and 900 *kPa*. Tyre loads and pressures were varied and a speed of 0.5 *m/sec* was maintained throughout.

Their results were a good fit to the relationship described by the equation

$$LFC = LFC_{\max}\,(1-e^{-B\alpha}) \tag{2.2}$$

where

LFC = Lateral force coefficient

$LFC_{\max}$, B = Constants for particular conditions

α = Slip angle

They then tried to correlate the results with four different forms of mobility number, of which the two most important were :

$$EMOB = \frac{C\,b\,d}{W}\sqrt{\delta/h}\;\frac{1}{1+b/2\,d} \tag{2.3}$$

$$\phi MOB = \frac{c\,b\,d}{W}\sqrt{\delta/h}\;\frac{1}{1+b/2\,d}\;\phi^{n} \tag{2.4}$$

Relationships between these numerics and two parameters in equation (2.1) were sought : namely $LFC_{\max}$ and $B.LFC_{\max}$ which is the initial slope of the *LFC* vs. α curve. Examples of the results using *EMOB* were :

$$LFC_{\max} = 0.89-0.14\,EMOB \tag{2.5}$$

$$B.LFC_{\max} = 2.18+0.38\,EMOB \tag{2.6}$$

Equation (2.5) was not statistically significant though it provided a good subjective fit to the data, whereas equation (2.6) was significant at the 2% level.

McAllister's work [1981,84] used six different tyres including tractor front, implement and trailer tyres in 38 field conditions. Tyres size were 7.50 x 16 and 12.00 x 18 and forward speed was 1 *m/sec* throughout. Details of the test rig are given in reference [1984] and measurements were made up to slip angle of 40^{o}.

McAllister found good correlation between measured results and equation (2.1). His attempts to correlate the results with mobility number led to the following expressions :

For cross-ply tyres

$$LFC_{\max} = \frac{0.69}{EMOB} + 0.61 \qquad (2.7)$$

(significant at 5% level)

$$B.LFC_{\max} = 2.34 + 0.088\, EMOB \qquad (2.8)$$

(significant at 0.1% level)

For radial-ply tyres

There was no significant relationship between $LFC_{\max}$ and $EMOB$, but :

$$B.LFC_{\max} = 2.79 + 0.16\, EMOB \qquad (2.9)$$

These are compared with Gee-Clough's results in Fig.(2.5). Equation (2.7) is a surprising result because it indicates that maximum lateral force increases as soil strength (described by cone index values) decreases.

There have been two recent and important contributions to the lateral tyre forces generation presented at the 1981 I.S.T.V.S. conference. Schwanghart [1981] described measurements made on two tractor front tyres, a 7.50 x 18 with a T85 non-driven type profile and a 6.50 x 20 with an A7 lugged profile. A specially designed frame towed behind a Unimog tractor was used on 8 different surfaces. Slip angle was varied from 0 to 30^{o} and vertical tyre load varied from 1 to 8 *kN*, so that a wide range of conditions was covered . Only a sample of the results are published in his work and the lateral force data for a 7.50 x 16 tyre are shown in Figs.(2.6 and 2.7). The relationship of

lateral force with vertical load is given in Fig.(2.6) and the classic lateral force coefficient/slip angle curves are shown in Fig.(2.7). The curves which are fitted to the data are second and third order polynomials respectively.

There is a lot of information to digest here and obviously it is subject to considerable experimental scatter. From Fig.(2.7), however, it appears that the effect of vertical load varies dramatically with the surface.

The work done by Janosi, Kamm and Wray [1981] concentrated on three military truck tyres in the range 9.00 x 20 to 10.00 x 20. An interesting measuring rig was adopted using a four wheel drive military truck. The front wheel hubs were instrumented to measure forces in three directions and slip angles were achieved by adjusting the toe-in or toe-out values of both front wheels. The effect of braking or tractive forces on lateral force as shown in Fig.(2.8) could be studied by braking or driving the appropriate axle on the vehicle.

This technique, which could be applied to a four wheel drive tractor for example, appeared to be successful although it was only used up to slip angles of 9^{o}. The parameters varied were vertical load, tyre pressure and braking and tractive force to give a total of 1300 measurements over the three surfaces used; smooth concrete, hard soil and the same soil scarified to produce a 6 inch soft sandy top layer.

The results of particular interest are those in which braking or tractive forces were used. The examples are shown for concrete, hard soil and soft soil surfaces. They appear to substantiate the proposed friction ellipse model. The authors comment that although the analysis of results is not yet completed, there is a trend for the maximum longitudinal force to be greater than the maximum lateral force, implying a friction ellipse rather than a friction circle relationship.

It is worth summarising their initial findings : -

1) Lateral force decreases with decreasing tyre pressure on concrete and hard soils whereas on soft soils it increases.

2) The greater the load and the lower the tyre pressure, the smaller the difference in lateral force on soft and hard surfaces.

3) The greater the load, the higher the sensitivity to inflation pressure.

4) Lightly loaded tyres at low inflation pressure produce the most uniform handling characteristics over different surfaces.

5) In soft soil, the lateral force peaks at lower slip angles and is less sensitive to load and inflation pressure than on the hard surfaces.

6) At high inflation pressures, there was little difference between the radial and cross ply tyre results ; at low pressure the radial tyre always generates more lateral force.

Both Schwanghart [1981] and Janosi et al [1981] included measurements on road surfaces. Of particular interest are the comparisons between a wet and dry road Fig.(2.7). In certain cases, e.g. 10^{o} slip angle with a lightly loaded tyre, the lateral force coefficient changes from 0.9 to 0.05 in going from a dry to a wet surface.

The overall conclusion to be drawn from the measured results is that vehicles which travel both on and off the road have special problems. The tyre characteristics vary dramatically between surface conditions and so the vehicle handling behaviour will also be affected. Tractors with different lug patterns on the front and rear tyres will be especially sensitive to changes in the handling balance due to different surfaces. Different tyre pressures for on and off the road operation are indicated if optimum performance is aimed for.

This is analogous to the conflicting tyre pressure requirements of low pressure for tractive performance and higher pressures for transport and road work. However, if changes in inflation pressure to match the task are impractical, the lightly loaded tyres of low inflation pressures offer the best compromise for consistent lateral force

behaviour.

When the tyre is driven or braked, the lateral force behaviour is modified significantly. This was shown in 1973 by Krick [1973] who measured lateral forces at up to 35° of slip angle for various driven tyres in a soil bin with sandy loam soil. Under these conditions, he calculated that the approximate relationship between lateral and longitudinal force was given by :-

$$F_y = (1 \pm C_T F_x) C_\alpha \ \alpha \qquad (2.10)$$

where

F_y = Lateral force

F_x = Tractive (+) or braking (-) force

α = Slip angle

C_α = Cornering stiffness at $F_x = 0$

C_T = Coefficient relating the variation in lateral force with tractive or braking force.

The plus/minus sign in equation (2.10) refers to braking or tractive force respectively. For a given slip angle, lateral force decreases as tractive force increases but increases as braking force increases. This behaviour agrees with Krick's measured results for a 7.50 x 18 tyre although they were measured for relatively small variations in longitudinal force and so the application of equation (2.10) should be restricted to this range.

The only other published data on combined lateral and longitudinal forces for off-road tyres were measured by Janosi, Kamm and Wray [1981]. Cross country truck tyres, 9.00-20 and 11.00-20, were used in this work and an example of their results is shown in Fig.(2.8). The soft soil surface had a 150 *mm* top layer of scarified sand. These results are rather different from Krick's and show similar trends to those expected from road tyre experience. When these results are extended to the limiting conditions in any direction they are referred to as friction-ellipse characteristic of the tyre.

2.1.2. AN EMPIRICAL MODEL OF TYRE FORCE GENERATION

In order to model either lateral or longitudinal behaviour independently of each other, equations (2.2) and (2.11), can be used. However, when both forces are generated in combination the following approach offers an approximate representation of behaviour.

The shape of the lateral force coefficient vs. slip angle curve is assumed to be controlled by the tractive or braking force generated ;

$$LFC = LFC_{\max}\,(1-e^{-B\alpha}) \tag{2.2}$$

where $LFC_{\max}$ is now given by the equation :

$$\left(\frac{LFC_{\max}}{LFC'_{\max}}\right)^2 + \left(\frac{COT}{COT_{\max}}\right)^2 = 1 \tag{2.11}$$

where

$LFC'_{\max}$ = maximum value of $LFC_{\max}$ at COT = 0

$COT_{\max}$ = maximum value of $COT_{\max}$ at LFC = 0

This relationship is shown in Fig.(2.9), plotted in the friction ellipse form for the measured results shown earlier.

If equation (2.11) is to be used in any vehicle dynamics study, there are several other points to consider. First, the vertical load (F_z) on each tyre will normally by varying and the above analysis assumes a linear relationship between lateral and tractive forces with vertical load. If the variations of load are small, then the above analysis is satisfactory , the "constants" $LFC'_{\max}$, $COT_{\max}$ and B being referred to the mean load condition. If the variations in load are great, then the above parameters should be included as function of (F_z). Second, the relationships only apply to the case in which the wheel is rolling. If it is locked and therefore sliding, then the distinction between lateral and longitudinal forces ceases to be meaningful.

There is only one resultant force and it may be assumed to act in the opposite direction to the resultant sliding velocity, although there are few measurements available in these conditions. Since $LFC'_{\max}$ and $COT_{\max}$ may not, in general, be the

same, a friction ellipse characteristic occurs again and the resultant force can be calculated from the angle of the resultant velocity, Fig.(2.10) shows the angle of the resultant velocity for which :

$$Resultant\ force = \frac{F_z\, COT_{max}\, LFC'_{max}}{\sqrt{LFC'^2_{max}\cos^2\alpha + COT^2_{max}\sin^2\alpha}} \qquad (2.12)$$

Third, the relationships assume steady state conditions. However, for any change in operating condition, i.e. change in wheelslip or slip angle, tyres have a finite response time relating to the time taken for the contact region to assume a new distorted shape. For road vehicle tyres, this aspect of dynamic response has been widely measured and can be approximated by :-

$$F = F_{ss}\,(1-e^{-x/l_r}) \qquad (2.13)$$

where

F = Force, lateral or longitudinal

F_{ss} = Steady state value of force

x = Distance

l_r = Relaxation length

The relaxation length, l_r, for the case of lateral force build up is approximately equal to the rolling radius of the tyre. Although no published measurements are available for off-road tyres, this type of response characteristic is a fundamental property of the tyre and there is no reason to expect off-road tyres to behave differently from road tyres. In the time domain, the response is of first order lag with break frequency, $\frac{1}{T} = \frac{U}{l_r}$. For road vehicle parameters the break frequency is sufficiently high that tyre dynamic response does not affect the vehicle response. But for off-road vehicles, where U is low and l_r can be large, e.g. tractor rear tyres, the tyre dynamic response may be important. In transfer function terms, equation (2.13) becomes :

$$\frac{F}{F_{ss}} = \frac{1}{1+S\,T} \qquad (2.14)$$

where

S = Laplace operator

T = Time constant = $\frac{l_r}{U}$

For example, if $l_r = 1\ m$ and $U = 1.5\ m/sec$, the break frequency = 1.5 *rad/sec* (0.24 *Hz*). So for these conditions, the tyre dynamic response would be important since the frequency range of interest goes up at least 3 *Hz* for handling motion and say 4 to 5 *Hz* for lateral ride motions.

2.1.3. ANALYSIS OF LATERAL TYRE FORCE GENERATION

Three simplified analyses of lateral tyre force generation on off-road surfaces have been done by the following authors :

Schwanghart [1968,81], Grecenko [1969,75], Jurkat and Brady [1981]. In addition, Karafiath and Nowatzki [1978] have proposed a finite element based model to predict all soil-tyre forces under any condition of load, longitudinal and lateral slip. This model, however, is rather too elaborate to use in vehicle handling studies since the calculations required for each set of conditions are extensive and to incorporate it in a vehicle model would require the calculations to be repeated every time step.

The other three models have distinct similarities in their approach. The main features are as follows :

1) A pressure distribution in the contact region is either assumed or calculated. This involves the important assumption that the force systems in the vertical and lateral directions can be decoupled, i.e. that the lateral force and slip angle do not affect the normal pressure distribution. Clearly, this is not the case since the soil in the contact region is subjected to three dimensional stress, but as a first order approximation it is reasonable.

2) The lateral force generated is a function of two parameters :-

a. Lateral deformation of the tyre.

b. Soil lateral deformation due to soil shear.

The first of these implies a force at the soil-tyre interface due to a displacement of the tyre tread or carcass. The force is usually assumed to be a linear function of lateral tyre deflection. For the second, the displacement can be described by the well-known relationship as :

$$\tau_{soil} = \tau_{max} (1 - e^{-j/K}) \qquad (2.15)$$

where

$$\tau_{max} = (P_g \tan\phi + c) \qquad (2.16)$$

Although all three models use the same basic approach, there are differences. Schwanghart is the only one to assume a deep rut, and so he calculates an additional lateral force component acting on the tyre sidewall. He does not, however, include longitudinal forces in his analysis whereas the other two theories include the longitudinal force vs. wheelslip relationship. Finally, a slightly different approach to calculating the tyre deformation is used in each model.

The analysis of Del Rosario [1980] is not included as a separate model here because it is based on Grecenko's work, apart from the passive soil terms. He assumes that the total lateral force has three components, due to soil-rubber friction, soil shear in the contact region and passive soil failure against the tyre sidewall. He describes the shear stress due to friction by the equation :-

$$\tau_{friction} = (C_a + \sigma \tan\delta_f) \qquad (2.17)$$

where

C_a = adhesion

δ_f = Soil-rubber angle of friction

He also uses a friction forces vs. creep relationship which is similar in form to equation (2.15) and has a similar deformation constant. Hence, the analysis for the shear stresses due to friction and soil shear are identical. A simplified version of Grecenko's theory is used in which the longitudinal slip of the tyre is ignored and the normal pressure distribution is assumed to be governed by a pressure vs. sinkage relationship of the form :

$$P = \left(\frac{K_c}{b} + K_\phi\right) Z^n \tag{2.18}$$

where the sinkage, Z, increases linearly from zero at the front of the contact patch to its maximum and the decreases linearly to zero at the back of the contact patch.

where

n = an exponent

K_c, K_ϕ = Bekker's sinkage parameters

b = Width of the contact area

This gives a parabolic pressure distribution in the contact region rather than the constant pressure distribution assumed by Grecenko.

2.1.3.1. ANALYSIS OF SCHWANGHART

For tyres with deep treads, he assumes that tyre deformation is dominated by bending of the lugs and so carcass deformation can be neglected. Thus, the shear force arising from the lug is :

$$\tau_{tread} = C' \eta \tag{2.19}$$

where η is deformation of the tyre tread and the stiffness, C', can be measured by applying static lateral forces to the tyre. Soil shear stress, τ_{soil} is given by equation (2.15).

Then, for a slip angle, α, the total lateral displacement, y, depends on the longitudinal coordinate in the contact region, λ , i.e. :

$$y = \lambda \tan\alpha \tag{2.20}$$

This is the same as the line { defined in Fig. (2.3) } that the tyre centreline would follow under ideal kinematic conditions if there were no slip or soil shear. Recognising that the total lateral displacement results from (i) tread deformation, (ii) soil deformation, and (iii) slip after exceeding maximum soil deformation, Schwanghart writes :

$$j + \eta = \lambda \tan\alpha \tag{2.21}$$

where the terms (ii) and (iii) are both included in j. Then combining equations (2.19), (2.20) and (2.21) gives :

$$-K \log \left\{ 1 - \frac{\tau_{soil}}{\sigma \tan\phi + c} \right\} + \frac{\tau_{tread}}{C'} = \lambda \tan\alpha \tag{2.22}$$

For equilibrium at any small area in the contact region, the shear stress generated in the soil must equal that due to tyre deformation i.e.

$$\tau_{soil} = \tau_{tread} = C' \eta \tag{2.23}$$

and so substituting this in Equation (2.22) gives :

$$\eta - K \log \left\{ 1 - \frac{C' \eta}{\sigma \tan\phi + c} \right\} + \frac{\tau_{tread}}{C'} = \lambda \tan\alpha \tag{2.24}$$

This allows, η, to be found and hence, j, and then the total shear stress. Schematically, these parameters are plotted throughout the contact region in Fig.(2.11) for two assumed pressure distributions. Schwanghart differentiates between soil deformation and slip by approximating equation (2.24) to a bilinear form in which :

$$\tau = \left(\frac{j}{K} \right) \tau_{max} \tag{2.25}$$

until τ_{max} is reached. This is shown in Fig.(2.12). When τ is defined by equation (2.25), he calls it soil deformation, whereas when $\tau = \tau_{max}$ it is referred to as slip. Not surprisingly, as tyre slip angle is increased, the point in the contact region at which this changeover occurs, moves forward.

The component due to the sidewall of the tyre is calculated from the expression for the passive soil resistance of a blade moving through the soil as given by Reece [1965].

The importance of this term depends on the particular tyre and soil condition. Schwanghart's calculations for a 6.00 x 20 tyre in loose soil gave an average sinkage of 12 *cm* and he showed that for these conditions the sidewall component was of a similar order of magnitude to the contact patch component. With less sinkage and shallower rut, its effect is less important and the following two authors ignore it in their analyses.

2.1.3.2. ANALYSIS OF GRECENKO

The main assumptions of his analysis are that :

1) The contact area is rectangular.

2) The total resultant force, $U = \sqrt{H^2 + Y^2}$

as seen in Fig.(2.13) acts at an angle, ξ, to the wheel plane.

3) Rolling resistance force arises mainly from compaction and is constant for slip angles less than 40^o, where, γ = slip angle.

4) The rut is shallow.

5) The normal pressure distribution is constant.

The total deformation in the horizontal plane, *j*, arises from soil deformation. From Fig.(2.13) and for steady-state conditions, Grecenko derives the relationship :

$$j = u\,x \tag{2.26}$$

where

x = distance along the contact patch.

u = a constant depending on the particular slip and slip angle conditions.

This assumes that the resulting contact patch does not distort relative to the wheel centreline, so the tyre deformation is ignored and the force generated is due solely to the effect of soil deformation.

The force, U, and displacement vector, j, act in the same direction. The force on a small element, dx, of the contact region is :

$$dU = \tau\, b\ \ dx \tag{2.27}$$

where τ = soil shear force.

Therefore, the total force is obtained by integrating this expression over the whole contact region :

$$U = b \int_0^l \tau\ dx \tag{2.28}$$

where

$$\tau = \tau_m\,(1 - e^{-j/K})$$

τ_m = Soil shear strength.

Substituting for j, and integrating gives :

$$U = b\ l\ \tau_m \left\{ 1 - \frac{(1 - e^{-J_k})}{J_k} \right\} \tag{2.29}$$

where $J_k = \frac{u\,l}{K}$, a deformation coefficient. The maximum resultant force, U, as $u \rightarrow \alpha$ is :

$$U_m = b\,l\,\tau_m \tag{2.30}$$

so that the generalised resultant force, α_u, may be expressed solely in terms of the parameter J_k as :

$$\alpha_u = \frac{U}{U_m} = 1 - \frac{(1-e^{-J_k})}{J_k} \tag{2.31}$$

Alternatively, Grecenko derives a similar relationship but based on the bilinear form of the shear stress vs. displacement equation rather that the exponential form given in equation (2.15).

Grecenko then goes on to compare the forces generated as a function of wheelslip and slip angle.

$$\textit{Wheelslip},\ s = \frac{j_x}{x} = \frac{j\cos\xi}{x} = \frac{u\sin\xi}{1-s} \tag{2.32}$$

$$\textit{Slip angle},\ \tan\gamma = \frac{j_y}{x-j_x} = \frac{j\sin\xi}{x-j\cos\xi} = \frac{u\sin\xi}{1-s} \tag{2.33}$$

Equations (2.32) and (2.33) can be combined to give :-

$$u = \sqrt{(1-s)^2\ \tan^2\gamma + s^2} \tag{2.34}$$

Now, substituting into equation (2.20) for two special cases, gives :-

$$\text{for } s=0,\ \alpha_u = f_1(\tan\gamma)\ \textit{at}\ H=0 \tag{2.35}$$

$$\text{for } \gamma=0,\ \alpha_u = f_2(s)\ \textit{at}\ Y=0 \tag{2.36}$$

Since these two functions are identical :

$$f_1(\tan\gamma) = f_2(s) \tag{2.37}$$

Grecenko refers to this as the "principle of equivalence". It means that for a given set of soil and tyre parameters, the relationship between longitudinal force and wheelslip (at

zero slip angle) is the same as that between lateral force and the tangent of slip angle (at zero wheelslip).

In the more general case when both forces (H and Y) are present, these forces may be calculated from a knowledge of the wheel motion described by s and γ. Alternatively, knowing the forces, the wheel motion may be calculated.

Notice that equation (2.29) is identical to the result of Schwanghart for the special case in which $H = s = 0$ and C' is very stiff so that the tyre deformation, η, approaches zero.

2.1.3.3. ANALYSIS OF JURKAT AND BRADY

This model is based completely on an early version of a road vehicle tyre model developed by Dugoff, Fancher and Segel [1970] at U.M.T.R.I., Michigan. It is modified by introducing an extra failure mode due to soil shear in addition to the possibility of exceeding the available friction force in the contact region.

The assumed distortion of the tyre under longitudinal and lateral forces is shown in Fig.(2.14). Point P is in the contact patch whereas P' is in the centre plane of the tyre. When no forces act, P' is directly above P but when forces act they cause a distortion of the contact patch and P moves away from P'. Notice that λ is defined in the tyre coordinates whereas λ' is defined in the contact patch, the relationship between them being:

$$\lambda' = \lambda (1-s) \tag{2.38}$$

The position of P relative to a point directly below P' is defined by the vector :

$$\underline{s} = \left\{\lambda s,\ \lambda \tan\alpha \right\} \tag{2.39}$$

whose magnitude $j = | s |$

As the distance into the contact region, λ, increases the distortion between P and P' increases. At some point, the shear force due to tyre deformation equals the

minimum of

a. tyre/ground friction,

b. soil shear strength.

This point is defined by λ'_s. So for $\lambda' < \lambda'_s$ elastic deformation of the tyre occurs with no skid or soil shear. And for $\lambda' > \lambda'_s$ the tyre/ground friction or soil strength cannot support further tyre deformation and skid or soil shear occurs.

In the initial part of the contact region, the elastic shear stresses, τ_{e_x} and τ_{e_y}, are assumed to be linearly related to the strains so :

$$\tau_{e_x} = k_{x_n} \lambda s \tag{2.40}$$

$$\tau_{e_y} = k_{y_n} \lambda \tan\alpha \tag{2.41}$$

where

$$k_{x_n} = \frac{C_s}{b\, l^2} \tag{2.42}$$

$$k_{y_n} = \frac{C_\alpha}{b\, l^2} \tag{2.43}$$

$$\text{and } C_s = C_s(F_z) = \frac{\partial F_x}{\partial s} \Big|_{s=\alpha=0} \tag{2.44}$$

$$C_\alpha = C_\alpha(F_z) = \frac{\partial F_y}{\partial \alpha} \Big|_{s=\alpha=0} \tag{2.45}$$

and are determined empirically.

Thinking of the contact region as being divided into strips of length $d\lambda$ and width , b, the shear density, $\tau_e(\lambda)$, for each strip is approximately :-

$$\tau_e(\lambda) = \sqrt{(k_{x_n}(\lambda)\, s)^2 + (k_{y_n}(\lambda) \tan\alpha)^2} \tag{2.46}$$

This stress increases as λ increases and λs may exceed the stress due to :

$$\textit{friction}, \ \tau_k(\lambda) = \mu\, \sigma(\lambda) \tag{2.47}$$

$$\textit{or soil shear}, \ \tau_s(\lambda) = (c + \sigma(\lambda) \tan\phi)\,(1 - e^{-j/K}) \tag{2.48}$$

Therefore, $\lambda'_s = \lambda s\,(1-s)$ defines the coordinate of the point at which :

$$\tau_e(\lambda) = \min\left\{\tau_k(\lambda),\ \tau_s(\lambda)\right\} \tag{2.49}$$

In the region $0 < \lambda < \lambda'_s$, the forces are given by :

$$F_{x_e} = b\int_0^{\lambda'_s} \tau_{e_x}(\lambda)\,d\lambda = k_{x_n}\,s\,b\,\frac{\lambda'^2}{2\,(1-s)} \tag{2.50}$$

$$F_{y_e} = b\int_0^{\lambda'_s} \tau_{e_y}(\lambda)\,d\lambda = k_{y_n}\tan\alpha\,b\,\frac{\lambda'^2}{2\,(1-s)} \tag{2.51}$$

The total forces over the whole contact region consist of the above terms plus the components developed in the region $\lambda'_s < \lambda < 1$:

$$F_x = F_{x_e} + \frac{b\,s}{\sqrt{s^2+\tan^2\alpha}}\int_{\lambda'_s}^{l} \min\left\{\tau_k(\lambda),\ \tau_s(\lambda)\right\}d\lambda \tag{2.52}$$

$$F_y = F_{y_e} + \frac{b\tan\alpha}{\sqrt{s^2+\tan^2\alpha}}\int_{\lambda'_s}^{l} \min\left\{\tau_k(\lambda),\ \tau_s(\lambda)\right\}d\lambda \tag{2.53}$$

Jurkat and Brady point out the important fact that for road surfaces $\tau_s(\lambda)$ will be very much greater than $\tau_k(\lambda)$ and their model conveniently reduces to one already commonly used for road vehicle handling studies .

The force generated by the side wall of the tyre is calculated in the analysis of Schwanghart [1968] and Del Rosario [1980]. The other authors assume that for small values of sinkage, this component may be ignored. Both analyses are based on the fundamental equation of earthmoving mechanics for passive soil resistance of a wall or blade embedded in the soil :-

$$P' = (\gamma Z^2 N_\gamma + c\,Z\,N_c + q\,Z\,N_q)\,\cos\delta_f \tag{2.54}$$

where

P' = Soil resistance/unit length

γ = Soil specific weight

c = Soil cohesion

q = Surcharge load/unit area

Z = Sinkage

δ_f = Soil-rubber angle of friction

N_γ, N_c, N_q = Soil coefficients

The use of this equation and charts containing the soil coefficient are discussed by Reece [1965] and Hettiaratchi [1969].

In Schwanghart's use of this equation, he substitutes a parabolic distribution of sinkage in the contact region. He also calculates surcharge load by first calculating the volume of soil which is displaced laterally by the tyre and then assuming that this can be taken as an additional distributed load acting on the shear zone. This results in a value for P' as a function of distance in the contact patch which is then integrated over the contact length to give a total force.

Del Rosario [1980] identifies another possible mode of failure in addition to the passive failure described by equation (2.54). Following the work of Hettiarachi [1966], he points to the case in which a soil wedge appears and becomes part of the interface. The resultant force is then given by :-

$$P = P_e N_w + \gamma Z_w^2 N_{\gamma w} + c_w Z_w N_{cw} \qquad (2.55)$$

where P_e = Soil reaction force against the pseudo interface and suffix, w, simply relates to the case in which a wedge is formed.

In using equation (2.54), he assumes a linear relationship between sinkage and distance in the contact patch and he also assumes that there is no surcharge load. He does, however, calculate an extra small contribution to the total force due to the adhesion force acting along the interface.

Overall, therefore, these two approaches are similar and hinge around the application of equation (2.55) which is slightly more difficult for a rolling, slipping wheels than for a rigid plate. The importance of this term in the total lateral force generated by the tyre depends on the value of tyre sinkage in the soil.

2.1.4. SPOKED TYRE MODEL ON HARD SURFACE

The spoke tyre model is depicted in Fig.(2.15) and represented as a single plane wheel consisting of a multi-spoke structure. The spokes are cantilevers fixed to the wheel hub at their inner ends. The other ends form a complete circle in the unloaded condition.

The wheel model diameter is equal to the real tyre diameter, and the number of spokes are chosen to make the calculation economical on the one hand, and hopefully realistic on the other. The spokes are radially flexible as shown in the Fig. (2.14). They are also assumed to be flexible in the circumferential and lateral directions. The summations of the spoke stiffnesses in the normal, circumferential and lateral directions are considered to be comparable with the pneumatic tyre stiffnesses.

The spokes are free to deflect in the radial, longitudinal and lateral directions when the wheel is rolling along. These deflections will be related to the normal and shear forces generated. Because there is no connection between the spoke tips, the spokes outside the contact line are unstressed and, therefore, unstrained until they enter the contact region.

The spoke tips are assumed not to slide across the surface until the elastic forces in the surface plane implied by the absence of any sliding become greater than the friction force available. When sliding occurs the spoke tips will move across the road to establish a balance between the elastic force and the friction force.

El-Nashar [1985] predicted results that qualitatively agree with those obtained from a range of published work. His model is built on fundamental ideas and does not include any empirical formula. Consequently, the model behaviour reflects rather than closely follows that of a real tyre. The model can, therefore, be used to give the user an

improved appreciation of the relationship between tyre carcass stiffness properties, tyre/road friction properties and the shear force generation process.

Sharp and El-Nashar [1986] have recently reviewed and studied tyre behaviour. Their study is based on an mathematical model called a multi-spoke tyre model for predicting the generation of tyre shear forces. The model specifies wheel motion which in turn leads to a complete tyre force and moment system, and has been aimed at economical digital computer simulation. The model consists of a single plane of equi-spaced discrete radial spokes interconnected through the wheel hub, each spoke having radial, lateral and longitudinal tip flexibilities. The force components are normal to ground and in ground plane, so that the total force and moment system acting on the tyre can be obtained by summation over all the spokes in the contact region.

A transform axis system as shown in Fig.(2.17) was used to calculate tyre force components generated under steady-state condition on a hard surface. To explain this analysis, Fig.(2.18) shows the simple example for a rolling tyre in a straight running condition, with zero camber angle, i.e. a two dimensional case.

According to Fig.(2.18), point O, represents the position of the tyre centre at time zero and, OP, the first spoke just entering into the contact region at this time. OP, will have length, R, called the free radius of each spoke, and will be at an angle, ε, to the vertical plane. At time, t, the tyre centre will be at O', where, $OO' = U\,t$, the spoke tip will be at Q, and $O'Q$ will have components as follows :

$(R+\rho)\ Sin(\varepsilon-\Omega t)+\zeta\ Cos(\varepsilon-\Omega t)$ along the X direction.

$(R+\rho)\ cos(\varepsilon-\Omega t)-\zeta\ sin(\varepsilon-\Omega t)$ along the Z direction.

For Q and P to be at the same height (steady-state condition) :-

$$R\ Cos\varepsilon=(R+\rho)\ cos(\varepsilon-\Omega t)-\zeta\ sin(\varepsilon-\Omega t) \qquad (2.56)$$

$$R\ Sin\varepsilon=(R+\rho)\ sin(\varepsilon-\Omega t)+\zeta\ cos(\varepsilon-\Omega t)+U\,t \qquad (2.57)$$

Sharp and El-Nashar assumed that the spokes are positioned at 1^{o} intervals and chose t such that $\Omega t=\frac{\pi}{180}$. They then solved equations (2.56) and (2.57) for ρ and ζ.

These values of ρ and ζ then become ρ_0 and ζ_0, which are the initial second estimated for the next spoke. By using a bisection method, they corrected values of spoke tip deflections if there was not sufficient friction available to prevent sliding.

The normal force applied to the spoke tip by the ground surface is :-

$$f_z = \phi(\rho)\cos(\varepsilon - \Omega t) - \zeta\ K4\ \sin(\varepsilon - \Omega t) \qquad (2.58)$$

and the shear force is :

$$f_x = \phi(\rho_0)\sin(\varepsilon - \Omega t) + \zeta\ K4\ \cos(\varepsilon - \Omega t) \qquad (2.59)$$

where $\phi(\rho_0)$ is the radial force an the spoke tip and $K4$ is the constant circumferential spoke tip stiffness.

The main idea of their model is that the wheel motion and properties (spoke radius, spoke stiffnesses and spoke tip to road friction coefficient) will be specified and the force system will then be deduced. The calculations started from the point when the spoke whose motion is to be followed is right at the front of the contact region.

2.1.5. COMPARISONS OF MEASURED AND PREDICTED DATA

From the previous work concerning the relationship between the lateral force coefficient and slip angle, it is concluded that the tyre and soil data are the most predominant parameters in this relation.

Comparison between the measured and predicted results for the above relation is shown in Figs.(2.19 to 2.25). Fig.(2.19) shows the comparison between Schwanghart's results and those predicted by Grecenko for a 5.50-16 tractor front tyre under soft soil condition. The plot shows that the characteristics of the curves follow a similar pattern except that the rate of change of the slope in the measured results is higher than that of the predicted one. The results also show a quantitative agreement at a point where the two curves intersect at about 16^o of slip angle and slight discrepancies over the other range of slip angles.

For results measured by Del Rosario, Fig.(2.20) he indicates that the measured and predicted results have similar trends although in quantitative terms, there are some differences. The same behaviour as Fig.(2.19) is shown in Fig.(2.21) with slight variation in agreement and pattern for McAllister's results. The intersection between the two curves occurs at about 15^{o} of slip angle.

In Fig.(2.22) the intersection between the curve measured by Krick and predicted results occurs at about 18^{o} of slip angle. Figs.(2.23) and (2.24) show the same overall behaviour as Fig.(2.20) for a different tyre size and range of operating conditions. Both figures have the same trends and the predicted results are consistently higher than the measured results.

Measured results obtained by Gilfillan show a maximum value of lateral force at about 18^{o} of slip angle as seen in Fig.(2.25). The intersection between the measured and predicted results are in the range from 10 to 25^{o} of slip angle.

These figures {Figs.(2.19 to 2.25)} show the typical measured data compared with predicted results based on Grecenko's theory [1975], this theory being adaptable for each set of conditions. Some of the measured results were obtained from the field and some of them obtained by laboratory tests. It is necessary to estimate various parameters that are not described in the experimental data. This obviously introduces a degree of uncertainty into the results, but the exercise does attempt to test the theory over a reasonably wide range of conditions. Comparison of measured data and predicted results is often difficult because of the lack of soil and tyre parameters quoted in the reports of measurements.

2.2. BASIC SOIL MECHANICS

In agricultural soil mechanics, the most relevant soil properties are the reactions of soils to applied forces. For simplicity these properties are called "strength properties". For a given soil they will change with time under the influence of climate, soil management and plant growth. The strength properties of a given soil and their change with time are

determined by the following factors :-

1) Number of particles per unit of volume.

2) Spatial distribution of particles.

3) Moisture content as a percentage of total volume.

4) Moisture distribution.

5) Bonds between particles.

6) Distribution of bonds.

2.2.1. A HISTORICAL PERSPECTIVE

The development of a traction theory for off-road vehicles (agricultural, construction and forestry) dates from the 1940's. A considerable role in this development was played by Bekker [1956,60,69,74]. Traction theory depends upon the measurement of the fundamental soil shearing strength and the establishment of a "deformation modulus" to characterise the variation of shearing strength with deformation.

Significant research effort from the 1950's through the 1970's was directed toward the development of analysis systems for evaluating mobility and predicting tractive performance. These research efforts have led to systems which permit evaluation of new traction mobility vehicles and concepts which minimise experimental effort.

Terrain-vehicle problems involving self-powered vehicles, have a lengthy history. Current trends of traction and mobility technology and their applications to vehicle design have been discussed recently by Burt and Turner [1983]. In terms of the relevance of traction and mobility calculations to vehicle, a number of problems still remain. In particular, the descriptions of soil strength remains today as a major obstacle

to the development of a fully acceptable and accurate soil-mobility terrain mechanics description.

2.2.2. SOIL-VEHICLE TRACTION PERFORMANCE

The various approaches that have been taken to analyze soil-vehicle systems can be broadly categorised into three types :-

2.2.2.1. Semi-empirical methods

This modelling approach is based on theoretical mechanics concepts (equilibrium and soil strength theories) coupled with empirical pressure-sinkage relationships for soil. The maximum thrust developed by a tractive device is taken to be the local value of the maximum soil shear stress underneath the device, integrated over the contact area. The maximum soil shear stress acting on the device is estimated from simple Mohr-Coulomb Failure Theory for cohesive-frictional soils.

An empirically developed pressure-sinkage relationship for soil is used to calculate motion resistance to forward movement. Net pull force of a traction element is calculated as the difference between developed thrust and forward motion resistance.

The semi-empirical approach was developed by Bekker [1956,60] for applications to rigid wheels, pneumatic tyres and tracked vehicles. This analysis technique has not been widely adopted for use in off-road vehicle design.

2.2.2.2. Empirical methods

Empirical analysis methods based on the theory of dimensional analysis and have been developed and applied to a variety of soil-vehicle problems. The basic approach involves the identification of dimensionless groups of pertinent variables relevant to the problem, followed by experimentation in order to empirically relate these parameters.

Thus, modelling laws are empirically derived through experimentation as opposed to analytically derived through solution of fundamental equations which describe the

phenomena of interest. Through application of this approach one can possibly avoid explicit formulation and solution of the governing (typically differential) equations of the system.

One of the first attempts at applying the theory of dimensional analysis to tyre-soil systems was reported by Freitag [1968]. This report successfully derived tyre mobility numbers, i.e. independent dimensionless terms that led to empirical prediction equations for tyre traction and rolling resistance performance in dry sand and saturated clay soils. The mobility numbers comprise variables which describe tyre and soil properties.

Most importantly, cone index can be measured in field conditions with a relatively simple instrument, unlike most other common measurements of soil strength. Empirical equations were experimentally validated over a practical spectrum of tyre-soil conditions relative to agricultural earthmoving and forestry applications. These equations allow prediction of maximum tractive effort and rolling resistance of a single tyre based on tyre geometry, normal load, rate of slip and soil cone index.

Nevertheless, empirical methods using cone index was found to be much more reliable than the semi-empirical methods as reported by Domier and Williams [1979].

2.2.2.3. Analytical methods

This approach to vehicle-soil mobility is an outgrowth from the application of soil plasticity concepts to foundation and footing stability problems. The first attempt to apply soil plasticity analysis to problems of vehicle mobility, was reported by Karafiath [1970]. This work was motivated by an interest in problems associated with lunar locomotion.

The assumption of perfectly plastic soil behaviour is inherent in this analysis, thus situations in which elastic soil deformation is of importance as referred to by Karafiath and Nowatzki [1978] cannot be treated.

Another analytical method that is beginning to evolve for application to soil-vehicle problems is the "finite element method". This is a technique which provides a means of representing differential equations with approximate algebraic equations. The technique has received much attention since the early 1960's and has been applied to a variety of physical phenomena, stress, deformation, heat transfer, fluid flow, diffusion processes and electromagnetic fields.

Numerous applications of the finite element method to problems of soil and rock mechanics have appeared only over the last decade. Far less effort has been directed towards finite element modelling of soil traction problems. This modelling approach reported by Chung and Lee [1975] was more ambitious and treated the soil as a nonlinear viscoelasto-plastic material.

The finite element method will most likely be the vehicle for implementation of the theory. The major disadvantages of this method are associated with the large computer resource and costs and the complexity of the software required to conduct a general nonlinear analysis.

2.3. CRITICAL SUMMARY AND CONCLUSIONS

The above survey has shown that, most of the tyre studies to date have been directed towards the tractive behaviour of off-road tyres. In contrast, for fewer measurements have been concerned with the lateral behaviour of off-road tyres.

Reports of measurements of combined lateral and longitudinal forces are even more scarce and consequently, empirical or analytical descriptions of the behaviour of off-road tyres in generating these forces are not generally accepted although some attempts have been made to develop such descriptions.

Because of the small amount of work done on lateral off-road tyre behaviour and on measurements of the associated soil parameters, little success has been achieved either in relating tyre forces to soil properties or in developing predictive expressions from a fundamental soil mechanics viewpoint.

According to the above summary and literature survey, it is suggested that better off-road tyre models are needed, firstly, to represent tyre behaviour more accurately, secondly, to understand the tyre-soil interaction in more detail and finally, for use in off-road vehicle handling and stability models.

2.4. OBJECTIVE OF THE THESIS

The objectives of the work described in this thesis are :-

(a) to understand the mechanisms by which tyres generate forces on deformable surfaces.

(b) to develop models of varying degrees of complexity to describe this behaviour.

(c) to compare results predicted by these models with available data for tyre forces.

(d) to draw conclusions about the accuracy of the models and make recommendations about their usefulness in off-road vehicle dynamics problems.

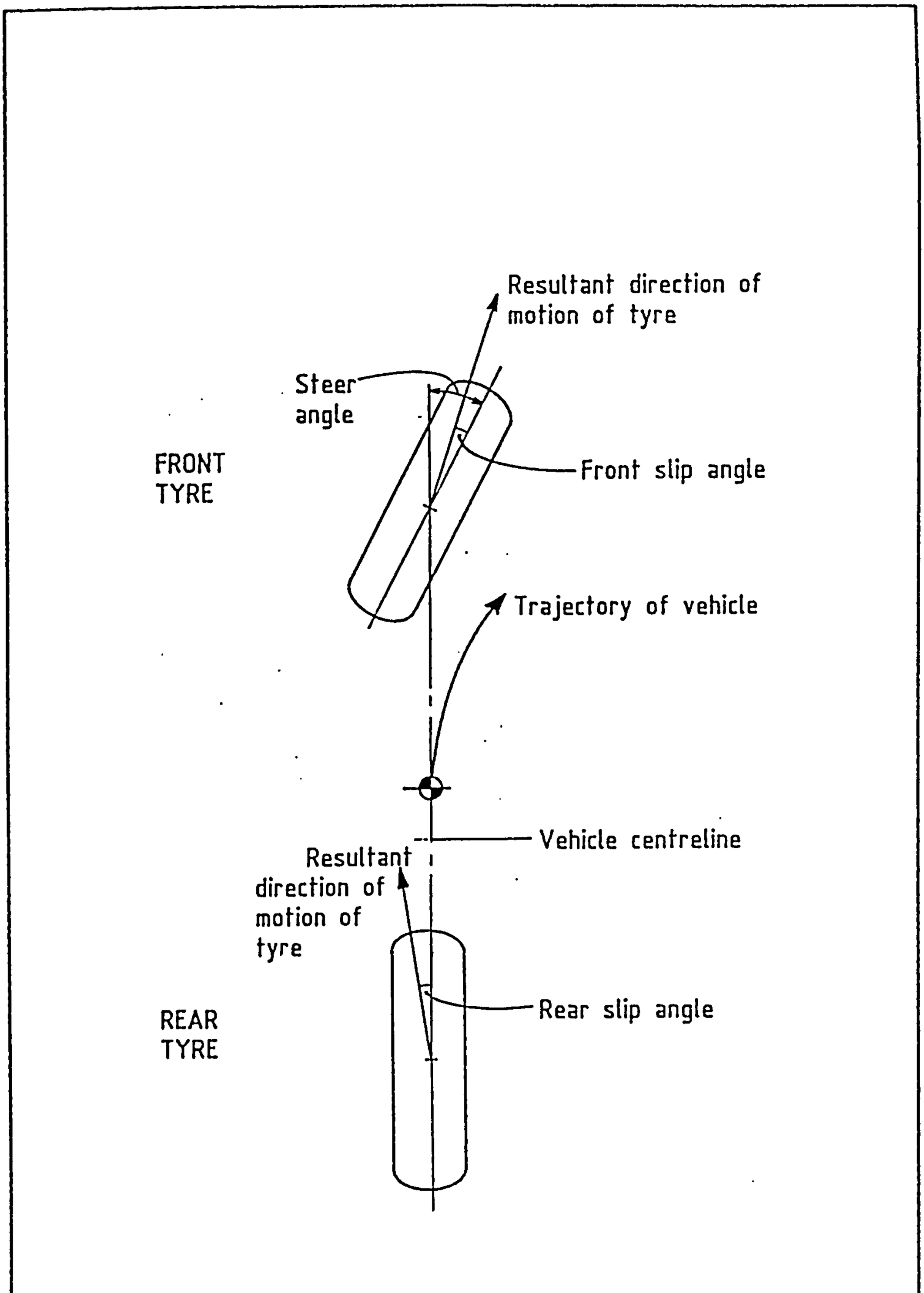

Fig. (2.1) Slip angles assumed by a vehicle during cornering.

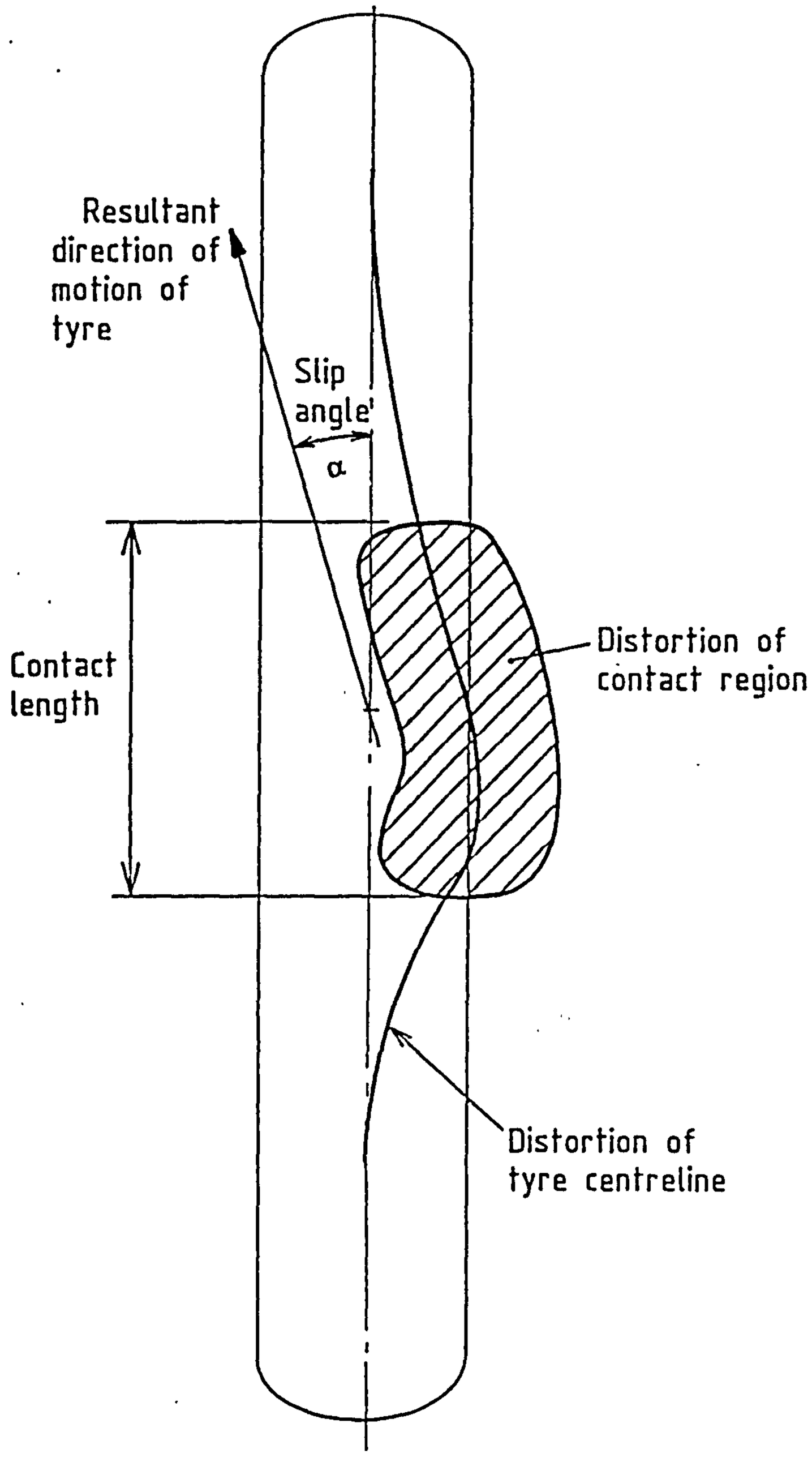

Fig. (2.2) Distortion of the contact patch of a tyre operating at a slip angle.

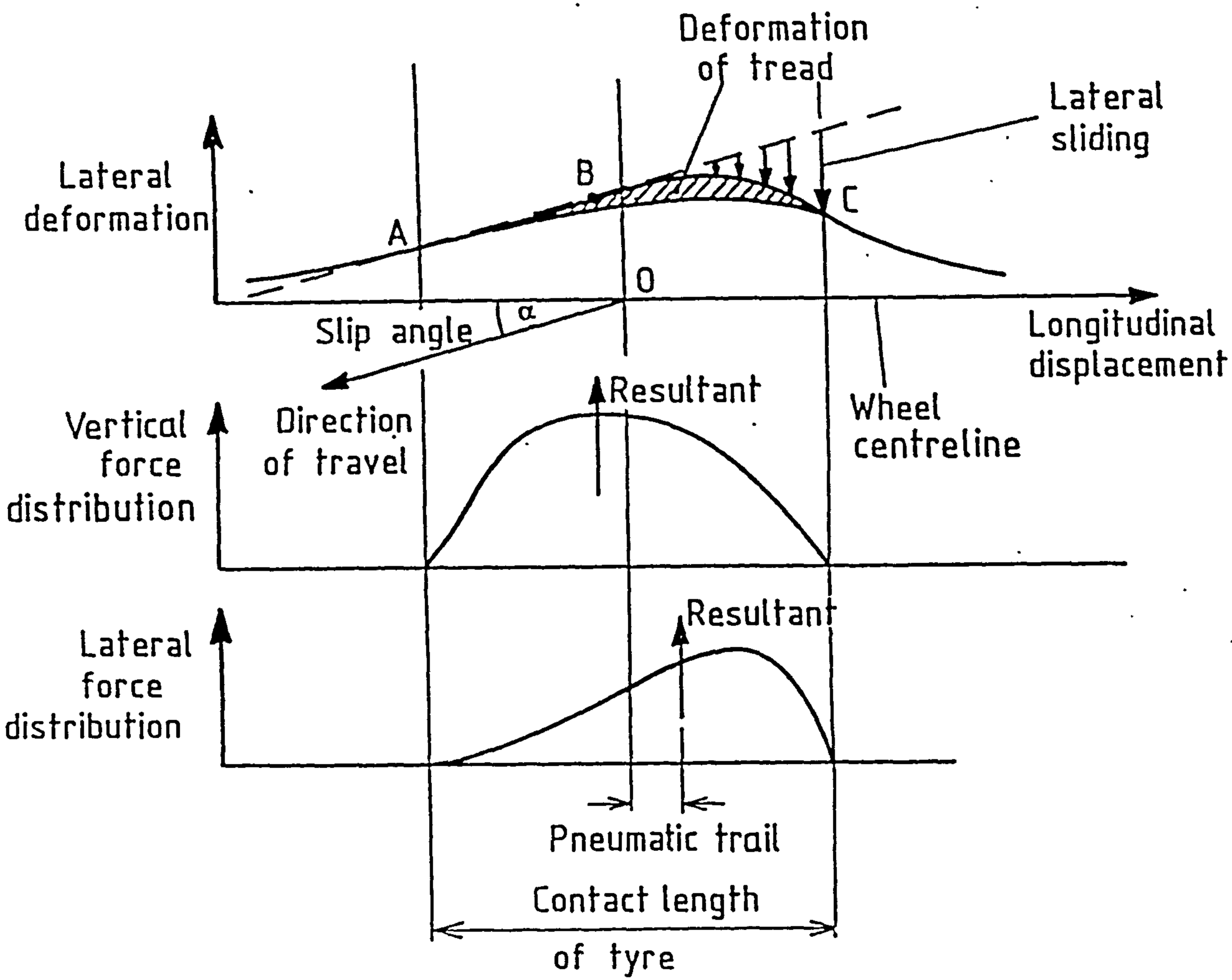

Fig. (2.3) Force distributions and lateral defomation of a tyre operating at a slip angle on hard surface.

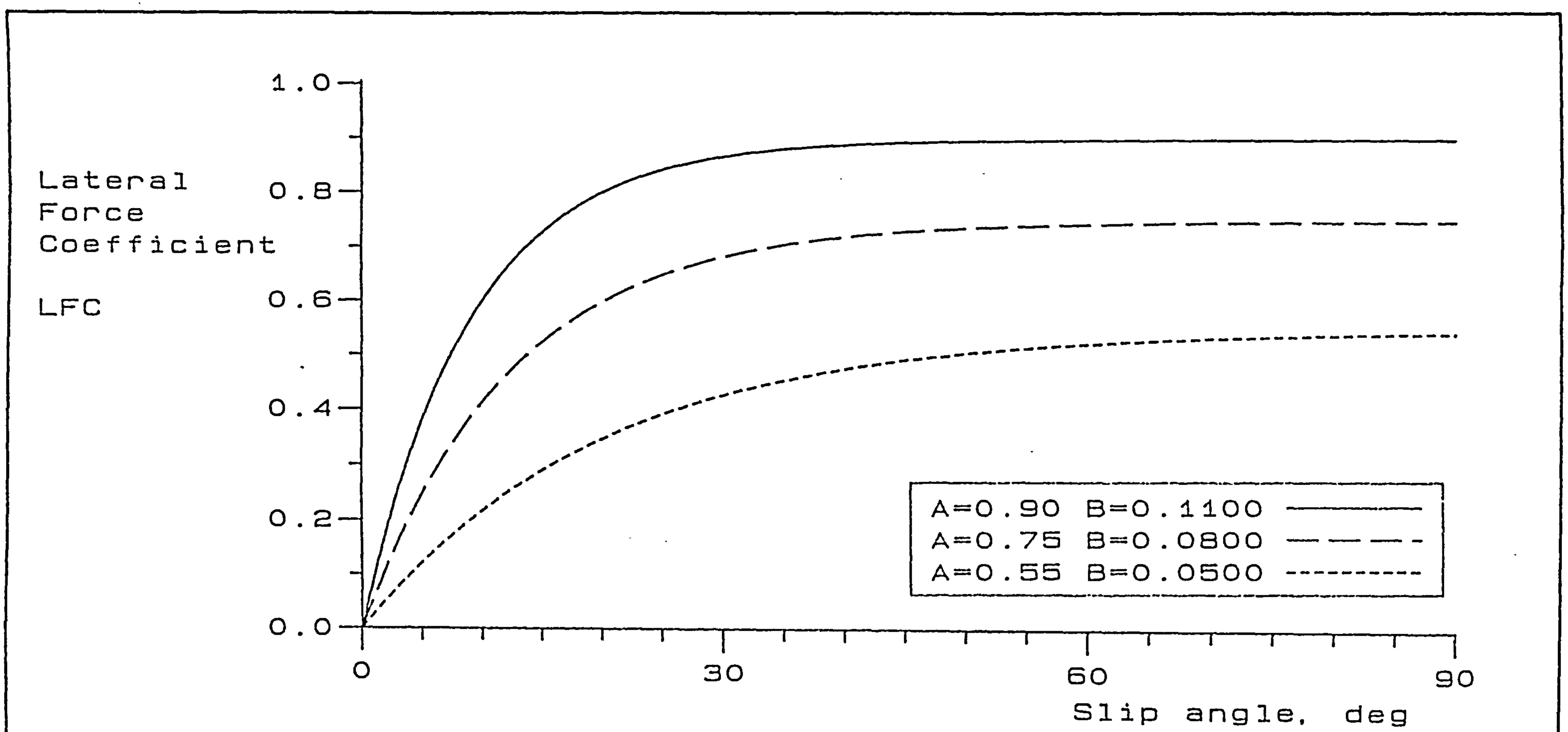

Fig. (2.4) Typical relationships of lateral force coefficient with slip angle for an off-road tyre on three different surfaces.

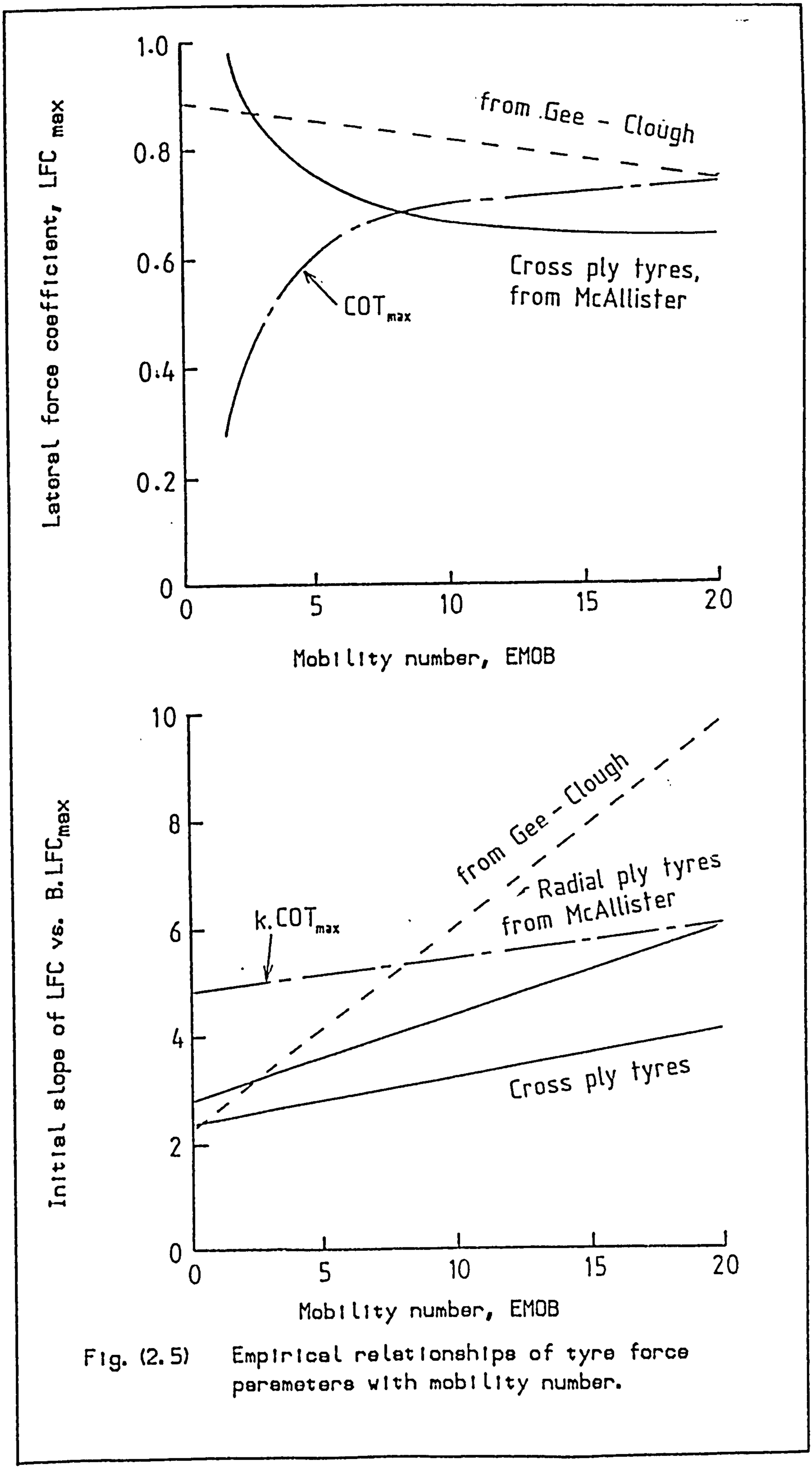

Fig. (2.5) Empirical relationships of tyre force parameters with mobility number.

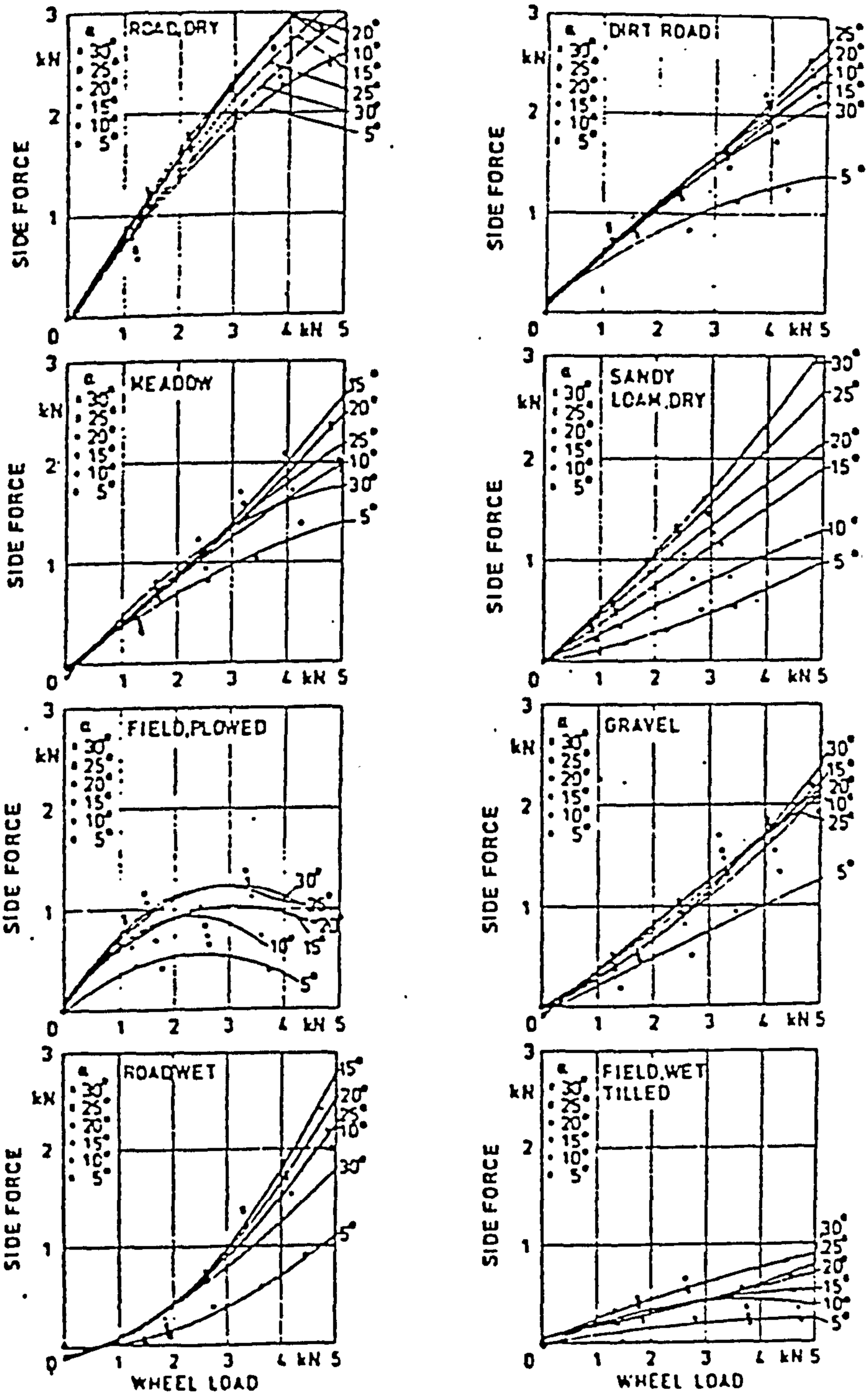

Fig. (2.6) Effect of vertical load on the lateral force for a tractor tyre on 8 different surfuces with various slip angles, Schwanghart 1981.

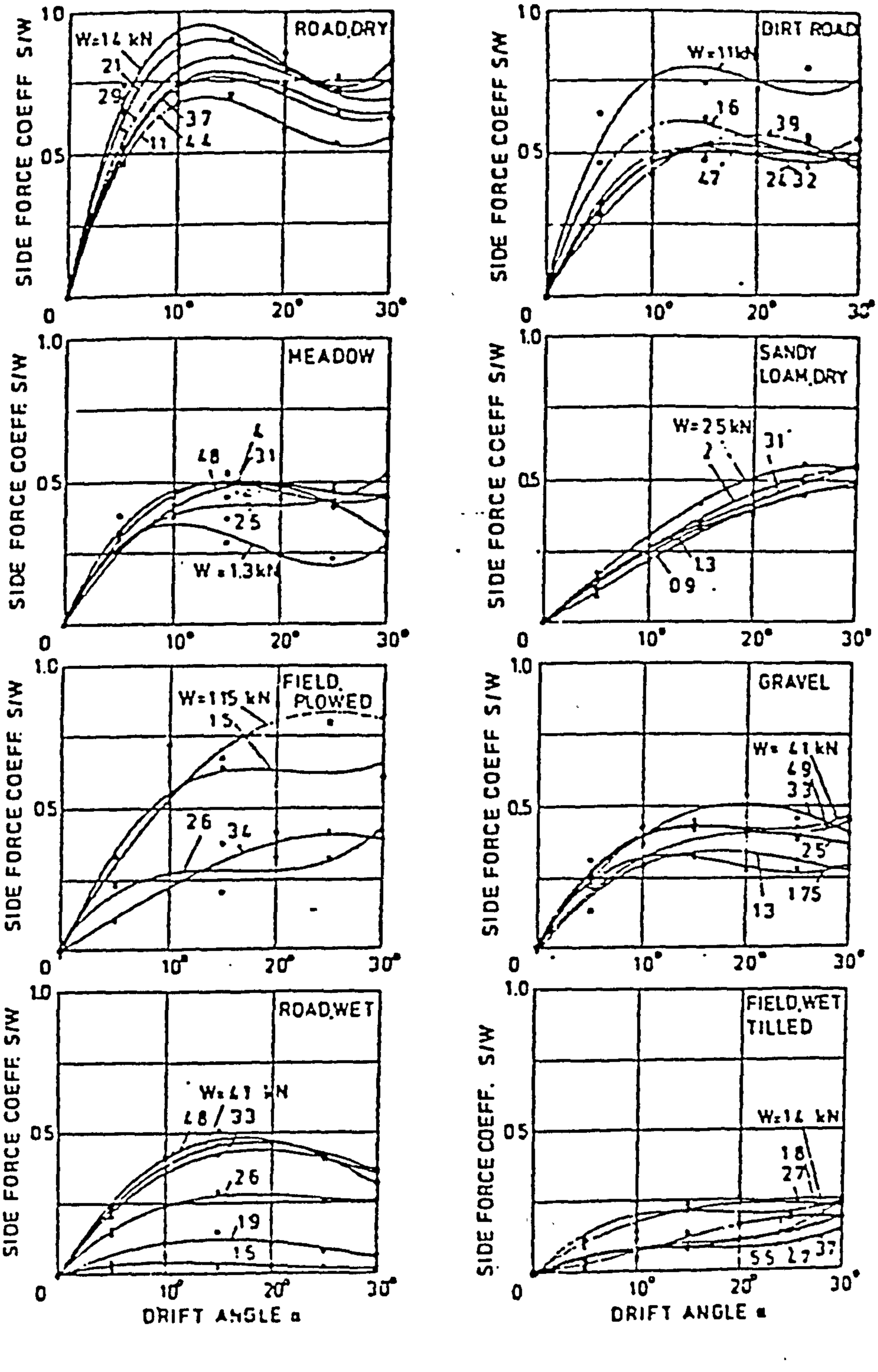

Fig. (2.7) Lateral force coefficient/slip angle relationships for a 7.50 x 16 tyre with different vertical load, Schwanghart 1981.

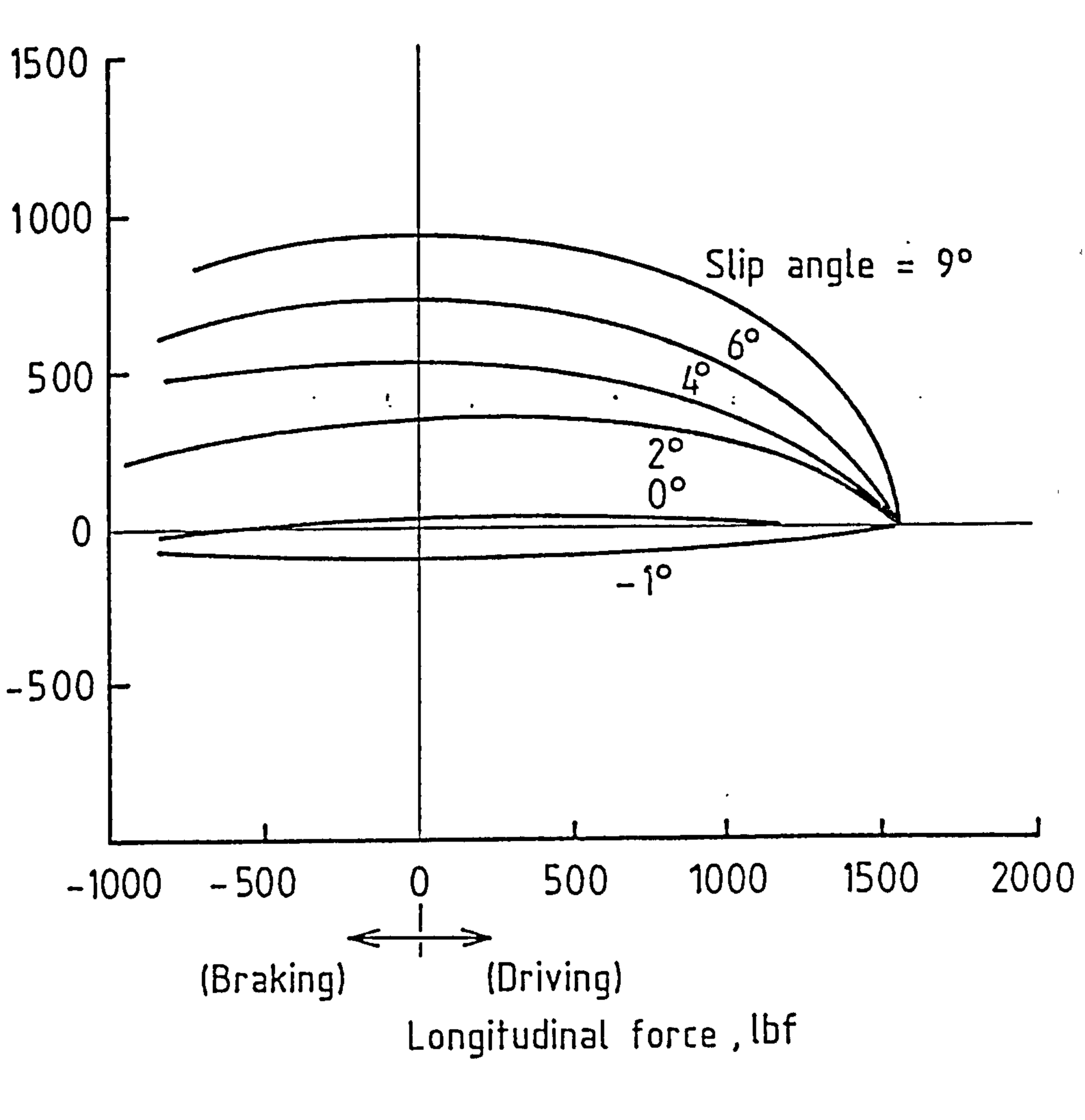

Fig. (2.8) The forces measured by Janosi 1981 for a tyre on soft soil.

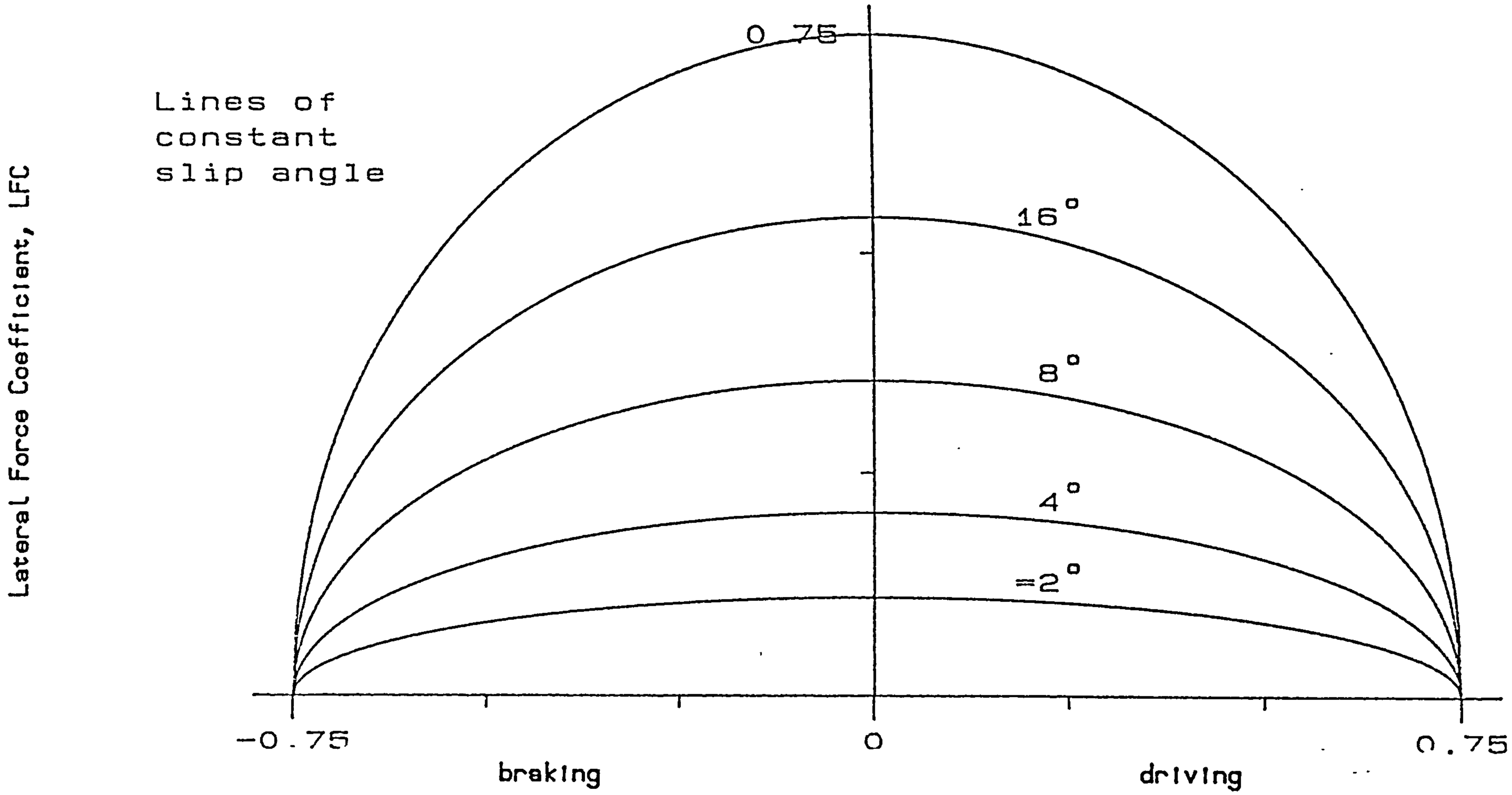

Fig. (2.9) Combined lateral and longitudinal tyre force generation characteristics as described by equations (2.2) and (2.15).

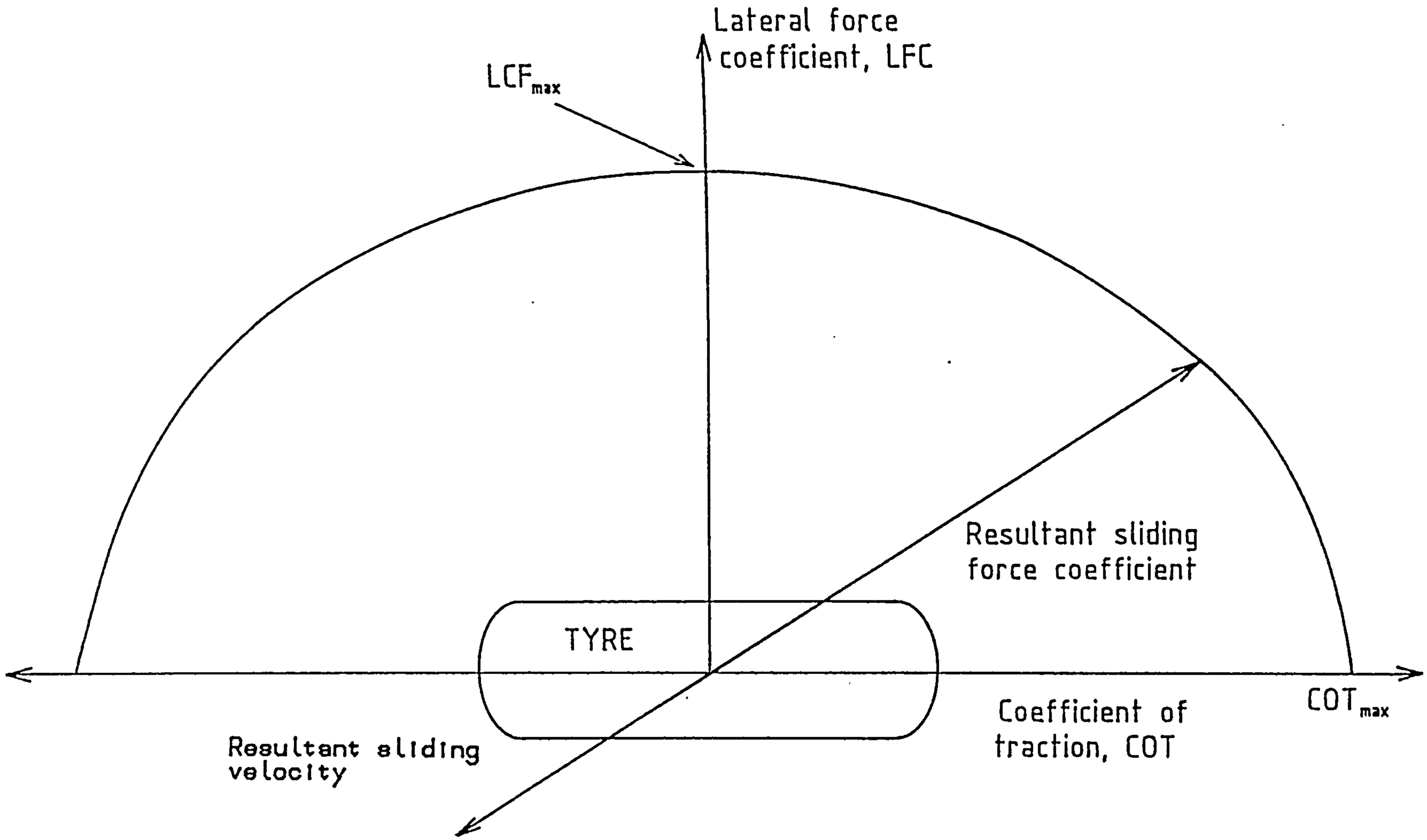

Fig. (2.10) Resultant force acting on a locked, sliding tyre.

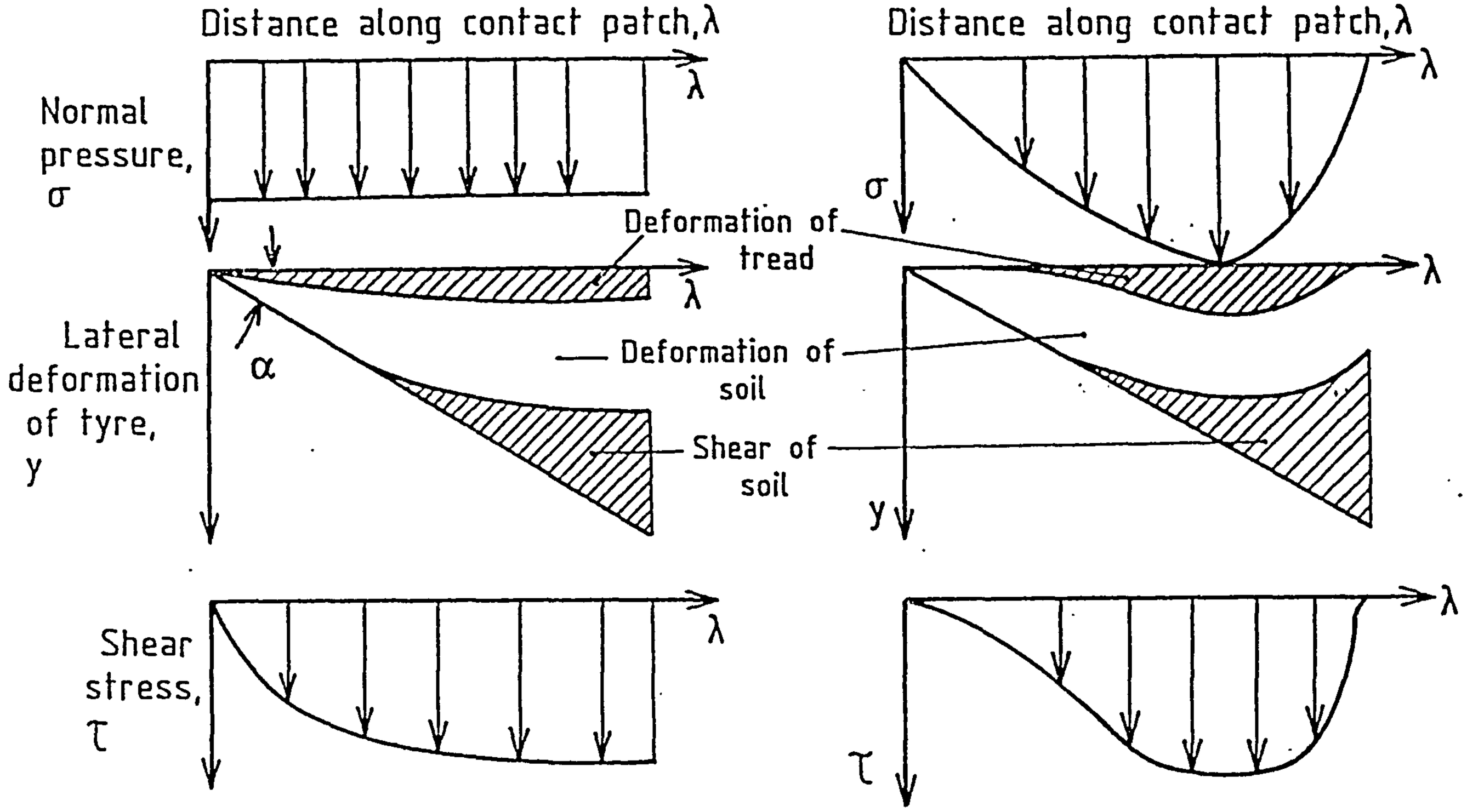

Fig (2.11) Lateral deformatin and soil shear stress in the contact region for two assumed normal pressure distributions by Schwanghart, 1968.

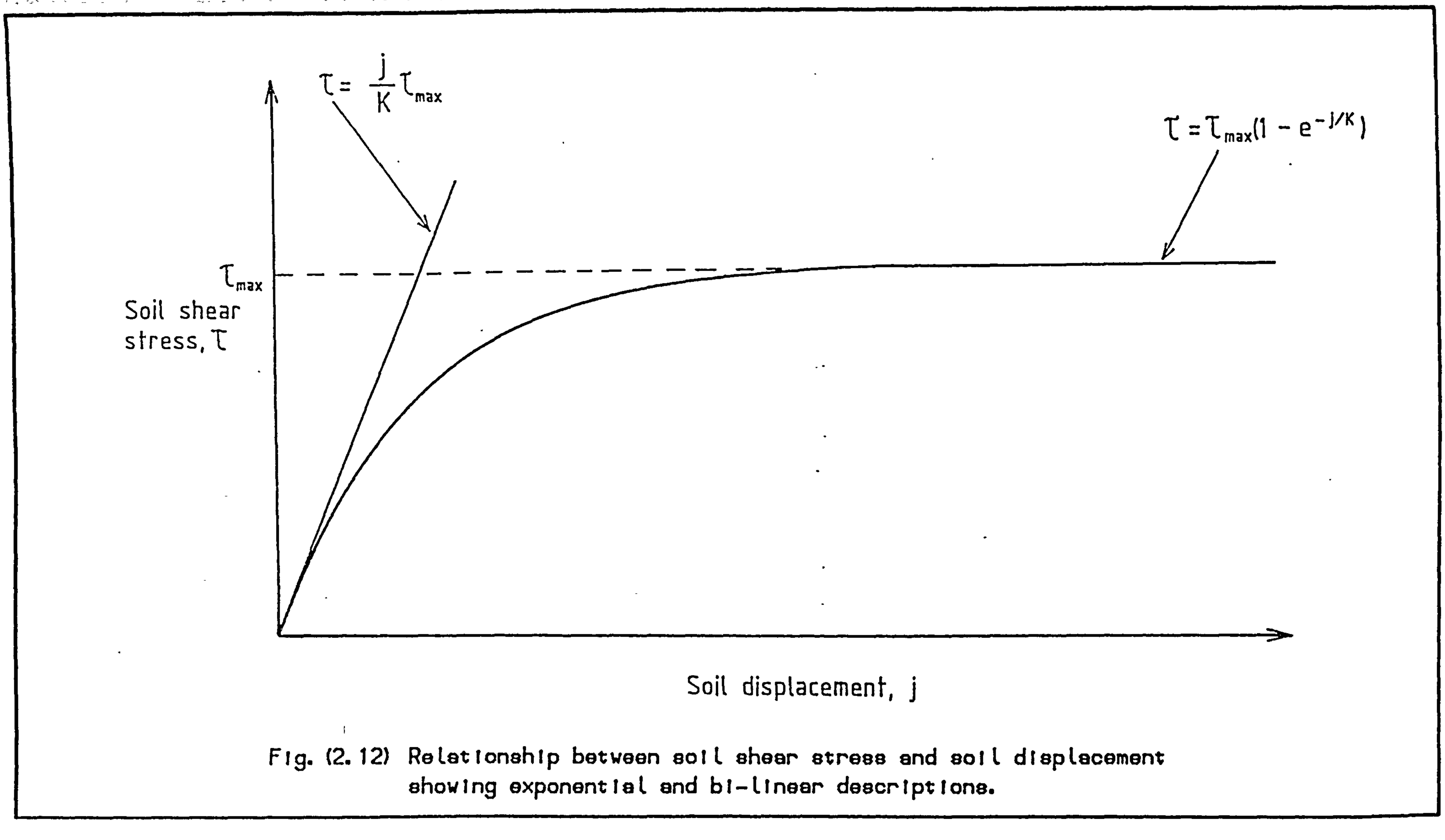

Fig. (2.12) Relationship between soil shear stress and soil displacement showing exponential and bi-linear descriptions.

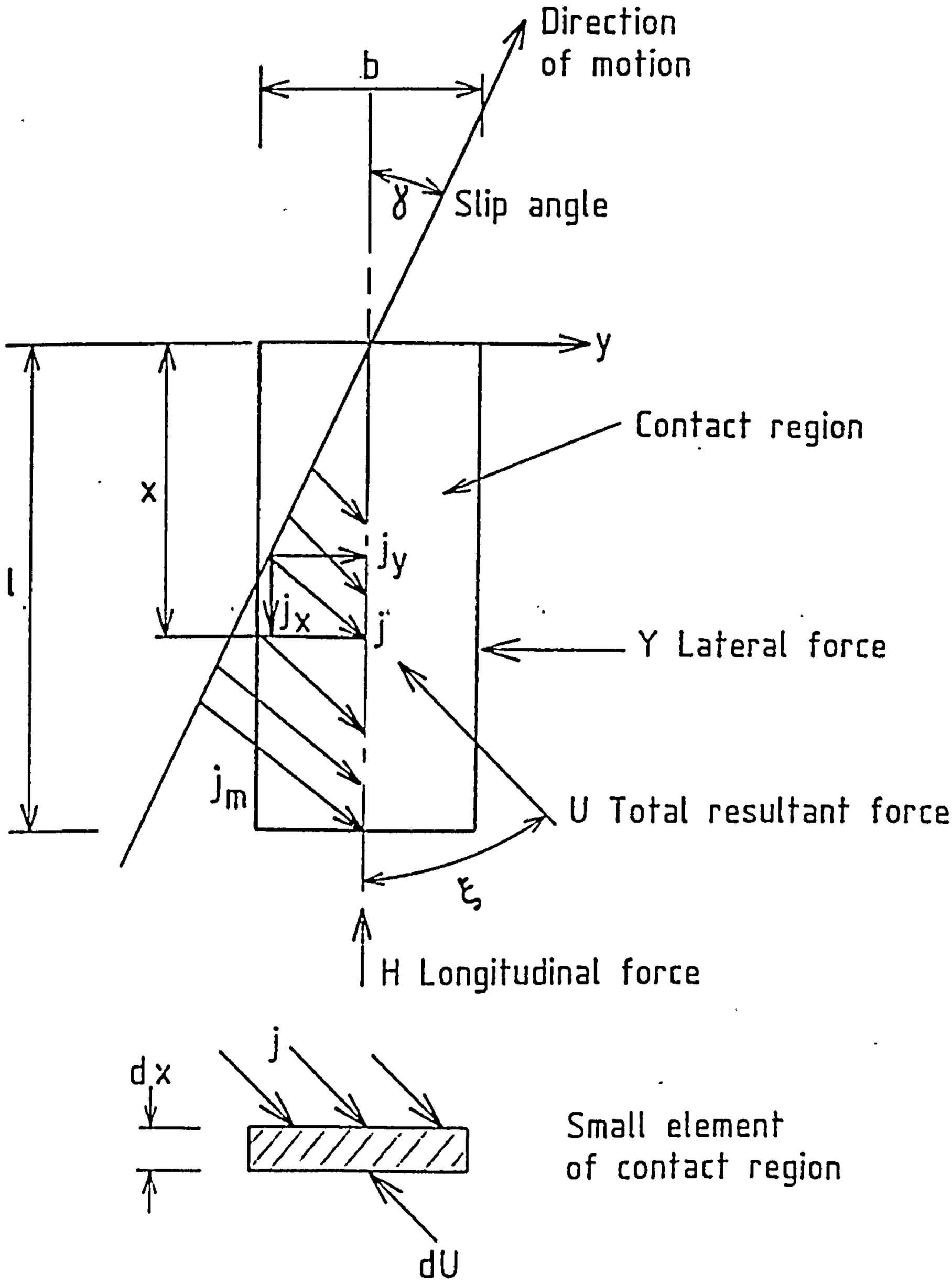

Fig. (2.13) Description of behaviour in the contact region according to Grecenko 1975.

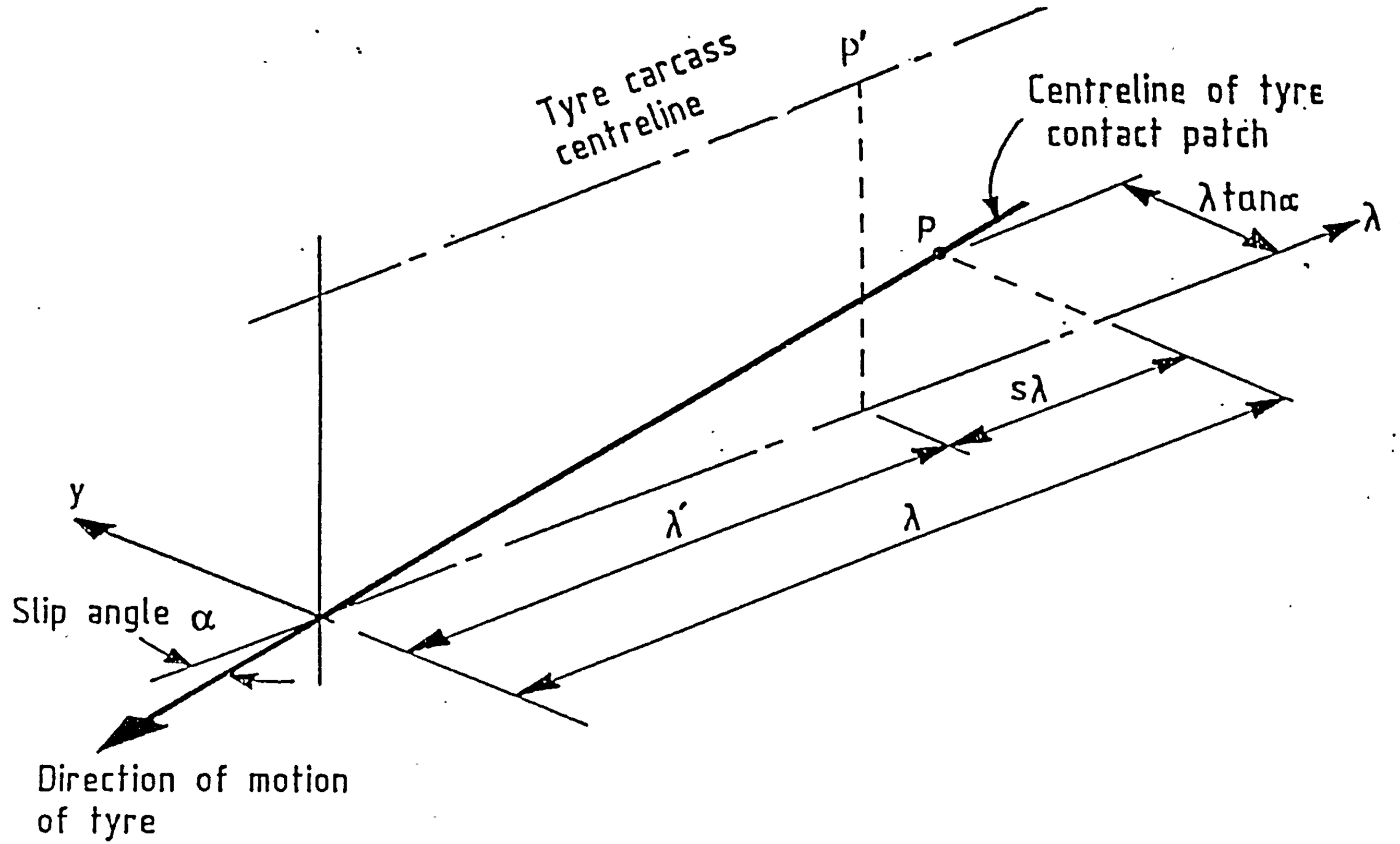

Fig. (2.14) Distortion of the tyre contact patch assumed by Jurkat and Brady, 1981.

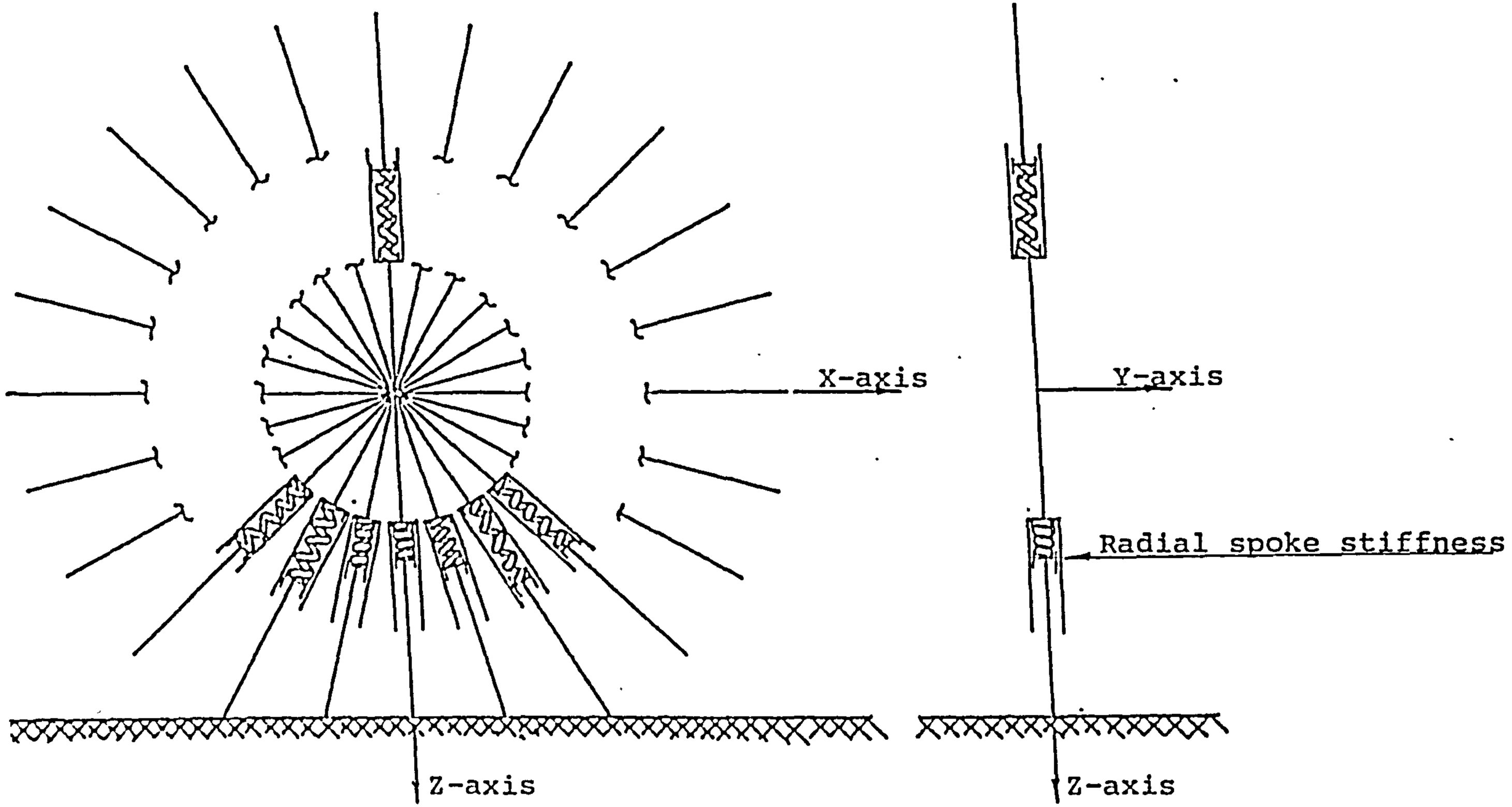

Fig. (2.15) Multi-spoke tyre model as a single plane of radial spokes assumed by Sharp and El-Nashar 1986.

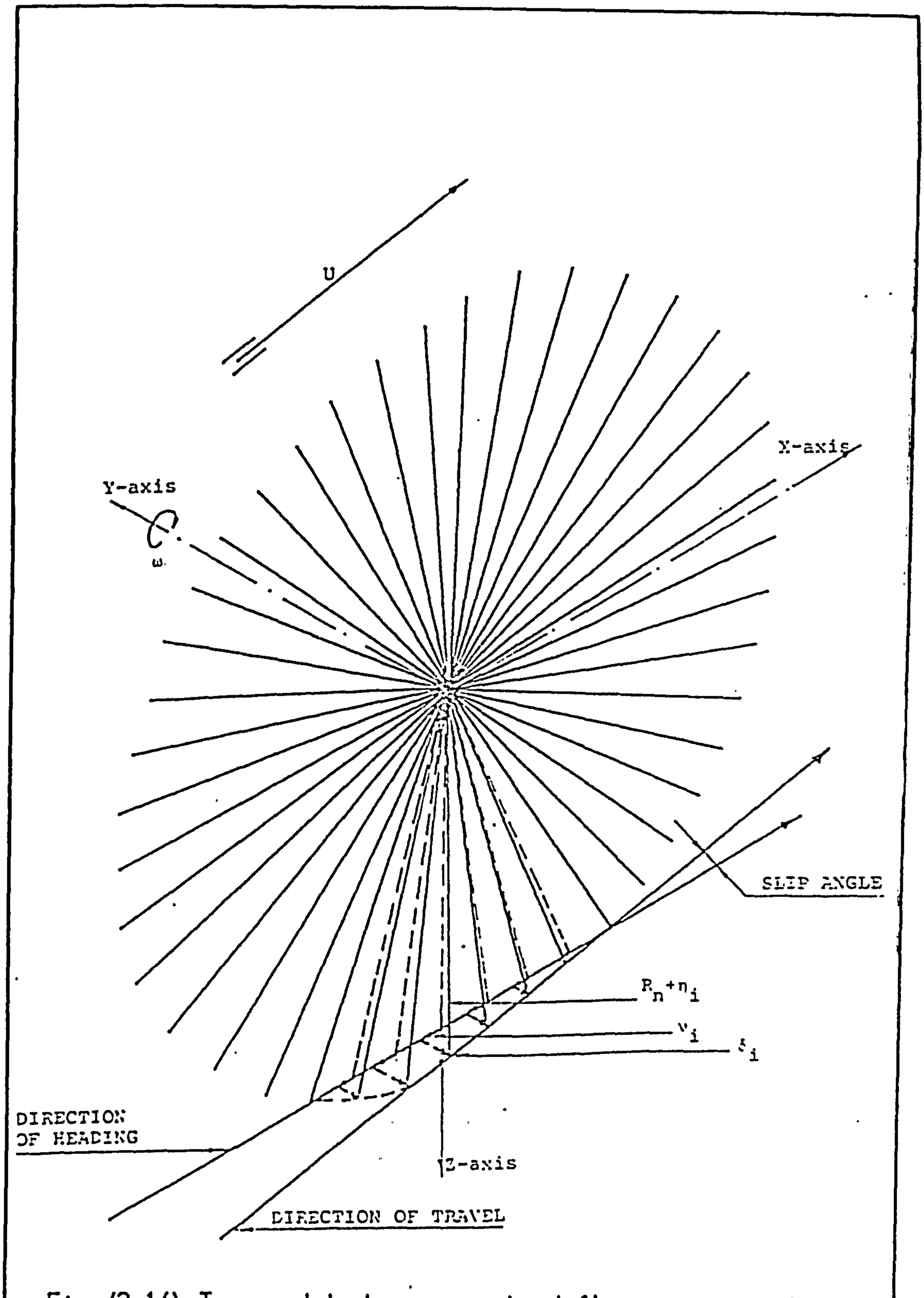

Fig. (2.16) Tyre model showing spoke deflections in radial, circumferential and lateral directions.

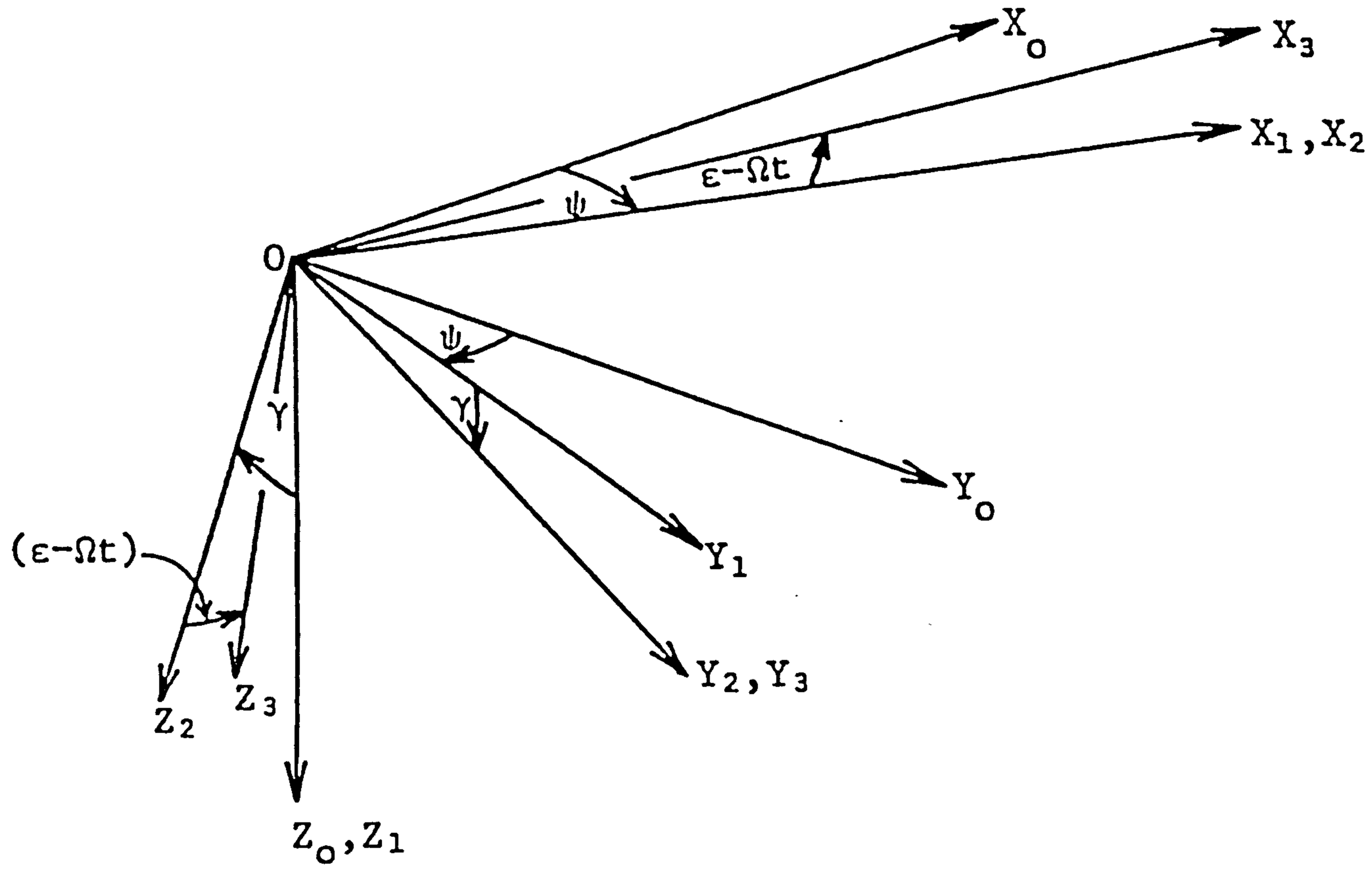

Fig. (2.17) Reference axis systems assumed by Sharp, 1986.

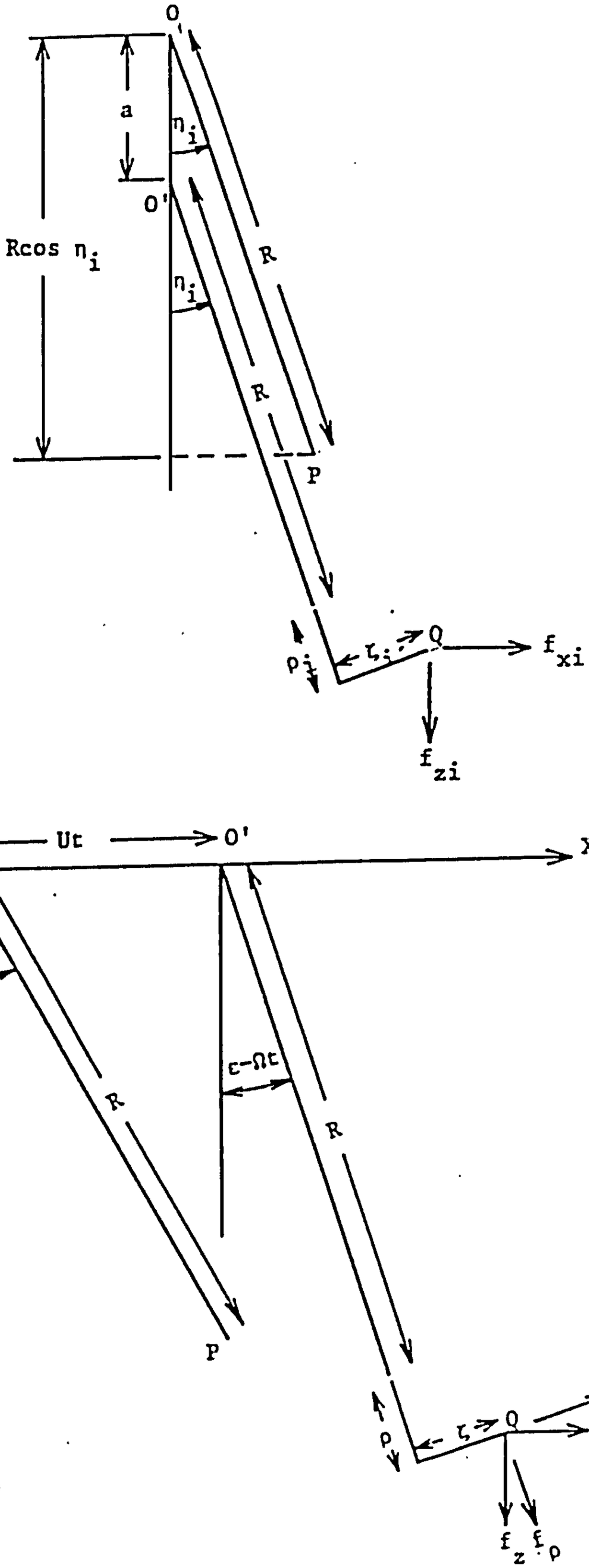

Fig. (2.18) Model geometry for tyre motion at zero camber angle and steady-state operating conditions.

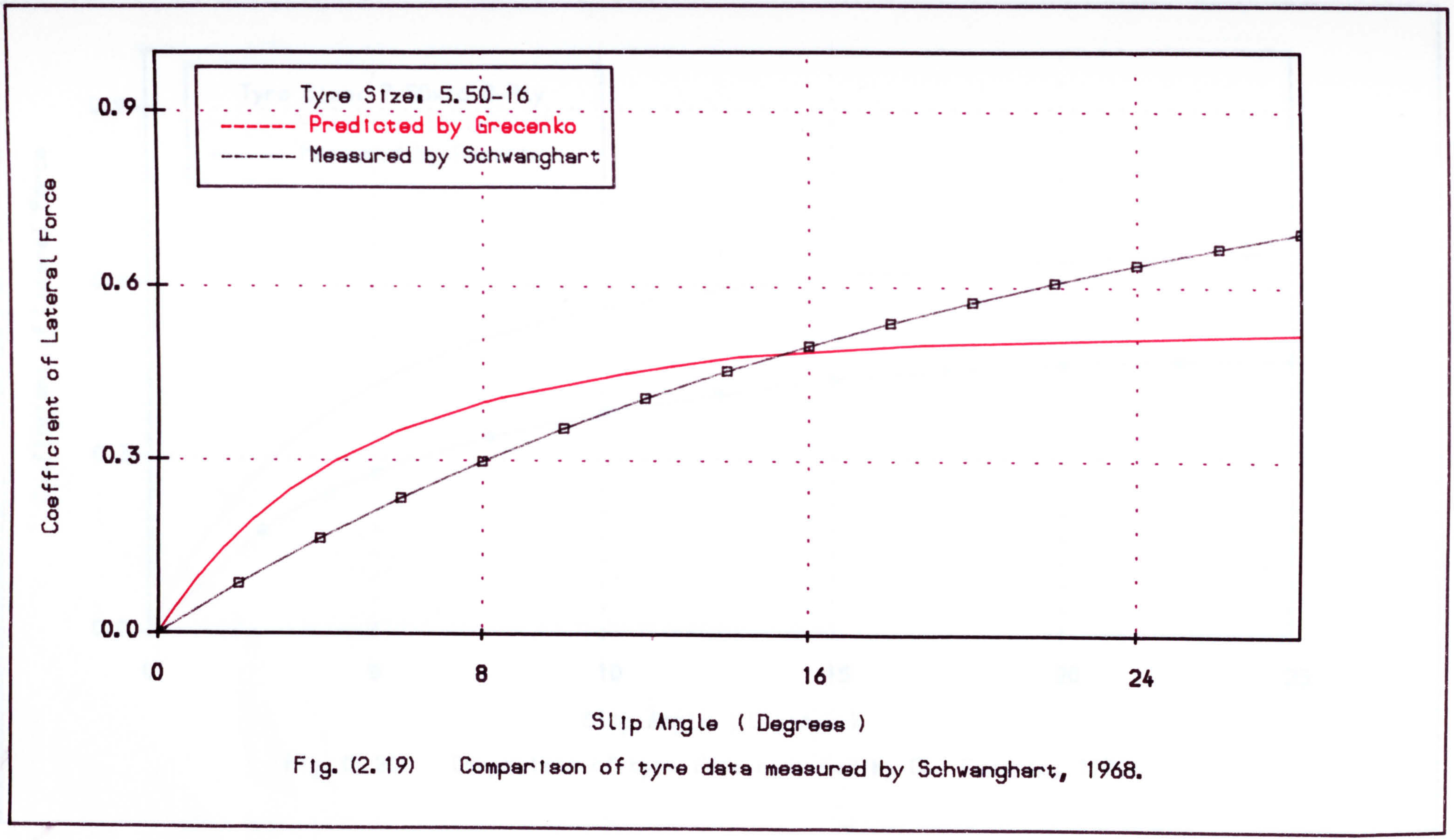

Fig. (2.19) Comparison of tyre data measured by Schwanghart, 1968.

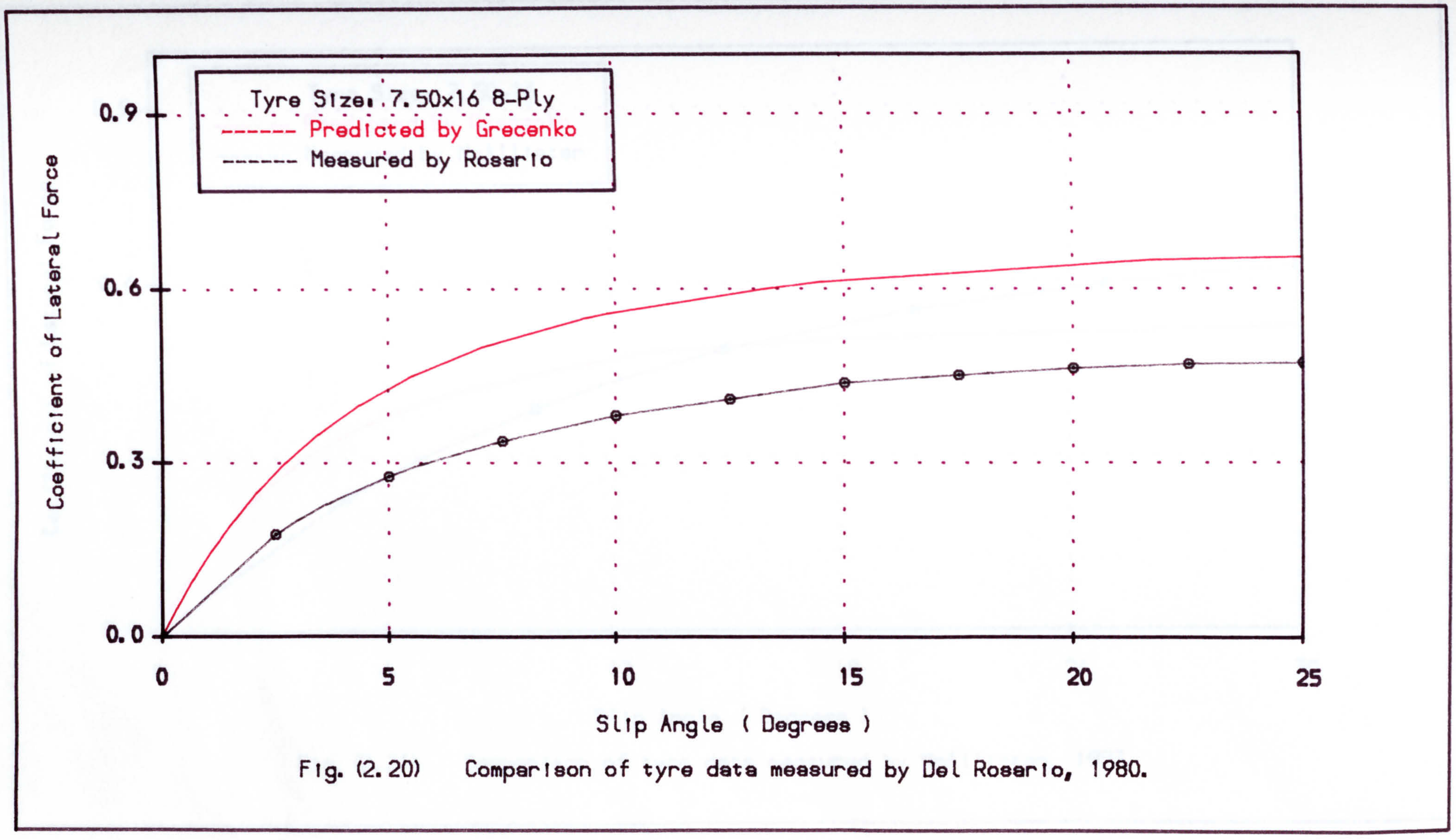

Fig. (2.20) Comparison of tyre data measured by Del Rosario, 1980.

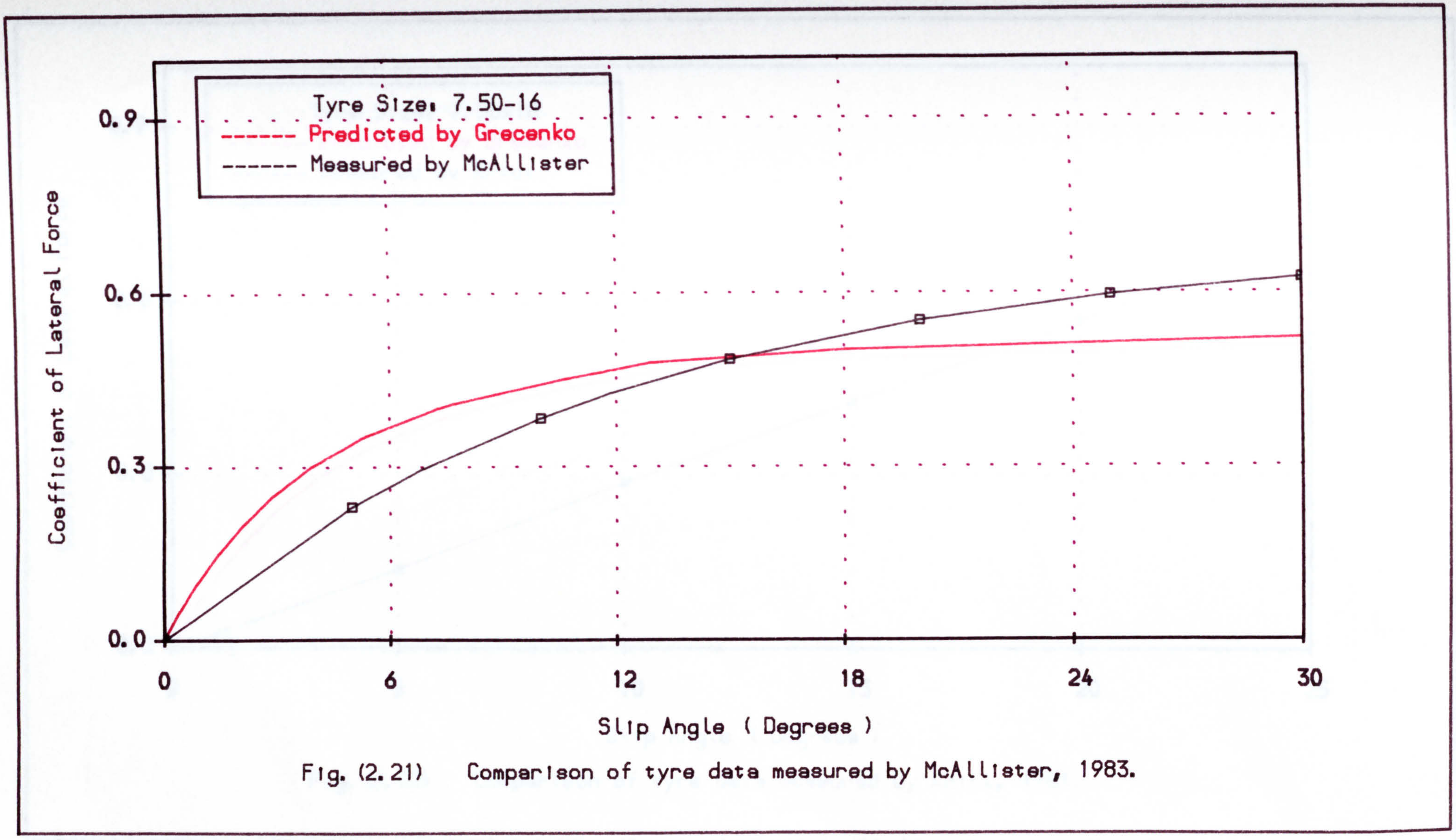

Fig. (2.21) Comparison of tyre data measured by McAllister, 1983.

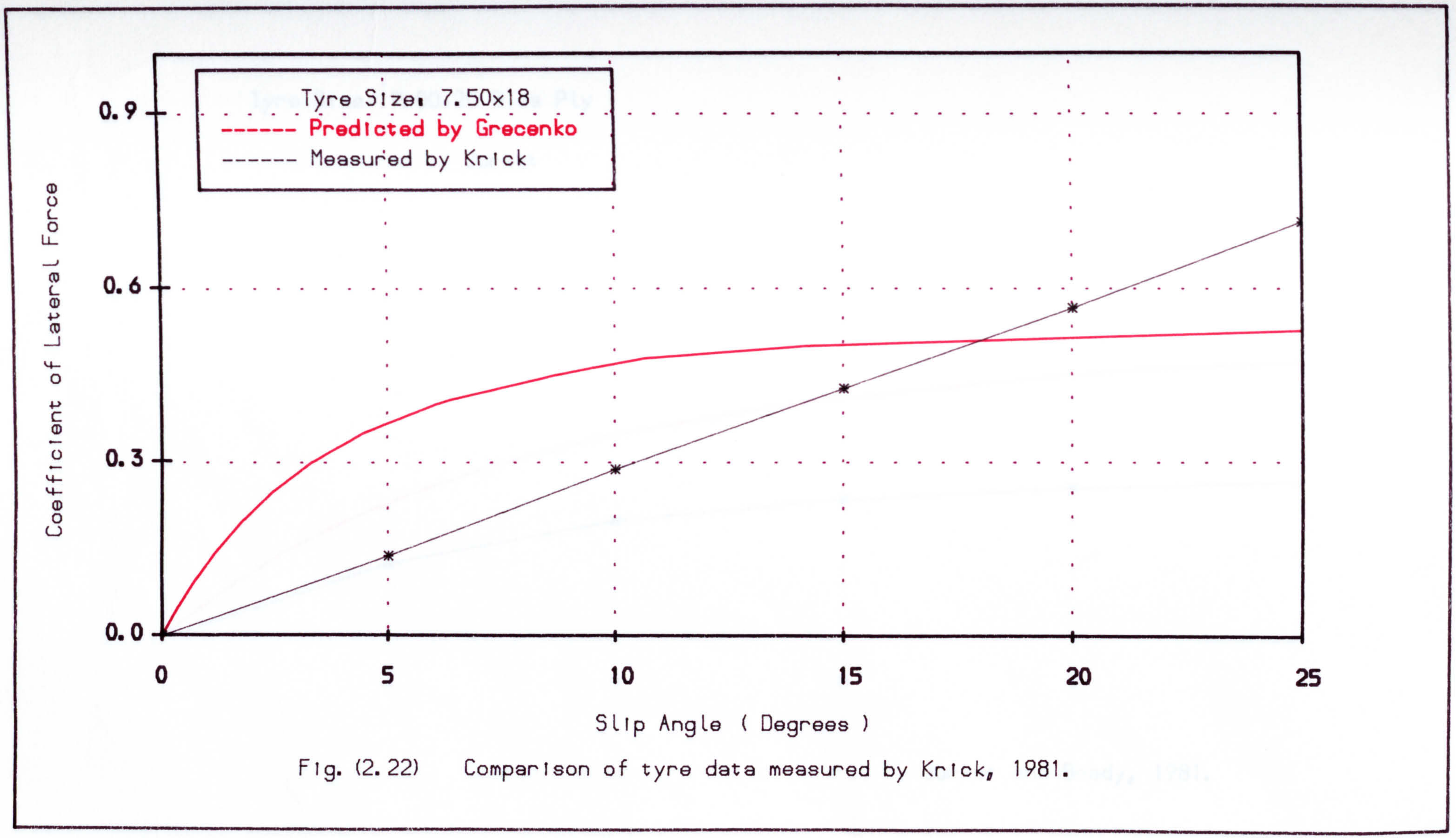

Fig. (2.22) Comparison of tyre data measured by Krick, 1981.

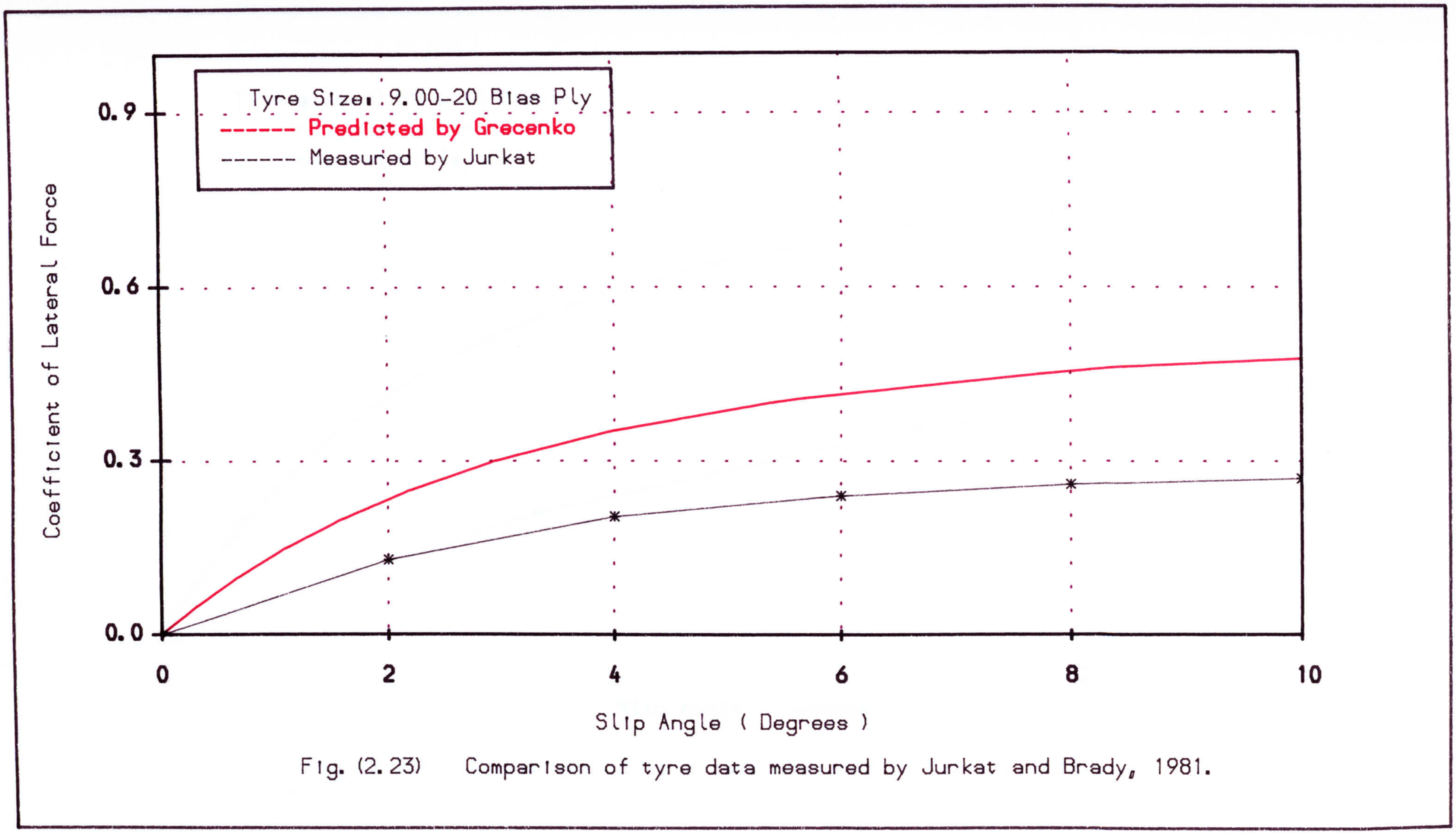

Fig. (2.23) Comparison of tyre data measured by Jurkat and Brady, 1981.

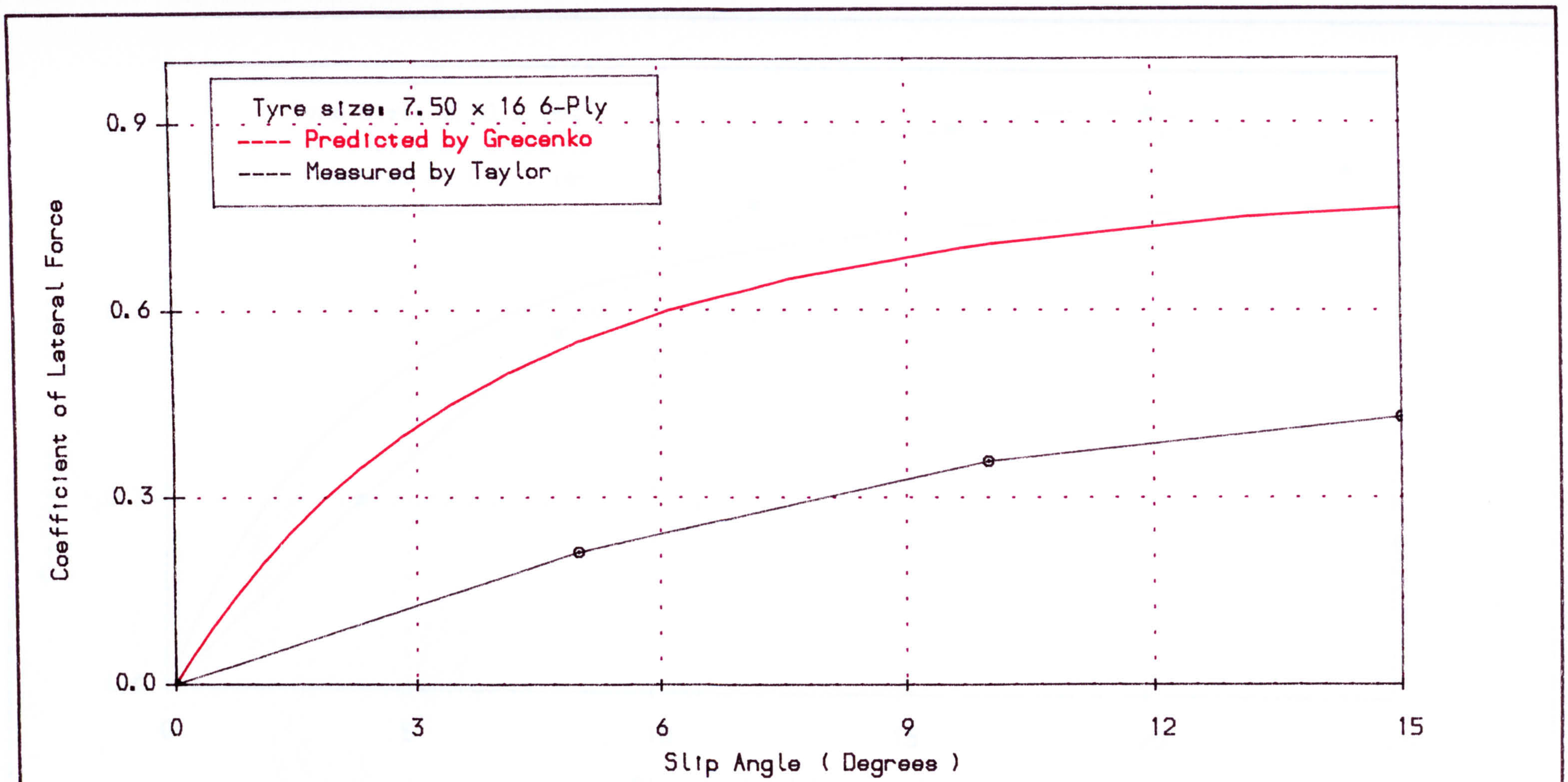

Fig. (2.24) Comparison of tyre data measured by Taylor, 1967.

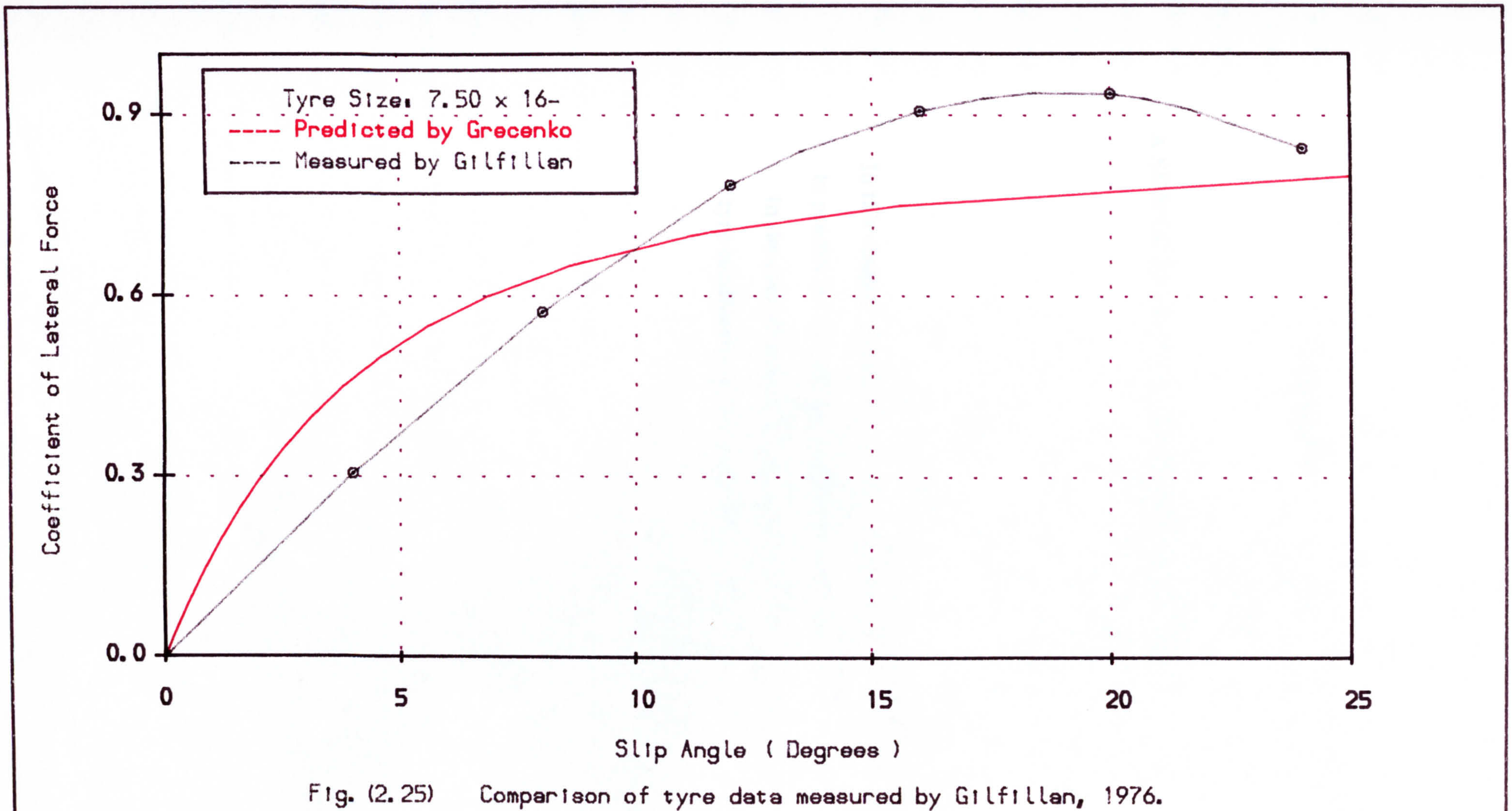

Fig. (2.25) Comparison of tyre data measured by Gilfillan, 1976.

CHAPTER 3

A SIMPLE TYRE FORCE GENERATION MODEL

In this chapter a simple tyre model is presented to predict the vertical and longitudinal forces in the case of stationary and steady state tyre conditions on a deformable surface.

3.1. INTRODUCTION

Using existing work on modelling the behaviour of on-road tyres as a background, a new simple model to represent the tyre forces generated between a tyre and a deformable surface is developed. It is based on a simplified calculation involving the combination of a multi-spoke representation of the tyre and simple soil mechanics equations.

The model predicts the forces in the vertical and longitudinal directions for a stationary and rolling tyre in steady state conditions. Distributions of the forces throughout the contact region are presented and discussed. The effect of tyre stiffness and soil strength parameters are discussed and the model is intended to establish a basis for further off-road tyre model studies.

Most previous studies to describe the behaviour of off-road tyres in generating longitudinal and vertical forces are based on one of the three following points :-

1) The soil is compact and harder than the tyre. In this situation, the deformation of the tyre is completely dominant, and the interface is assumed to be flat. Therefore, the proposed model becomes exactly like those used for road vehicle tyres with differences in parameters to describe the off-road tyre.

2) The tyre is harder than the soil, thus the tyre deformation is smaller and the interface has a convex shape. The proposed model then becomes similar to those used to describe the behaviour of a rigid wheel in soil.

3) The case in between the previous cases, in which there is tyre deformation in the contact region, and at the same time the ground is affected and deformed by the tyre load. This case, which is obviously closest to the practical situation, is the one which has received little attention in the literature.

3.2. STATIC TYRE ON DEFORMABLE SURFACE

Let us consider a tyre, standing on ground either hard or deformable at tyre load, *W*, with zero camber angle, γ, as shown in Fig.(3.1). The shape of the contact surface depends on the tyre deflection. In general, the shape of the surface is slightly shorter and wider than would follow from an imaginary, intersecting plane between the tyre in its unloaded shape and the supporting surface. The shape of the contact region depends on the particular tyre type and the inflation pressure. However, Fig.(3.1a) shows the cross section of the impression that is obtained when a non-rotating (static) tyre is lowered vertically onto hard ground. An entirely different impression is found when the tyre inflation pressure is increased to the maximum range (as a rigid wheel), and lowered vertically onto a soft surface as shown in Fig.(3.1b).

If the tyre has a low inflation pressure and is standing on a soft surface, it will deflect and sink to a certain extent. The process in the contact region incorporates aspects of the tyre on a hard ground as well as aspects of a rigid wheel (or tyre at high inflation pressure) with sinkage. Fig.(3.1c) shows the tyre standing at tyre load, *W*, on a deformable soil.

It is interesting to note that the most the soils are deformed when subjected to load. This deformation is elastic when the soil regains its original shape upon removal of the load. Plastic deformations occur for stresses exceeding the elastic limit of the soil, and elasto-plastic deformations occur in soils which have no clearly defined elastic limit (or properties). In general, when the load is removed from the soils, very little deformation is recovered by elastic rebound, as illustrated in Fig.(3.2). This is because the principal soil deformations are state changes caused by relative particle motion. Only a very small amount of the soil deformation occurs from particle distortion and is elastically recoverable.

To sum up, when the soil shear stress becomes equal to the soil shear strength, and the normal load is released, which is indicated by "A", then if is there no elastic recovery for this soil, the soil shear stress decreases to zero value at "B'", but if the soil

has an elastic recovery behaviour then the soil shear stress will decrease to zero value at "B".

3.2.1. LOAD-DEFLECTION BEHAVIOUR

To describe the behaviour of off-road tyres and the forces acting on them, it is necessary to define an axis system that serves as a reference for the definitions of various parameters. The axis systems used in this tyre model are shown in Fig.(3.3). The origin of the axis system is the centre of the line of tyre contact with the ground. The X axis is the intersection of the wheel plane and the ground plane with a positive direction forward. The Z axis is perpendicular to the ground plane with a positive direction downward. The Y axis is in the ground plane, its direction being chosen to make the axis system orthogonal.

There are three main forces acting on the tyre from the ground, longitudinal force, f_x, which is the component in the X direction of the resultant force acting on the tyre, lateral force, f_y, which is the component in the Y direction and normal force, f_z, which is the component in the Z direction of the resultant force acting on the tyre from the load. With this axis system many performance parameters of the tyre can conveniently be defined.

3.2.2. EQUILIBRIUM FORCE EQUATIONS

When the tyre load applied to the deformable surface exceeds a certain limit, the stress level within a certain boundary of the surface may reach a point which is denoted by K on the idealised stress-strain relationship shown in Fig.(3.4). An infinitely small increase of stress beyond point K produces a rapid increase of strain, which constitutes plastic flow. The state that precedes plastic flow is usually referred to as plastic equilibrium.

There are a number of criteria proposed for the failure of soils under tyre load and of other similar materials. One of the widely used and simplest criteria is that due to

Mohr-Coulomb. It postulates that the shear stress in the material is related to displacement according to the following condition :-

$$\tau_s = (c + P_g \tan\phi)(1 - e^{-j/K}) \tag{3.1}$$

where

τ_s = Soil shear stress

P_g = Normal ground pressure

c = Soil cohesion

ϕ = Soil internal angle of friction

j = Soil shear displacement

K = Soil deformation modulus

The basis of the Bekker theory [1969] is a relationship between the ground pressure, P_g, and soil sinkage, Z, as follows :-

$$P_g = (\frac{K_c}{b} + K_\phi)\ Z^n \tag{3.2}$$

where

K_c = Cohesive soil moduli

K_ϕ = Frictional soil moduli

b = Width of tyre contact patch

n = Exponent of soil deformation

in which K_c, K_ϕ and n are empirically measured, soil describing constants.

The use of basic equations (3.1) and (3.2) can perhaps best be appreciated by considering the case of a static tyre on deformable surfaces. At the interface between the tyre and the off-road surface an element of tyre surface area is acted upon by forces which can be expressed as two components, one perpendicular to the contact region, called the normal force, f_g, and other tangential to the contact region, called shear force, f_s. This is shown in Fig.(3.5). The idea behind the modelling is that at any point

point of the interaction between the tyre and ground, the shear and normal forces must equal the bending and radial forces generated by the tyre. Accordingly the tyre and soil forces are :-

$$f_s = (c + P_g \tan\phi)(1 - e^{-j/K}) A_c \tag{3.3}$$

$$f_g = (\frac{K_c}{b} + K_\phi) Z^n A_c \tag{3.4}$$

$$f_b = \eta_x K_x \tag{3.5}$$

$$f_r = DR\, K_r \tag{3.6}$$

where

A_c = Horizontal contact area

η_x = Circumferential deflection

K_x = Circumferential tyre stiffness

DR = Radial tyre deflection

K_r = Radial tyre stiffness

The equilibrium force equations can be written as following :-

$$f_s = f_b \tag{3.7}$$

$$f_g = f_r \tag{3.8}$$

Substitution of equations (3.3) to (3.6) into equations (3.7) and (3.8) give :

$$(c + P_g \tan\phi)(1 - e^{-j/K}) A_c = \eta_x K_x \tag{3.9}$$

$$(\frac{K_c}{b} + K_\phi) Z^n A_c = DR\, K_r \tag{3.10}$$

and from the tyre geometry as shown in Fig.(3.5), the relation between the tyre deflections and the soil sinkage at any point through the contact region is :-

$$R\, Cos\theta_1 + Z + \eta_x\, Sin\theta = (R - DR)\, Cos\theta \tag{3.11}$$

where

R = Undeflected tyre radius

$d\theta$ = Spoke angle position

θ_1 = Entry angle

$\theta = \theta_1 - d\theta$ and

$j = \eta_x$

The simplified model contains two main assumptions :

1) The area of contact region between the tyre and the surface is assumed to be rectangular, i.e. ($area = b\ l$) and divided into infinitely thin strips.

where l is length of the tyre contact patch.

2) The tyre load/deflection relationship is assumed to be a linear function.

Equilibrium force equations (3.9), (3.10) and (3.11) can be solved for DR, η_x and Z.

The vertical and horizontal tyre force components would be :-

$$f_z = DR\ K_r\ Cos\theta + \eta_x\ K_x\ Sin\theta \tag{3.12}$$

$$f_x = DR\ K_r\ Sin\theta + \eta_x\ K_x\ Cos\theta \tag{3.13}$$

The summation of vertical tyre force components is :-

$$F_z = \sum_{\theta=\theta_1}^{\theta=-\theta_1} f_z \tag{3.14}$$

$$F_z = \sum_{\theta=\theta_1}^{\theta=-\theta_1} (DR\ K_r \cos\theta + \eta_x\ K_x \sin\theta) \tag{3.15}$$

The total vertical force, F_z, must be equal to the tyre load, W. If not, then there is a subroutine called "Angle" to recalculate the correct value of θ_1 for which $F_z \approx W$. Fig.(3.6) shows the load distribution of a 7.50 x 18 front tractor tyre along the length of the contact region. The longitudinal shear force distribution is shown in Fig.(3.7).

3.2.3. EFFECT OF RADIAL TYRE STIFFNESS

Fig.(3.8) shows the influence of the radial tyre stiffness on the radial tyre deflection and the soil sinkage for a static tyre on deformable soil. Vertical and horizontal components of tyre force generation are affected by different values of radial tyre stiffness as shown in Fig.(3.9).

3.2.4. EFFECT OF TYPE OF SOILS

Simple tyre model results are affected significantly by three type of soils, clay soil, loose soil and sandy loam soil. Fig.(3.10) illustrates the radial tyre deflection and soil sinkage distributions along the length of the contact region. Vertical and horizontal force distributions are shown in Fig.(3.11).

3.3. ROLLING TYRE ON DEFORMABLE SURFACE

With constant forward speed, U, and constant spin velocity, ω, there will be combined tyre deflection and soil deformation. The deformations of the tyre and the soil are dependent on several important parameters, such as tyre stiffnesses, tyre inflation pressure, soil type and soil strength.

Fig.(3.12) shows how the tyre moves in steady state conditions on hard ground (a), rigid wheel on soft surface (b) and tyre on deformable surface (c). The entry angle, θ_1, in case (c) is greater than that in case (a), but less than that in case (b). However, the soil sinkage, Z, increases with increasing tyre inflation pressure until a maximum value, which is the same as the case of the rigid wheel, is reached.

According to Fig.(3.12), the interface between the tyre and a deformable surface is assumed to be split into two main regions as follows :-

1) Deformable region, that is the region at the front of the tyre contact patch, where all the soil deformation occurs.

2) Compacted region, that is the region at the rear of the tyre contact patch, the tyre forces are decreased and the soil reaches a maximum sinkage.

3.3.1. TYRE AND SOIL FORCES

As mentioned earlier in equations (3.3) and (3.4), the forces acting on the tyre from the ground are f_s and f_g. These forces must be equal to those forces generated by the tyre deformations. In order to describe the behaviour of the rolling tyre on deformable surfaces, the equilibrium force equations are :-

Deformable region

$$\left(\frac{K_c}{b} + K_\phi\right) Z^n A_c = DR\, K_r \tag{3.16}$$

$$(c + P_g \tan\phi)\,(1 - e^{-j/K})\, A_c = \eta_x K_x \tag{3.17}$$

$$R\, Cos\theta_1 + Z + \eta_x\, Sin\theta = (R - DR)\, Cos\theta \tag{3.18}$$

$$R\, Sin\theta_1 = U\, dt + (R - DR)\, Sin\theta + \eta_x\, Cos\theta \tag{3.19}$$

where

dt = time increment = $\dfrac{d\theta}{\omega}$

and $d\theta = 1^o$.

Equations (3.16) to (3.19) can be solved for DR, η_x, j and Z. Then the vertical and longitudinal tyre force components can be resolved :-

$$f_z = DR\, K_r\, Cos\theta + \eta_x K_x\, Sin\theta \tag{3.20}$$

$$f_x = DR\, K_r\, Sin\theta\, B + \eta_x K_x\, Cos\theta \tag{3.21}$$

Compacted region

To determine the tyre and soil force components in the second half of the tyre, the approximate relation between the entry angle, θ_1, and the rear angle, θ_2, is as follows :-

$$\theta_2 = \cos^{-1}\left(\cos\theta_1 + \frac{Z_{max}}{R}\right) \tag{3.22}$$

where Z_{max} is maximum soil sinkage.

The equilibrium force equations in this region are :

$$R\,Cos\theta_2 = (R-DR)\,Cos\theta + \eta_x\,Sin\theta \tag{3.23}$$

$$R\,Sin\theta_2 = U\,dt + (R-DR)\,Sin\theta - \eta_x\,Cos\theta \tag{3.24}$$

The solution of equations (3.23) and (3.24) in DR and η_x are used to calculate the tyre force components in vertical and longitudinal directions as follows :-

$$f_z = DR\,K_r\,Cos\theta + \eta_x\,K_x\,Sin\theta \tag{3.25}$$

$$f_x = DR\,K_r\,Sin\theta - \eta_x\,K_x\,Cos\theta \tag{3.26}$$

The total vertical tyre force through the length of contact region is :-

$$F_z = \sum_{\theta=\theta_1}^{\theta=-\theta_2} f_z \tag{3.27}$$

$$F_z = \sum_{\theta=\theta_1}^{\theta=-\theta_2} (DR\,K_r\,Cos\theta + \eta_x\,K_x\,Sin\theta) \tag{3.28}$$

Fig.(3.13) shows the behaviour of soil sinkage and the radial tyre deflection through the length of the contact region for rolling steady state tyre on sandy loam soil. Both soil sinkage and radial deflection reach a maximum value at the centre of the tyre. In the second half of the contact length, the soil sinkage stays. The radial deflection behaviour is similar to the soil sinkage up to the centreline of the tyre. After that point the soil sinkage remains constant because force decreases and soil behaviour is clearly not elastic recovery.

The longitudinal and vertical force distributions along the contact region of a rolling tyre moving under steady-state conditions on sandy loam soil are shown in Fig.(3.14). The longitudinal force distribution takes form which has a small part at the rear of the figure. Rolling resistance can be found by a summation of the longitudinal force over the length of the contact region. Pressure distribution along the contact region is presented also in Fig.(3.14). The centre of pressure remains in front of the tyre which is ahead of the centre of the contact region.

3.3.2. INFLUENCE OF TYRE STIFFNESS

For the steady state tyre, Fig.(3.15) illustrates the influence of the radial tyre stiffness on the radial tyre deflection and soil sinkage. With increasing tyre stiffness, tyre deflection is decreased, while the soil sinkage increases. The distributions of tyre force are indicated in Fig.(3.16) for various tyre stiffnesses. The soil parameters remain constant, an increase in tyre stiffness parameters results in less radial tyre deflection and a reduction, therefore, in the length of the contact region.

3.3.3. EFFECT OF SOIL STRENGTH

Fig.(3.17) and Fig.(3.18) show the influence of the soil strength on the tyre deflection, soil sinkage and force distributions for vertical and horizontal directions. The dominant feature is that since the tyre load is maintained constant, an increase in soil strength results in less sinkage and a reduction, therefore, in the length of the contact region and an increase in ground pressure.

3.4. CONCLUDING REMARKS

(1) A simple tyre model for vertical and longitudinal force generation of an off-road surfaces in the case of stationary and rolling tyre in steady state conditions has been presented.

(2) In predicting the longitudinal and vertical force distributions within an off-road tyre, the model forms a basis for an extension of the analysis to include lateral force behaviour.

(3) The presented results cover the static and steady state cases for a wide range off-road surfaces.

(4) A comparison between the vertical tyre load/deflection relationships and those obtained experimentally by Plackett [1983] for a 7.50 x 16 front tractor tyre under hard surface conditions is shown significantly in agreement in qualitative terms with the trends of the relationship. The quantitative agreement occurs at 4.15 kN/m radial tyre stiffness as depicted in Fig.(3.19).

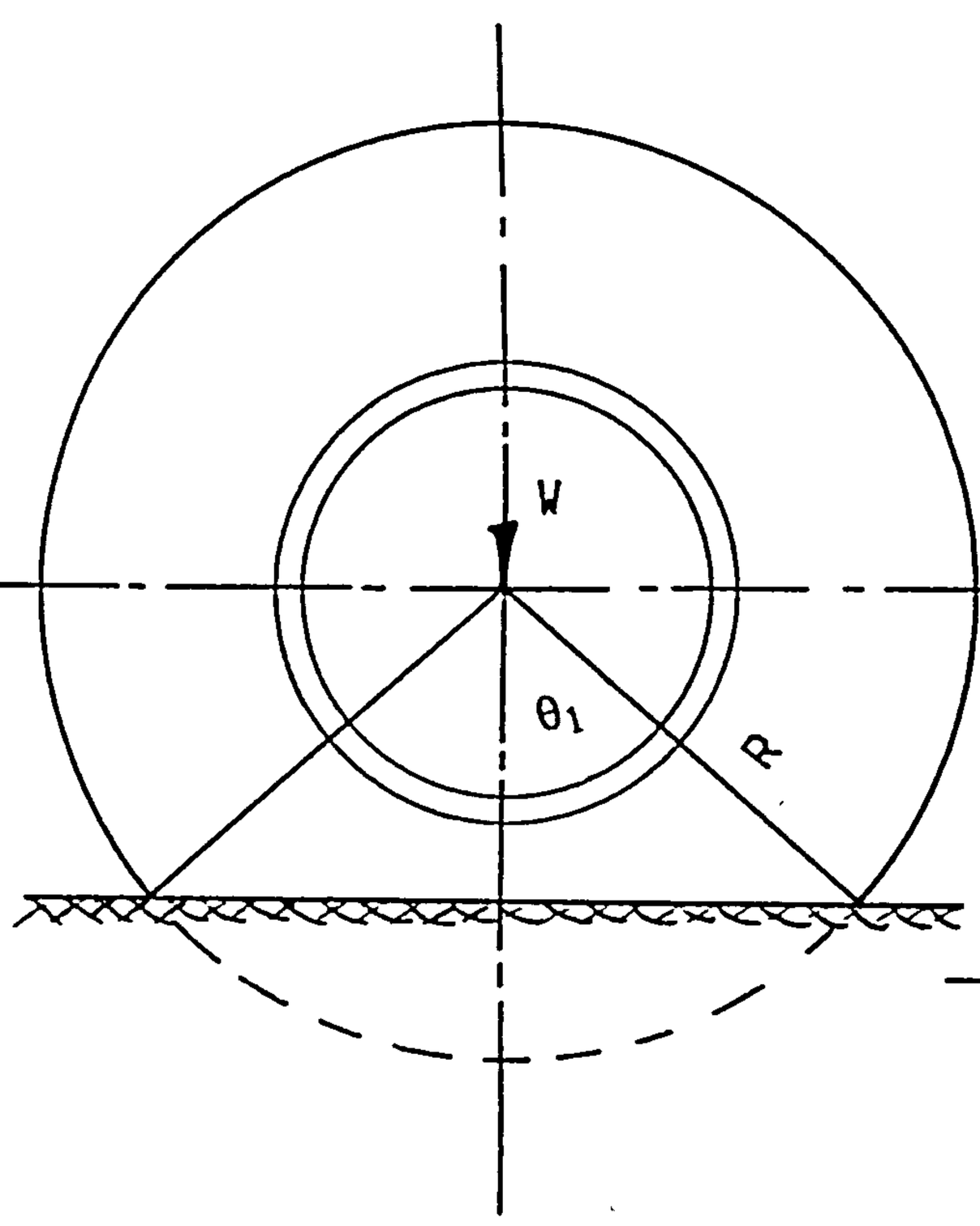

(a)

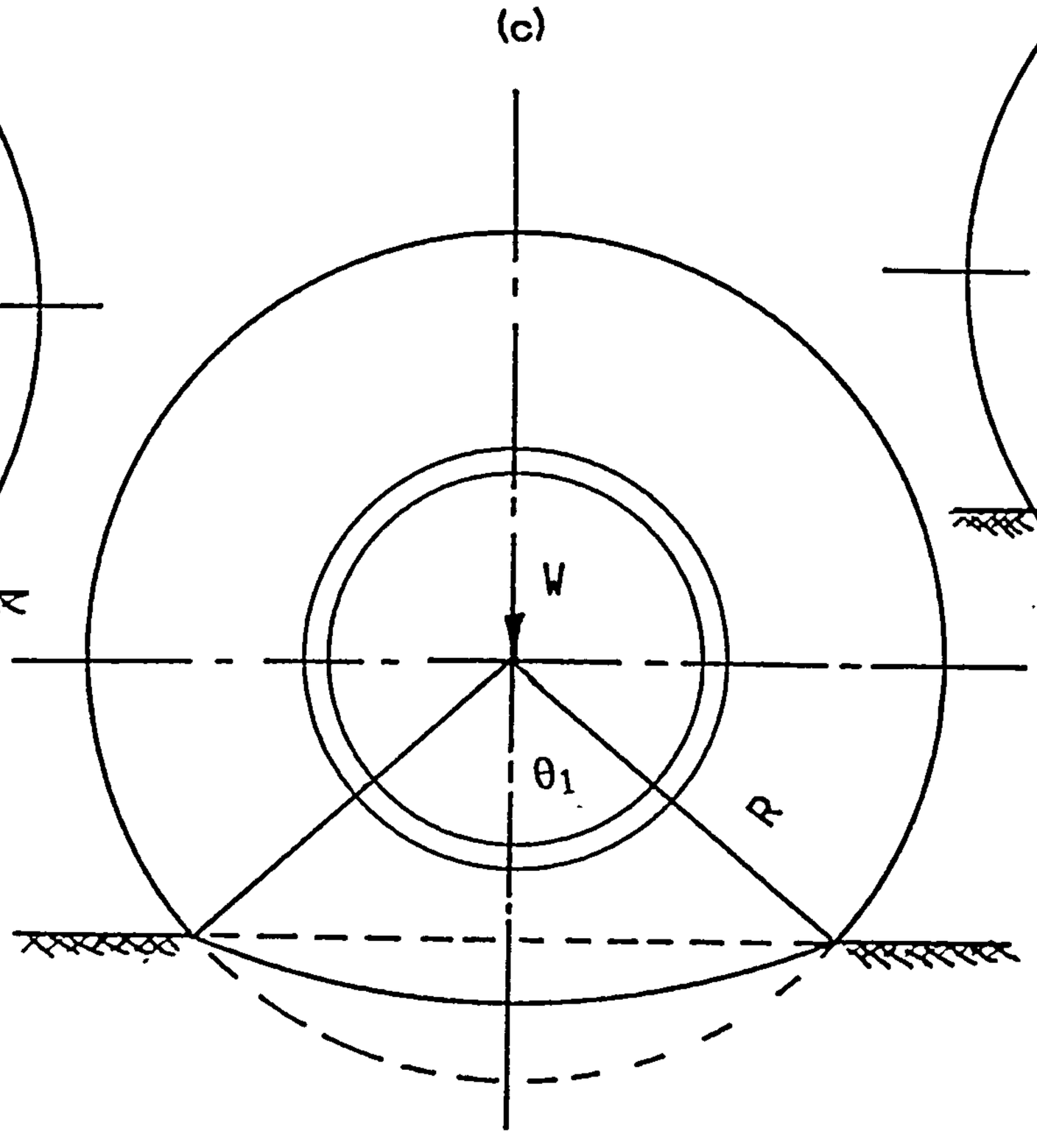

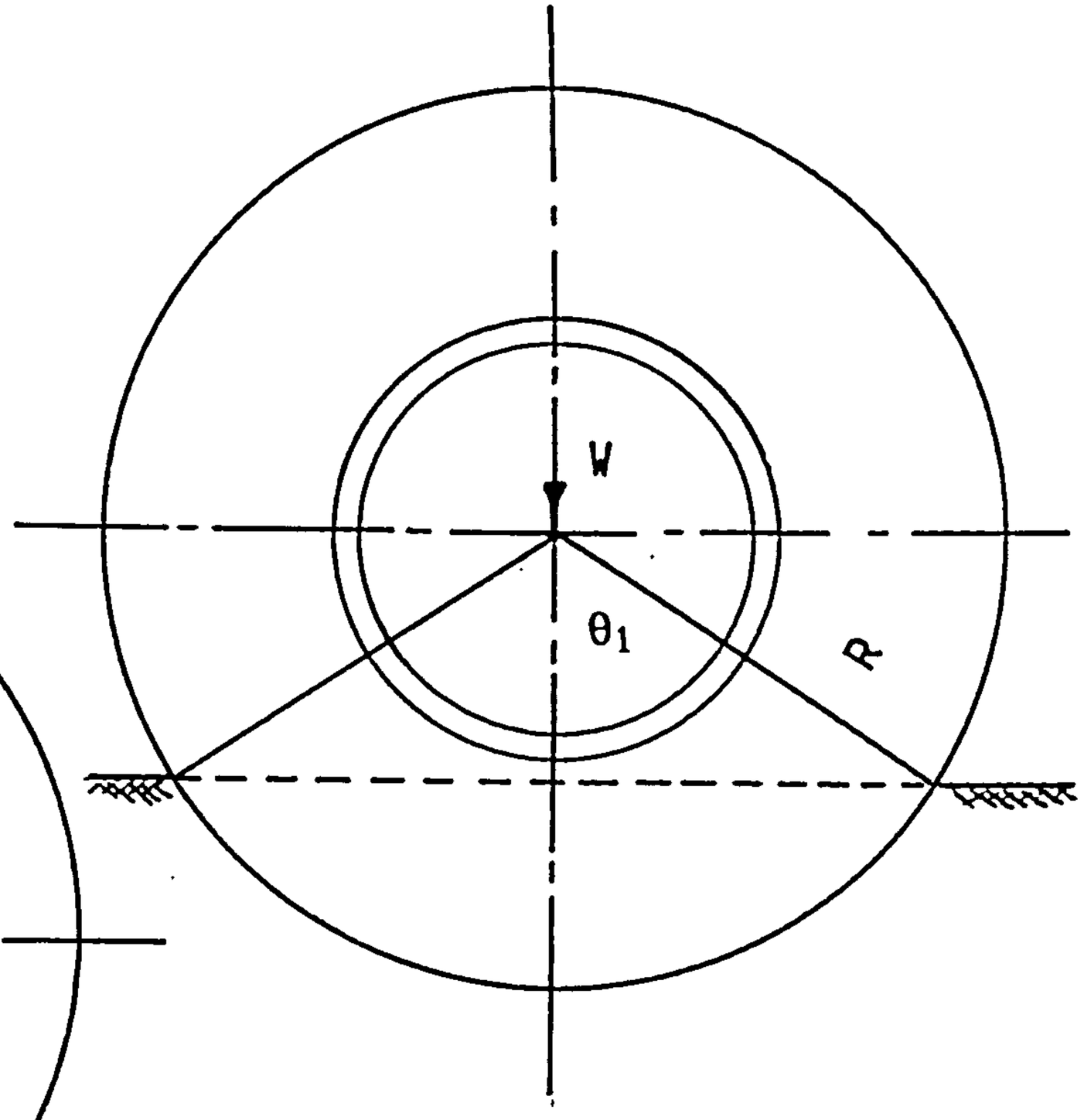

(b)

Fig. (3.1) The contact patch of interaction between the tyre on hard surface (a), rigid wheel on soft soil (b) and tyre on deformable surface (c).

Fig. (3.2) The elasto-plastic behaviour for a soil under application and release of the tyre load.

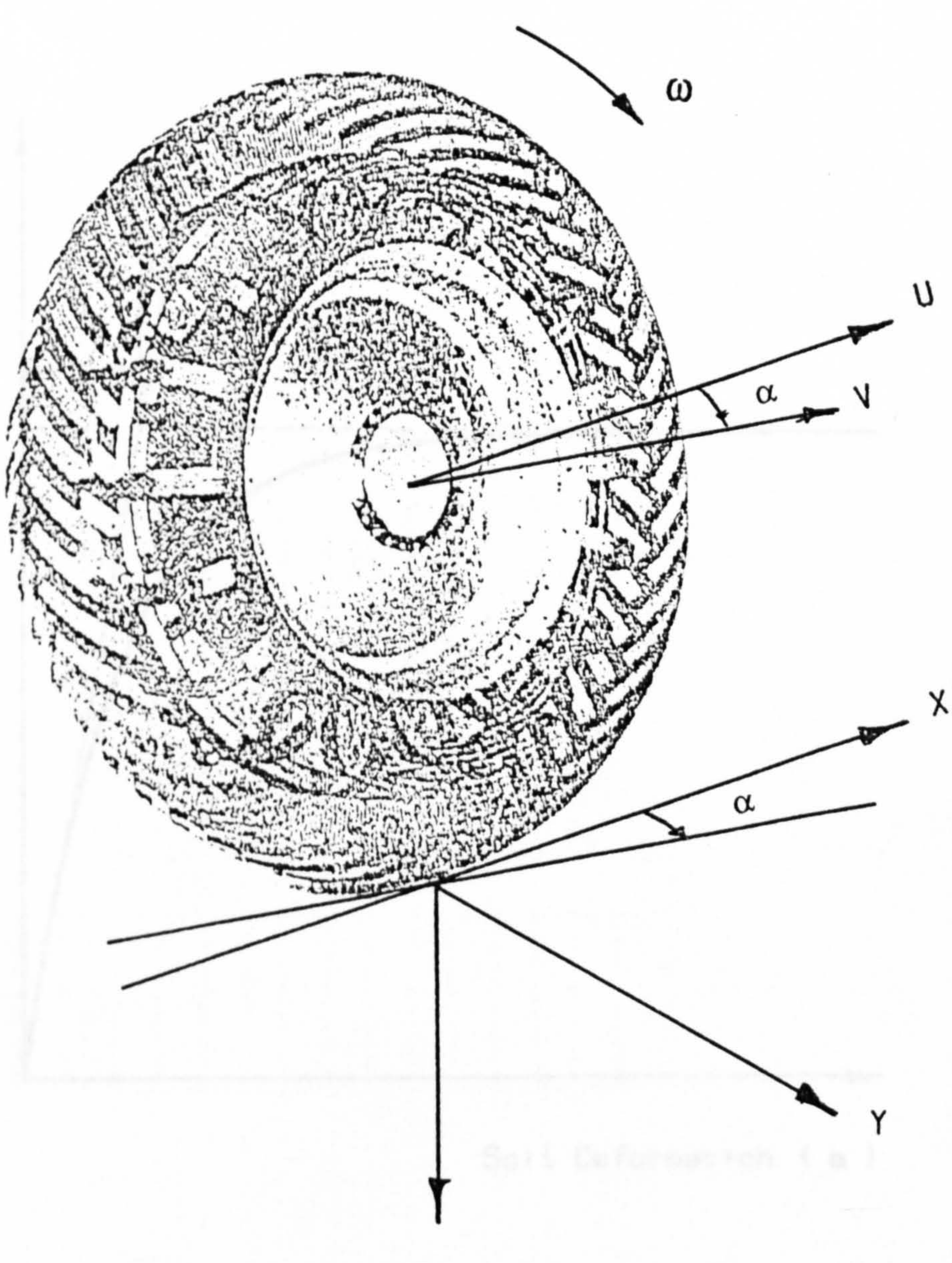

Fig. (3.3) Tyre axis system.

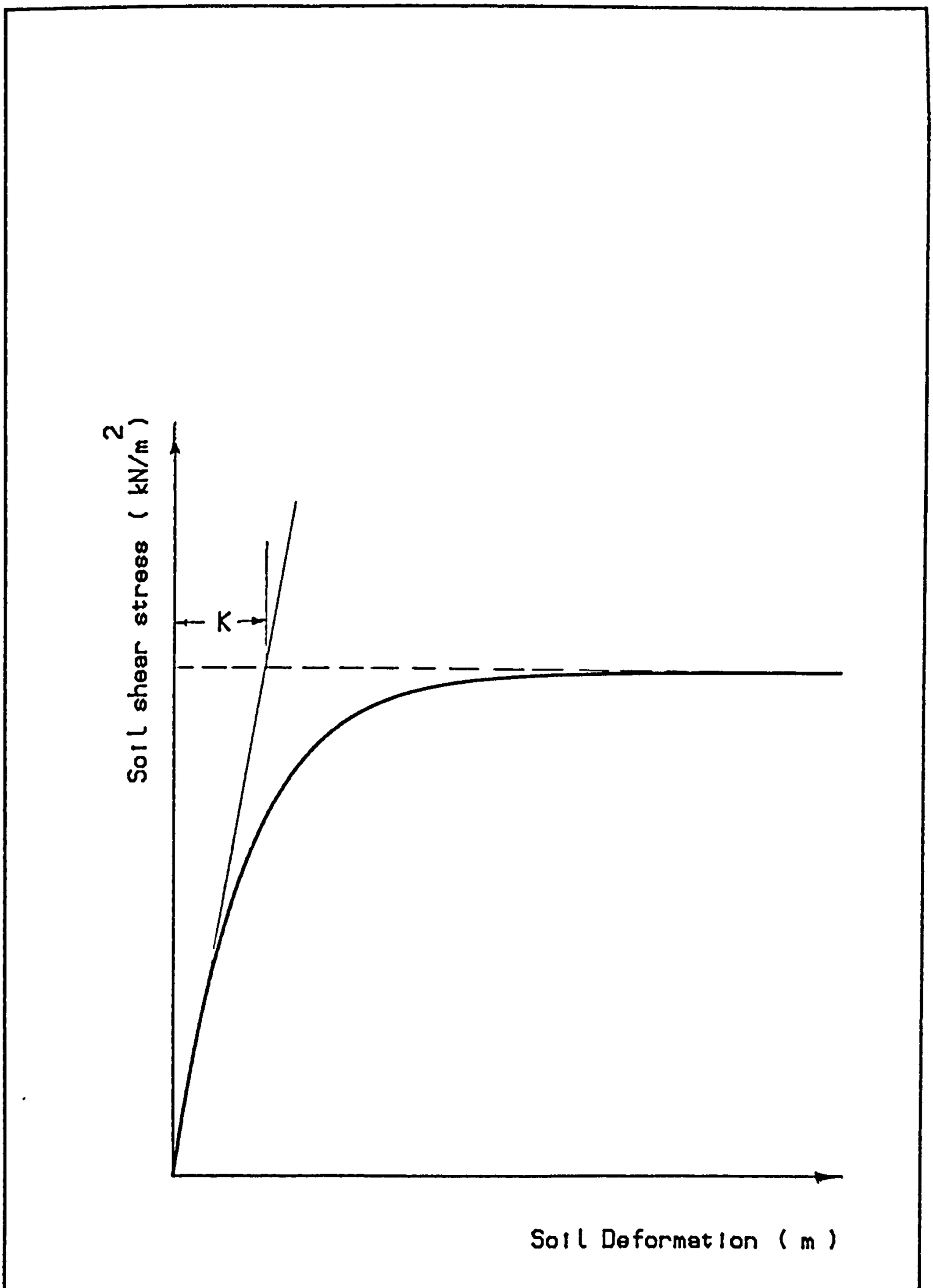

Fig. (3.4) Idealized soil stress-deformation relationship for loose soil.

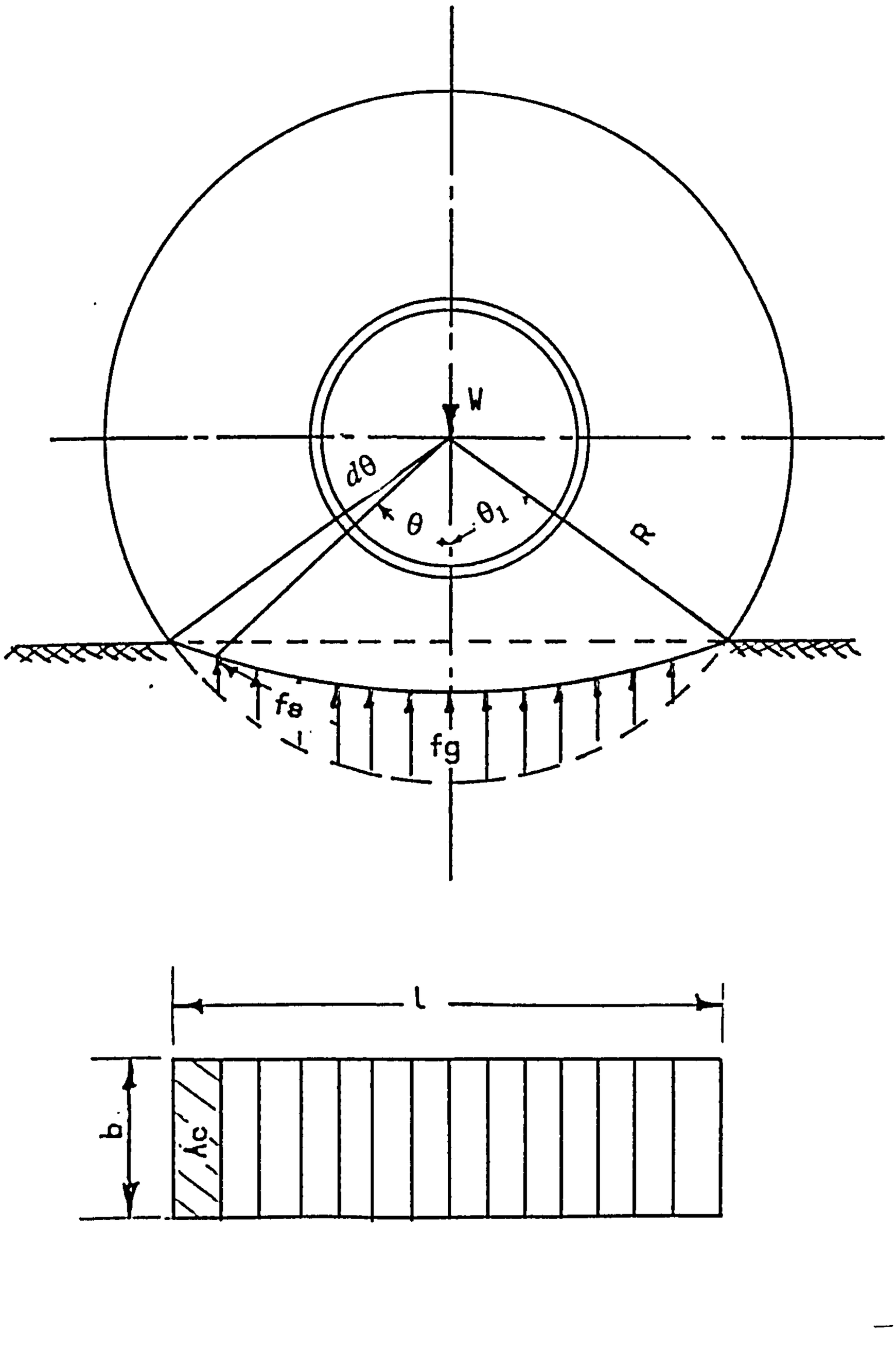

Fig. (3.5) The tyre geometry under stationary conditions on a deformable surface.

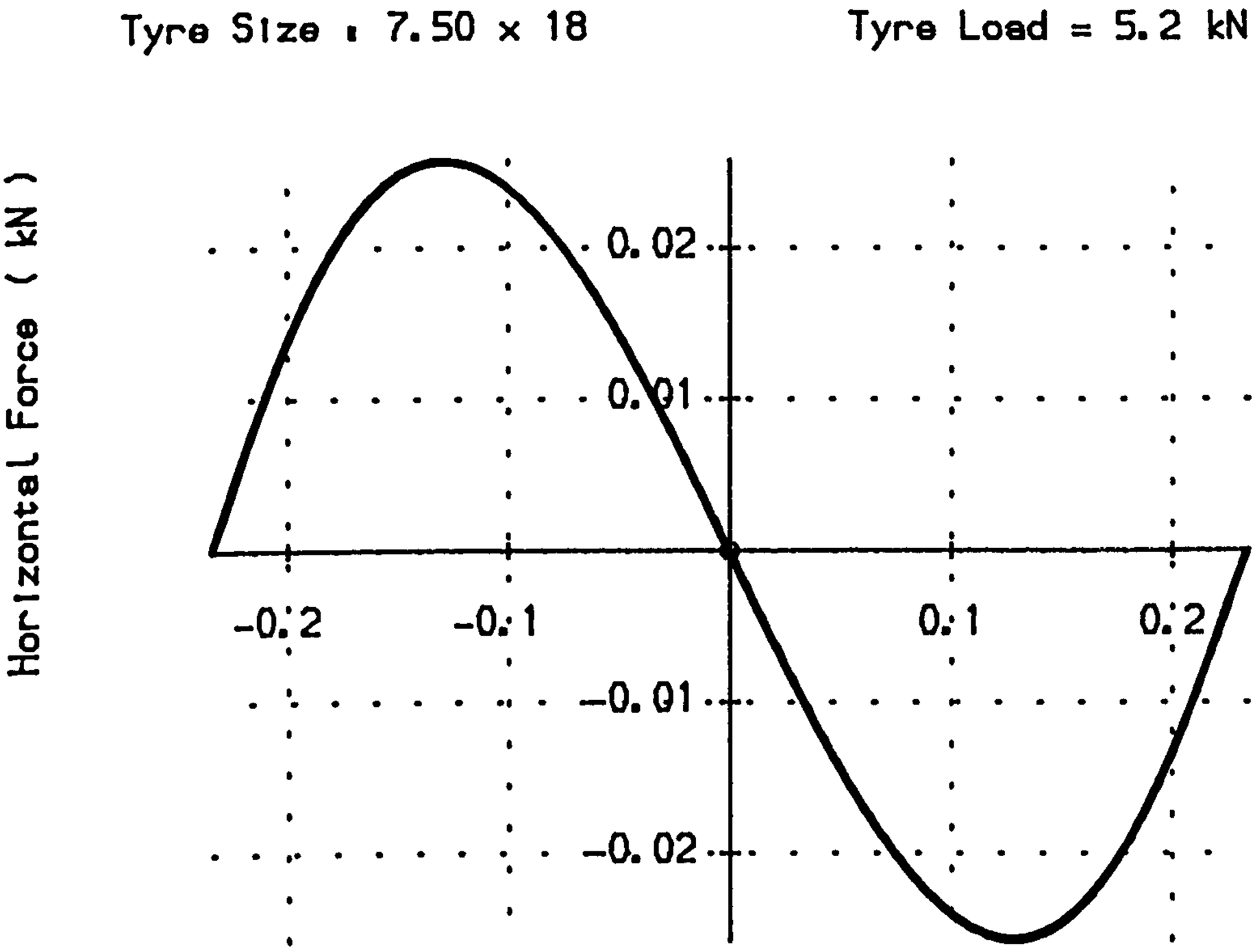

Fig. (3.6) Horizontal force distribution along length of the contact region for a static tyre on soft soil.

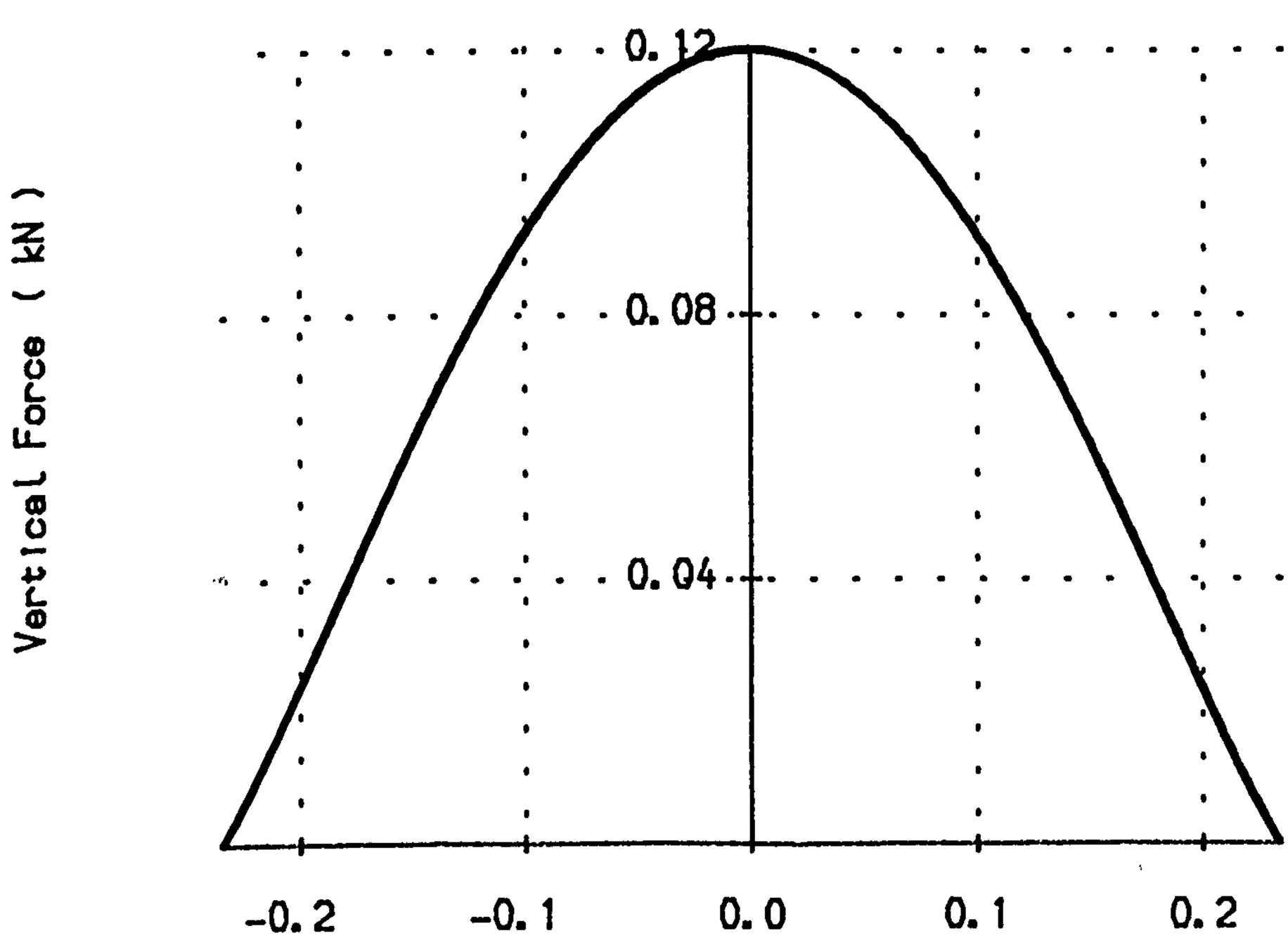

Fig. (3.7) Vertical load distribution along length of the contact region for static tyre on soft soil.

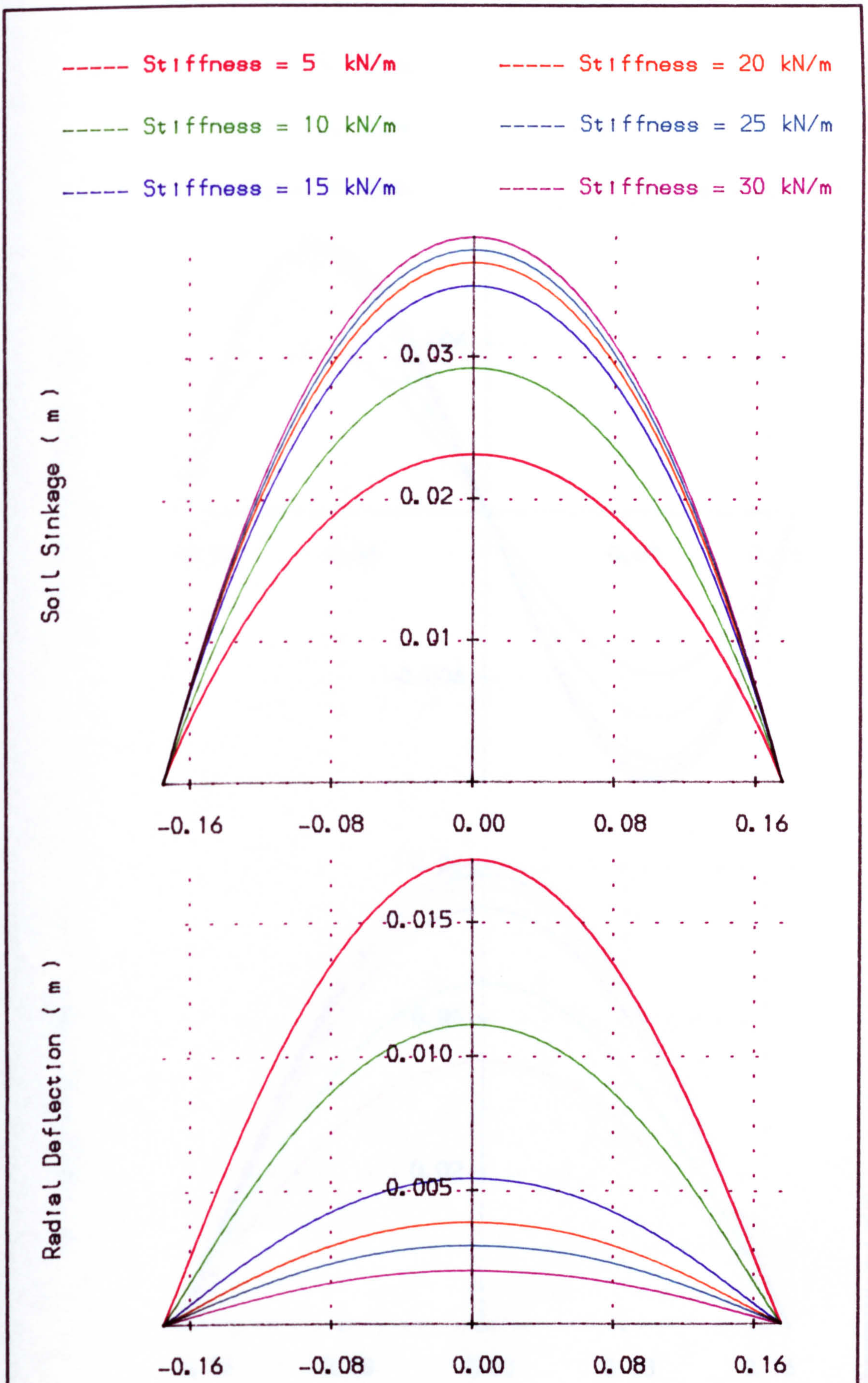

Fig. (3.8) Effect of radial tyre stiffness on the radial deflection and soil sinkage.

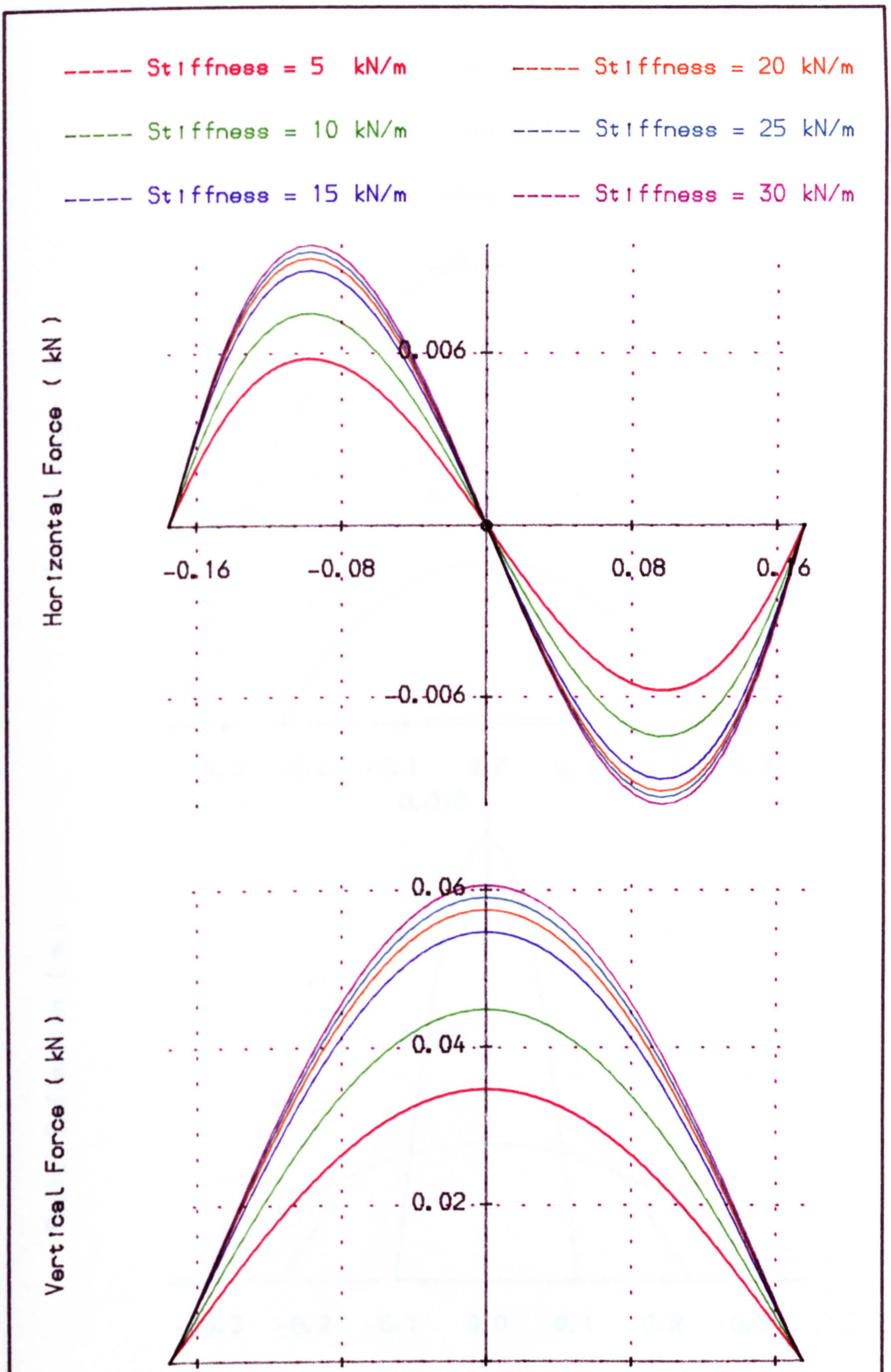

Fig. (3.9) Effect of radial tyre stiffness on the vertical and horizontal forces.

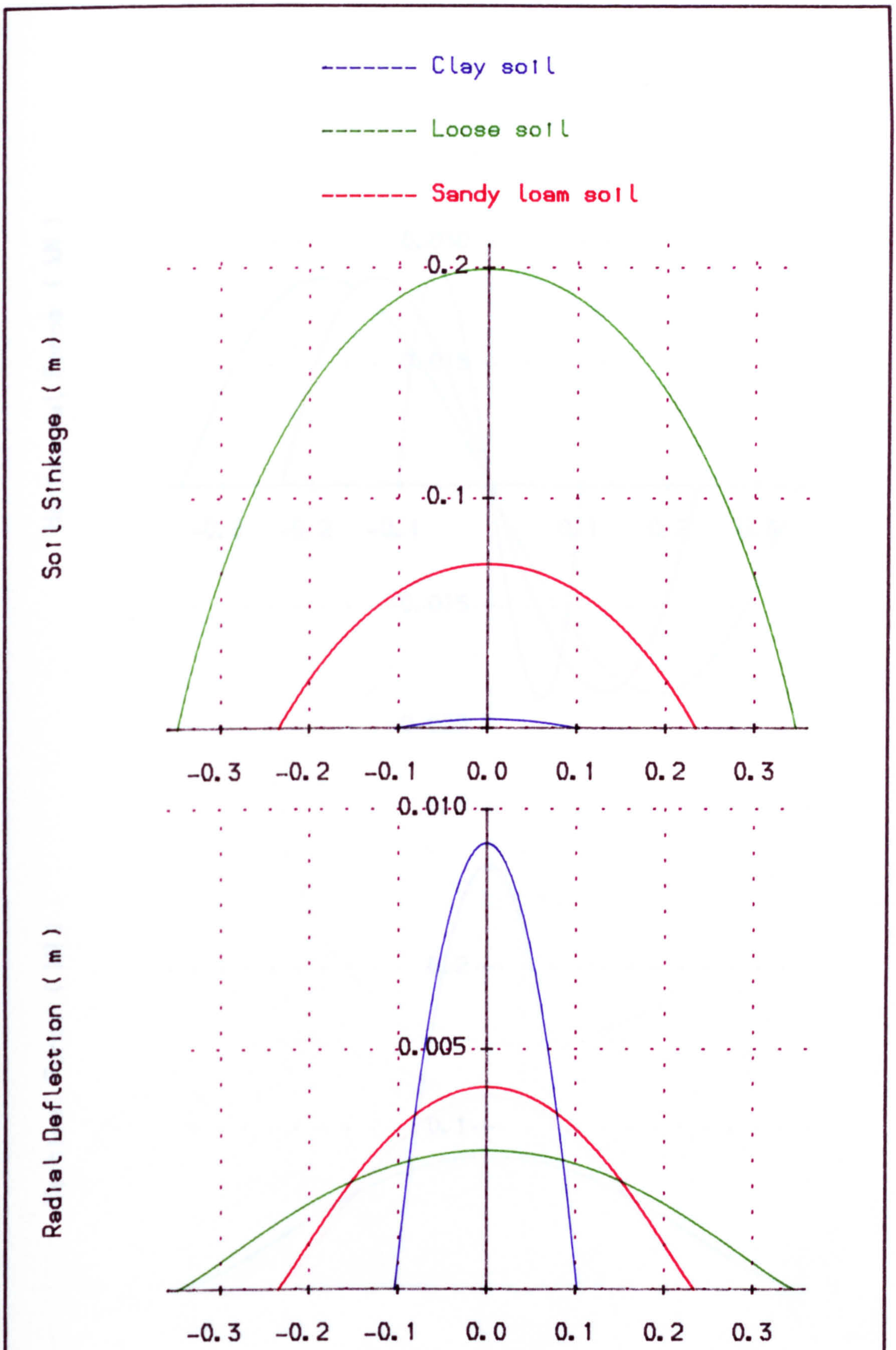

Fig. (3.10) Effect of type of soils on the radial deflection and soil sinkage for a static tyre condition.

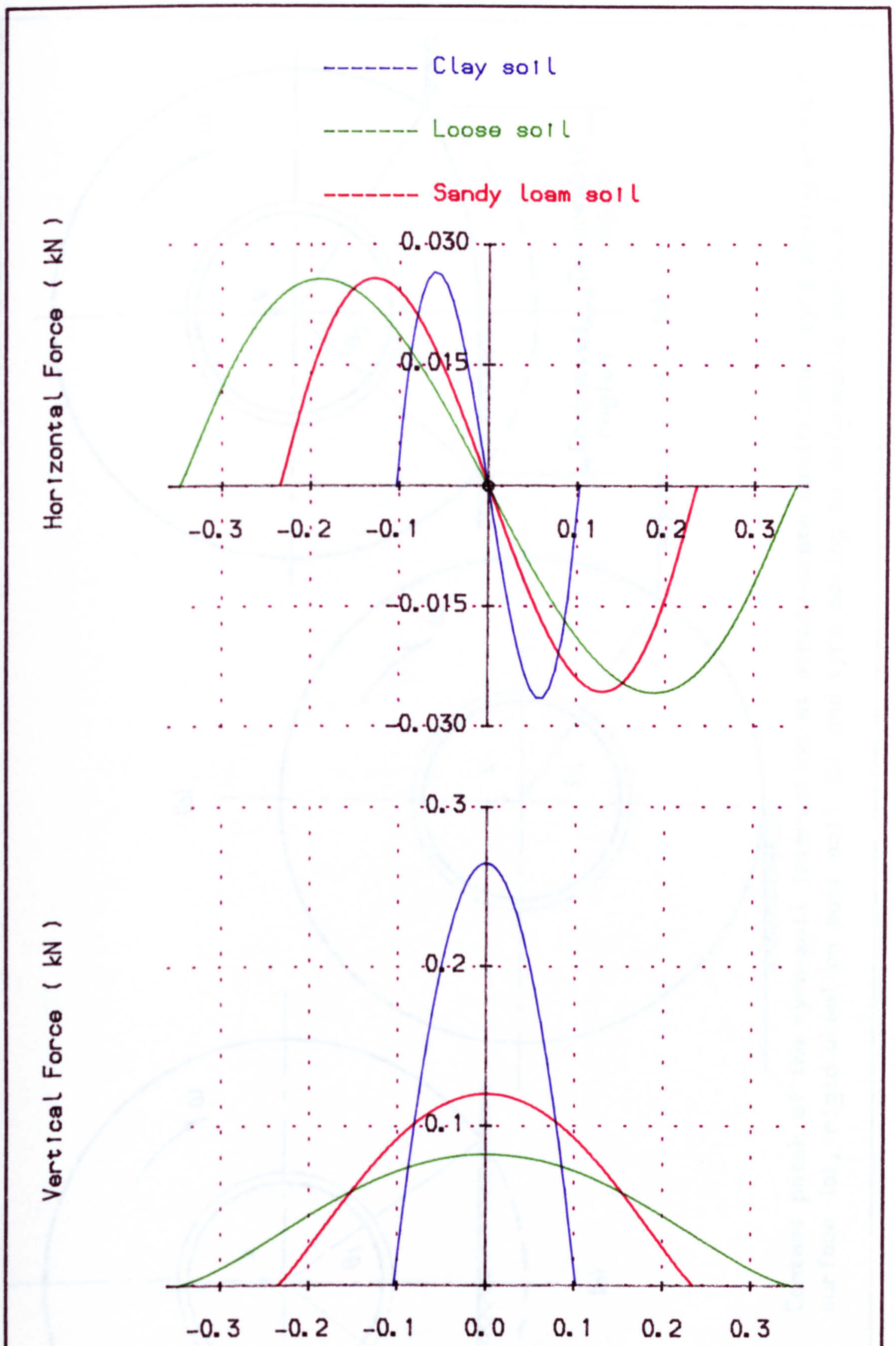

Fig. (3.11) Effect of type of soils on the vertical and horizontal forces for a static tyre.

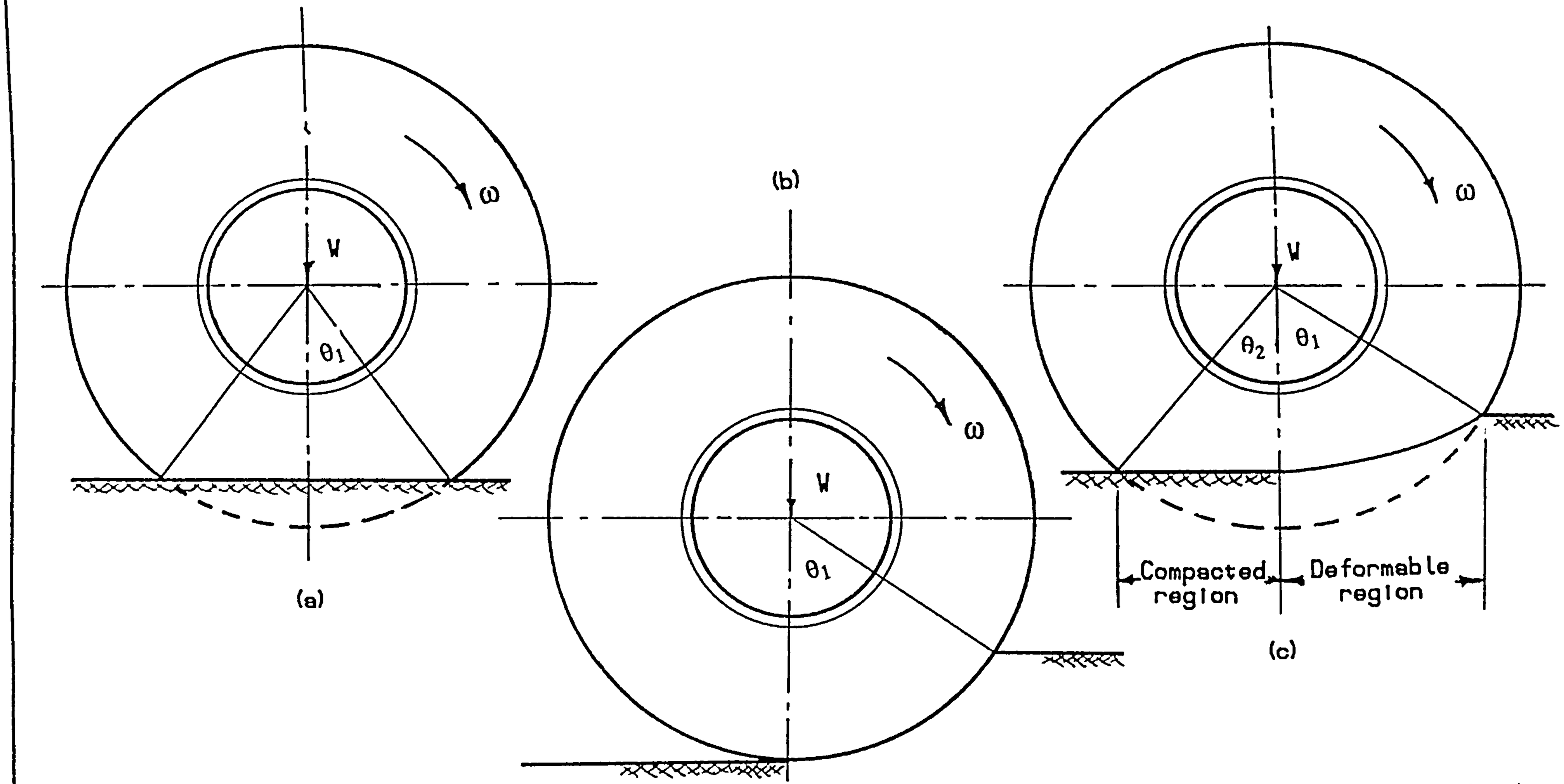

Fig. (3.12) Contact patch of the tyre-soil interaction at steady-state conditions, tyre moving on hard surface (a), rigid wheel on soft soil (b) and tyre moving on deformable surface (c).

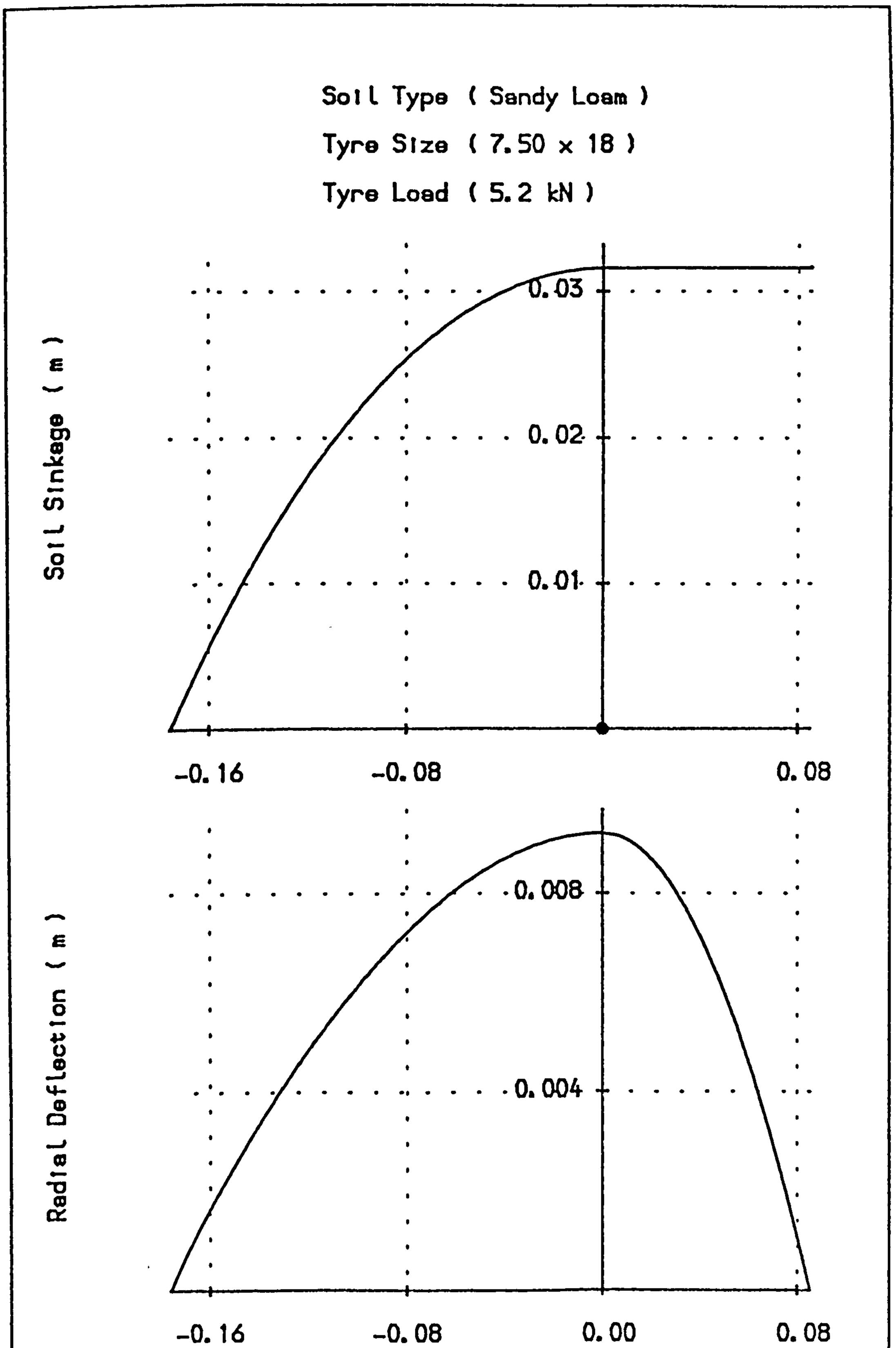

Fig. (3.13) Soil sinkage and the radial tyre deflection for a steady state tyre condition.

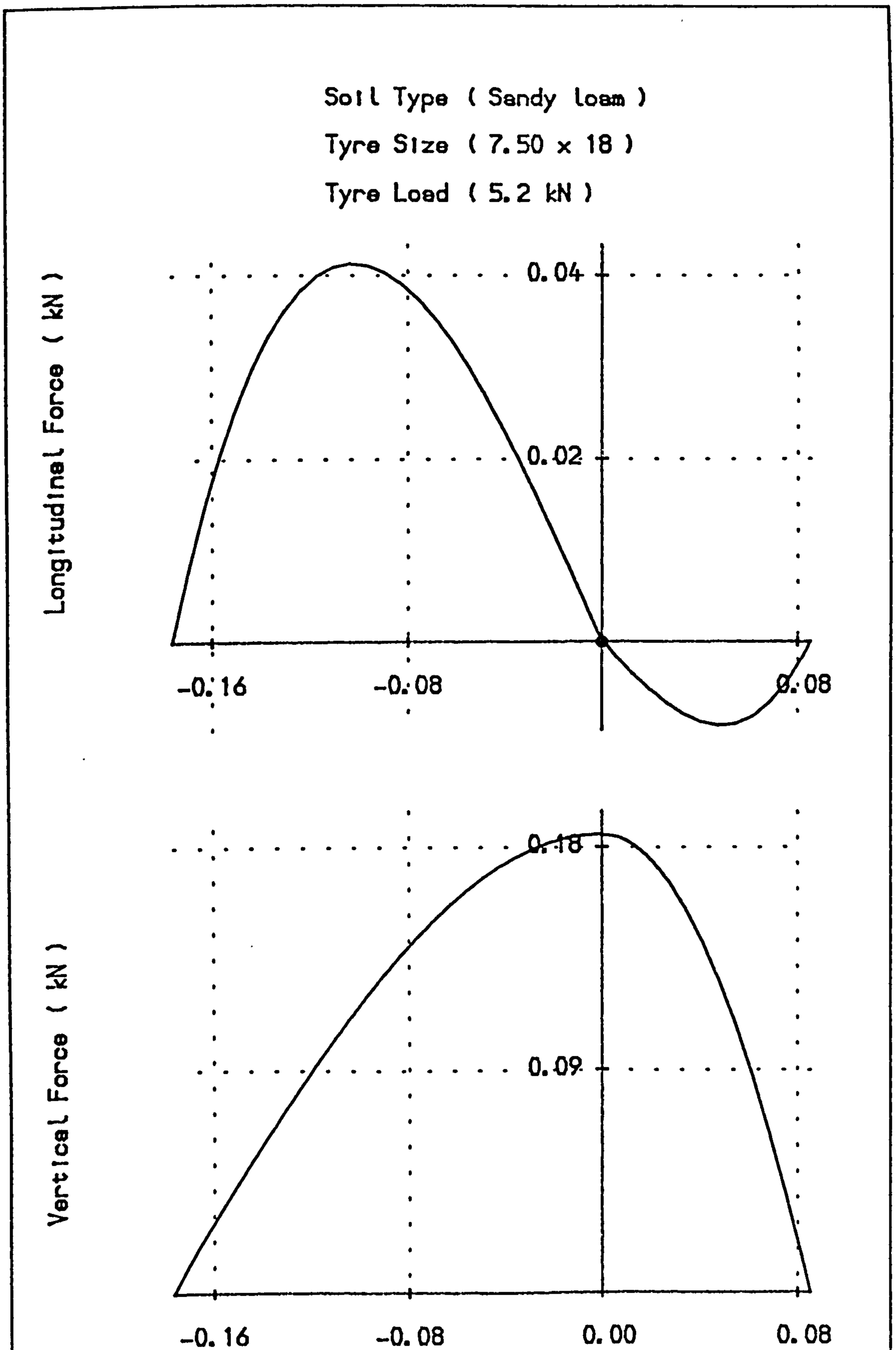

Fig. (3.14) The longitudinal and vertical force distributions along the length of the contact region for steady state tyre.

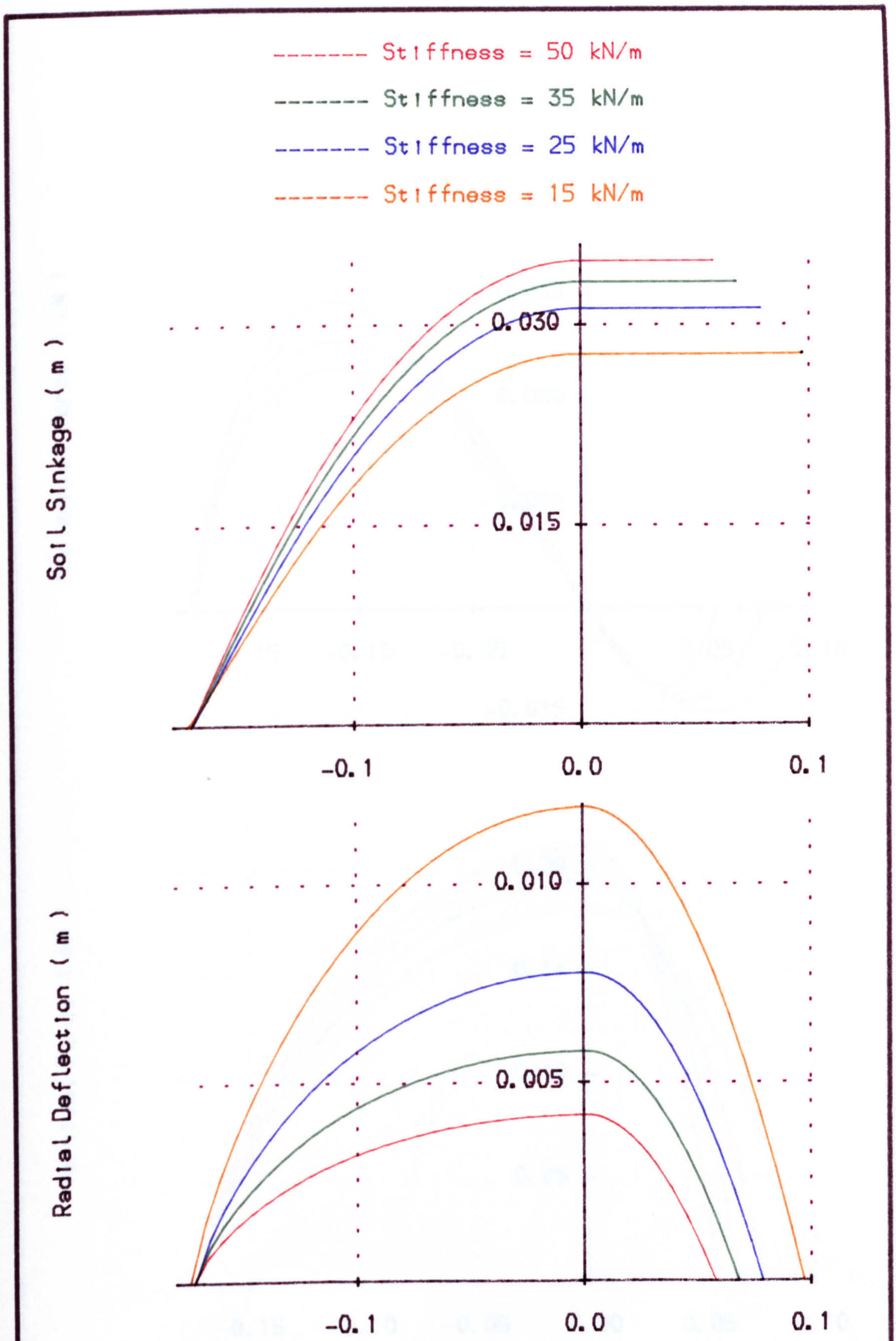

Fig. (3.15) Influence of the radial tyre stiffness on the radial tyre deflection and soil sinkage for a steady state tyre on deformable soil.

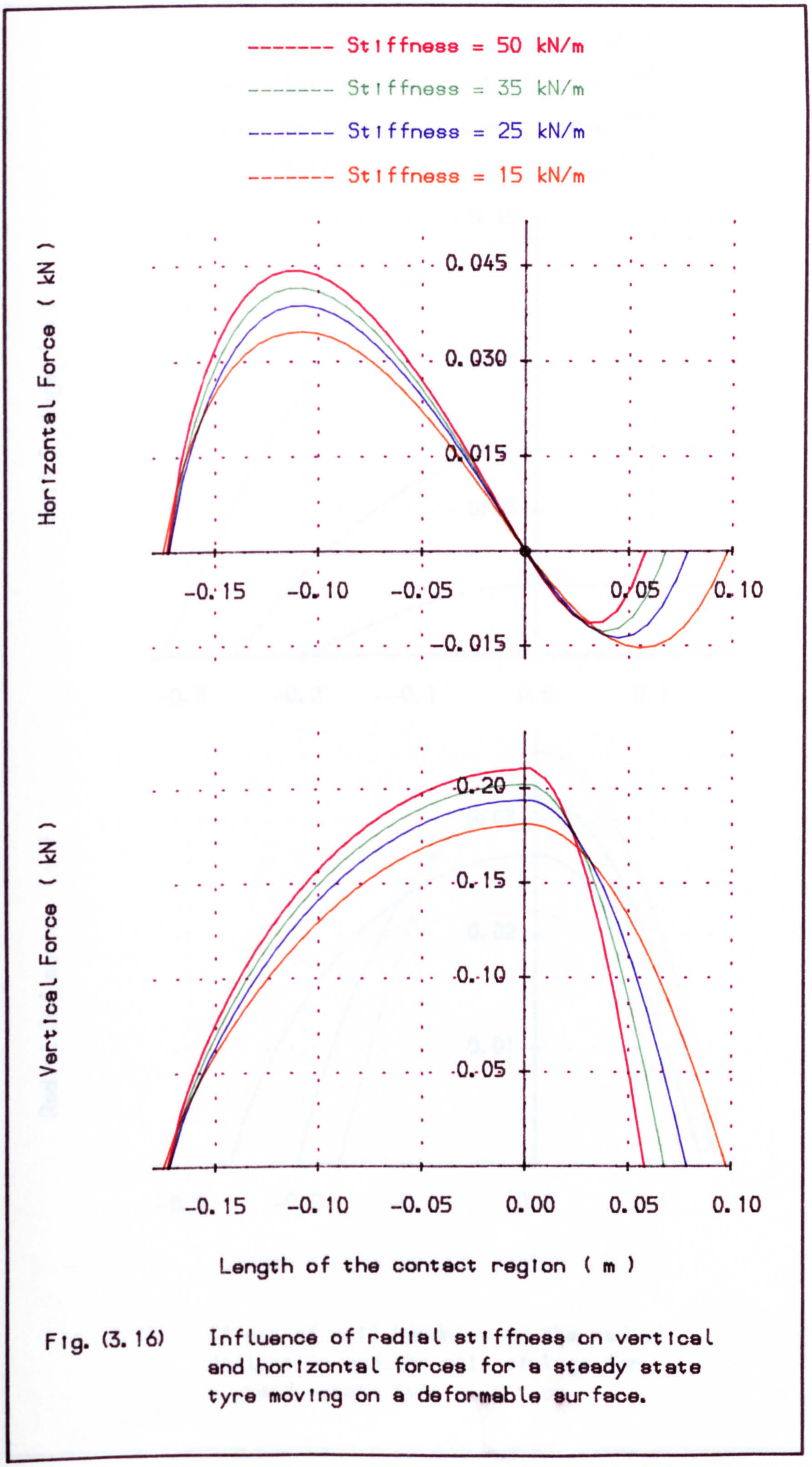

Fig. (3.16) Influence of radial stiffness on vertical and horizontal forces for a steady state tyre moving on a deformable surface.

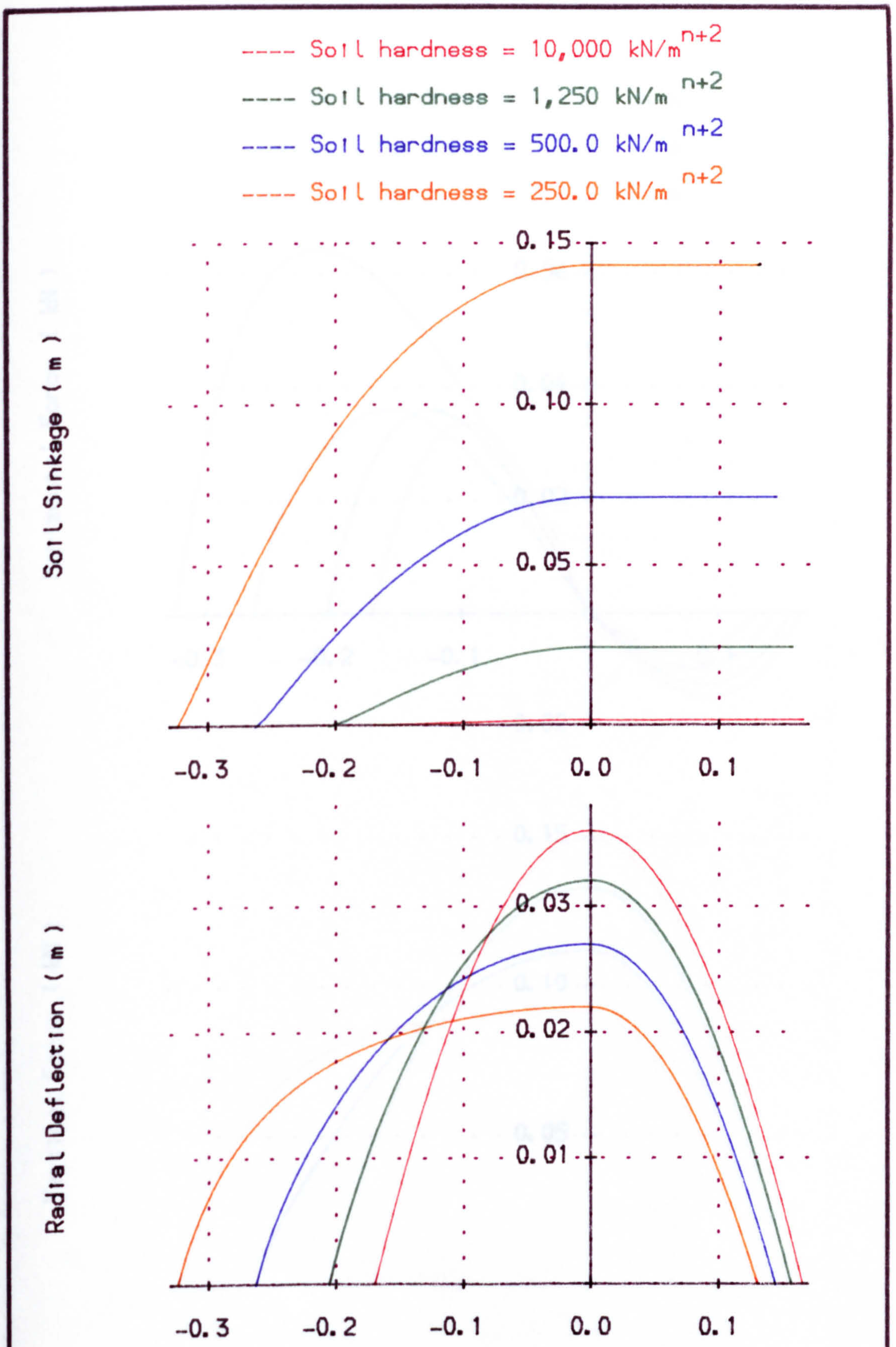

Fig. (3.17) Effect of soil hardness on the radial deflection and the soil sinkage for a steady-state tyre condition.

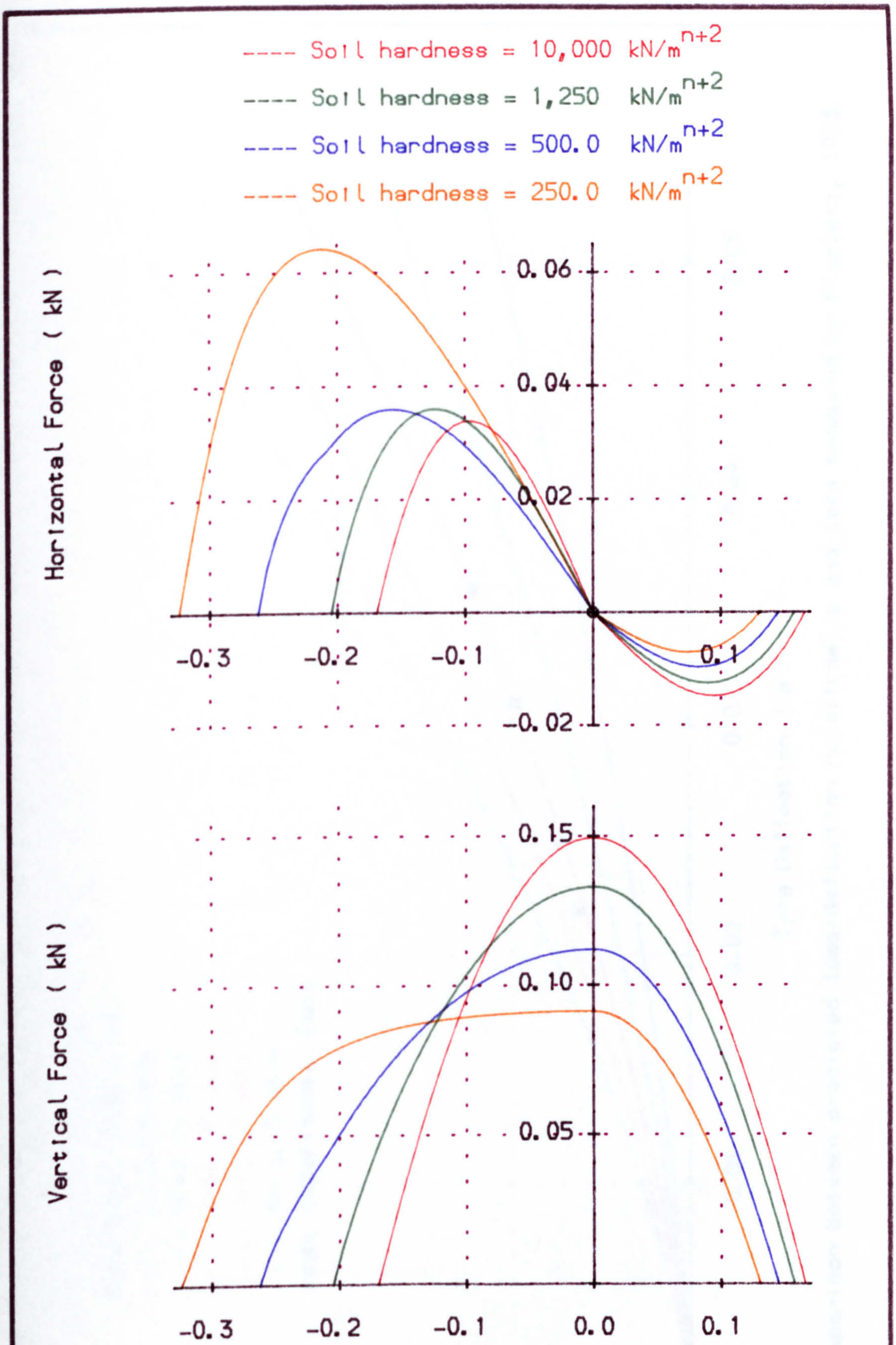

Fig. (3.18) Effect of soil hardness on the vertical and horizontal forces for a steady state tyre condition.

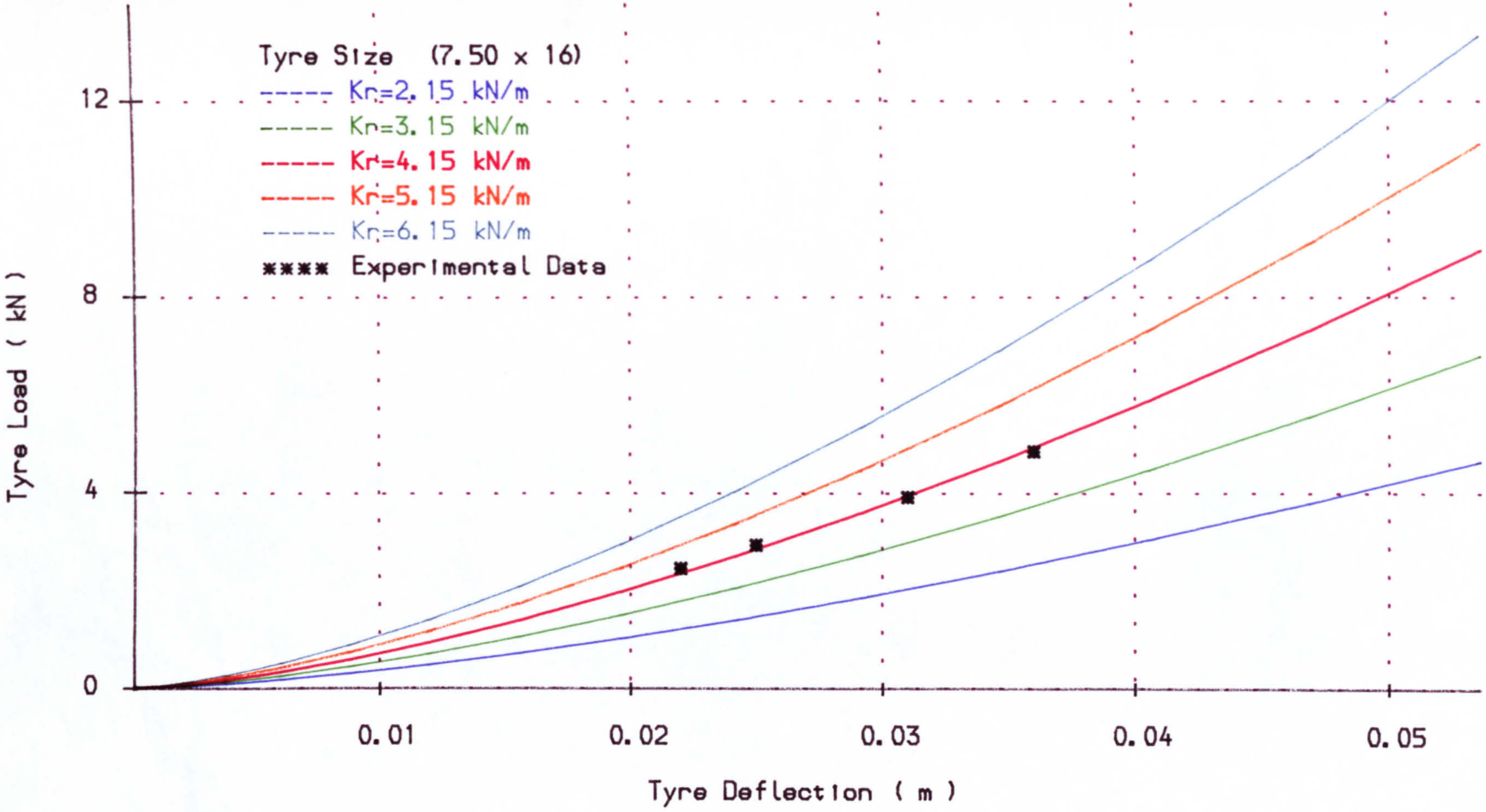

Fig. (3.19) Comparison between predicted load/deflection relationship and data measured by Plackett, 1983.

CHAPTER 4

AN EXTENDED MODEL FOR COMBINED LATERAL AND LONGITUDINAL TYRE FORCES

The extended model for combined lateral and longitudinal off-road tyre forces is presented. A fuller treatment of tyre/soil behaviour in the contact region than existed previously is outlined.

4.1. INTRODUCTION

A qualitative description of behaviour in the contact region is given in Fig.(4.1), for the case of a tyre operating at a slip angle but zero wheelslip. The tyre equatorial line is distorted relative to the wheel centreline. In fact, if there were no soil shear or sliding, the wheel equatorial line would follow the line (AD), in the resultant direction of motion of the tyre. However, in order to generate a force at the tyre/ground interface, soil shear occurs and the tyre equatorial line displaces to a new position at which :

$$\textit{FORCE DUE TO SOIL SHEAR} = \textit{FORCE DUE TO TYRE DISTORTION} \quad (4.1)$$

An exactly similar situation occurs in the longitudinal direction, though for clarity it is not shown on the diagram. This simple concept is the basis for the mathematical model.

The tyre distortion actually has two components, one due to carcass and the other due to tread deformation. However, the deformation due to the tread or lugs is normally much smaller than that due to the carcass, so it may be ignored. Also, the tyre carcass is distorted in the areas immediately in front of and behind the contact patch and these two areas are also ignored in the analysis.

Conceptually, the model is based on the idea of idealizing the tyre contact region into a number of individual points along the tyre equatorial line, writing equation (4.1) in full for the longitudinal and lateral directions, solving to obtain the appropriate displacements and finally summing the individual force components over the contact length to obtain the total tyre forces.

4.2. DEFORMATION-FORCE RELATIONSHIP

In this derivation of the model, the contact area is assumed to be rectangular ($b\ l$), and the pressure distribution is assumed to be constant over the contact area ($\sigma = \frac{F_z}{bl}$). The assumed distortion of a point in the contact region under the action of lateral and longitudinal forces is shown in Fig.(4.2), for the sideslip and braking conditions.

where

σ = Normal ground pressure

F_z = Tyre force in vertical direction

b = Width of tyre contact patch

l = Length of the tyre contact patch

The total tyre distortion, η, and the total soil deformation, j, are separated into longitudinal and lateral components denoted respectively :-

$$\eta_x, \eta_y \text{ and } j_x, j_y \tag{4.2}$$

where

$$j = \sqrt{(j_x)^2 + (j_y)^2} \tag{4.3}$$

From Fig. (4.2), the following equations for displacements can be written :-

$$\eta_x + j_x = \frac{s}{1-s}\,\lambda' \tag{4.4}$$

$$\eta_y + j_y = \frac{\tan\alpha}{1-s}\,\lambda' \tag{4.5}$$

where

η_x = Longitudinal tyre deflection

η_y = Lateral tyre deflection

j_x = Longitudinal soil deformation

j_y = Lateral soil deformation

s = Wheelslip

λ' = Longitudinal displacement

α = Tyre slip angle

The deformation in the contact region for the case of sideslip and traction are shown in Fig. (4.3). The displacement equations (4.4) and (4.5) are now :-

$$\eta_x + j_x = s\,\lambda' \tag{4.6}$$

$$\eta_y + j_y = (1-s)\,\lambda' \tan\alpha \tag{4.7}$$

The definitions of wheelslip used in equations (4.6 and 4.7) are :-

For tractive case

$$Wheelslip\ \ (s) = \frac{no\ slip\ velocity - actual\ velocity}{no\ slip\ velocity} \tag{4.8}$$

which is true for $0 < s < 1$

For braking case

$$Wheelskid\ \ (s) = \frac{actual\ velocity - no\ skid\ velocity}{actual\ velocity} \tag{4.9}$$

which is true for $-1 < s < 0$

The total shear stress in the soil is governed by the total soil displacement, j, and so the shear stress components in the X and Y directions depend on the magnitudes of j_x and j_y relative to j. Note that the soil cannot generate maximum shear stress, τ_{max} , in both directions simultaneously. Equating the shear stress in the soil to the shear stress resulting from the tyre deflection gives :

$$\frac{j_x}{j}\left\{\tau_{max}\,(1-e^{-j/K})\right\} = C'_x\,\eta_x = \tau_x \tag{4.10}$$

where

τ_{max} = Soil shear strength

τ_x = Component of soil shear stress in X-direction

τ_y = Component of soil shear stress in Y-direction

C'_x = Longitudinal tyre stiffness

C'_y = Cornering tyre stiffness

$$\frac{j_y}{j}\left\{\tau_{max}\,(1-e^{-j/K})\right\} = C'_y\,\eta_y = \tau_y \tag{4.11}$$

When equation (4.3) is substituted, equations (4.4) to (4.11) become a set of four simultaneous, non-linear equations in four displacements, j_x, j_y, η_x and η_y. The required data for a particular tyre and soil condition are summarised in Table (4.1), with example values for a 7.50 x 18 tyre on a sandy loam soil. The tyre stiffness parameters, C'_x and C'_y, are obtained empirically from the behaviour of the tyre on a hard surface. They are obtained from the initial slopes of the longitudinal and lateral forces with wheelslip and slip angle respectively.

$$C'_x = \frac{C_s}{b\, l^2} \tag{4.12}$$

$$C'_y = \frac{C_\alpha}{b\, l^2} \tag{4.13}$$

where

C_s = Initial slope of longitudinal force vs. wheelslip

C_α = Cornering stiffness at $F_x = 0$

α = Tyre slip angle

$d\lambda'$ = Length of the thin strip

C'_y = Cornering tyre stiffness

and

$$C_s = \frac{\partial F_x}{\partial s}\Big|_{s=\alpha=0} \quad \& \quad C_\alpha = \frac{\partial F_y}{\partial \alpha}\Big|_{s=\alpha=0} \tag{4.14}$$

The solution for the predicted forces are essentially found by integrating stresses over the contact area. Computationally, this is done as follows :-

1) The contact region is assumed to consist of a finite number of thin strips of length, $d\lambda'$.

2) For values of λ' from $\frac{d\lambda'}{2}$ to $(l - \frac{d\lambda'}{2})$, i.e. along the contact length, equations (4.7) to (4.10) are solved to obtain displacements.

3) The displacements are used to calculate the shear stress components, τ_x and τ_y, in the X and Y directions from equations (4.9) and (4.10).

4) The net forces on each strip are then :

$$dF_x = \tau_x \, b \, d\lambda' \tag{4.15}$$

and

$$dF_y = \tau_y \, b \, d\lambda' \tag{4.16}$$

where

dF_x = The net force on thin strip in X-direction

dF_y = The net force on thin strip in Y-direction

5) The total forces on the tyre are the summations of these force components throughout the contact region.

Repeating this procedure for a range of values of wheelslip and slip angle enables the complete force characteristics of the tyre to be built up. A computer programme was written in Fortran to do this and it incorporated a subroutine to obtain the solution to equations (4.7) to (4.10) using the bisection method. Thus, the structure of the computer programme is that for a given set of tyre and soil data, the input values are wheelslip and slip angle and the output values are longitudinal and lateral forces. This enables it to be linked as a subroutine to off-road vehicle handling programmes.

4.3. SOIL AND TYRE DEFORMATION

The deformation of the tyre and the soil at various points in the contact region is shown in Fig.(4.4). The values of 12^{o}. slip angle and 60% wheelslip represent a fairly extreme condition and were chosen so the components of displacement could be seen clearly. Only ten points are shown in this figure although the computation is actually done for more than 100 points.

4.4. EFFECT OF TYRE STIFFNESS PARAMETERS

The effect of the tyre stiffness parameters, C'_x and C'_y, are shown in Fig.(4.5) and Fig.(4.6). The lateral force coefficient is plotted against slip angle for the condition of zero wheelslip with different values of C'_x and C'_y. In Fig.(4.6), the longitudinal force coefficient is plotted against wheelslip for the condition of zero slip angle and the same variation of C'_x and C'_y.

As the tyre stiffness parameters increase, the predicted tyre forces at a particular wheelslip or slip angle also increase. In the limit as C'_x and C'_y approach infinity, the predicted forces approach those calculated in Grecenko's model [1975] which assumes that the tyre is rigid compared to the soil.

4.5. EFFECT OF SOIL DEFORMATION MODULUS

The sensitivity of the model predictions to one of the important soil parameters, i.e. the deformation modulus, K, is shown in Figs.(4.7) and (4.8). As the value of this modulus parameter increases, the predicted forces decrease because the soil becomes very stiff at lower values of soil deformation modulus.

It is interesting to note that as the soil parameters approach those of an "infinitely stiff" soil, i.e. a non-deformable, road surface, the model becomes the same as that originally proposed at the University of Michigan Transportation Research Institute [1970] and used by them for some vehicle handling studies.

As a general presentation of the results, Fig.(4.9) illustrates the influence of lateral force coefficient as a function of slip angle and wheelslip. It also shows the relationship between the longitudinal force coefficient and wheelslip with different slip angles. The slip angle ranged between 0 to 45^{o} and wheelslip ranged between 0 and 100%.

4.6. CONCLUDING REMARKS

(1) A model for the combined lateral and longitudinal force generation of an off-road tyre has been presented. It is based on the idea that in the tyre/ground contact region the forces due to soil shear must equal those due to tyre deflection at any point.

(2) Predicted force relationships with slip angle and wheelslip agrees qualitatively with those obtained from measured data.

(3) The model is in a form which is suitable for inclusion in vehicle models to predict handling and steering behaviour.

(4) The model agree quantitatively with the model predicted by Grecenko. The comparison and the model accuracy are presented in Chapter 6 later.

Soil data	
Cohesion, c	$4.0\ kN/m^2$
Internal angle of friction, ϕ	29^o
Deformation soil modulus, K	$0.029\ m$
Sinkage exponent, n	0.9
Cohesive modulus, K_c	$1.72\ kN/m^{n+1}$
Frictional modulus, K_ϕ	$1515\ kN/m^{n+2}$
Tyre data	
Tyre load, W	$5.2\ kN$
Width of the contact region, b	$0.204\ m$
Length of the contact region, l	$0.36\ m$
Longitudinal tyre stiffness, C'_x	$2950\ kN/m^3\ unit\ slip$
Lateral tyre stiffness, C'_y	$1115\ kN/m^3\ rad$

Table (4.1) Typical soil and tyre data parameters for a 7.50 x 18 tractor front tyre operating on medium sandy loam soil.

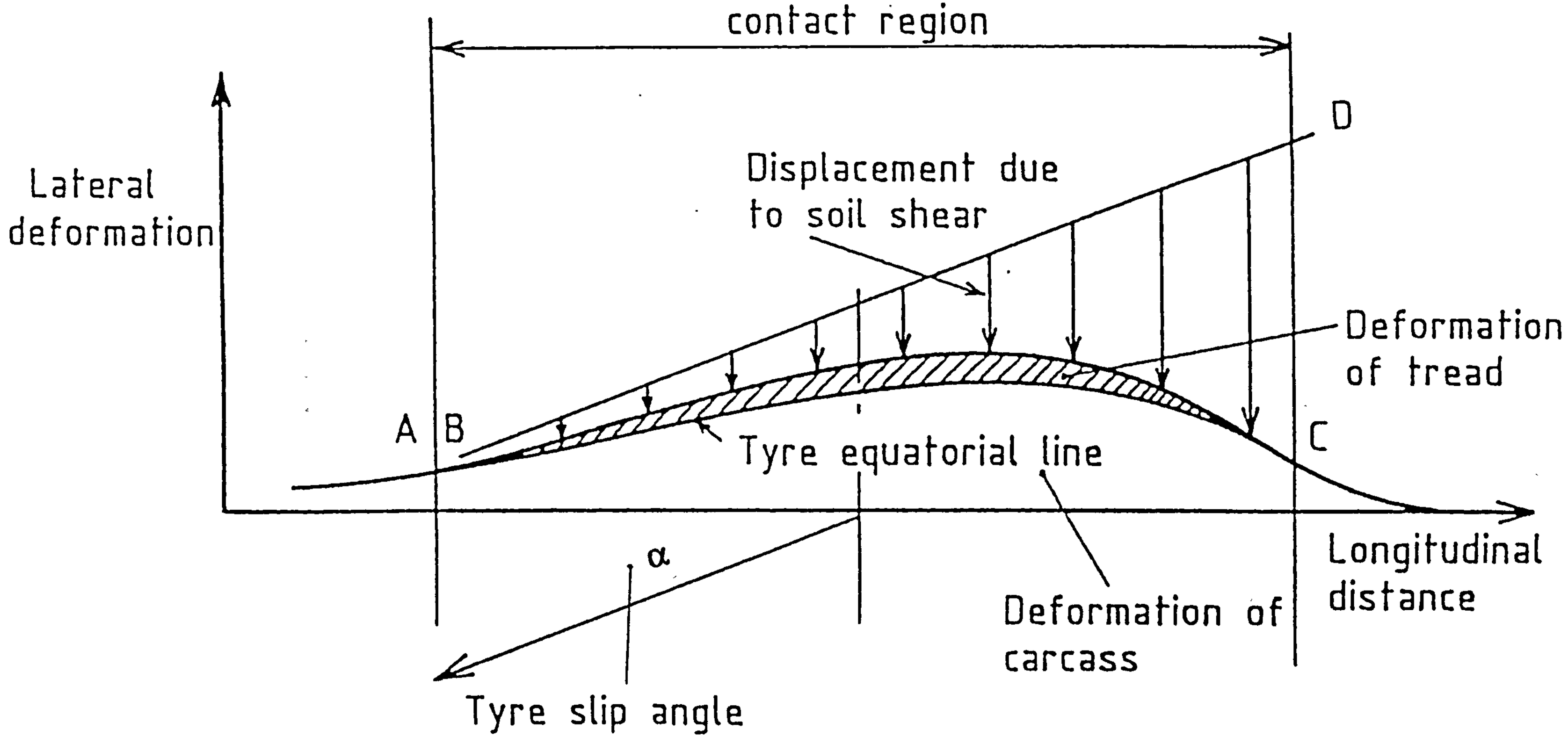

Fig. (4.1) Tyre and soil deformations in the contact region of a tyre operating at a slip angle on a deformable surface.

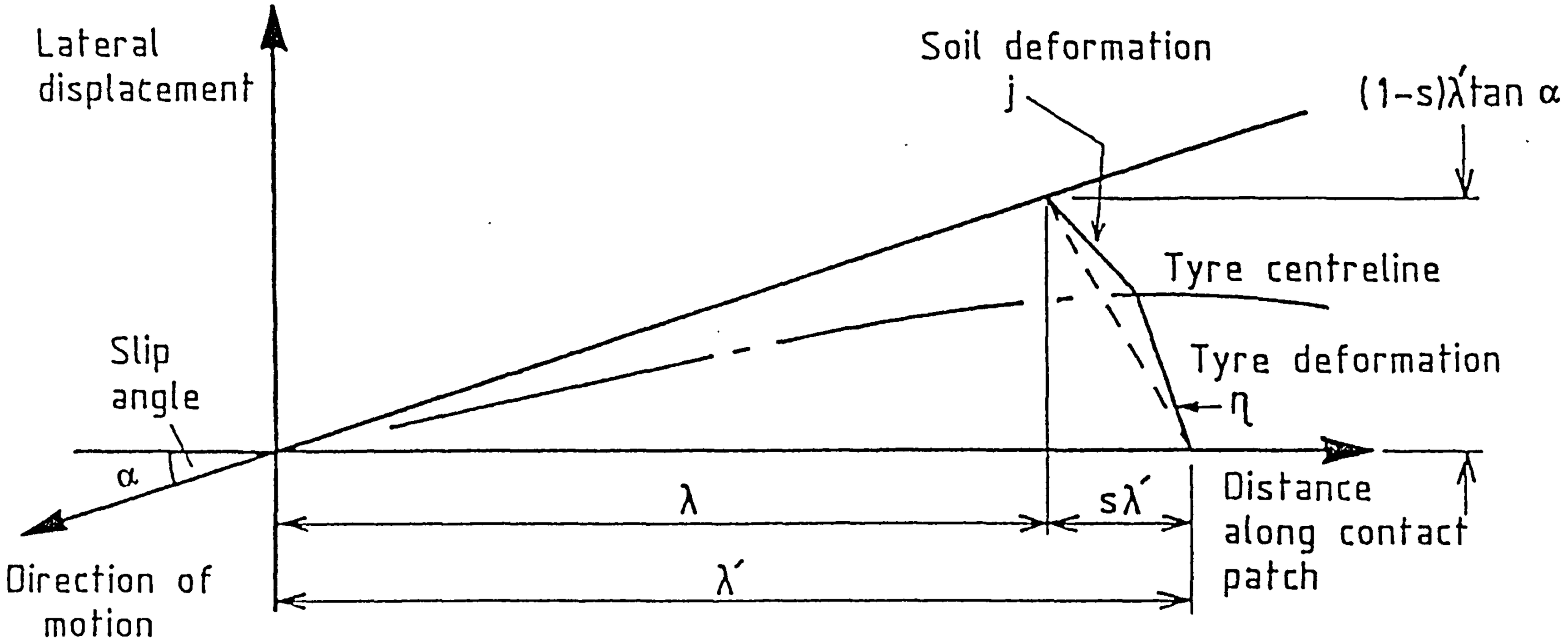

Fig. (4.2) Tyre and soil deformations for a tyre operating under sideslip and braking conditions.

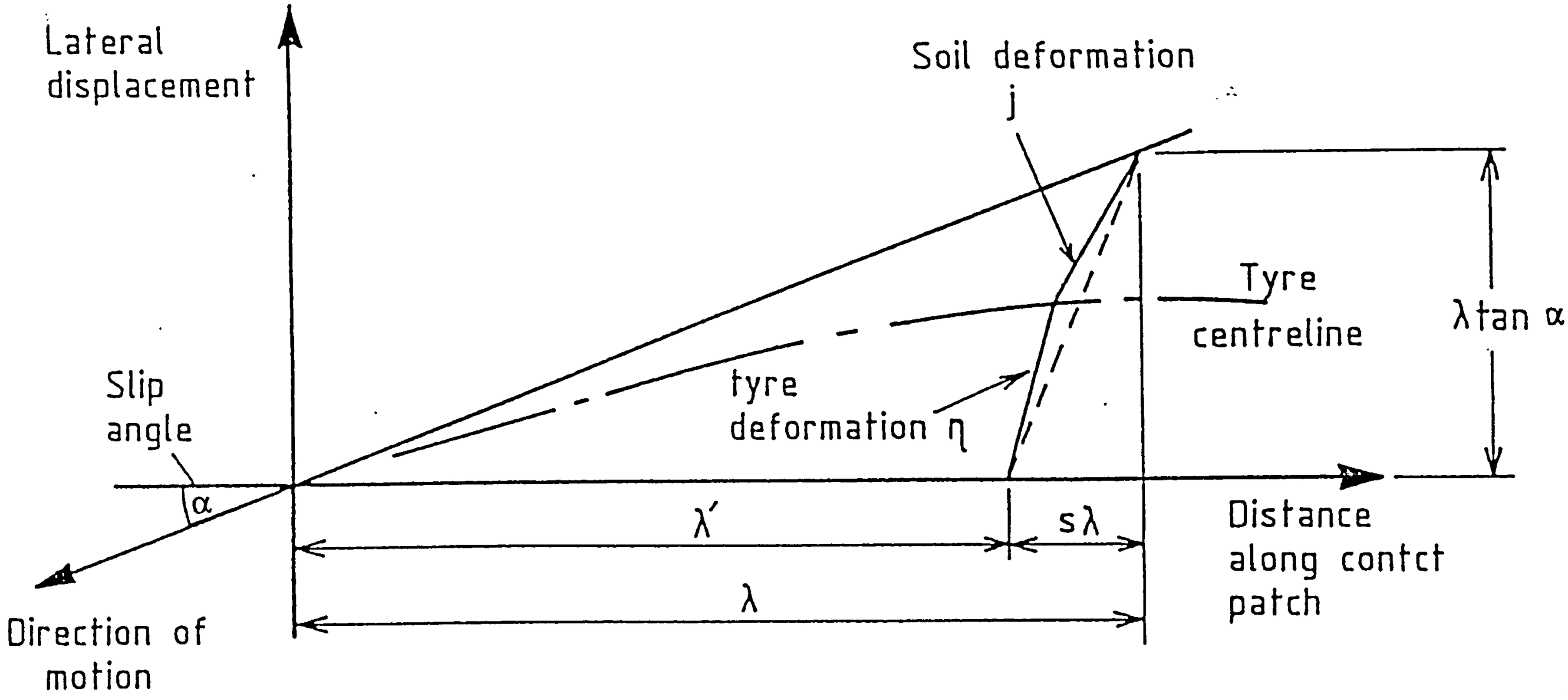

Fig. (4.3) Tyre and soil deformations for a tyre operating under sideslip and traction conditions.

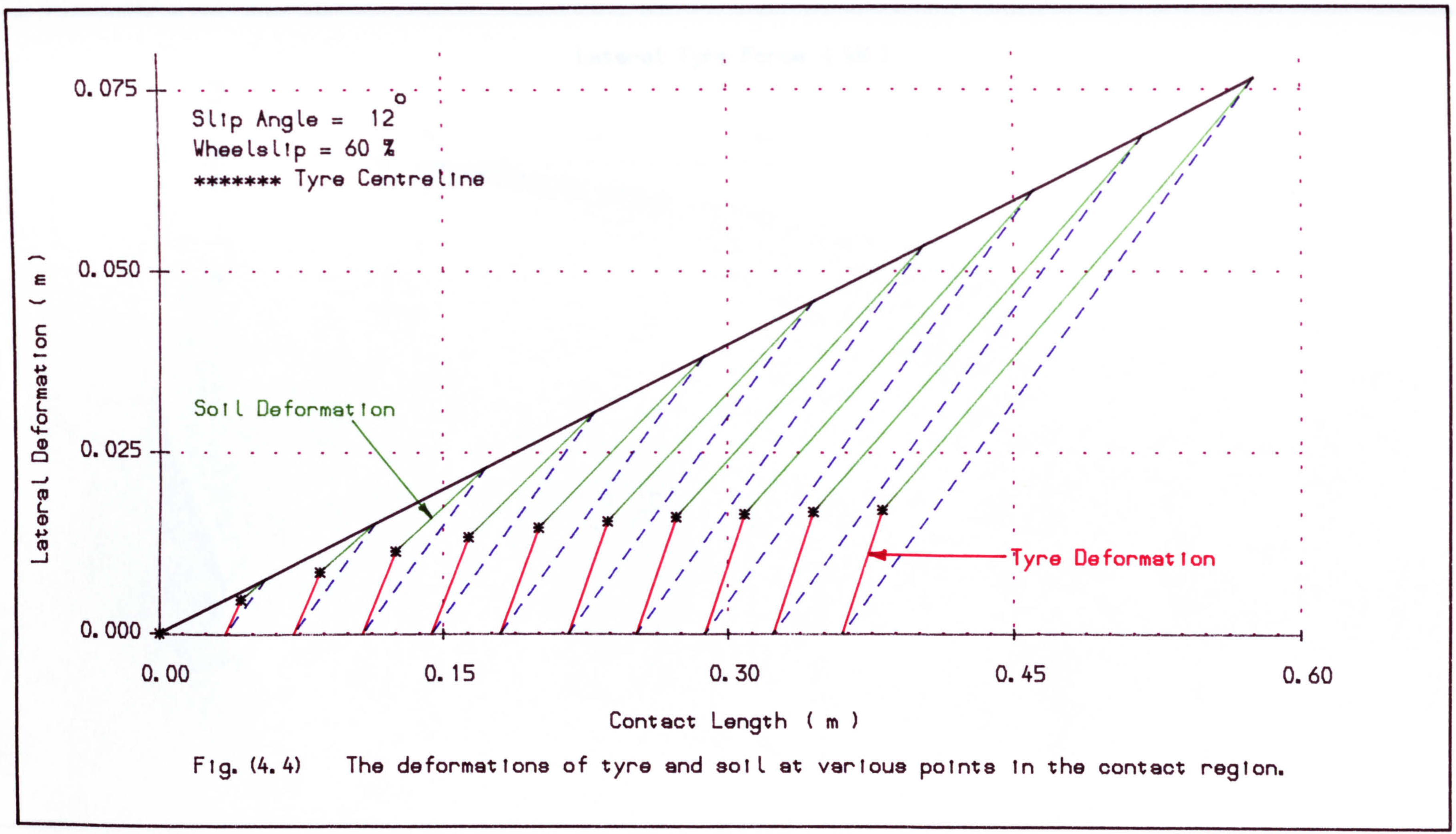

Fig. (4.4) The deformations of tyre and soil at various points in the contact region.

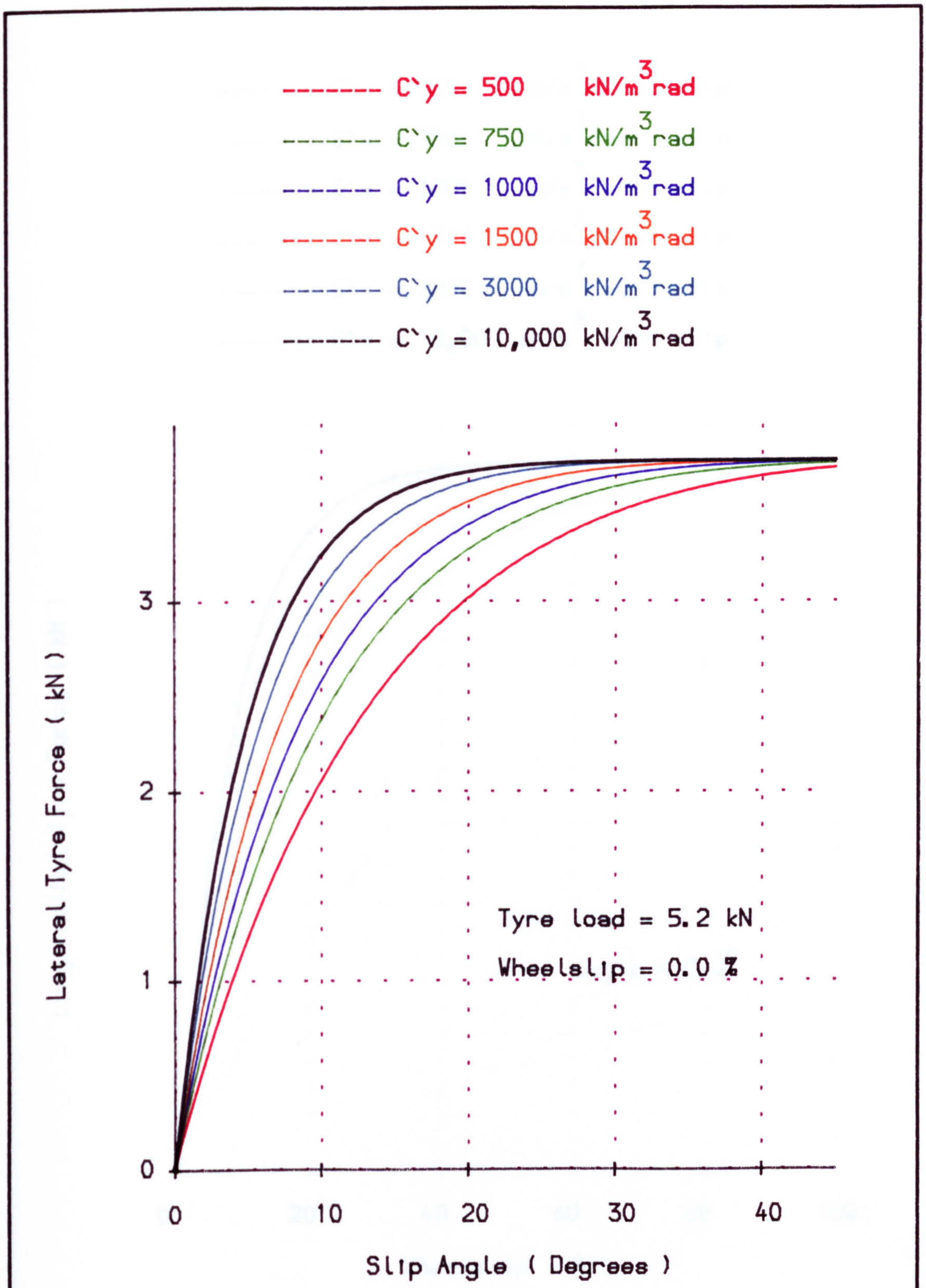

Fig. (4.5) Effect of the tyre stiffness parameter, C`y on the lateral tyre force.

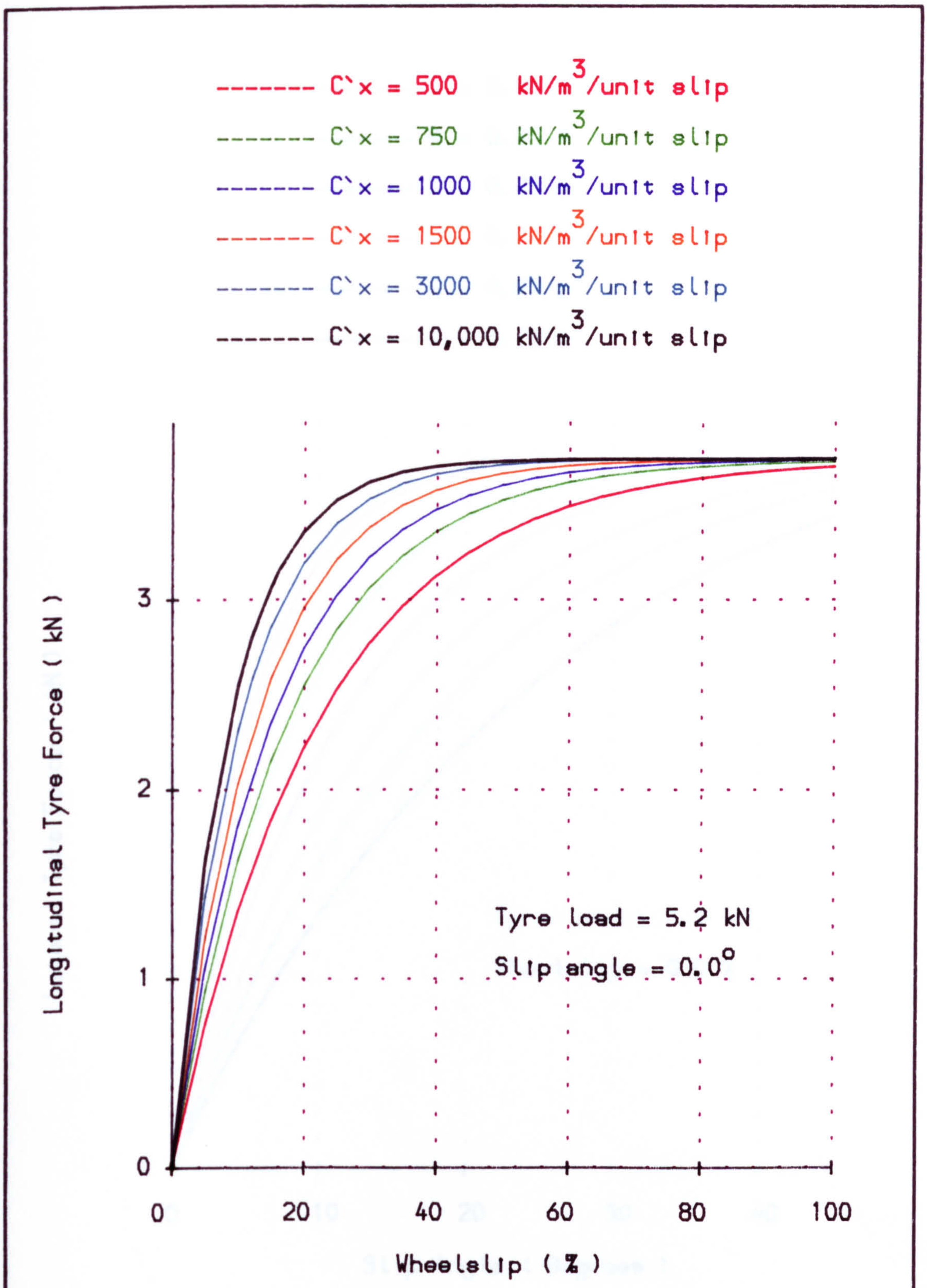

Fig. (4.6) Effect of the tyre stiffness parameter, C`x on the longitudinal tyre force.

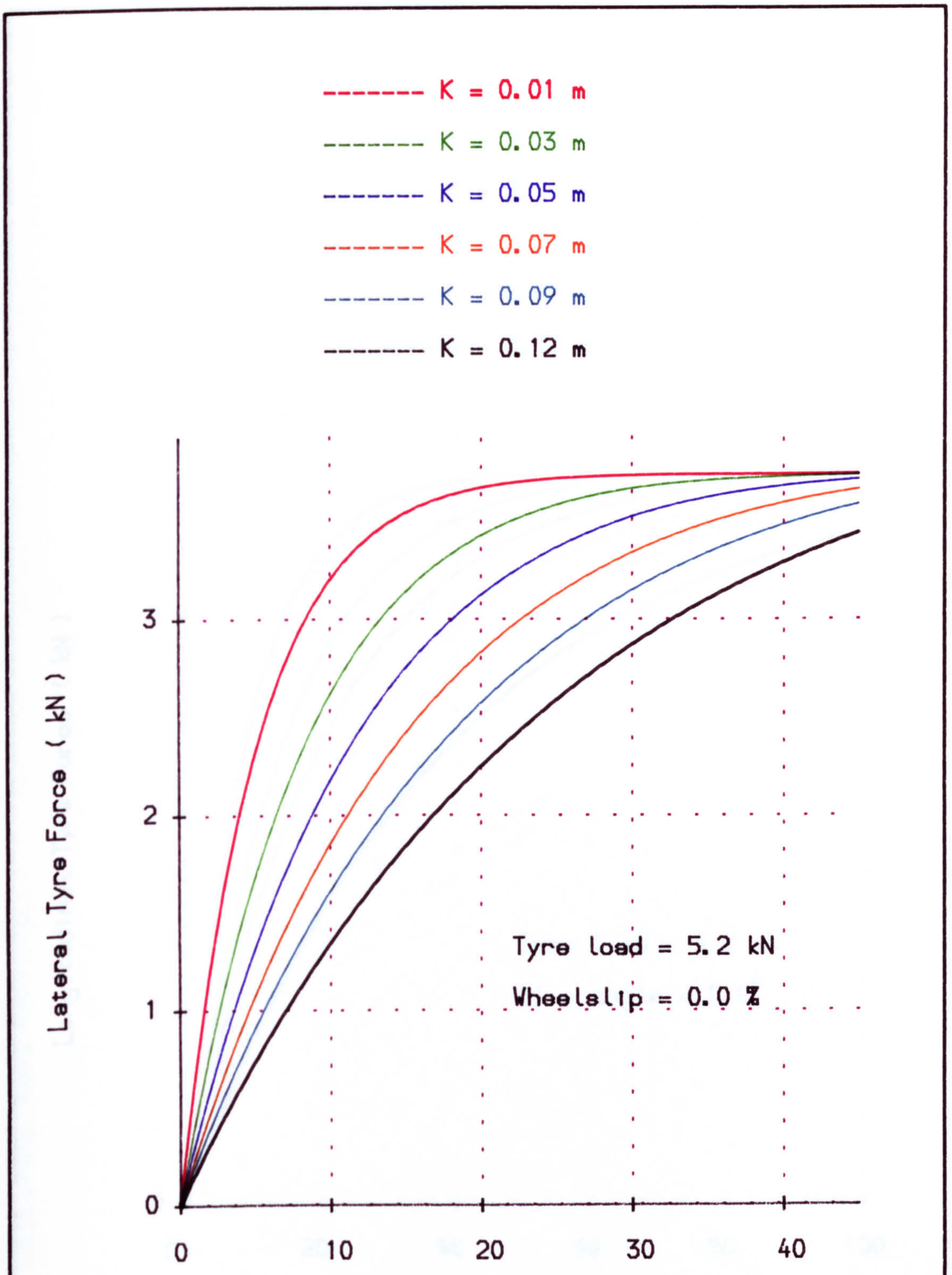

Fig. (4.7) Influence of soil deformation modulus, K, on the lateral tyre force/slip angle relationship.

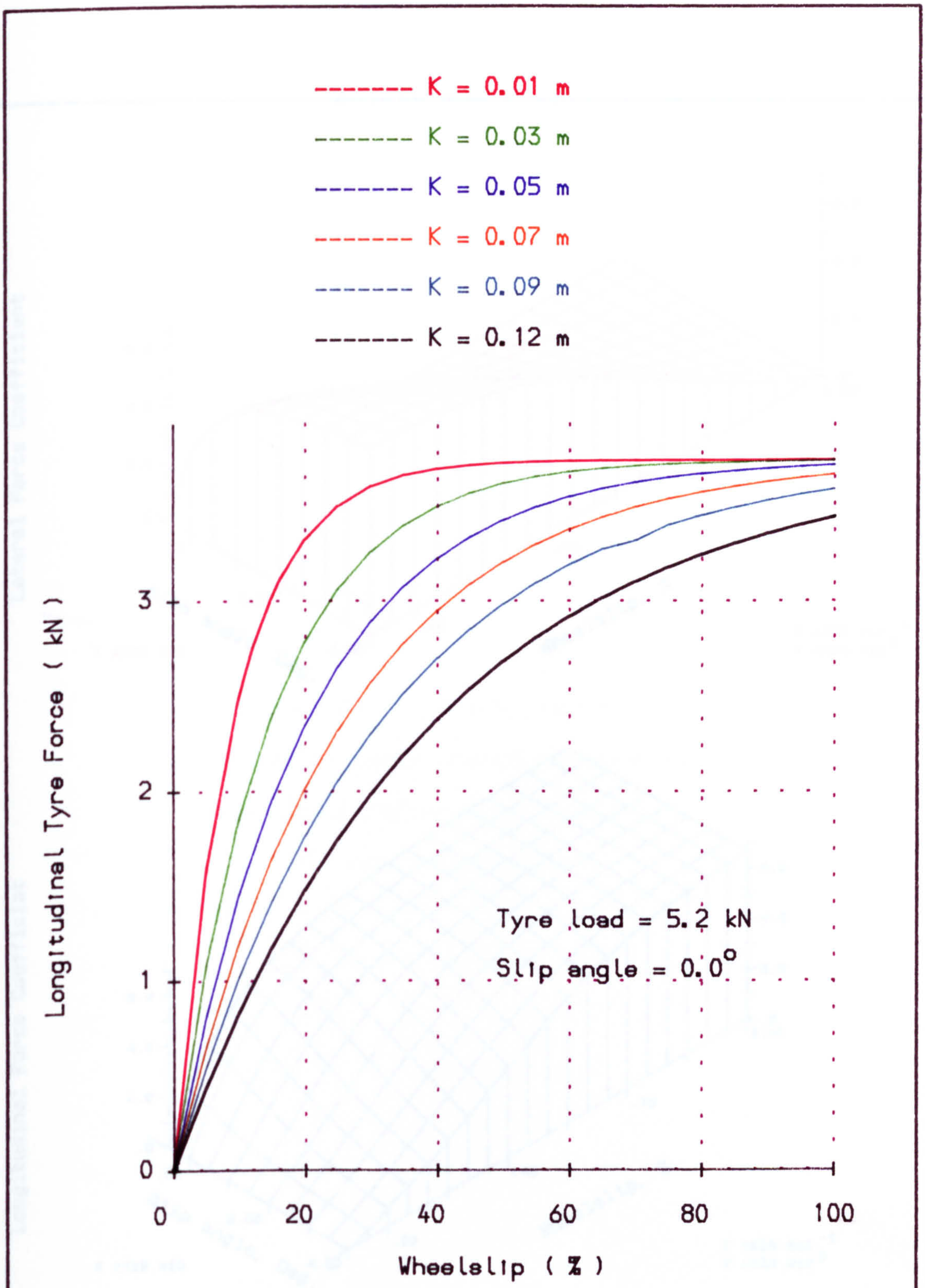

Fig. (4.8) Influence of soil deformation modulus, K, on the longitudinal tyre force/wheelslip relationship.

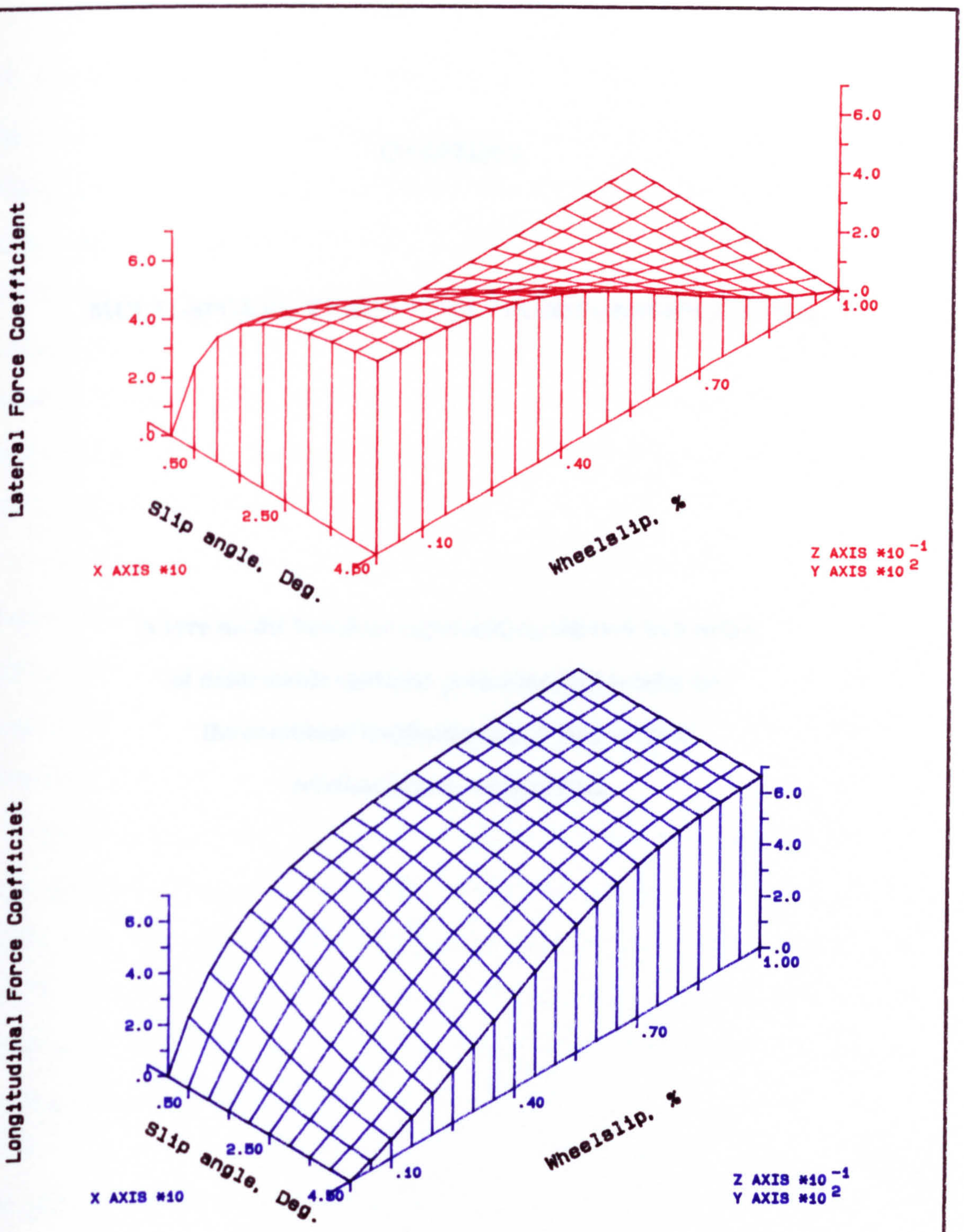

Fig. (4.9) Lateral and longitudinal force coefficient plotted as a function of slip angle and wheelslip.

CHAPTER 5

MULTI-SPOKED TYRE MODEL ON DEFORMABLE SOILS

A tyre model based on representing the tyre as a series of deformable spokes is presented and results for the combined longitudinal and lateral force relationships are calculated.

5.1. INTRODUCTION

The accurate prediction of the forces generated between the deformable soil and the rolling tyre is one of the most important and difficult problems in developing a mathematical tyre model simulation. In any study to predict the dynamic performance of off-road vehicles, it is vital to be able to model the off-road tyre accurately. Accordingly, predictions of tyre performance over a range of soil conditions are important. Also, the tyre model may be helpful in gaining a better understanding of the force distributions throughout the contact region and in establishing the detailed way in which tyre and soil parameters affect behaviour.

The model is represented by a series of individual spokes whose only connection to each other is through the hub of the wheel. The spokes have both radial and bending stiffness and solving the force equations at the tips of the spoke in the lateral, longitudinal and vertical directions is the basis of the mathematical tyre model simulation.

The modelling results are verified by comparisons with measured data and it is then argued that the model is sufficiently accurate and economical in computing requirements to be used in vehicle simulation studies. Accurate predictions of off-road tyre forces are essential when studying off-road vehicle handling and stability behaviour because these are the external forces which are responsible for guiding, braking and propelling the vehicle.

5.2. DEVELOPMENT OF MODEL

The key to developing a comprehensive model of an off-road tyre is the ability to predict accurately the force system at the tyre-soil interface. The behaviour of off-road tyres at the tyre-soil interface is governed by forces originating from external sources above the soil surface and reaction forces from the soil against them. This reaction comes through the tyres via the spoke contacts of the wheel on the soil surface.

The model can be described as a simple and straightforward approach utilising the idea of the tyre being formed by a series of radial spokes, each spoke having three degrees of freedom, laterally, longitudinally and radially. Fig.(5.1) illustrates the behaviour of the spoke tip under conditions of static tyre deformation on a deformable surface.

In the case of steady-state rolling conditions, Fig.(5.2) shows the spoke tip behaviour in the contact region, the spoke tips will deflect in three directions (if there is any lateral wheel movements) circumferentially, radially and laterally, though for clarity the lateral deflection is not shown in the diagram. The soil will also be deformed under these spoke tip movements. These spoke tip deflections will imply forces in longitudinal, radial and lateral directions respectively with the soil surface generating forces against them as shown in Fig.(5.3).

5.3. MATHEMATICAL ANALYSIS

As described in Fig.(5.3), the spoked tyre model is moving at a constant forward speed, U, with constant spin velocity, ω, and tyre load, W, under operating condition of wheelslip, s, and slip angle, α, on a deformable soil. Suppose the entry contact angle (angle between centreline of the tyre and forward position) is, θ_1, and the rear contact angle(angle between the centreline of the tyre and the rear contact position) is, θ_2.

Calculations start from the point when the first spoke enters into the soil surface at the front of the contact region. The tyre is moving forwards and rotates a small amount, the rotation being sufficient to make the particular spoke of interest become the second in the contact region. At this point, the next proceeding spoke has just touched the contact region.

Because the tyre movement in the time increment described are completely specified, the radial, lateral and longitudinal deflections can be related directly to instantaneous tyre forces and soil shear forces in the contact region. Referring to Fig.(3.12) in Chapter 3, the contact region is divided into two portions. The first portion

is defined as the deformable region and the other portion is defined as the compacted region.

The equations of the force equilibrium relationships through the length of the contact region can be described as follows :-

For the deformable region of the contact area

According to Fig.(5.3), the point, O, represents the position of the tyre centre at time zero and OA is the first spoke just to touch the contact region at this time. OA has an undeflected length, R, will be at an angle, θ_1, to the vertical. After a small time increment, δ_t, the spoke tip will be at B_1 (case of the rigid wheel with soft soil) or at B_2 (case of the hard surface). Because the surface is deformable and the spoke has radial, lateral and circumferential tip flexibilities, the spoke at point B needs to achieve equilibrium between the radial spoke tip force, f_r, and the component of ground reaction force, f_g. These equilibrium forces can be written as follows :-

$$f_r = f_g \, Cos\theta \tag{5.1}$$

where

$$f_r = K_1 \, (1 - e^{-K_2 \, DR}) \tag{5.2}$$

$$f_g = (\frac{K_c}{b} + K_\phi) \, Z^n \, CAH \tag{5.3}$$

where

K_1, K_2 = Tyre stiffness parameters

DR = Radial spoke deflection

P_g = Normal ground pressure

K_c = Cohesive soil modulus

K_ϕ = Frictional soil modulus

b = Width of tyre contact patch

Z = Soil sinkage

n = Exponent of soil deformation

CAH = Projected area of the contact patch

θ = Spoke angle

Then by substitution into equation (5.1), the equilibrium equation in the radial direction is :

$$\left(\frac{K_c}{b} + K_\phi\right) Z^n \, CAH \cos\theta = K_1 \left(1 - e^{-K_2 DR}\right) \tag{5.4}$$

Note that the spokes are free to deform in the radial, lateral and longitudinal directions, so that the spoke will be deforming circumferentially due to the soil shear displacement, j, as well as due to soil sinkage, Z. Fig.(5.4) indicates the spoke behaviour in the $X-Y$ plane with soil force components, f_{s_x} and f_{s_y} that can be written as :

$$f_{s_x} = \left(\frac{j_x}{j}\right) f_s \tag{5.5}$$

$$f_{s_y} = \left(\frac{j_y}{j}\right) f_s \tag{5.6}$$

where

$$f_s = (c + P_g \tan\phi)\left(1 - e^{-j/K}\right) \, CAH \tag{5.7}$$

and

$$j = \sqrt{j_x^2 + j_y^2} \tag{5.8}$$

where

j_x = Longitudinal soil deformation

j_y = Lateral soil deformation

K = Soil deformation modulus

ϕ = Soil internal friction angle

j = Soil shear displacement

The spoke tip also has two force components f_b and f_y in longitudinal and lateral directions respectively written as follows :

$$f_b = \eta_x K_4 \tag{5.9}$$

$$f_y = K_5 (1 - K_6 DR^{K_7}) \eta_y \tag{5.10}$$

where

K_4, K_5, K_6, K_7 = Tyre stiffness parameters

η_x = Longitudinal tyre deflection

η_y = Lateral tyre deflection

By substitution, the equilibrium equations in longitudinal and lateral directions become :-

$$\left(\frac{K_c}{b} + K_\phi\right) Z^n CAH \sin\theta + \left(\frac{j_x}{j}\right) f_s = \eta_x K_4 \tag{5.11}$$

$$K_5 (1 - K_6 DR^{K_7}) \eta_y = \left(\frac{j_y}{j}\right) f_s \tag{5.12}$$

With a loaded, steady state rolling tyre on a deformable surface, equilibrium occurs in between soil and tyre deformations. The soil deformation is plastic while the tyre deformation is elastic. However, the lateral deformation is divided into two main parts, one part due to spoke deformation and other part due to soil shear displacement as shown in Fig.(5.5). These deformations vary under any operating condition through the length of the contact region and can be described as :

$$j_x + \eta_x = \eta_{x_k} \tag{5.13}$$

$$j_y + \eta_y = \eta_{y_k} \tag{5.14}$$

where η_{x_k} and η_{y_k} are kinematic spoke tip deflections in circumferential and lateral directions respectively.

Once again, Fig.(5.3) shows the geometry of the spokes indicating clearly the first spoke tip position after entering into the soil surface. Equilibrium occurs at this point for which :

$$R\,Cos\theta_1 + Z + \eta_x\,Sin\theta = (R - DR)\,Cos\theta \tag{5.15}$$

Similar calculations for the compacted region are summarised as follows :-

For the compacted region of the contact area

The rear angle, θ_2, calculated as described in Chapter 3 :-

$$\theta_2 = Cos^{-1}\left(Cos\theta_1 + \frac{Z_{max}}{R}\right)$$

where

R = Undeflected tyre radius

Z_{max} = Maximum soil sinkage

So the equilibrium spoke tip force equations are :

$$P_g = \left[K_1\,(1 - e^{-K_2 DR})\cos\theta + \eta_x K_4 \sin\theta\right] / A_c \tag{5.16}$$

$$f_s = (c + P_g \tan\phi)\,(1 - e^{-j/K})\,A_c \tag{5.17}$$

$$\left(\frac{j_x}{j}\right) f_s = \eta_x K_4 \tag{5.18}$$

$$\left(\frac{j_y}{j}\right) f_s = K_5\,(1 - K_6\,DR^{K_7})\,\eta_y \tag{5.19}$$

$$j = \sqrt{j_x^2 + j_y^2} \tag{5.20}$$

$$j_x + \eta_x = \eta_{x_k} \tag{5.21}$$

$$j_y + \eta_y = \eta_{y_k} \tag{5.22}$$

$$R\,Cos\theta_1 + Z_{max} - \eta_x\,Sin\theta = (R - DR)\,Cos\theta \tag{5.23}$$

where b, R, K_c, K_ϕ, ϕ, c and n are quoted in Chapter 4, Table(4.1).

These calculations in both the deformable and compacted regions are then repeated for each time increment as the spoke passes through the contact region, with the forces being stored at each step. These steps continue until the spoke leaves the contact region and the total wheel tyre force system is then computed over all the length of the contact area.

The relationships between the tyre deflections and their corresponding forces, are modelled by rolling a tyre on hard ground and are described by a set of parameters called "spoke stiffness parameters" which are chosen and compared with experimental data obtained by Schwanghart [1981] for a 7.50 x 18 front tractor tyre rolling on a hard surface as shown in Figs.(5.6).

The objective in choosing the spoke stiffness parameters K_1, K_2, K_4, K_5, K_6 and K_7 is to match the shape of the relationships between the gross tyre forces and the tyre deflection and sideslip angle on hard ground. Parameters K_1 and K_5 govern the magnitudes of the maximum values of the radial and lateral spoke forces respectively. Other parameters are chosen to control the shape of the spoke tip force relationships with various deflections in order to get a good pressure distribution throughout length of the contact region. The remaining parameters concern the shear force and the soil shear displacement relationships between the spoke tips and the ground.

The spoke stiffness parameters used are :-

$$K_1 = 4.8\ kN$$

$$K_2 = 64\ m^{-1}$$

$K_4 = 14\ kN/m$

$K_5 = 15.4\ kN/m$

$K_6 = 100$

$K_7 = 1.95$ (with DR in metres)

Equations (5.4), (5.7), (5.8) and (5.11 to 5.15) become eight simultaneous equations in eight unknowns, j_x, j_y, j, Z, η_x, η_y, DR and f_s. To obtain a solution, a numerical analysis must be used and a computer programme is therefore required.

Finally, the spoke tip deflections and soil deformations are used to calculate tyre forces in the lateral, longitudinal and vertical directions via the stiffness parameters mentioned above. However, the total vertical force components must be equal to the input tyre load. This condition can thus be stated as :-

$$F_z = \sum_{i=1}^{i=N} f_z \text{ due bending} + \sum_{i=1}^{i=N} f_z \text{ due radial} \qquad (5.24)$$

As a result, the total vertical force is then expressed as :

$$F_z = \sum_{i=1}^{i=N} \eta_x K_4 \sin\theta + \sum_{i=1}^{i=N} K_1 (1 - e^{-K_2 DR}) \cos\theta \qquad (5.25)$$

where

i = Spoke number

N = Number of spokes in the contact region

Note that for a rolling tyre on a hard surface the spoke tip may remain stationary at the first point of contact with the ground or it may slide to an equilibrium position at which the carcass forces and friction forces are equal. In fact, the main difference between the spoke behaviour on hard and soft surfaces is that in case of off-road surfaces, the spoke tip is never in the kinematic (no sliding) condition. The spoke tips must always slide due to the soil shear displacement until an equilibrium position is

established.

With regard to the behaviour of the tyre on a hard surface, Fig.(5.7a) illustrates the small element for the tyre under braking conditions which describes the longitudinal deformation, δ_x, as follows :-

Suppose that A moves small a distance, x, and B moves distance, x', at the same time, δ_t, where ;

$$x = R\,\omega\,\delta_t \tag{5.26}$$

$$x' = U\,\delta_t \tag{5.27}$$

The difference between these two distances is called "the longitudinal deformation", can be expressed as :

$$\delta_x = x' - x = \left(1 - \frac{\omega R}{U}\right) x' \tag{5.28}$$

where

U = Tyre forward velocity

ω = Spin velocity of the tyre

δ_t = Small time increment

x, x′ = Distance in longitudinal direction

δ_x = Longitudinal tyre deflection

and as described in Chapter 4, the wheelslip, s, is equal to $\left(1 - \frac{\omega R}{U}\right)$, then

$$\delta_x = s\,x' \tag{5.29}$$

or

$$\frac{(1-s)}{s} = \frac{x}{\delta_x} \tag{5.30}$$

This gives the longitudinal deformation as :

$$\delta_x = \frac{s}{(1-s)}\,x \tag{5.31}$$

Therefore, the lateral deformation, δ_y, can then be calculated as :

$$\delta_y = \frac{\tan\alpha}{(1-s)}\, x \tag{5.32}$$

Similarly, Fig.(5.7b) indicates the small element for a rolling tyre under tractive operating conditions which leads to the longitudinal and lateral deformations as follows :-

$$\delta_x = s\, x \tag{5.33}$$

$$\delta_y = (1-s)\tan\alpha\; x \tag{5.34}$$

Note also that the longitudinal and lateral deformations described in equations (5.13), (5.14), (5.21) and (5.22) in the case of the traction condition, can be now expressed as :-

$$\eta_x + j_x = sx \tag{5.35}$$

$$\eta_y + j_y = \tan\alpha\,(1-s)\,x \tag{5.36}$$

and in the case of the braking tyre, these become :

$$\eta_x + j_x = \frac{s}{(1-s)}\, x \tag{5.37}$$

$$\eta_y + j_y = \frac{\tan\alpha}{(1-s)}\, x \tag{5.38}$$

where x is longitudinal displacement.

5.4. SPOKE TYRE COMPUTER PROGRAMME

The method of solution is summarised by the flow chart in Fig.(5.8). The flow chart shows the programme structure including seven subroutines called; Soft, Hard, Sharp, Adjust, Angle, Sinkage and Plot. The main programme is used to specify the running conditions and to call all these subroutines.

This programme is capable of showing graphically, the tyre and soil forces and their deformation distributions f_x, f_y, f_z, f_g, f_s, η_x, η_y, DR, j_x, j_y, j and Z. In order to

run this programme, it must be initialised with a set of running conditions {entry angle, soil data and the tyre data which are shown in Table (4.1) } and operating conditions (slip angle, wheelslip or wheelskid and tyre load).

Subroutine Soft calculates the values of spoke tip deflections, soil deformations, soil sinkage, spoke tip and ground forces under the deformable region. Subroutine Hard is used to calculate these parameters under the compacted region. By using subroutine Sharp, the values of η_{x_k} and η_{y_k} can be determined.

To calculate the entry angle, θ_1, and the correct number of spokes , N, in the contact region, subroutine Angle is used. Subroutine Sinkage is used in order to iterate entry angle and hence recalculate maximum soil sinkage, Z_{max}, in order for the summation of vertical component forces to equal the tyre load.

The bisection method inside the Adjust subroutine has been used in the programme in order to calculate the equilibrium point involving the balance between the soil shear force, f_s, and the elastic shear force required at spoke tip, f_t, as shown in Fig.(5.9). The soil shear force must be greater than or equal to the spoke tip force resultant where :

$$f_s \geq \sqrt{f_x^2 + f_y^2} \tag{5.39}$$

where

f_s = Soil shear force

f_x = Spoke force in fore and aft direction

f_y = Spoke force in lateral direction

Subroutine Plot is used to provide graphical output to the computer terminal with hardcopy to illustrate the results of the computer programme.

5.5. SPOKE TYRE FORCE CHARACTERISTICS

The behaviour of the tyre and soil through the length of the contact region are shown in Figs.(5.10 to 5.12). These diagrams should give an indication of tyre deflection and soil deformation. Fig.(5.10) shows the longitudinal distributions of tyre deflection and of soil deformation. Lateral deflection distributions are illustrated in Fig.(5.11). The variations of the radial tyre deflection and the soil sinkage through the contact region are depicted in Fig.(5.12). Fig.(5.13) shows the distributions of spoke tyre forces in longitudinal, lateral and vertical directions respectively under the operating condition of 10^{o} slip angle and 10% of wheelslip.

Typical results from the spoke tyre model operating on a sandy loam soil are shown in Figs.(5.14) and (5.15). The lateral tyre force as a function of tyre load and slip angle is plotted as a carpet plot in Fig.(5.14). The longitudinal tyre force behaviour as indicated in Fig.(5.15) for a 7.50 x 18 front tractor tyre is plotted with a wide range of operating conditions.

5.6. CONCLUDING REMARKS

(1) A model for predicted longitudinal and lateral off-road tyre forces which is in a form for use in vehicle handling and stability models is presented.

(2) Results from the off-road tyre model become the same as those obtained by the on-road tyre model when the soil parameters are changed to make the soil infinitely stiff.

(3) The magnitudes of the forces predicted by multi-spoked tyre model for off-road surfaces are generally lower than those predicted by an on-road tyre model as seen in Figs.(5.16) and (5.17) for a 6.50-16 tyre with hard ground and soft soil respectively.

(4) The model is computationally economical and applicable to a wide range of operating conditions to give tyre and soil force distributions in detail.

(5) The multi-spoke method for modelling the tyre shows advantages over other methods because the forces obtained can be investigated in greater detail throughout the contact region and there is an attempt to include the three dimensional aspect of the tyre-soil interface.

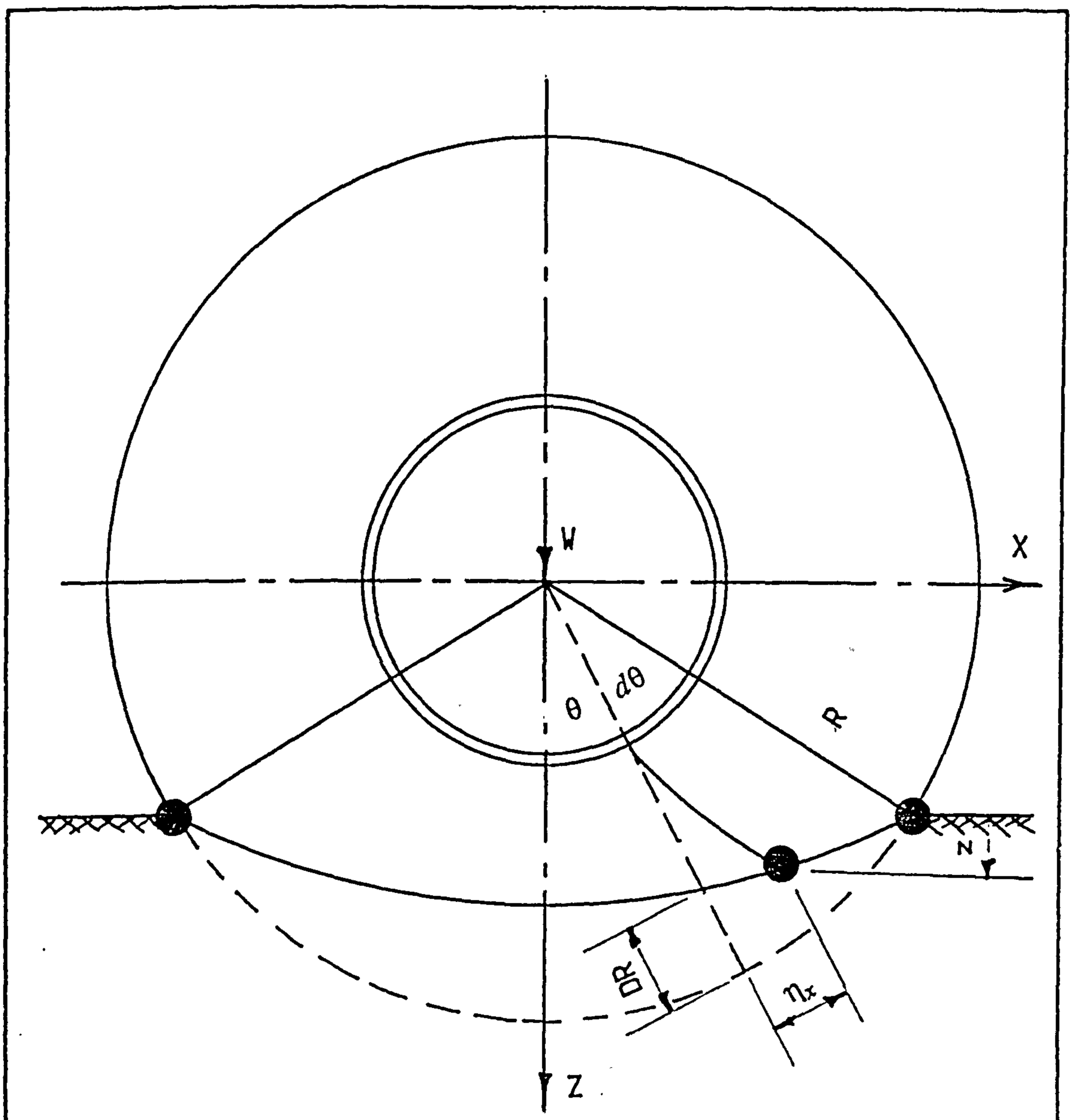

Fig. (5.1) Static multi-spoke tyre model on a deformable surface.

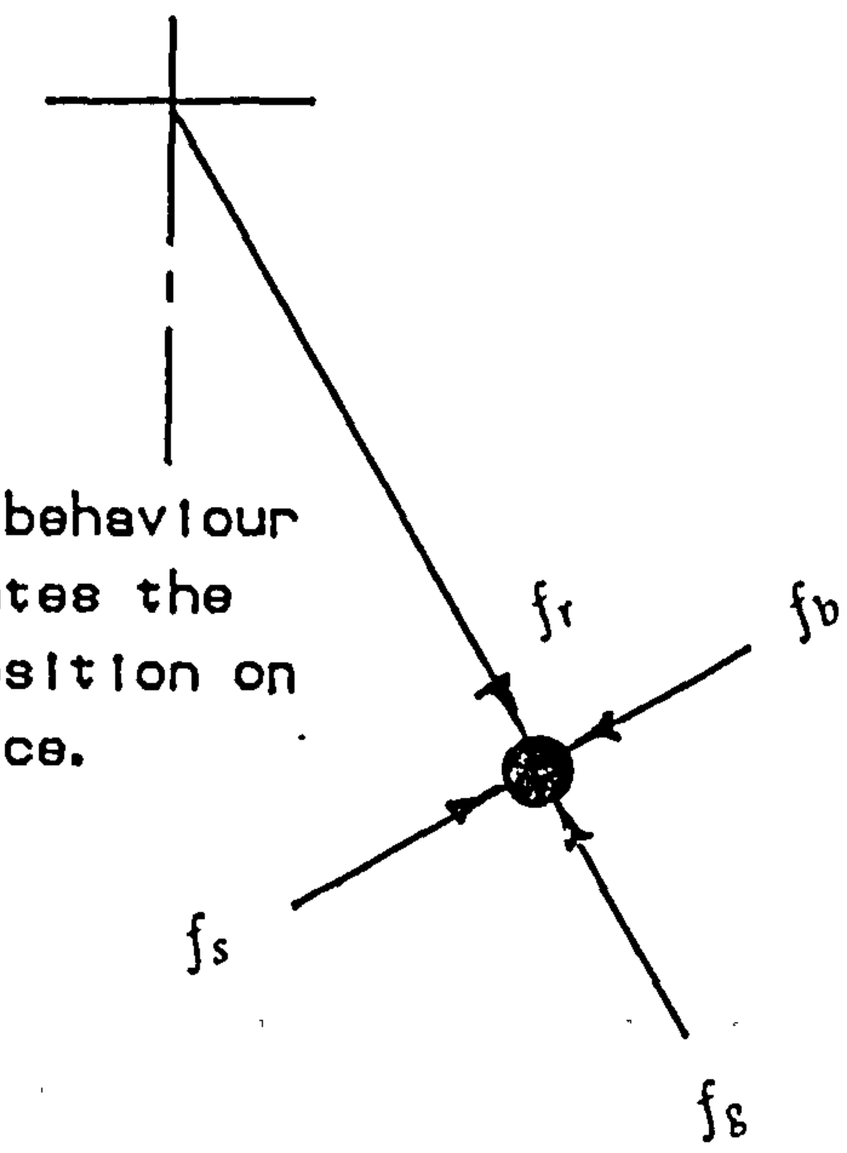

Fig. (5.2) The spoke tip behaviour which illustrates the equilibrium position on the soft surface.

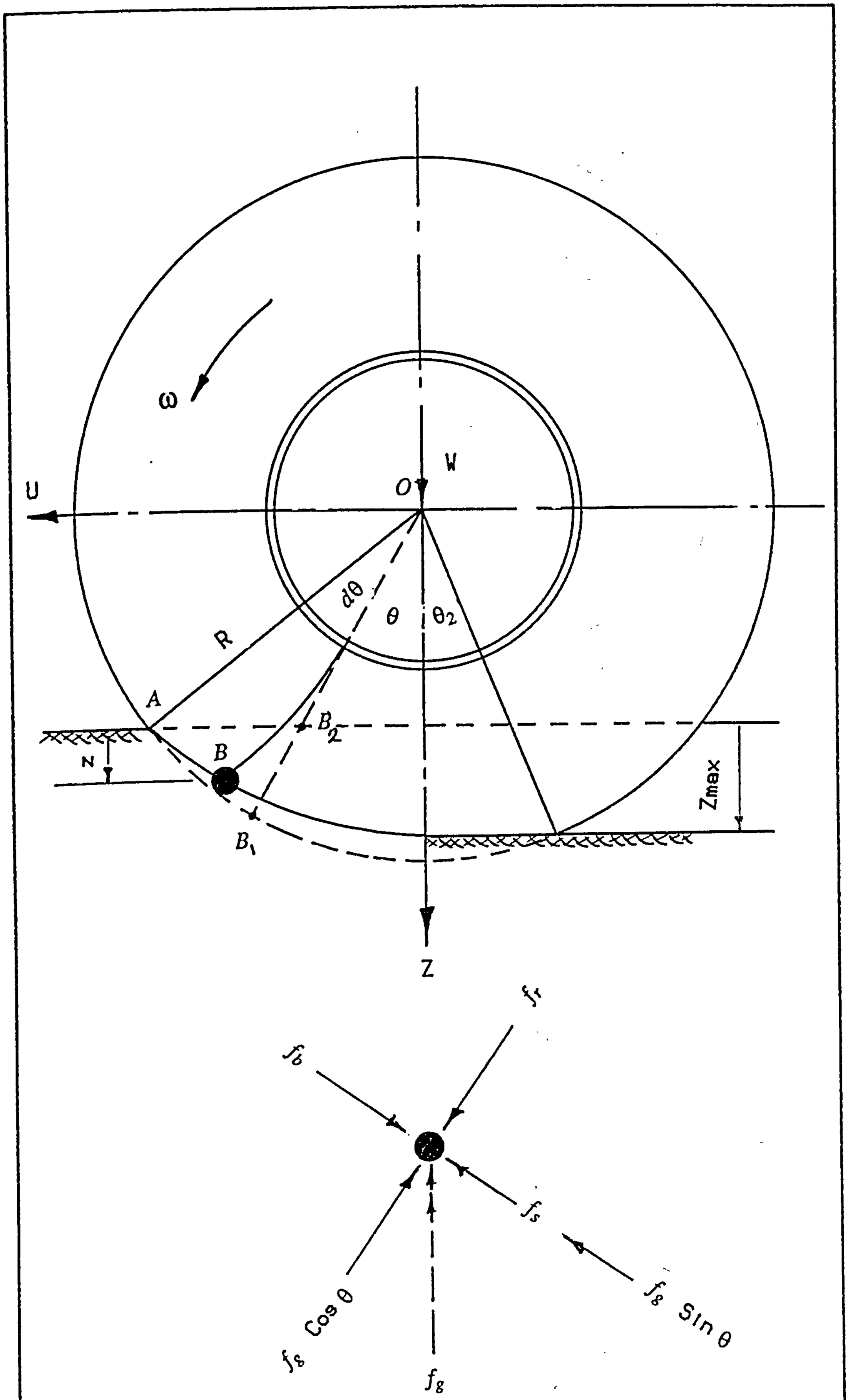

Fig. (5.3) Geometry of a spoke tip operating under steady-state conditions on a soft soil.

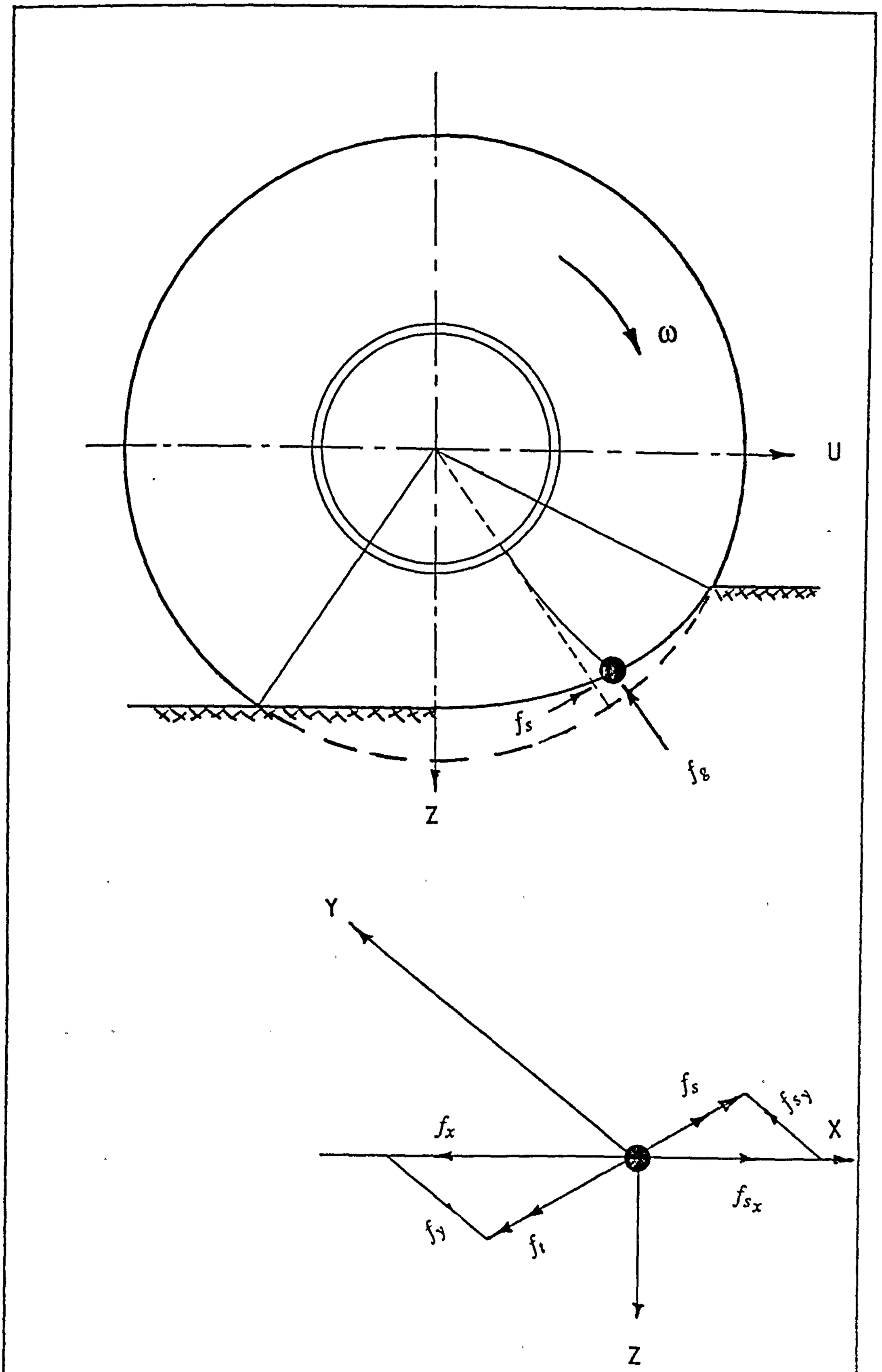

Fig. (5.4) The point which has a balance between the soil shear force and the elastic resultant spoke force in X-Y Plane.

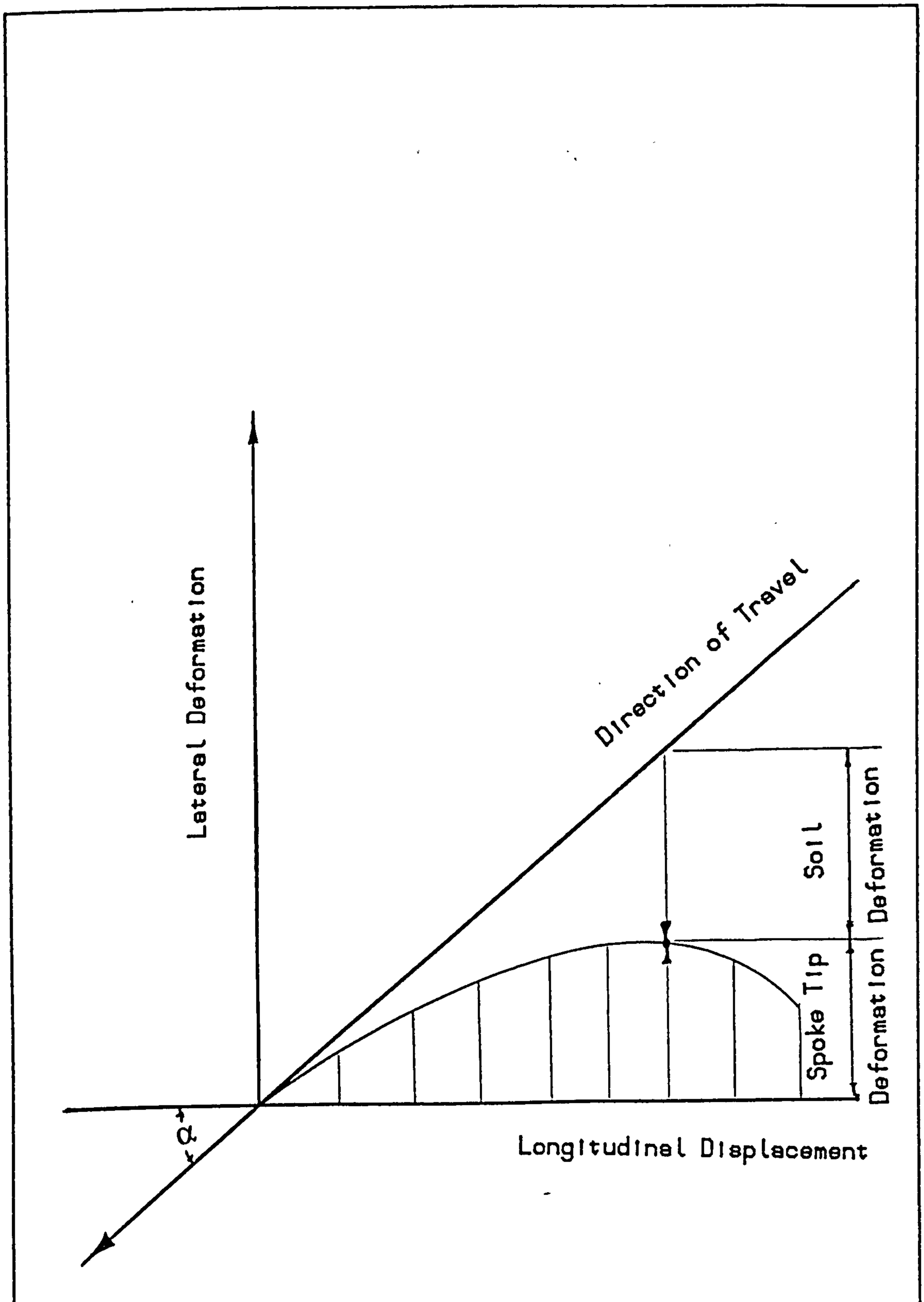

Fig. (5.5) The lateral deformations behaviour for a tyre moving on a deformable surface with zero wheelslip condition.

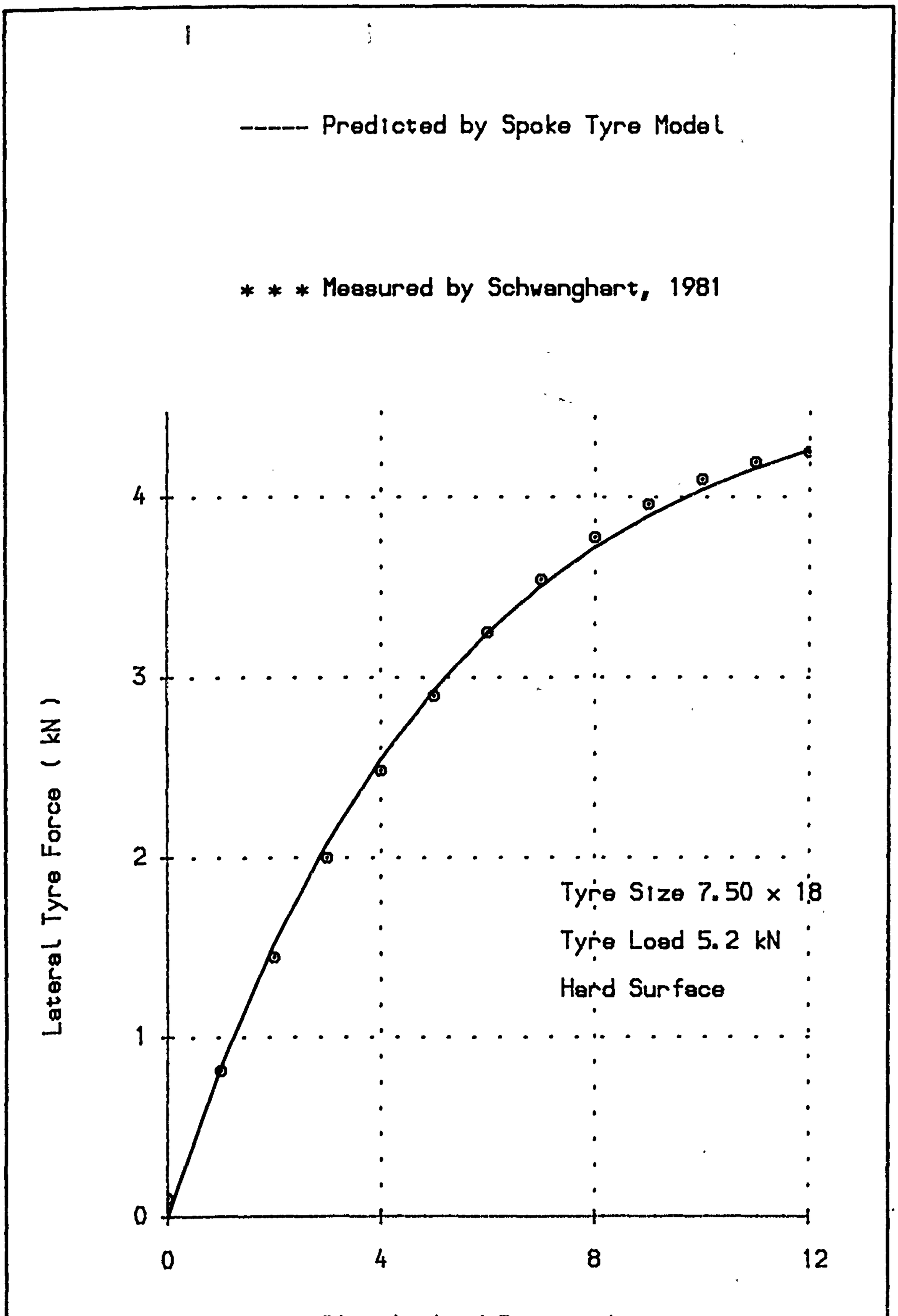

Fig. (5.6) Comparison between the predicted relationship between the lateral force and the slip angle and Schwanghart's data for a 7.50 x 18 tyre moving on hard surface.

(a)

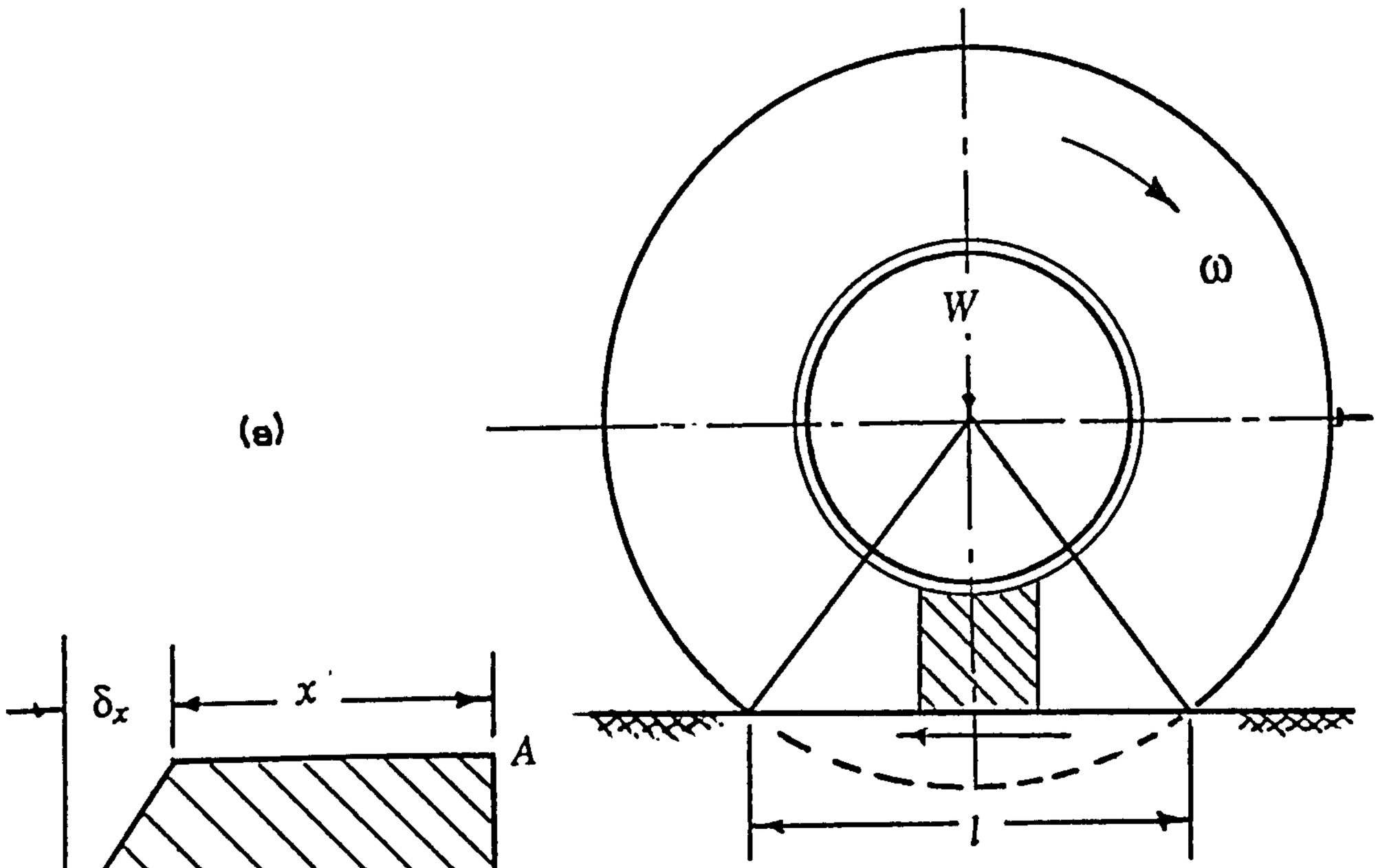

(b)

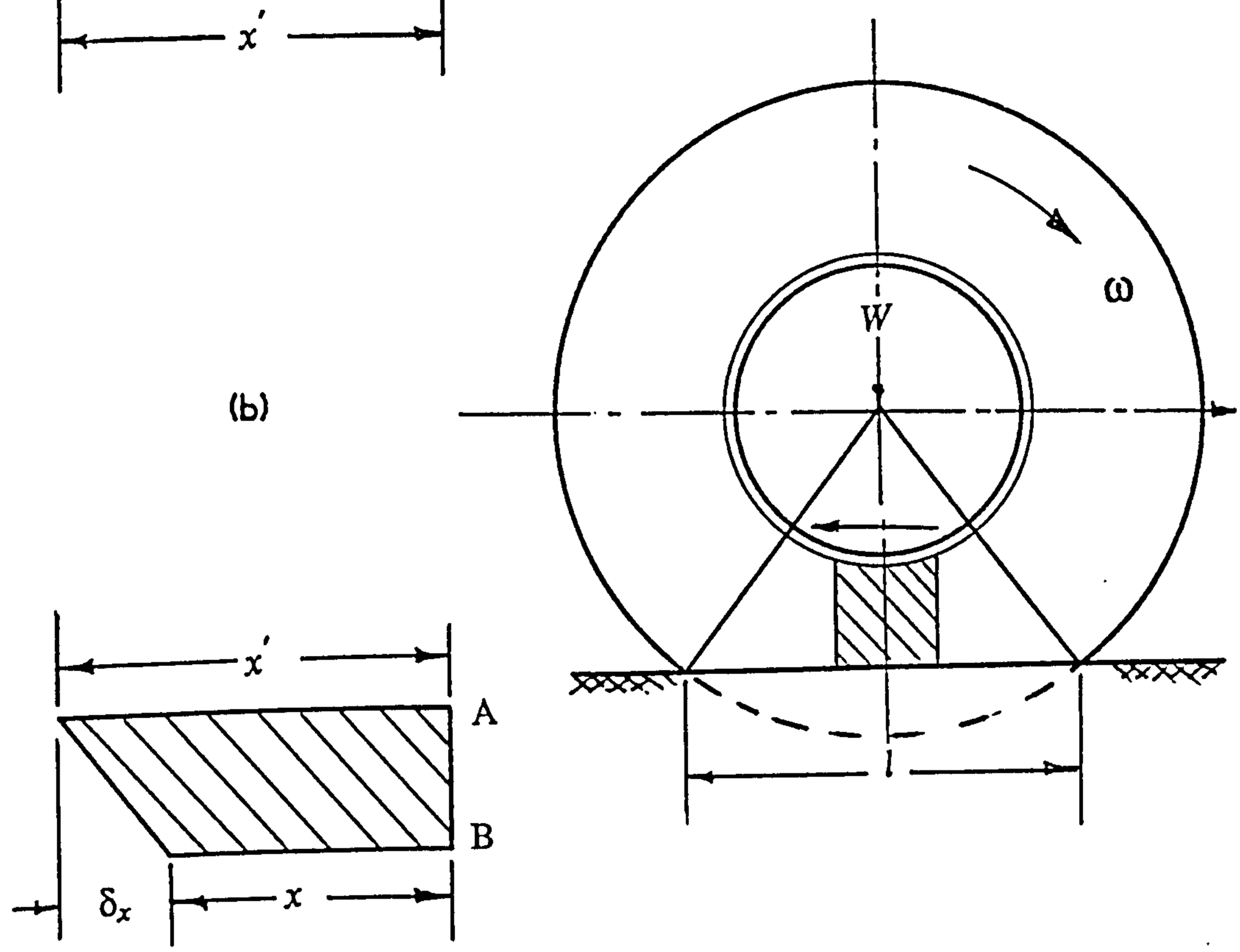

Fig. (5.7) The tyre behaviour under braking and tractive conditions for a rolling tyre on hard ground.

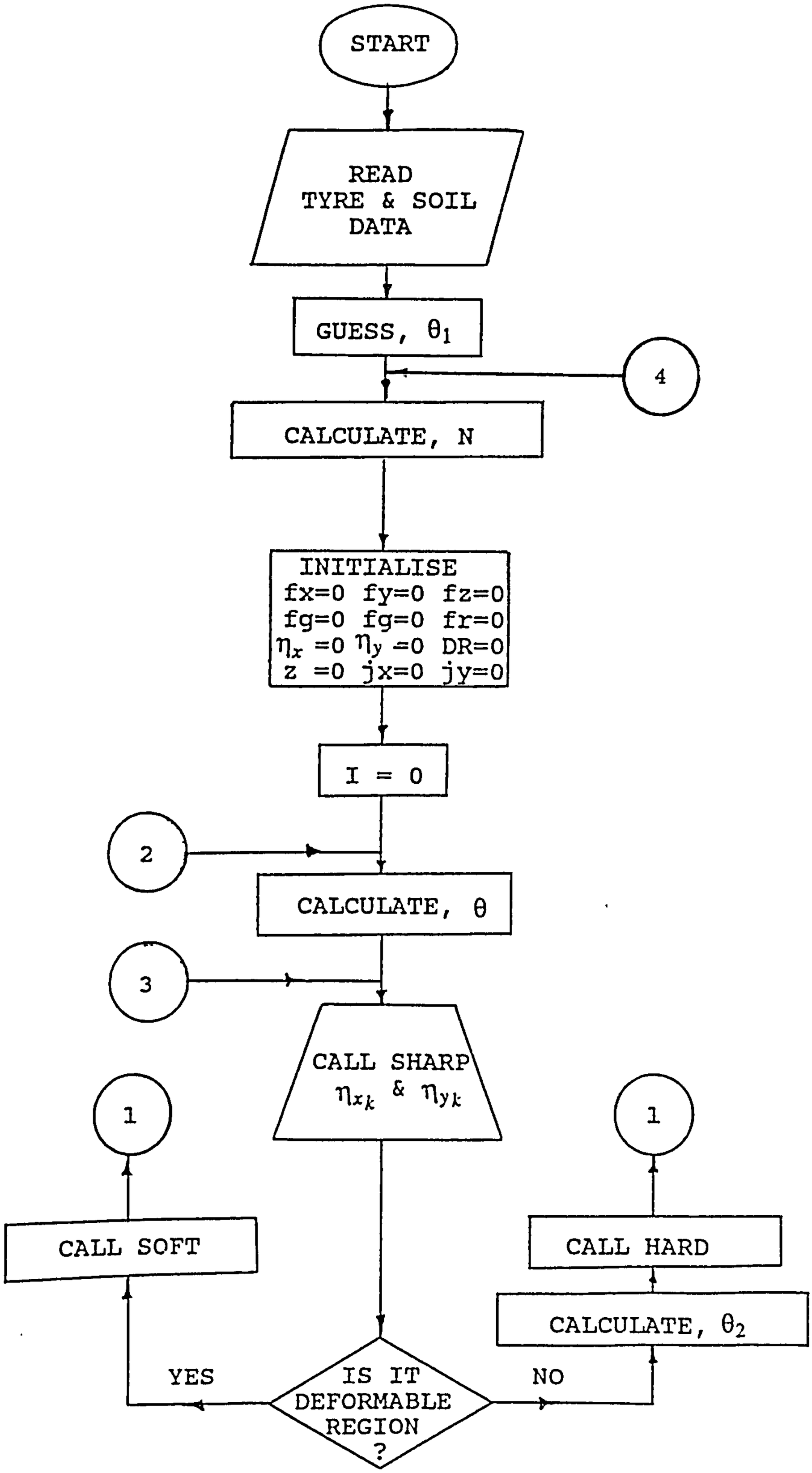
START
READ
TYRE & SOIL
DATA
GUESS, θ_1
4
CALCULATE, N
INITIALISE
fx=0 fy=0 fz=0
fg=0 fg=0 fr=0
η_x =0 η_y =0 DR=0
z =0 jx=0 jy=0
I = 0
2
CALCULATE, θ
3
CALL SHARP
η_{xk} & η_{yk}
1
CALL SOFT
1
CALL HARD
CALCULATE, θ_2
YES
IS IT
DEFORMABLE
REGION
?
NO

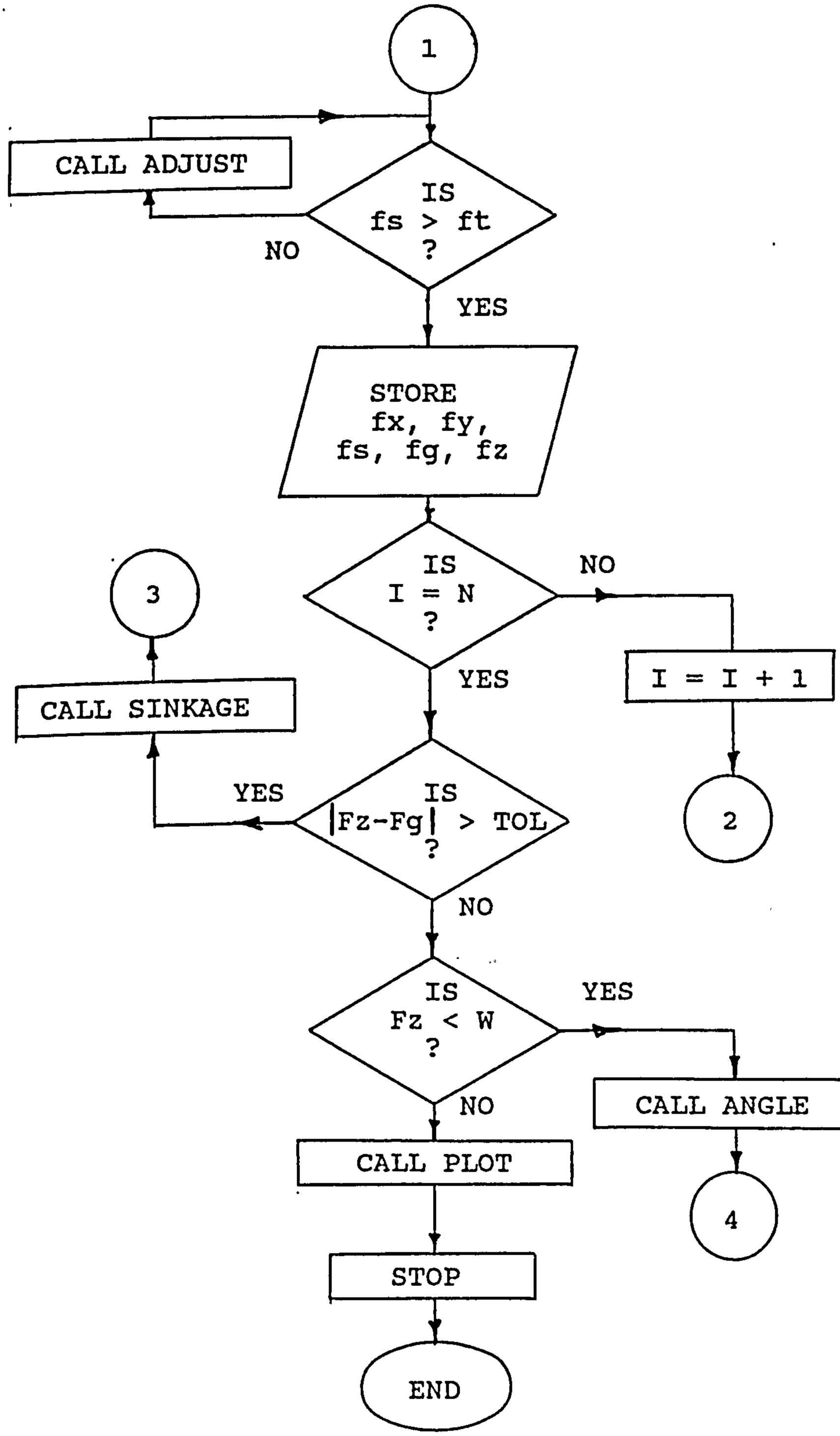

Fig.(5.8) The flow chart for the multi-spoke tyre model on off-road surfaces.

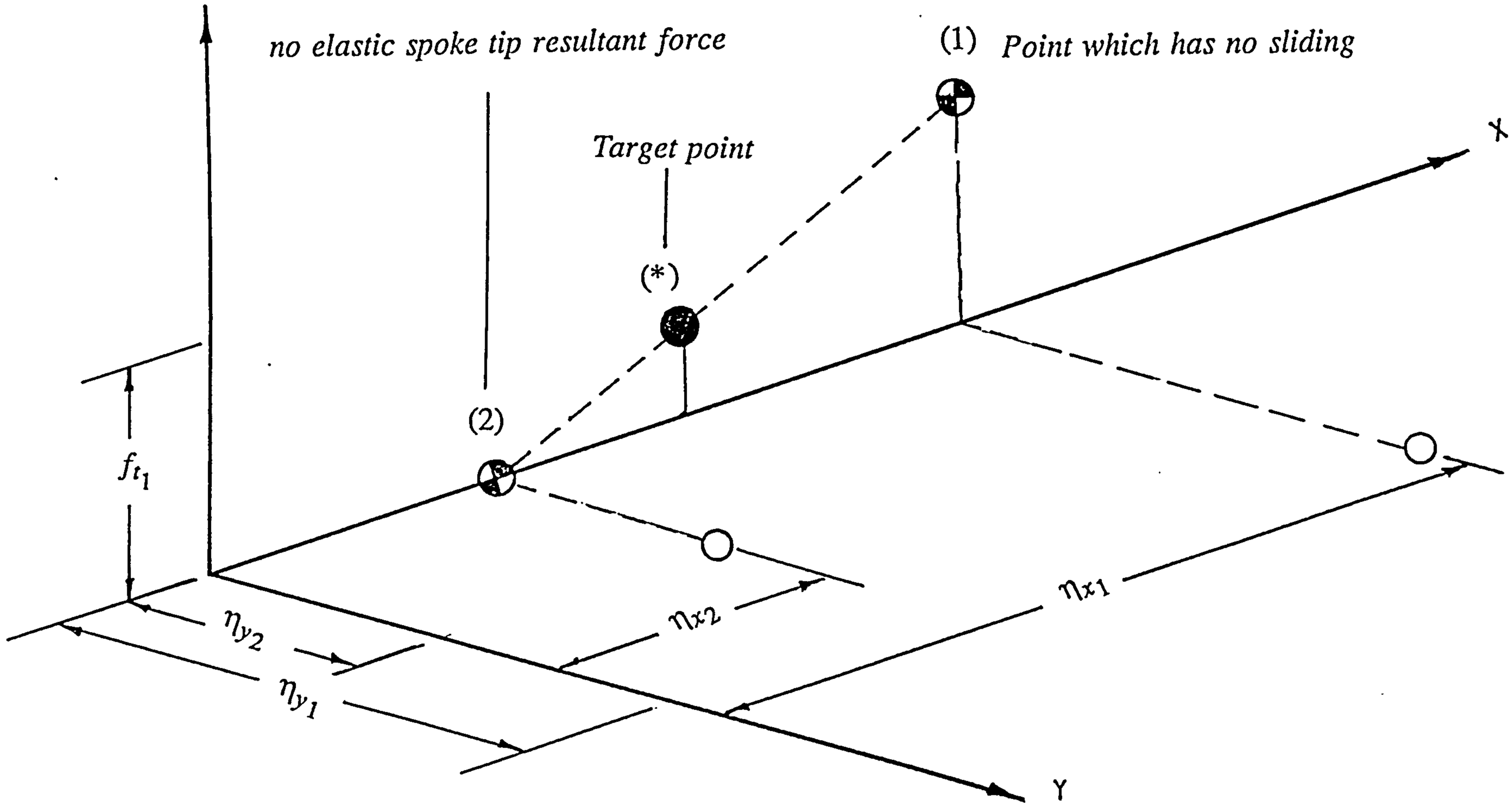

Fig. (5. 9) Using bisection method to get a point involving balance between the soil shear force and the elastic shear force required at spoke tip.

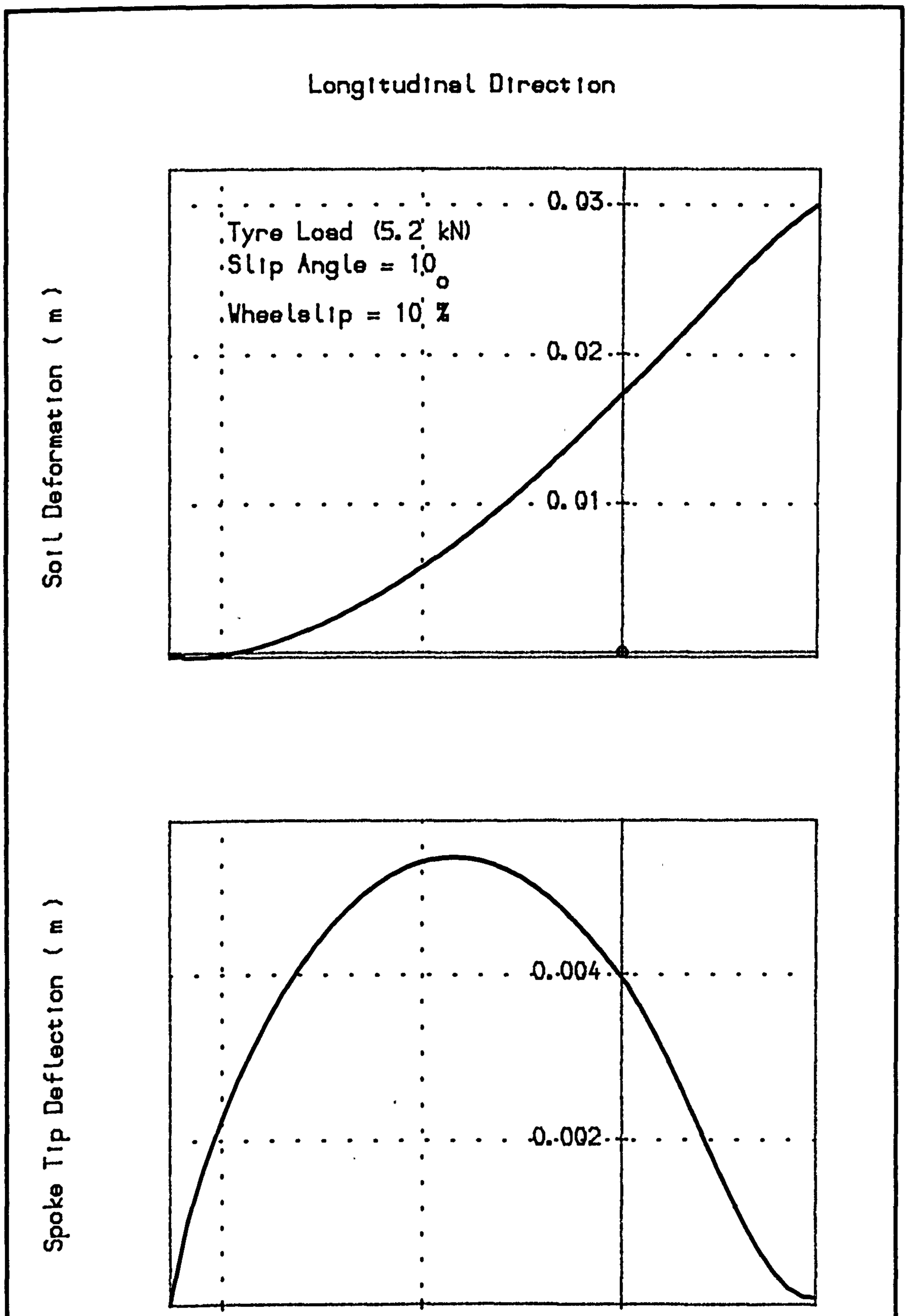

Fig. (5.10) The deformation of spoke tip and the soil in longitudinal direction on a sandy loam soil.

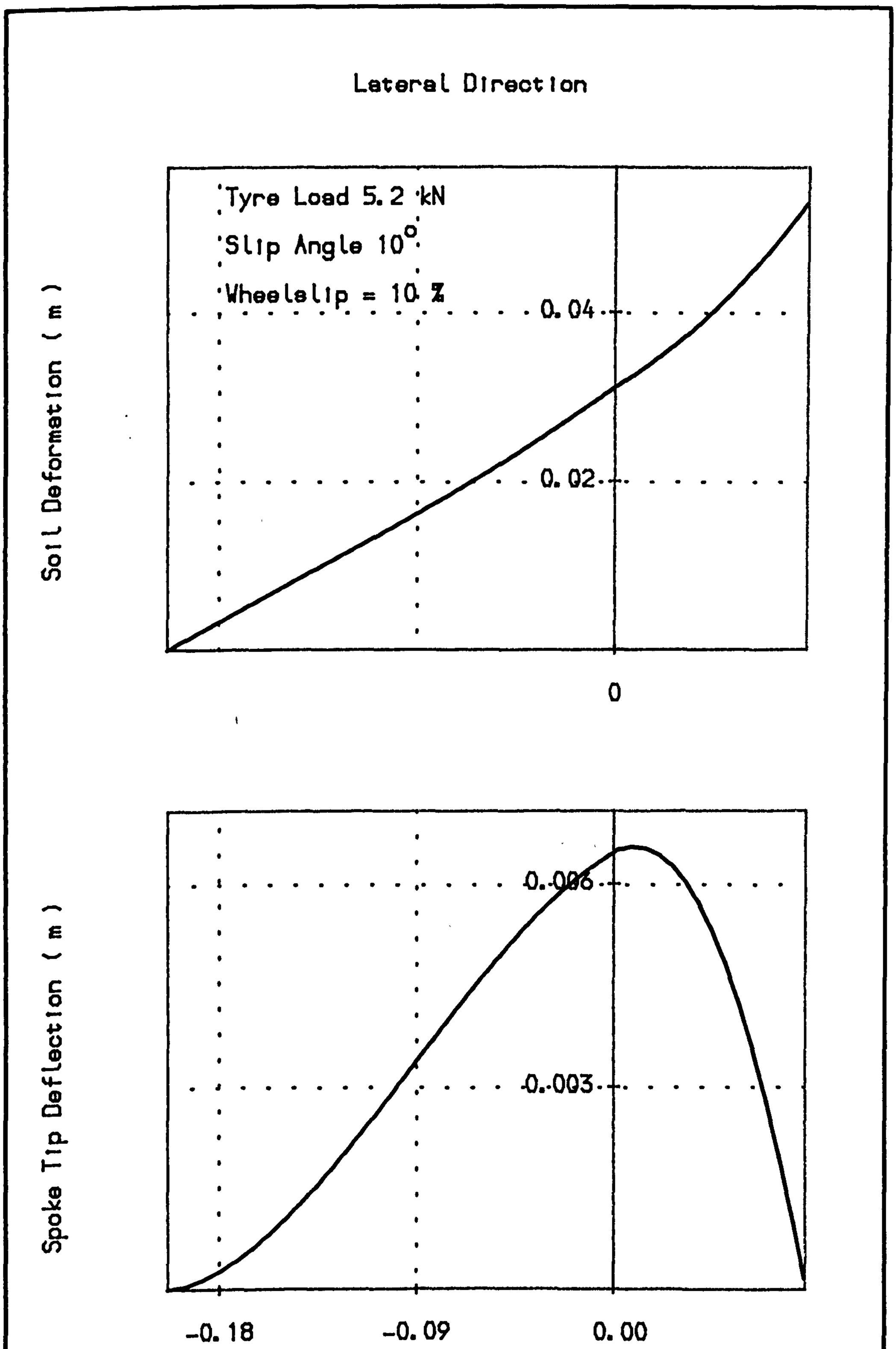

Fig. (5.11) Spoke tip deflection and soil deformation for a rolling tyre on sandy loam soil.

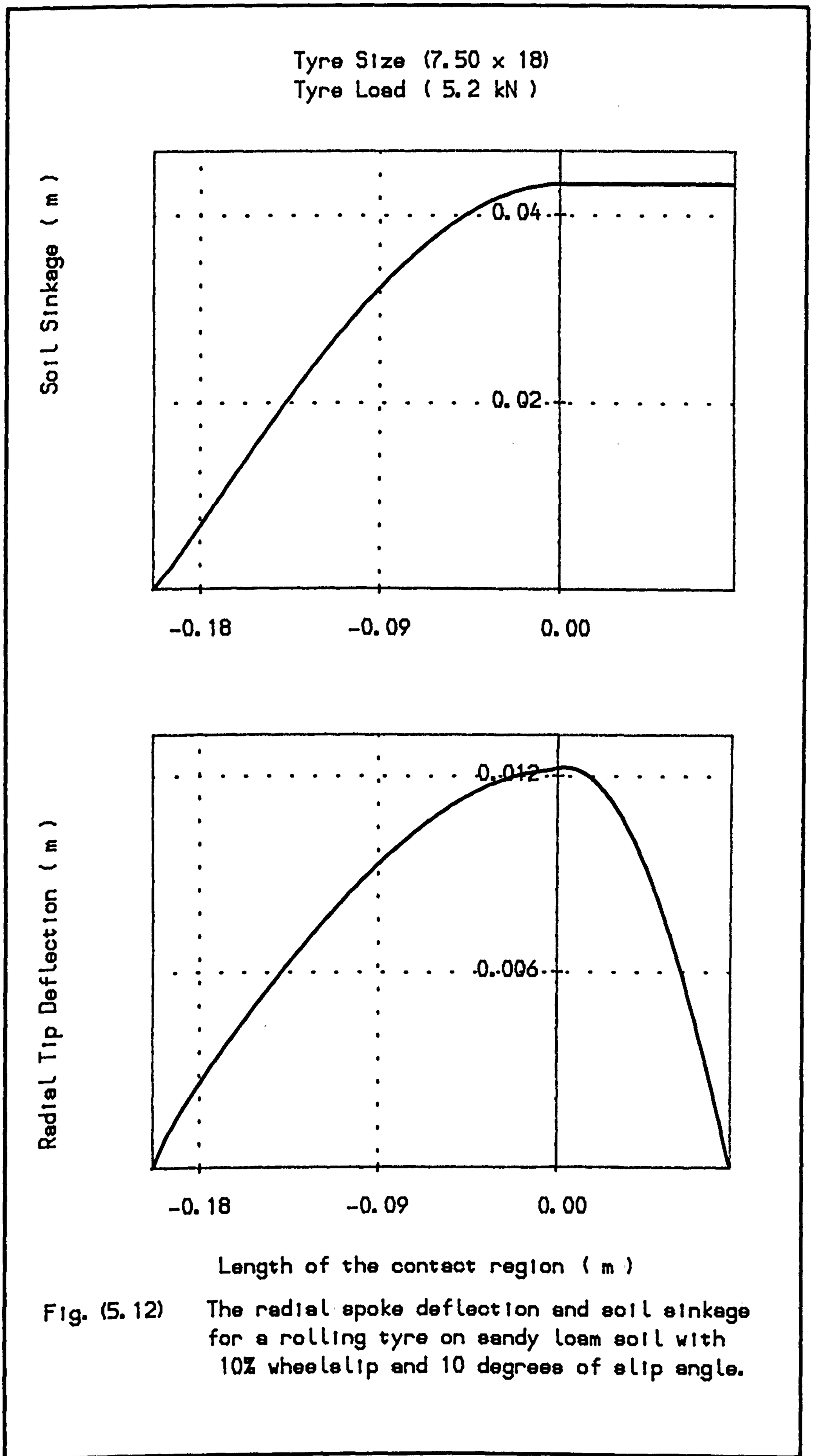

Fig. (5.12) The radial spoke deflection and soil sinkage for a rolling tyre on sandy loam soil with 10% wheelslip and 10 degrees of slip angle.

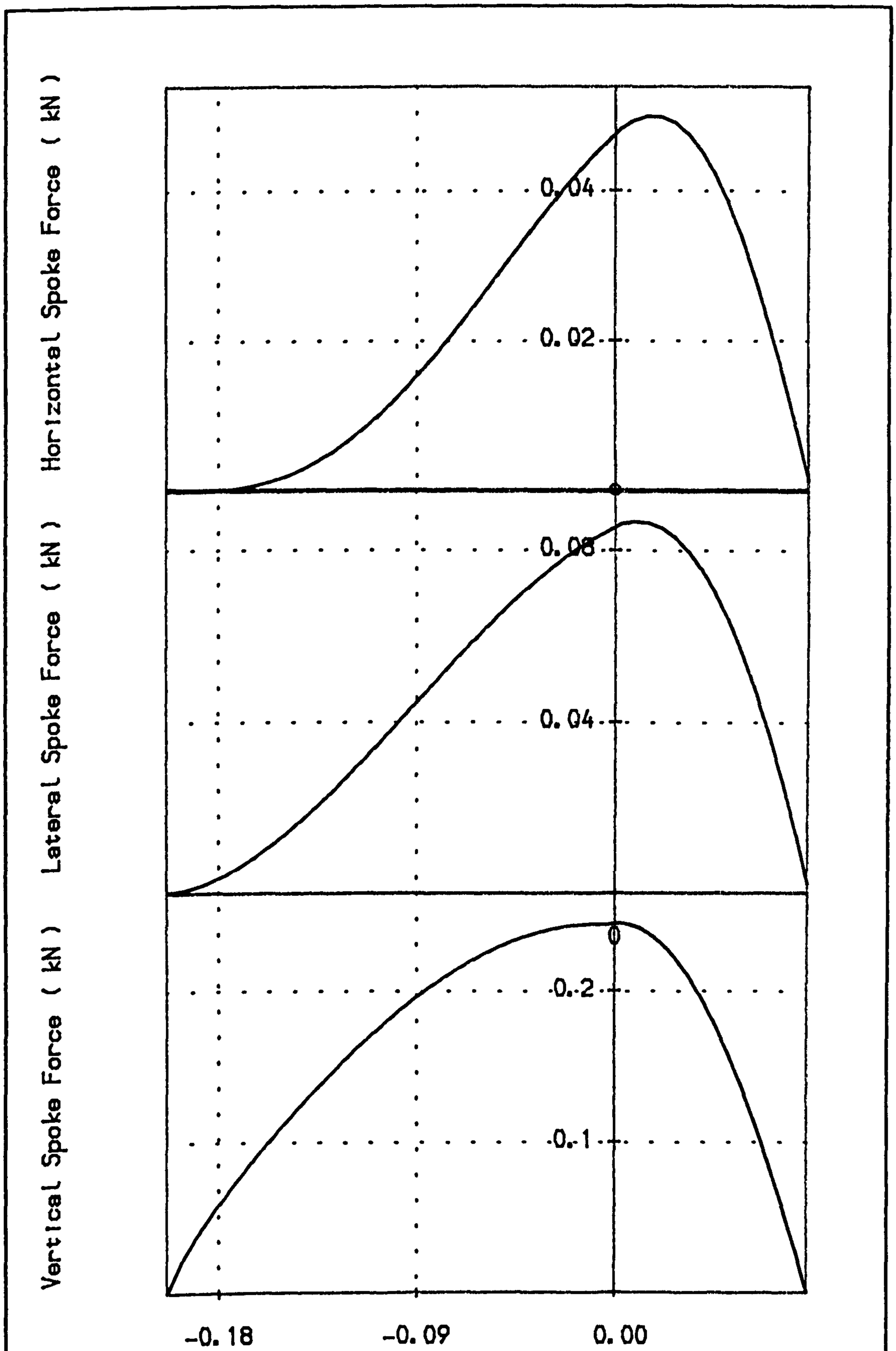

Fig. (5.13) Spoke force distributions along length of the contact region for a 7.50 x 18 tyre operating under conditions of 10% wheelslip, 10 deg of slip angle and 5.2 kN tyre load on loam soil.

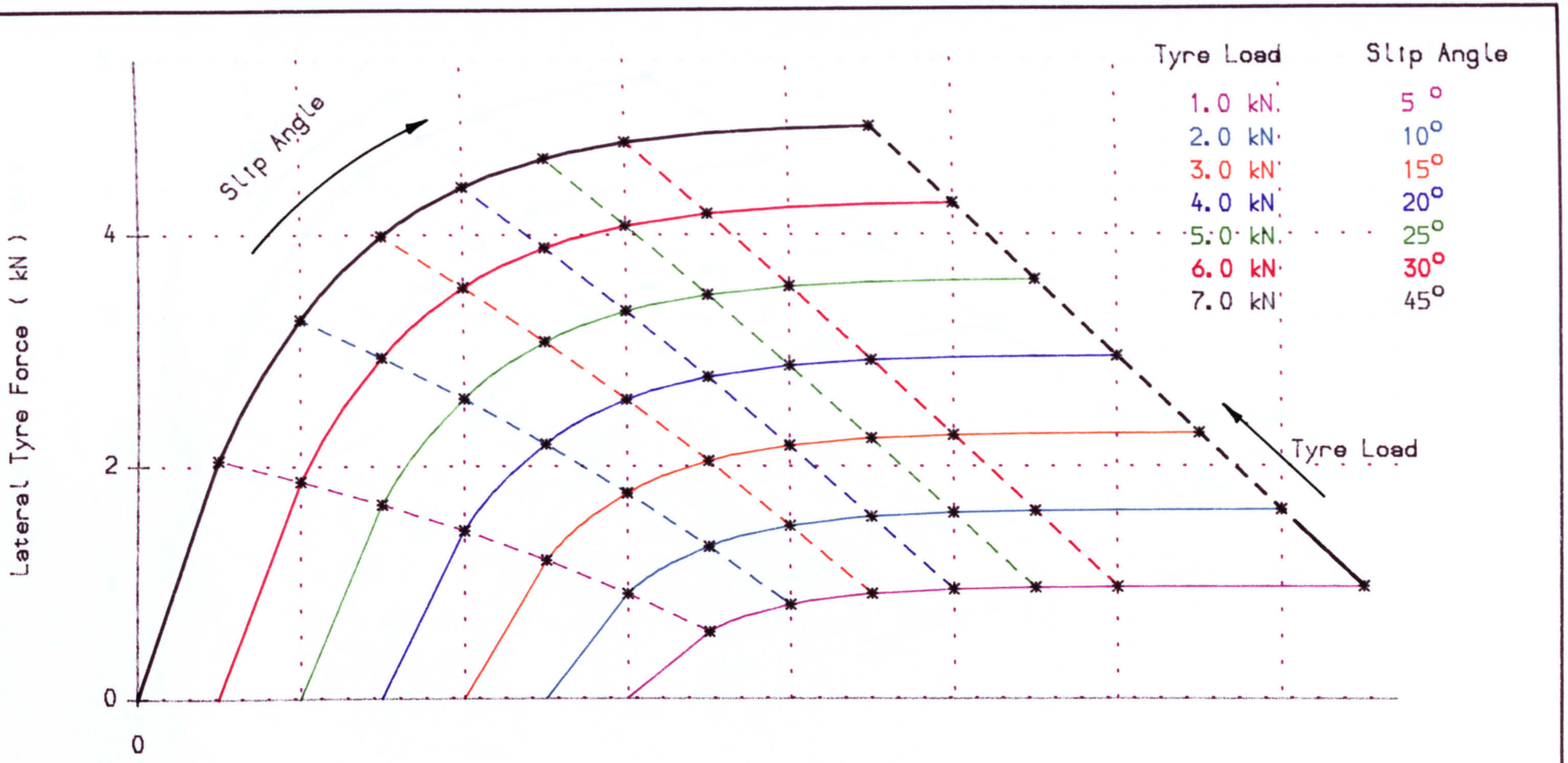

Fig. (5.14) Carpet plot of lateral tyre force as a function of tyre load and slip angle.

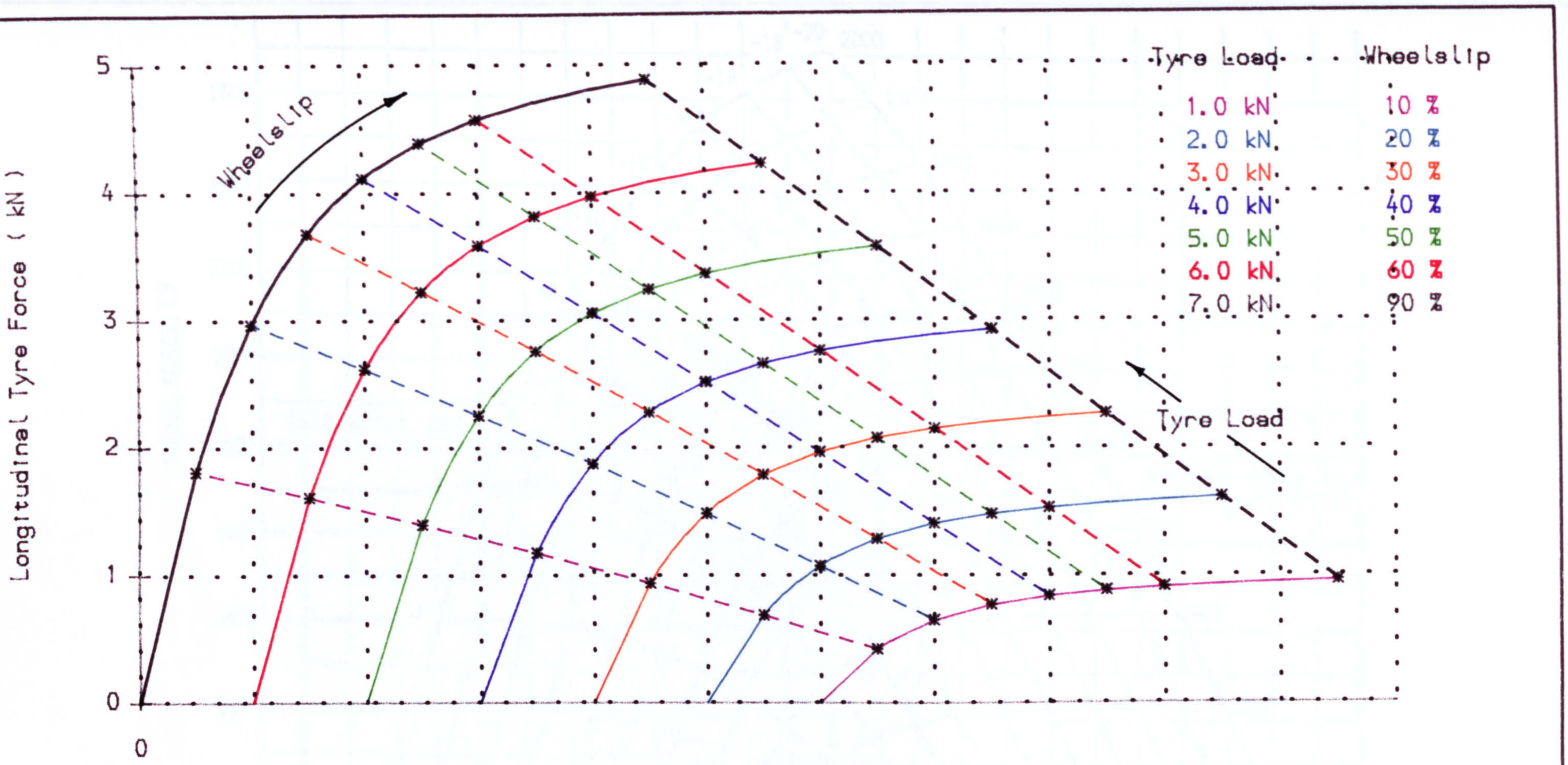

Fig. (5.15) Carpet plot of longitudinal tyre force as a function of tyre load and wheelslip.

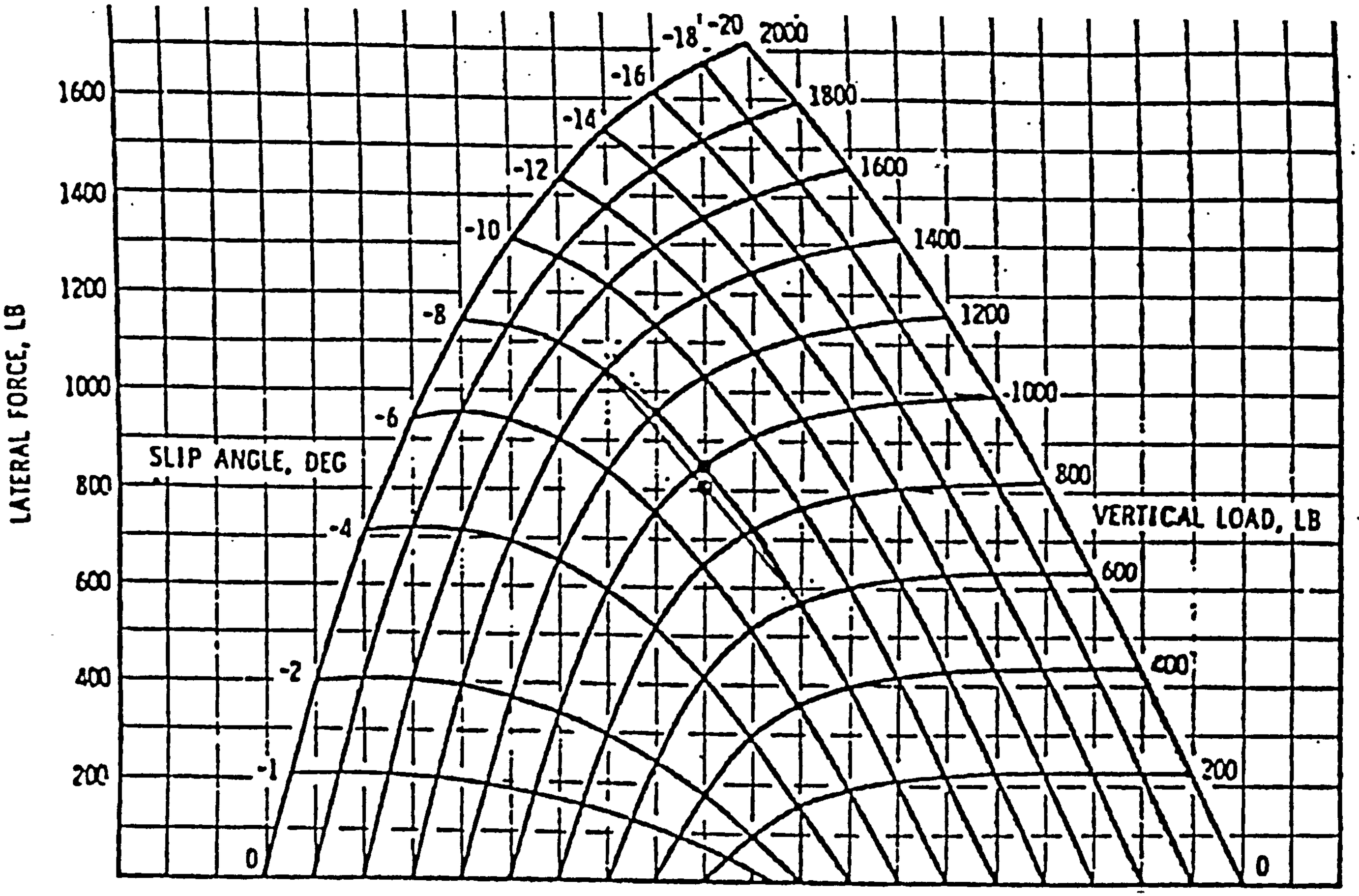

Fig. (5.16) The lateral tyre force as a funotion of tyre load and slip angle as obtaind by Nordeen, 1967 for a 6.50-15 tyre moving on hard surface.

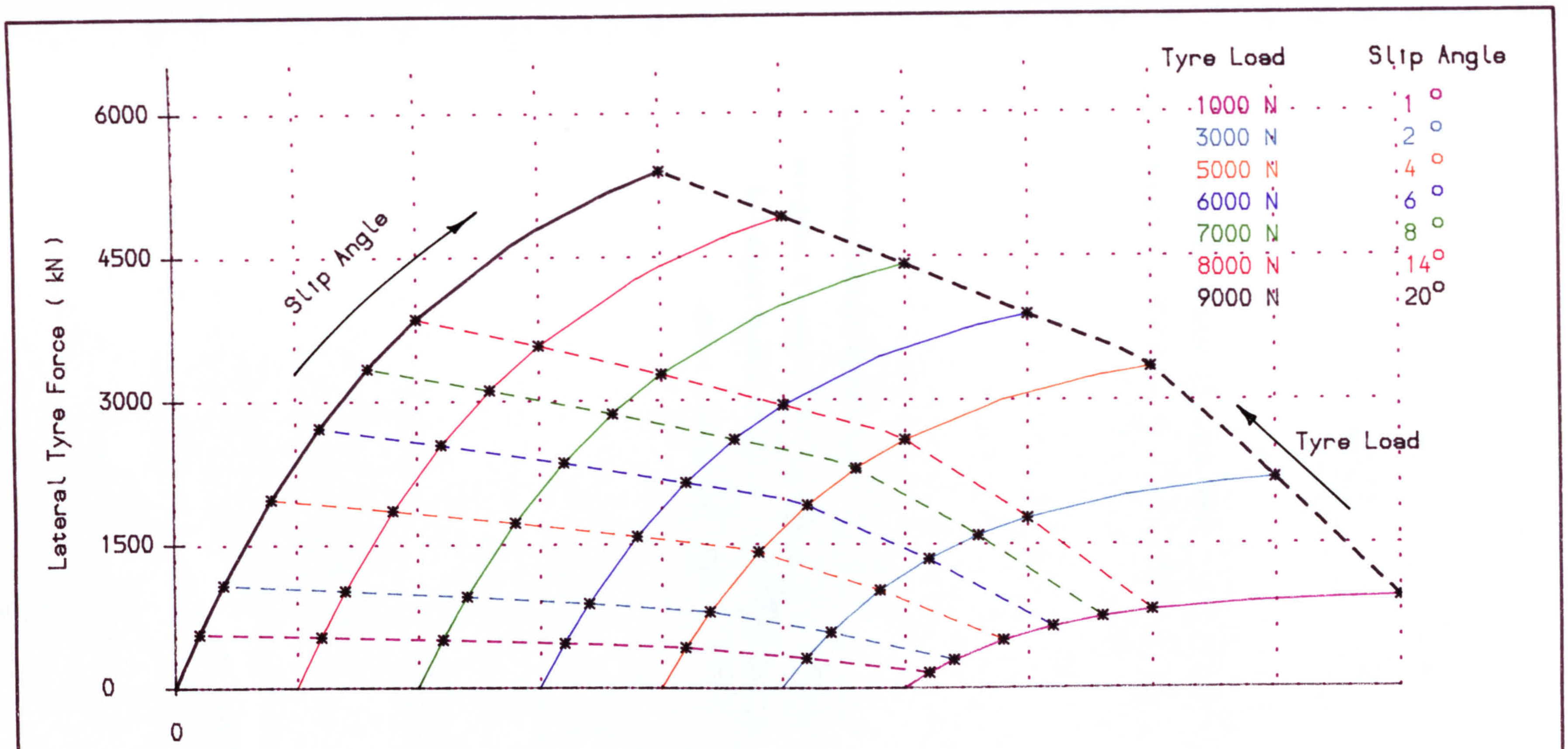

Fig. (5.17) Carpet plot of lateral tyre force as a function of tyre load and slip angle.

CHAPTER 6

COMPARISON BETWEEN RESULTS PREDICTED BY VARIOUS MODELS AND MEASURED RESULTS

Comparison between the predicted results and measured data are given. A large number of results are presented to investigate thoroughly a wide range of off-road tyre operating conditions.

6.1. INTRODUCTION

For a better understanding of off-road tyre behaviour on deformable surfaces sample plots have been generated from the various models presented in this thesis, and are compared with measured data recorded in the literature (Chapter 2) under a wide range of operating conditions.

The results predicted from the various models for off-road tyre forces can be categorised into three main sections. Firstly the simple tyre model, which only deals with generating tyre forces in longitudinal and vertical directions for a stationary and rolling tyre under steady state conditions. Second is the extended tyre model for combined lateral and longitudinal forces on a deformable surface. Finally there is the multi-spoked tyre model on deformable surfaces initiated in order to present a better understanding of off-road vehicle handling behaviour.

6.2. SIMPLE TYRE MODEL

The predicted contact area/tyre load relationships for a 7.50 x 16 front tractor tyre with three different soil types dry sand, artificial and sandy loam soils shown in Fig.(6.1) are significantly in agreement in qualitative terms with the trends of those results obtained experimentally by Yong et al [1978a] for a different tyre size on silty soil and by Prettyman [1981] for a static tyre on hard surface as shown in Figs.(6.2) and (6.3).

Fig.(6.4) presents a comparison between the theoretical and experimental relationships between the soil sinkage and the tyre load for a 7.00 x 16 tyre on artificial soil made by Bekker and Janosi [1960] compared with predicted results shown in Fig.(6.5). The soil sinkage increases significantly with the increase in tyre load. It should be noted however, that the slope of this relationship decreases with increasing tyre load. The difference between the predicted results and measured data may be expected due to the differences in soil parameters reported and used for tyre model input data.

Variation of rolling resistance with tyre load for a 7.00 x 16 tyre on wet plastic soil is shown in Fig.(6.6) as measured by Bekker and Semonin [1975]. This can be

compared with predictions by a simple off-road tyre model as shown in Fig.(6.7). The predicted relationship between the rolling resistance and the tyre load is similar to that obtained by Bekker and Semonin [1975], although again slight magnitude discrepancies occur due to different soil parameters.

6.3. EXTENDED TYRE MODEL

The results for the extended model for combined lateral and longitudinal tyre force become the same as those proposed by Grecenko [1975] as the tyre stiffness parameters, C'_x, and C'_y are increased. Fig.(6.8) illustrates this comparison, with the coefficient of lateral force plotted against slip angle at zero wheelslip and 500, 750, 1000, 1500 and 20,000 $kN/m^3\,rad.$ tyre stiffness. Fig.(6.9) shows the comparison between the coefficient of longitudinal force/wheelslip relationship and the results predicted by Grecenko under the same range of operating conditions and zero slip angle.

The measured results of the influence of slip angle on the relationship between lateral force and tyre load and the influence of tyre load on the relationship between lateral force and slip angle, obtained by Schwanghart [1981] for a 5.50-16 front tractor tyre shown in Figs.(6.10) and (6.11) are very close to those predicted by the model for the same operating conditions as seen in Fig.(6.12) and (6.13).

Figs.(6.14 to 6.21) present comparisons between results measured by different authors and results predicted by the extended off-road tyre models presented in chapter 4. The comparisons show the qualitative agreement in the curves. It is interesting to note that Fig.(6.21) does not show rolling resistance and therefore, looks significantly different from the predicted results shown in Fig.(6.20). In general, the behaviour of the tractive force for on and off-road tyre can be summarised as shown in Fig.(6.22). The rolling resistance is shown to be significantly influenced by the tractive behaviour. As a result, the rolling resistance of the tyre on hard surfaces is primarily caused by the hysteresis in the tyre material due to the deflection of the carcass while rolling. But in case

of a rigid wheel moving on a deformable surface, the rolling resistance occurs due to the soil shear deformations.

Fig.(6.23) shows comparison between the computed and measured lateral/longitudinal force relationship as obtained by Matejka [1977] for a 6.0 x 16 driven wheel on field (wheat stubble on soil). These results are in significant agreement with the same relationship predicted by the off-road tyre model under varying operating conditions of 10, 20, 30, 40 and 50% of wheelslip and 10, 20, 30 and 40° of slip angle as seen in Fig.(6.24).

A better presentation of the tyre characteristics was achieved by Grecenko [1975], presented in Fig.(6.25) compared with the extended tyre model results in Fig.(6.26) for the same operating conditions. The results from two models become similar as the tyre stiffness in the extended tyre model increases.

6.4. SPOKED TYRE MODEL

The load and shear force distributions along the length of the contact region are shown in Fig.(6.27) obtained by Krick [1969] under soft soil operating conditions. Similar relationships in Fig.(6.28) measured by Burt [1987] are compared with results predicted by the off-road tyre model operating on a deformable surface as shown in Fig.(6.29).

By increasing the soil parameter values the soil becomes effectively very stiff compared to the tyre, the contact region between the tyre and the surface becomes smaller, so the spoked tyre model results should be the same as those predicted by the Sharp and El-Nashar [1986] model on a hard surface. These results are shown in Figs.(6.30) and Fig.(6.31) for the relationship between side force and longitudinal slip and the relationship between side force and longitudinal force (braking or traction) respectively. These results are compared under typical operating conditions with results predicted by the multi-spoked tyre model for off-road surfaces in Figs.(6.32) and (6.33). However, the comparison shows the quantitative differences that can be

expected due to the dependence on the tyre input data.

Fig.(6.34) and Fig.(6.35) illustrate the relationship between the longitudinal force/wheelslip and the lateral force/slip angle at two different soil hardness values, 4500 and 20,000 kN/m^{n+2}, compared with predicted results obtained by Sharp and El-Nashar [1986]. For an accurate comparison of off-road tyre model results with any other model results, Figs.(6.36) and (6.37) show a comparison with the same tyre size data and operating conditions (except different soil types). Not surprisingly, the forces predicted for hard ground (stiff soil) conditions are generally higher than those predicted for soft soil conditions.

The relationship between tyre load and the contact length predicted by Sharp and El-Nashar [1986] is shown in Fig.(6.38), compared with results from the spoked tyre model on hard surface conditions as shown in Fig.(6.39).

To demonstrate the multi-spoked tyre model, Fig.(6.40) shows the relationship between side force and longitudinal force with different slip angles of –1, 2, 4, 6 and 9° obtained by Janosi [1981] compared with predicted results in Fig.(6.41) from the spoked tyre model under the same operating conditions. This is the classic tyre force ellipse curve and shows how readily the tyre model can emulate actual experimental results.

6.5. CONCLUDING REMARKS

(1) The figures show that the forces generated by various off-road tyre models in longitudinal, lateral and vertical directions under a wide range of operating conditions, follow the same general trends as the measured results obtained by a wide range of authors.

(2) The plots illustrate the capability of off-road tyre models in representing tyre behaviour over a very wide range of operating conditions. The results obtained from these models show a very good qualitative agreement with published

experimental results obtained and collected from a wide range of sources as seen in "LIST OF REFERENCES".

(3) Comparisons of results of off-road tyre models and measured data are recognised to be often difficult because of the lack of soil and tyre parameters quoted in reports of measurements. However, despite these difficulties, qualitative agreement between the predicted results and measured data is generally good.

(4) Since the comparisons between the results predicted from various tyre models and those measured for a wide range of different operating conditions are in agreement qualitatively it is suggested that this validation of models is sufficient to justify their usefulness for vehicle handling and stability studies.

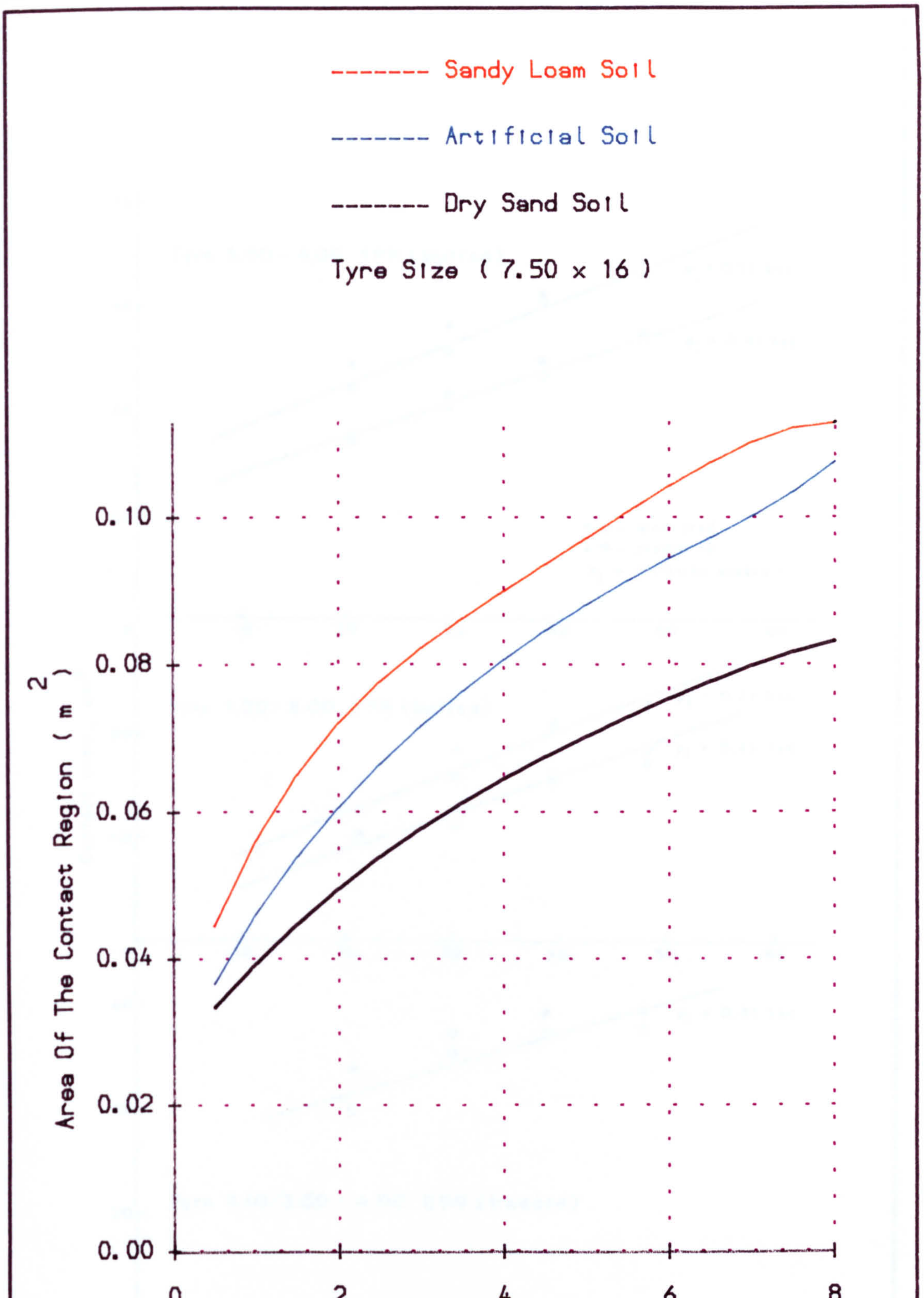

Fig. (6.1) Variation of the contact area between the tyre and three different soils for a static tyre condition

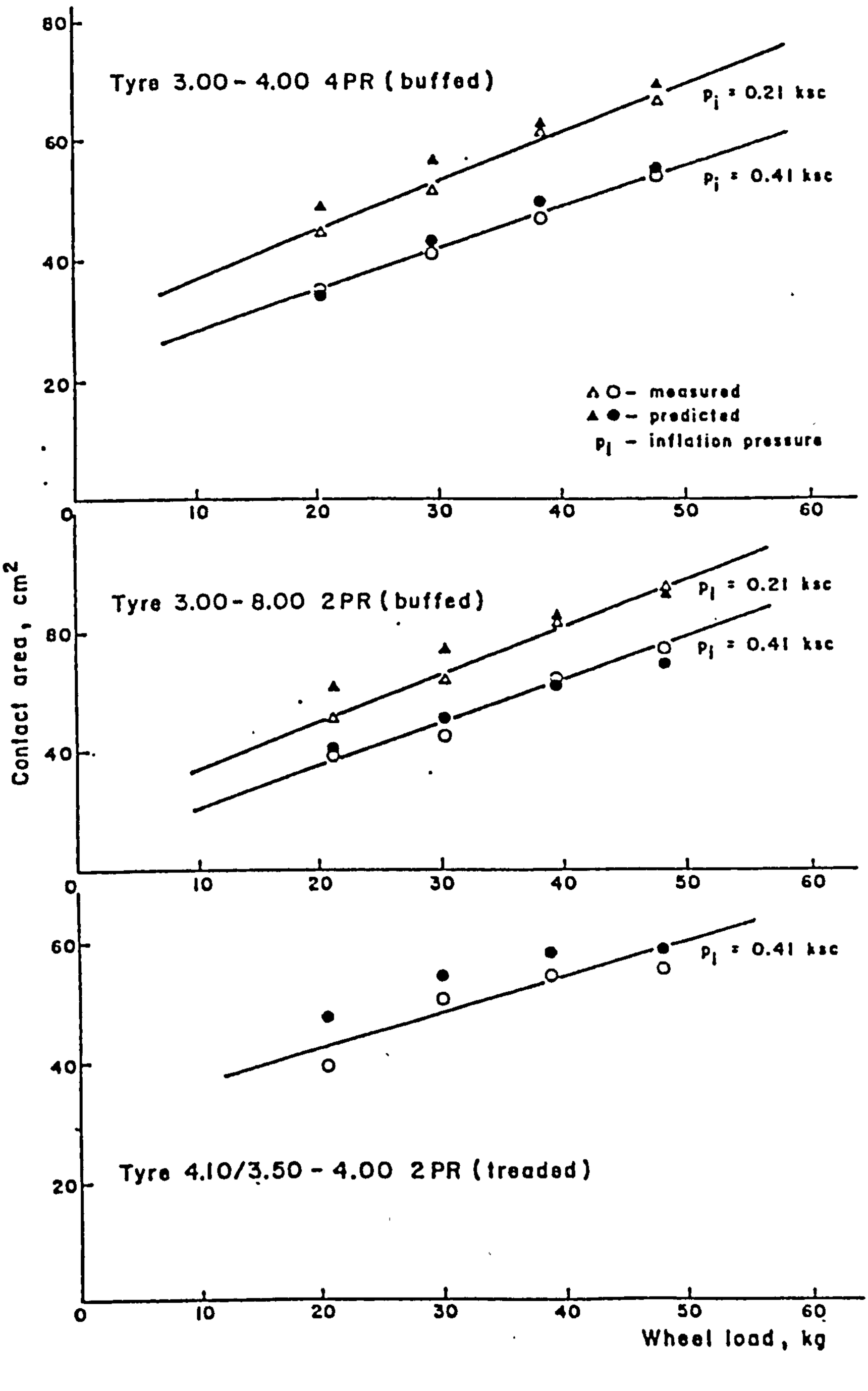

Fig. (6.2) The relationship between the contact area and the tyre load obtained by Yong et al, 1978a for differet tyre size on silty soil.

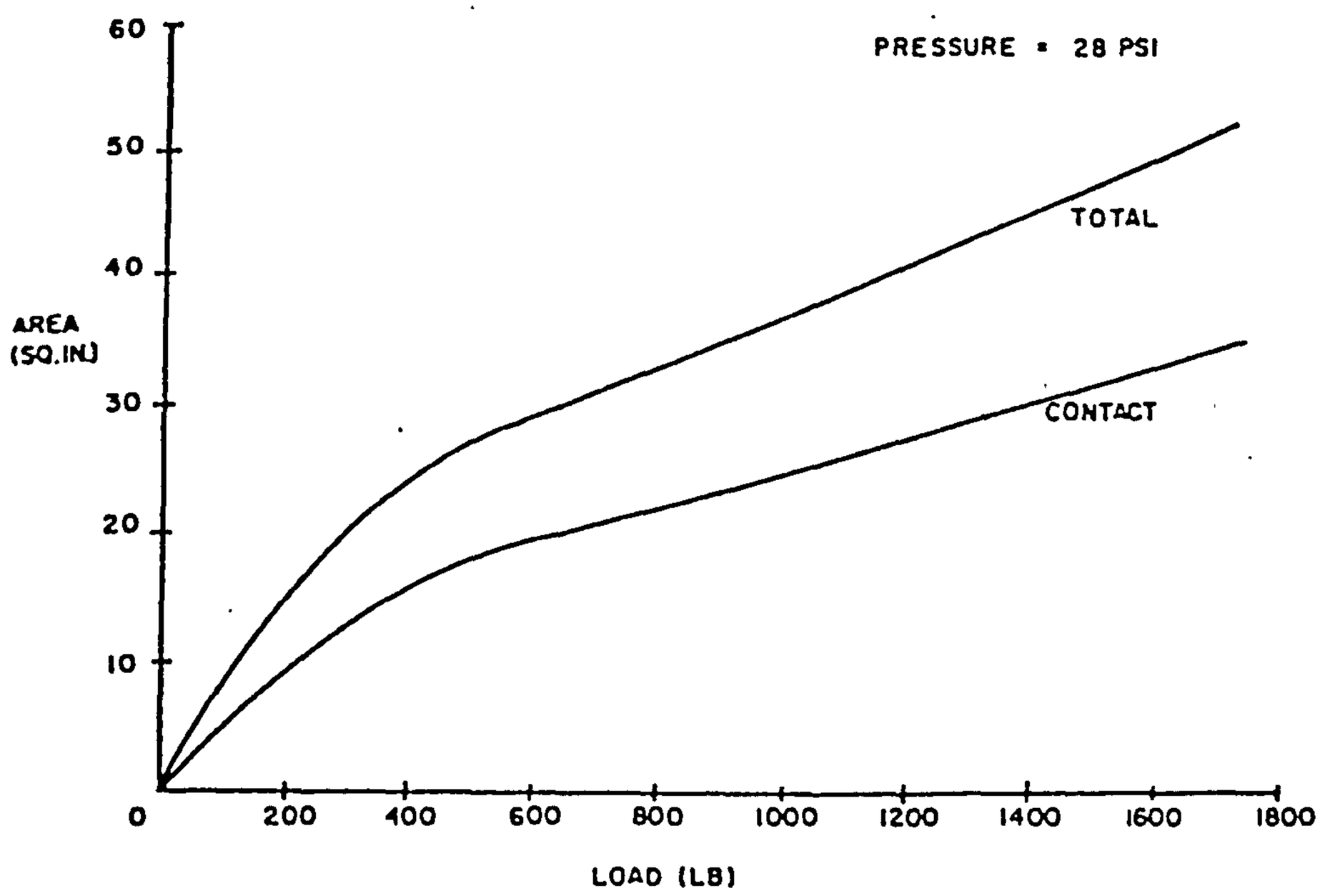

Fig. (6.3) The variation of footprint and the total contact area with the tyre load as measured by Prettyman, 1981 on hard surface.

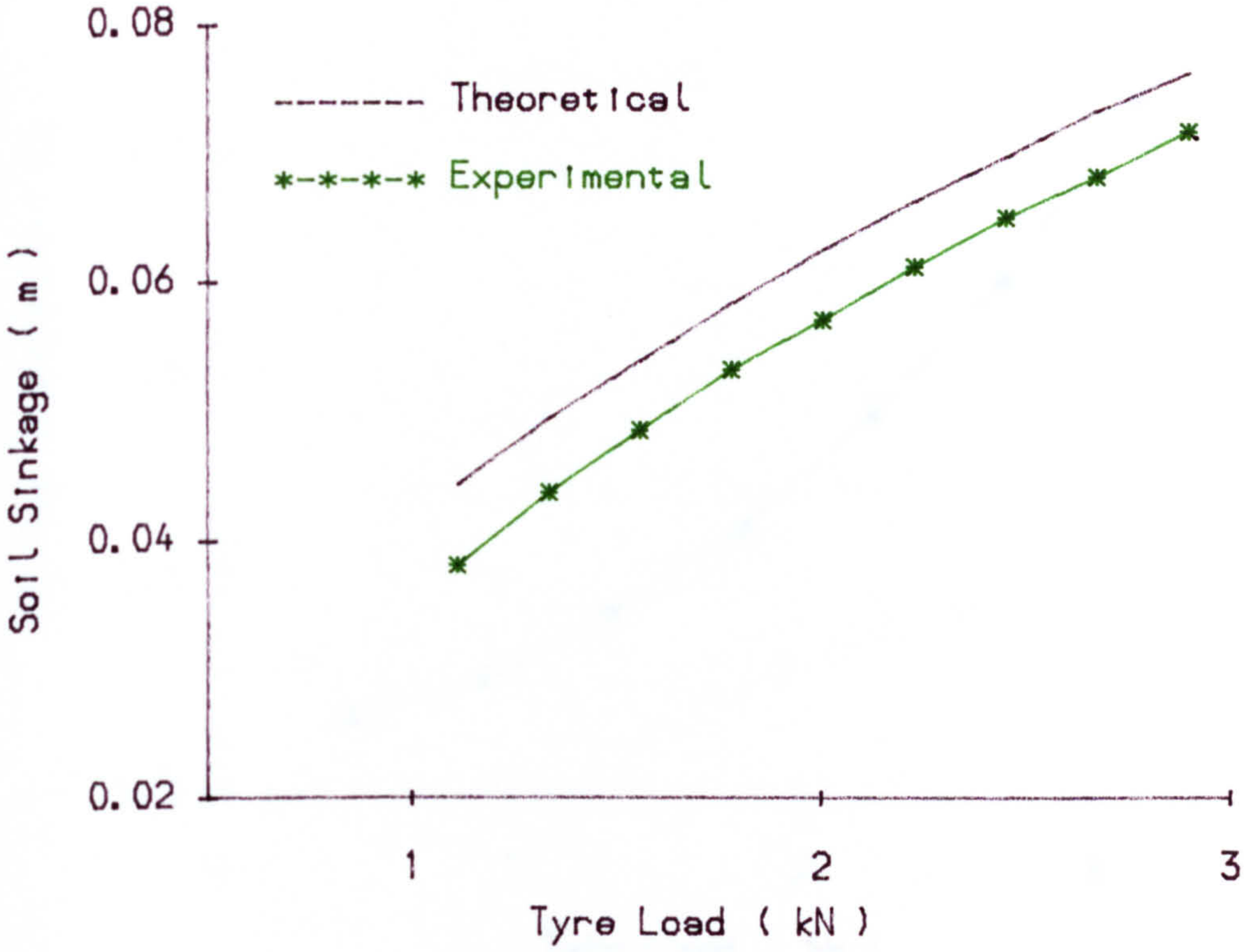

Fig. (6.4) Experimental and theoretical relationship between tyre load and soil sinkage obtained by Bekker and Janosi, 1960.

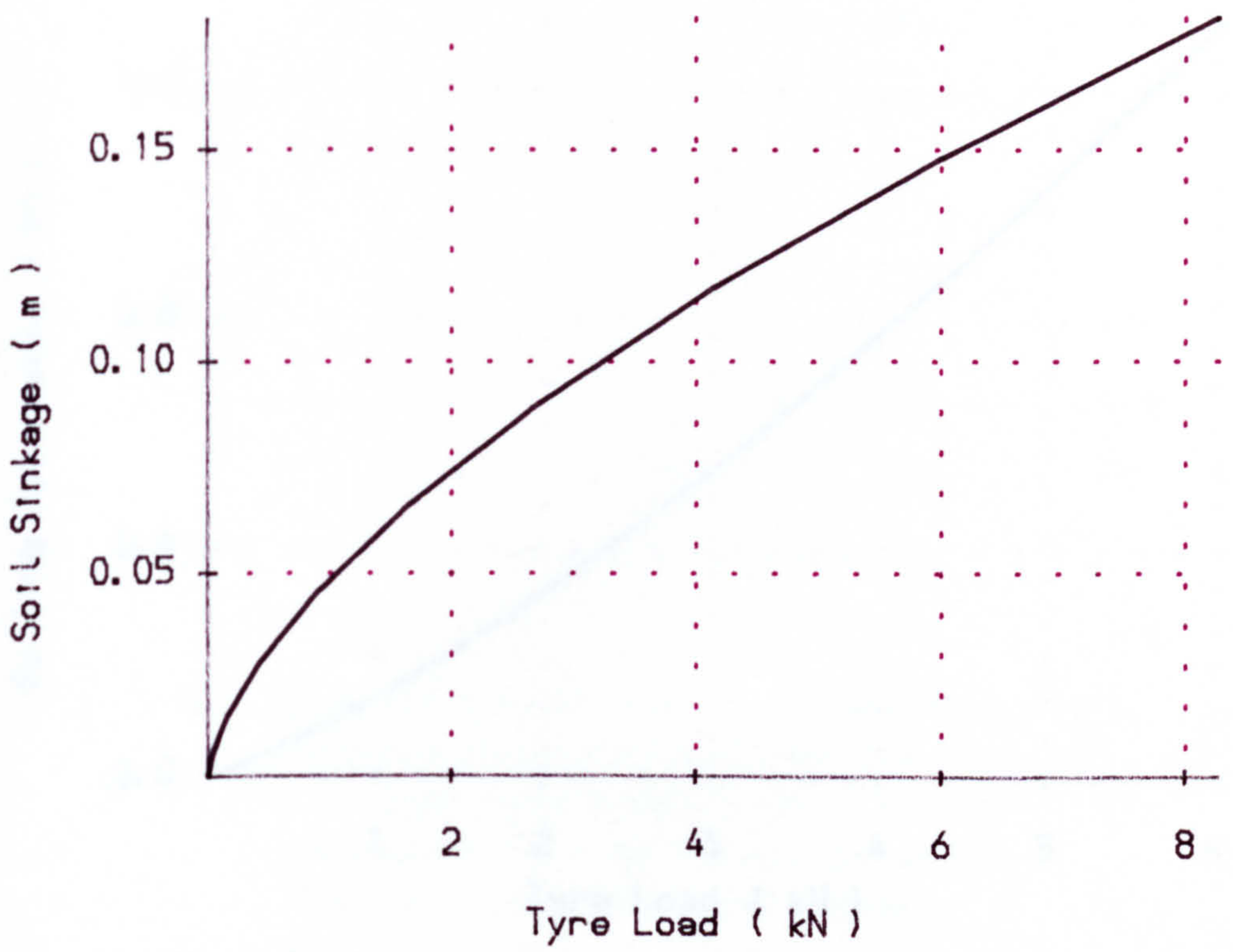

Fig. (6.5) Predicted relationship between soil sinkage and tyre load for a 7.50 x 18 tractor front tyre on sandy loam soil.

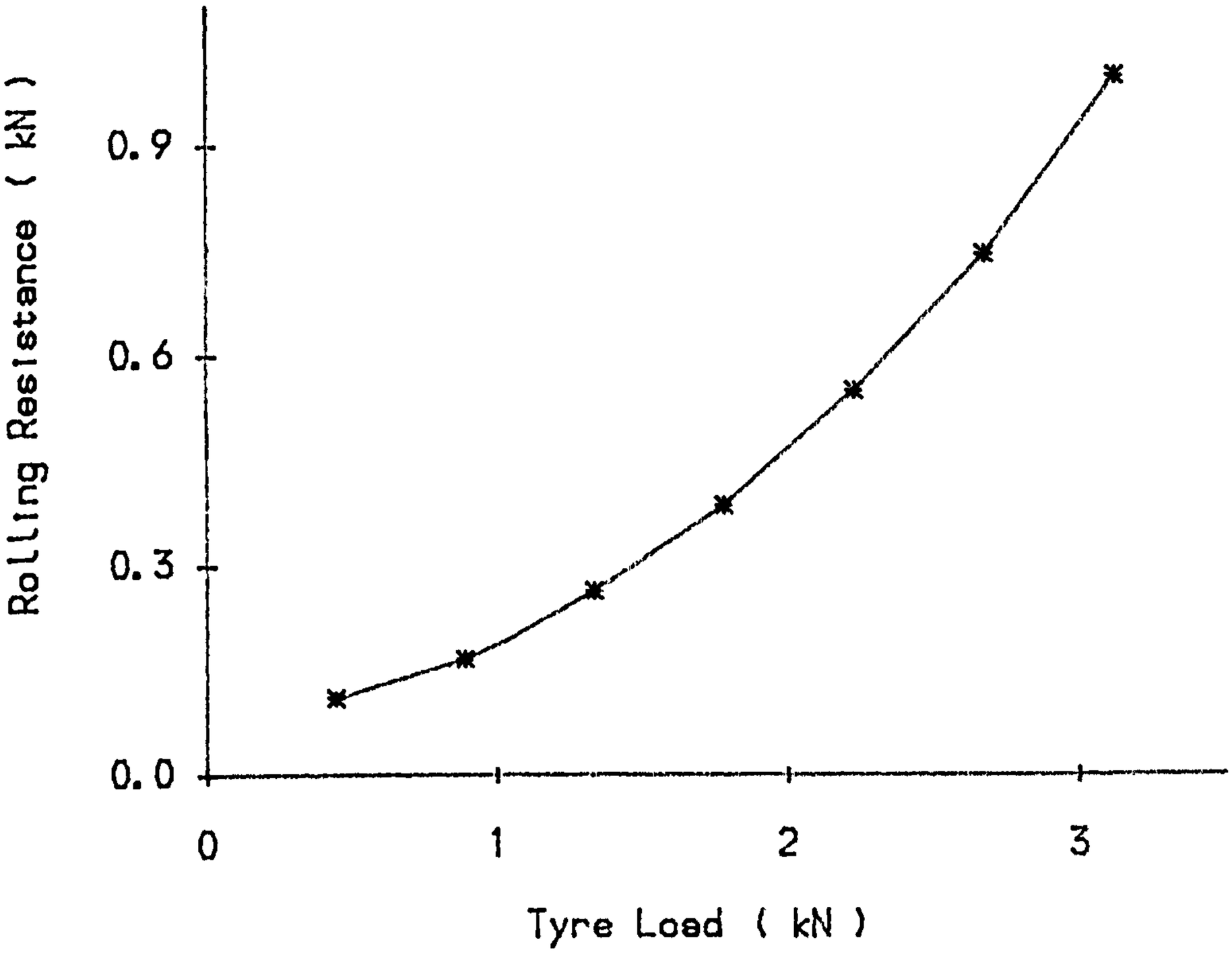

Fig. (6.6) Rolling resistance as a function of tyre load for a tyre on wet plastic soil measured by Bekker and Semonen, 1975.

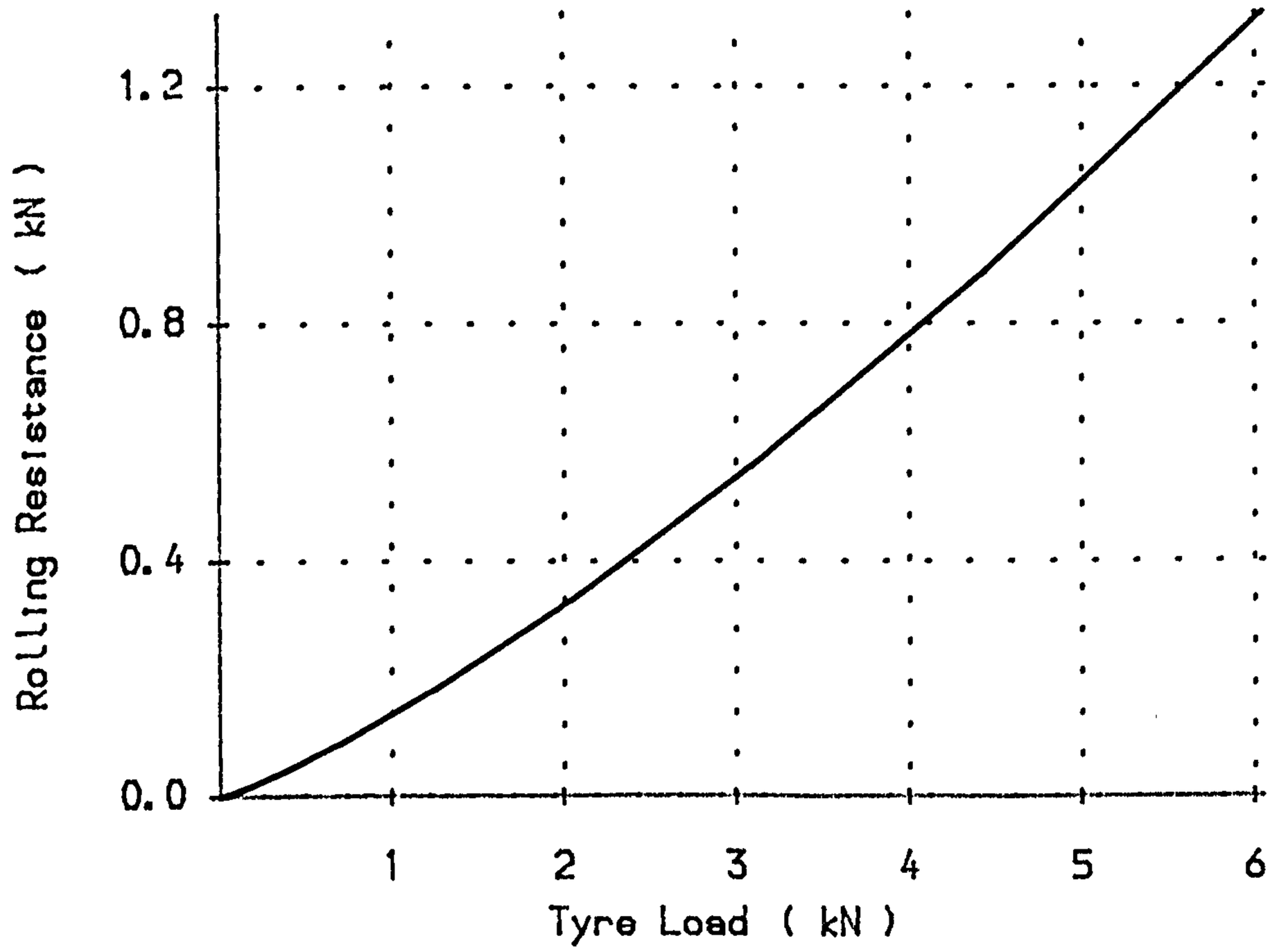

Fig. (6.7) Influence of tyre load on the rolling resistance for a tyre moving on soft soil.

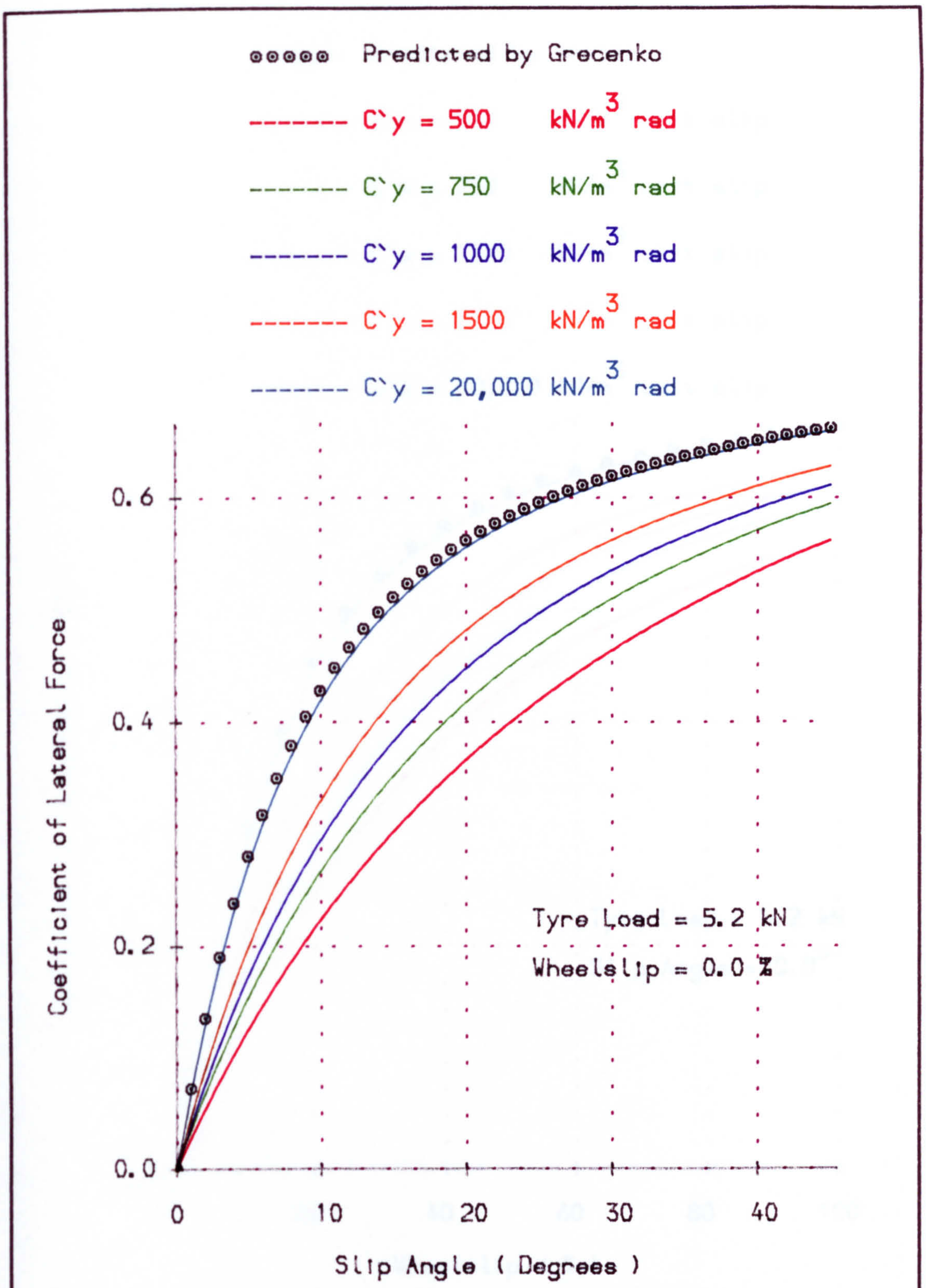

Fig. (6.8) Coefficient of lateral force/slip angle relationship predicted by the combined off-road tyre model with different values of tyre stiffness parameter compared with Grecenko's model.

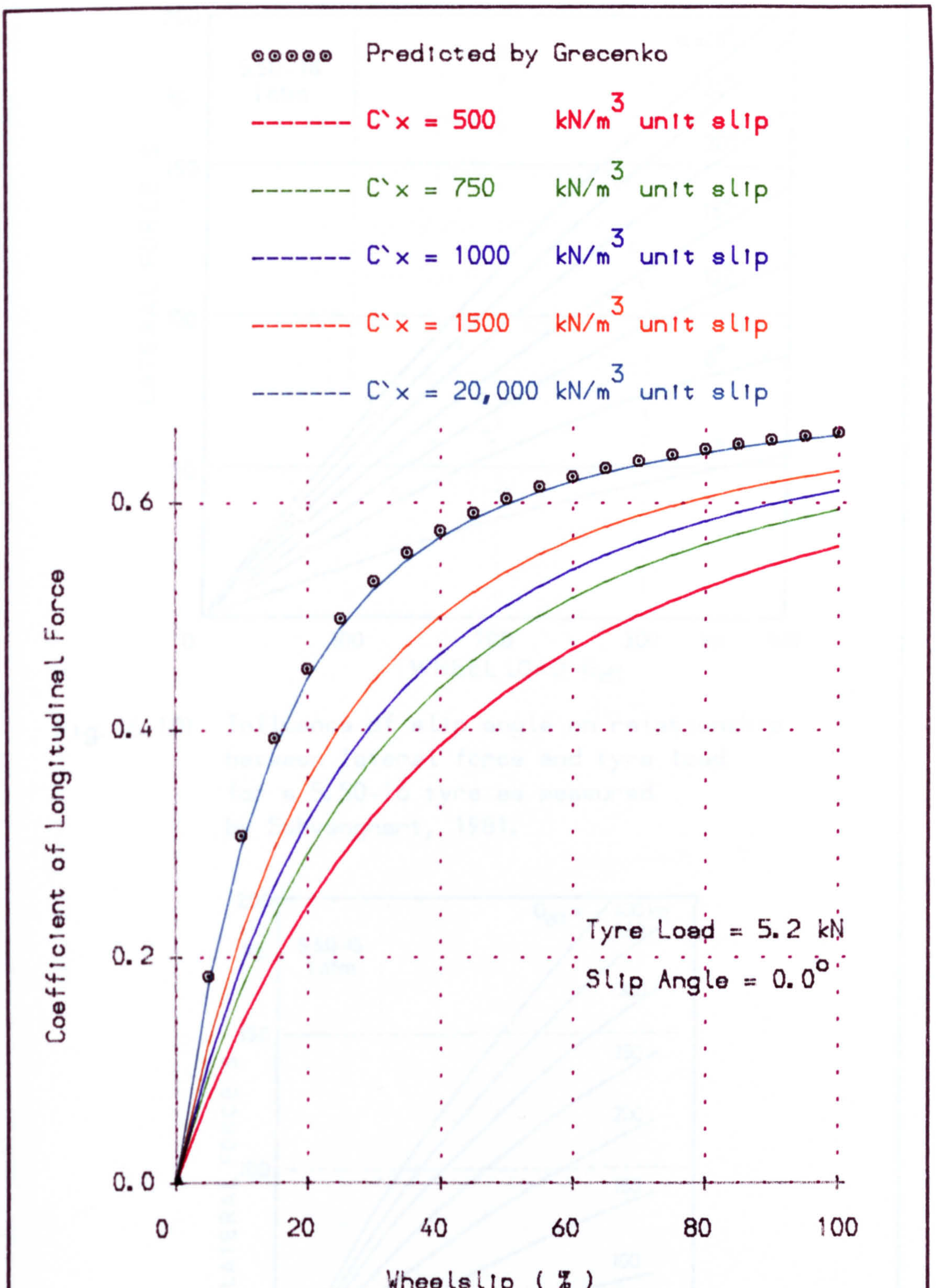

Fig. (6.9) Relationship between longitudinal force coefficient and wheelslip compared with those predicted by Grecenko's model.

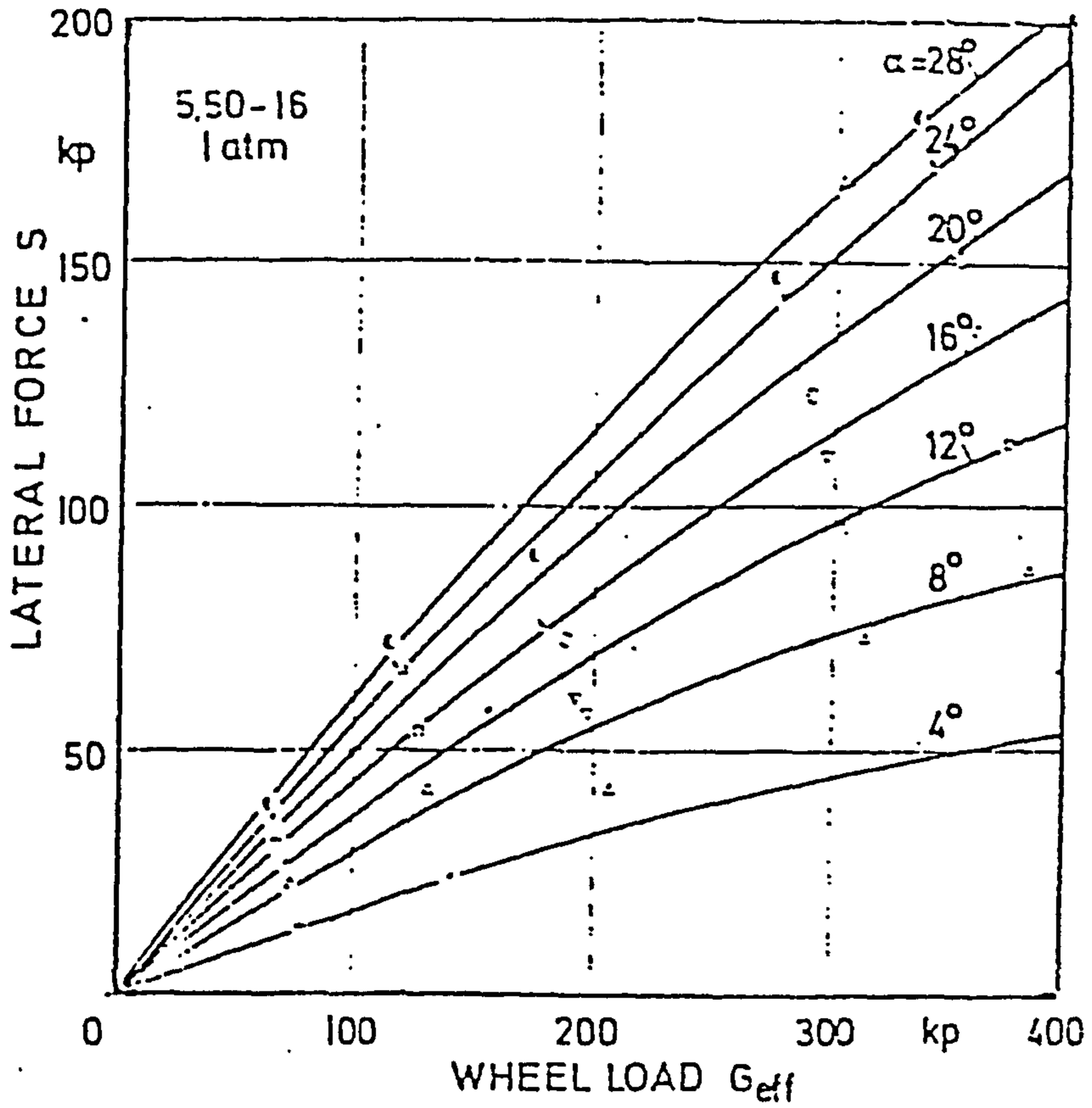

Fig. (6.10) Influence of slip angle on relationship between lateral force and tyre load for a 5.50-16 tyre as measured by Schwanghart, 1981.

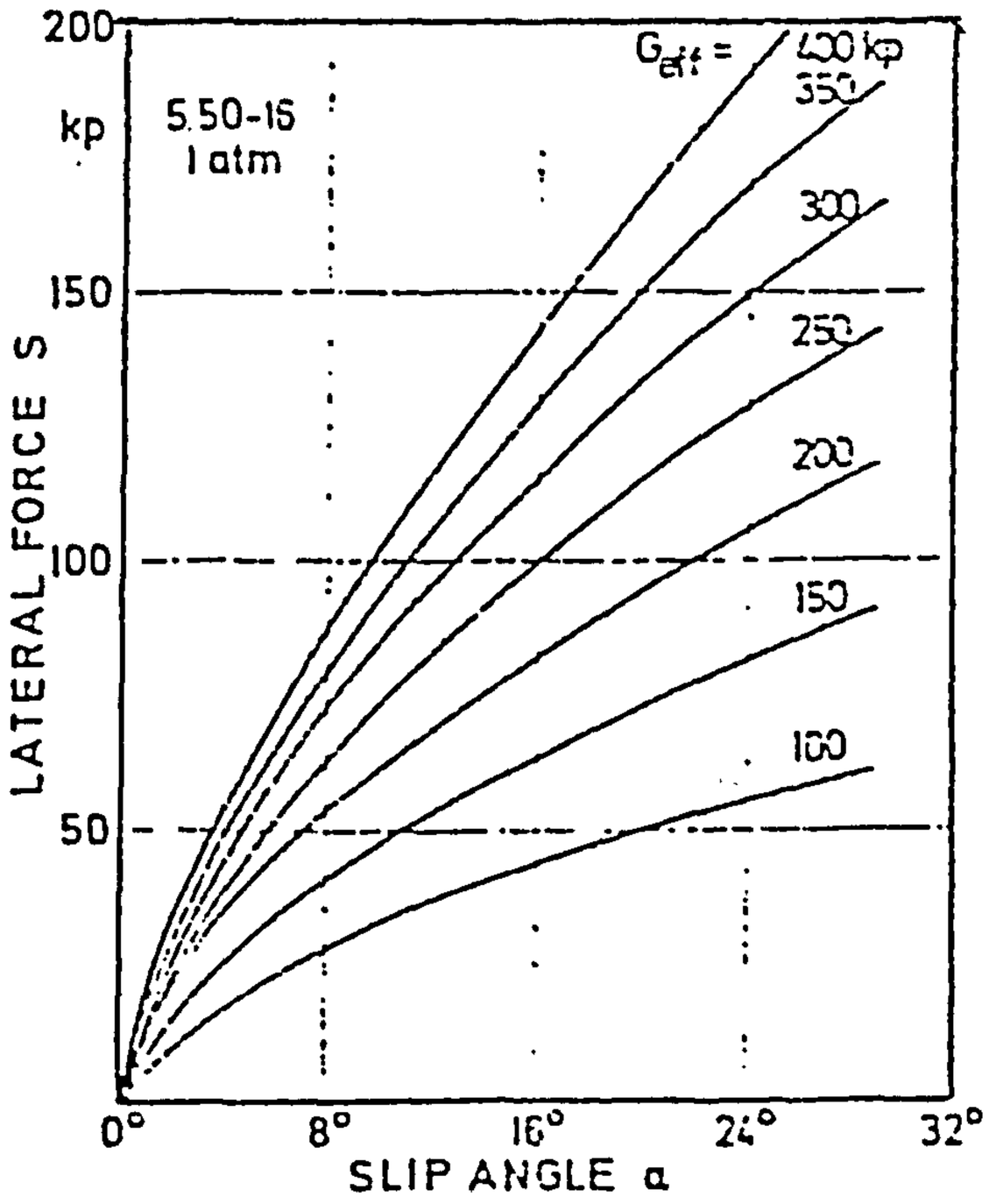

Fig. (6.11) Influence of tyre load on relationship between lateral force and slip angle for a 5.50-16 tyre as measured by Schwanghart, 1981.

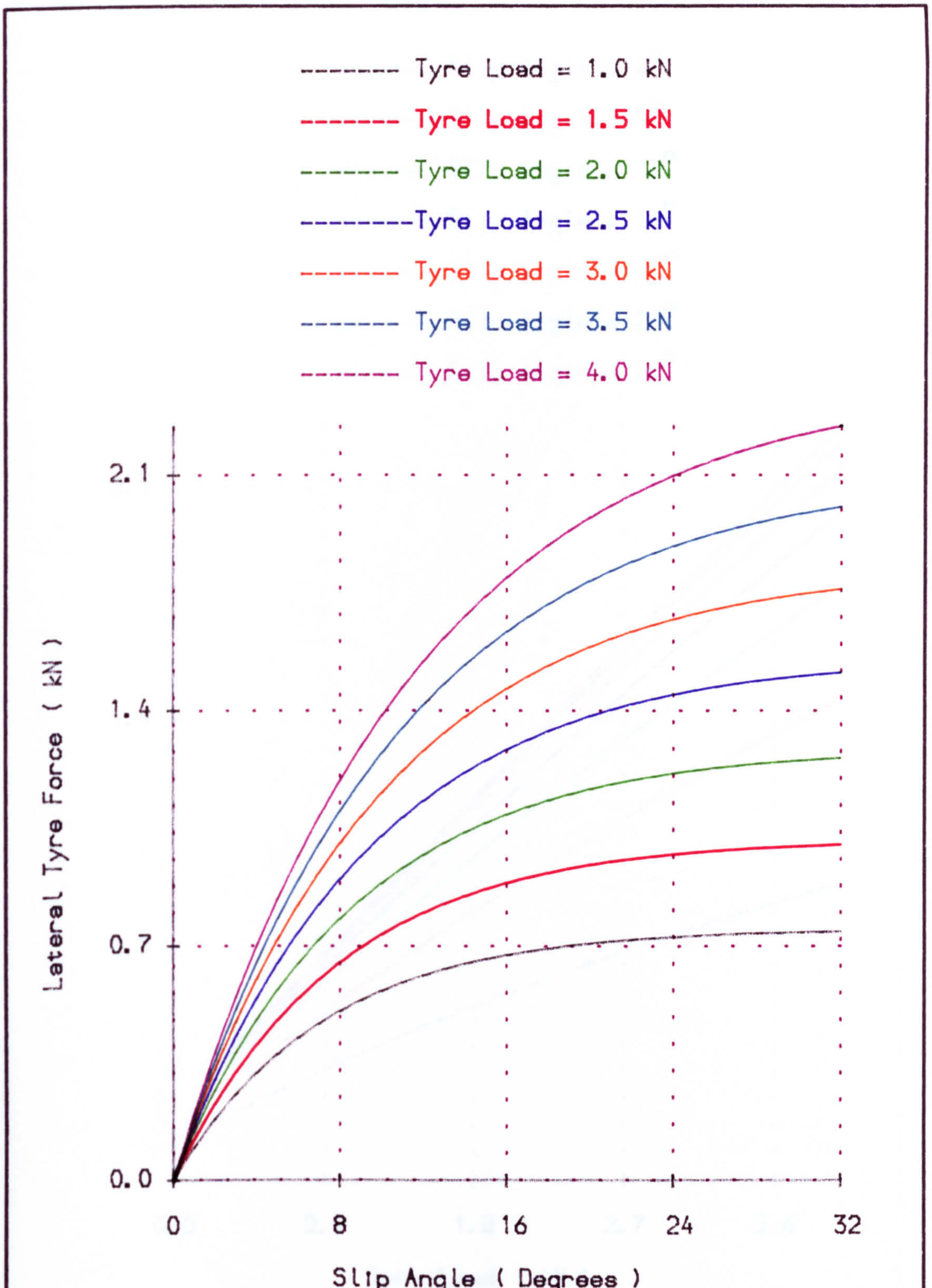

Fig. (6.12) Variation of lateral tyre force against slip angle with different tyre load for the extended off-road tyre model using Schwanghart`s data.

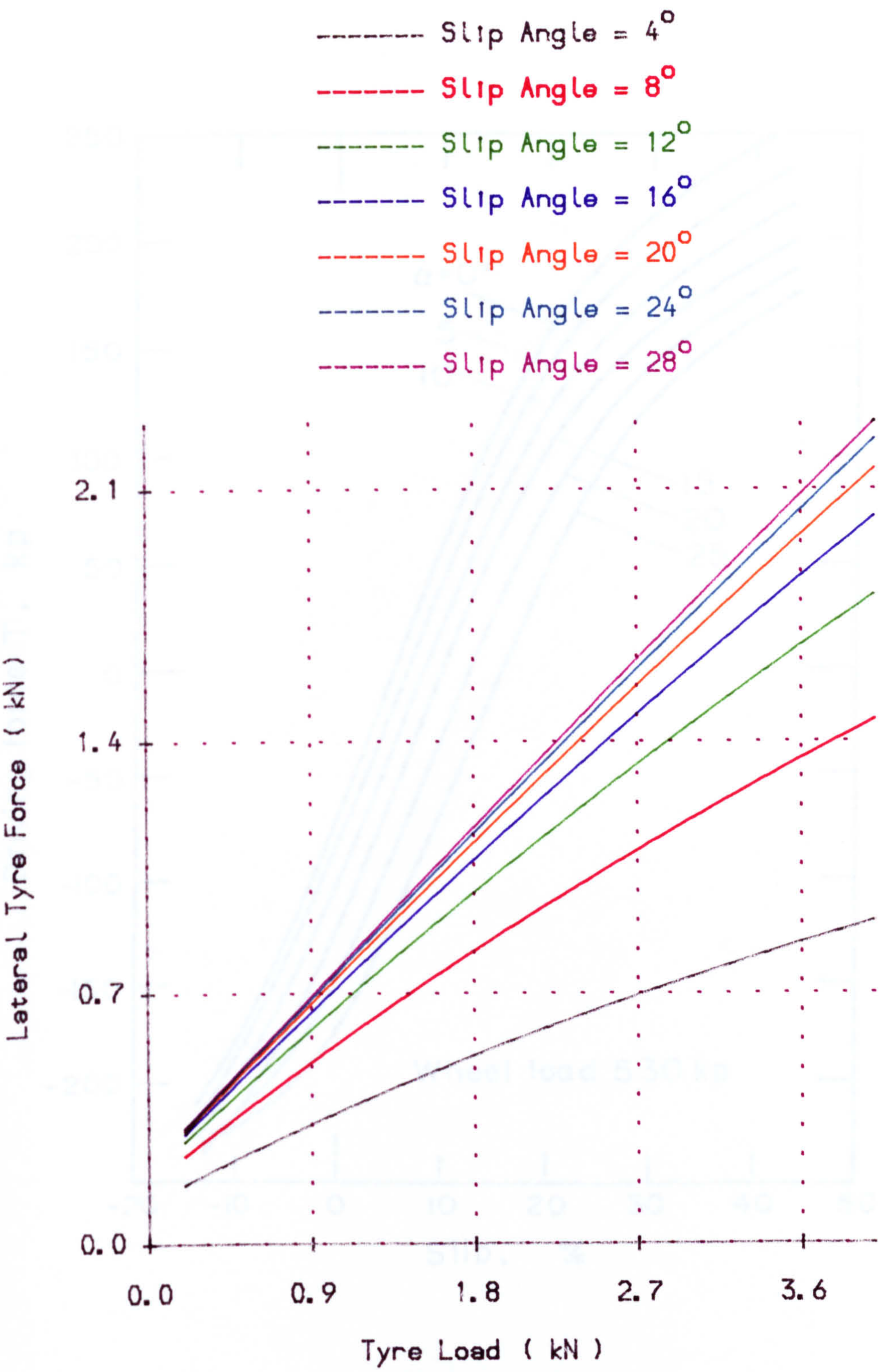

Fig. (6.13) Variation of lateral tyre force against tyre load with different slip angles using Schwanghart`s data.

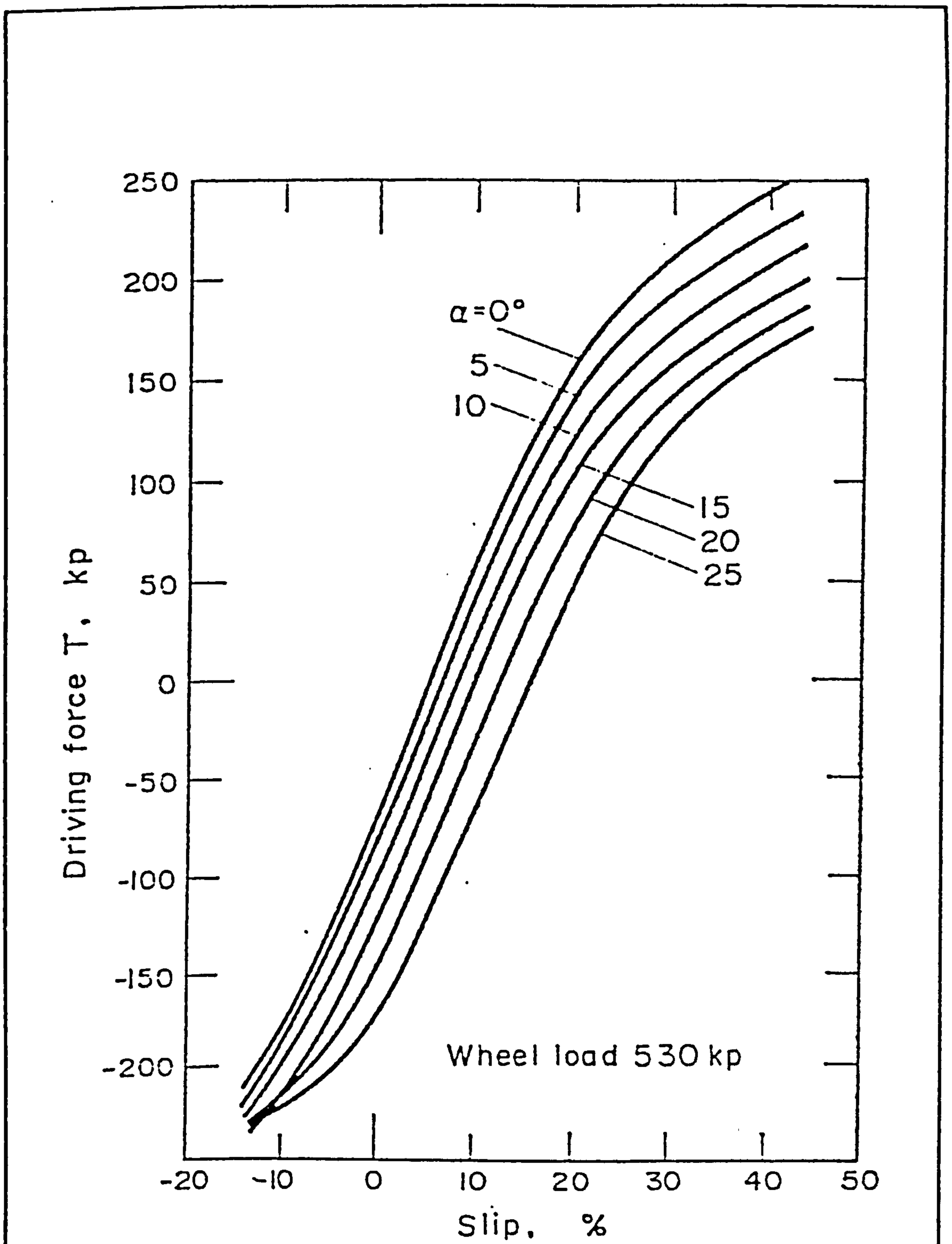

Fig. (6.14) Driving force against wheelslip with different slip angles measured by Krick, 1973.

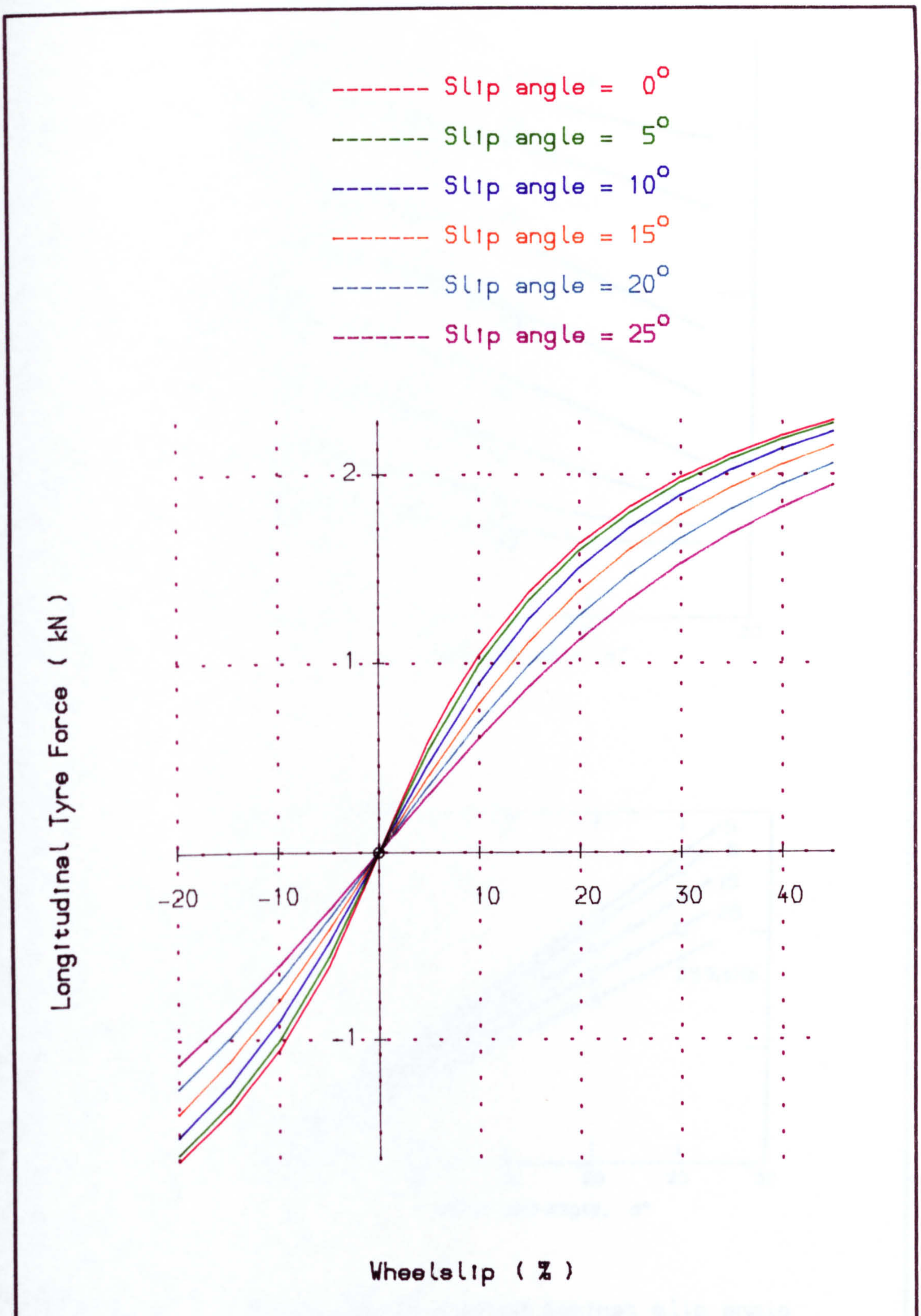

Fig. (6.15) **Longitudinal force/wheelslip relationship for the** extended off-road tyre model with different slip angles.

(a)

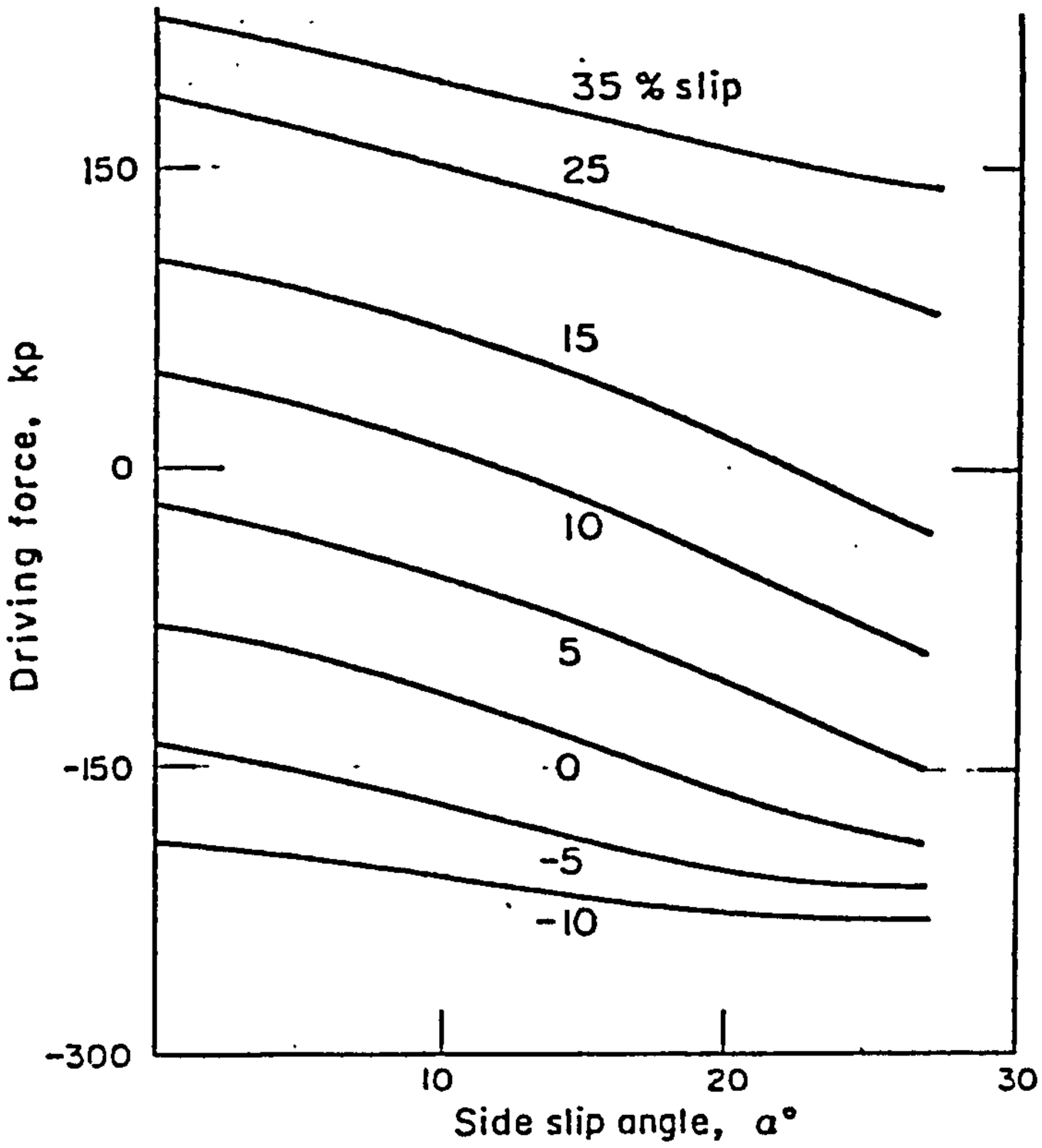

(b)

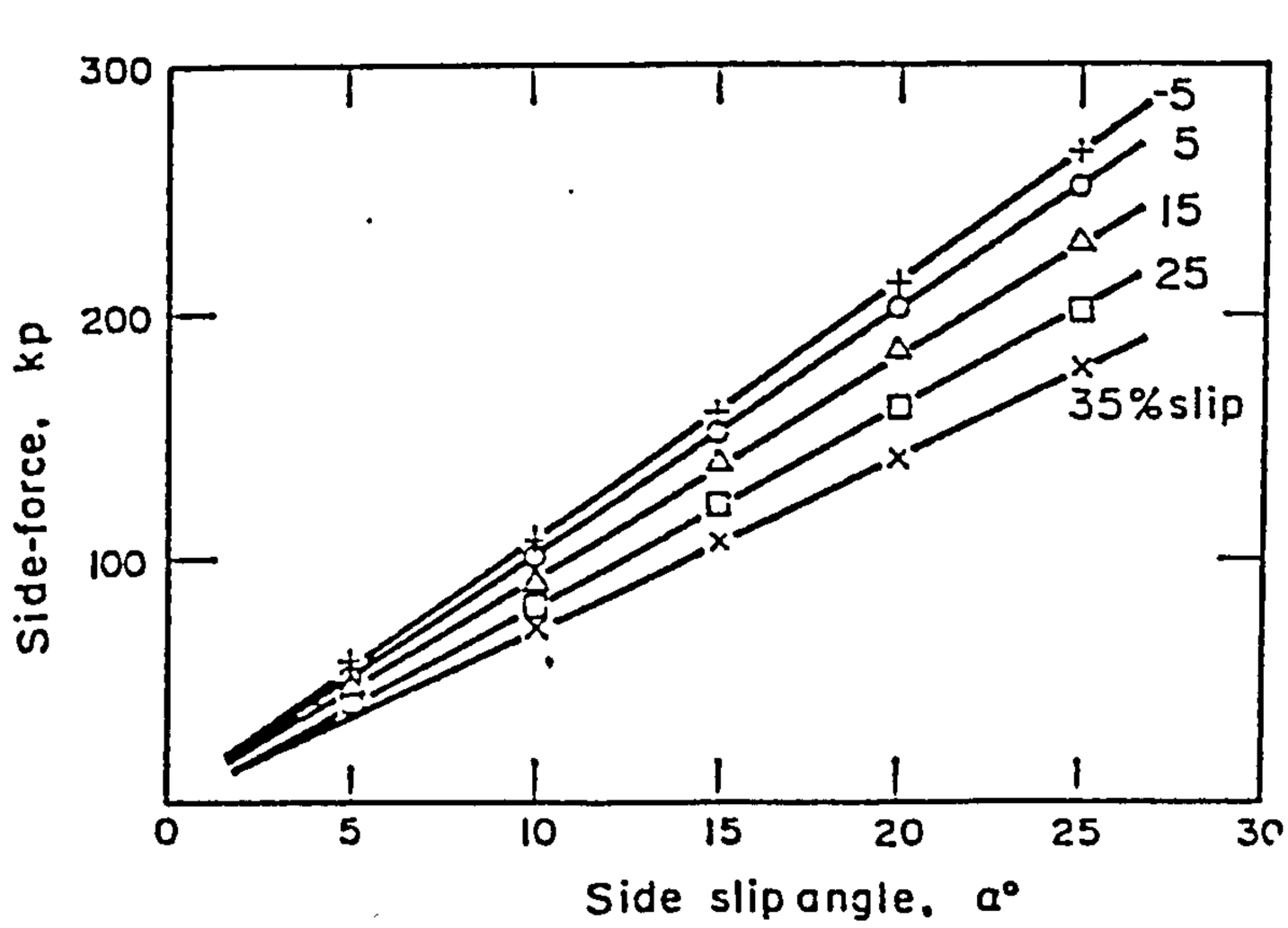

Fig. (6.16) Driving force plotted against slip angle (a) and side force plotted against slip angle with different wheelslip (b) as measured by Krick, 1973.

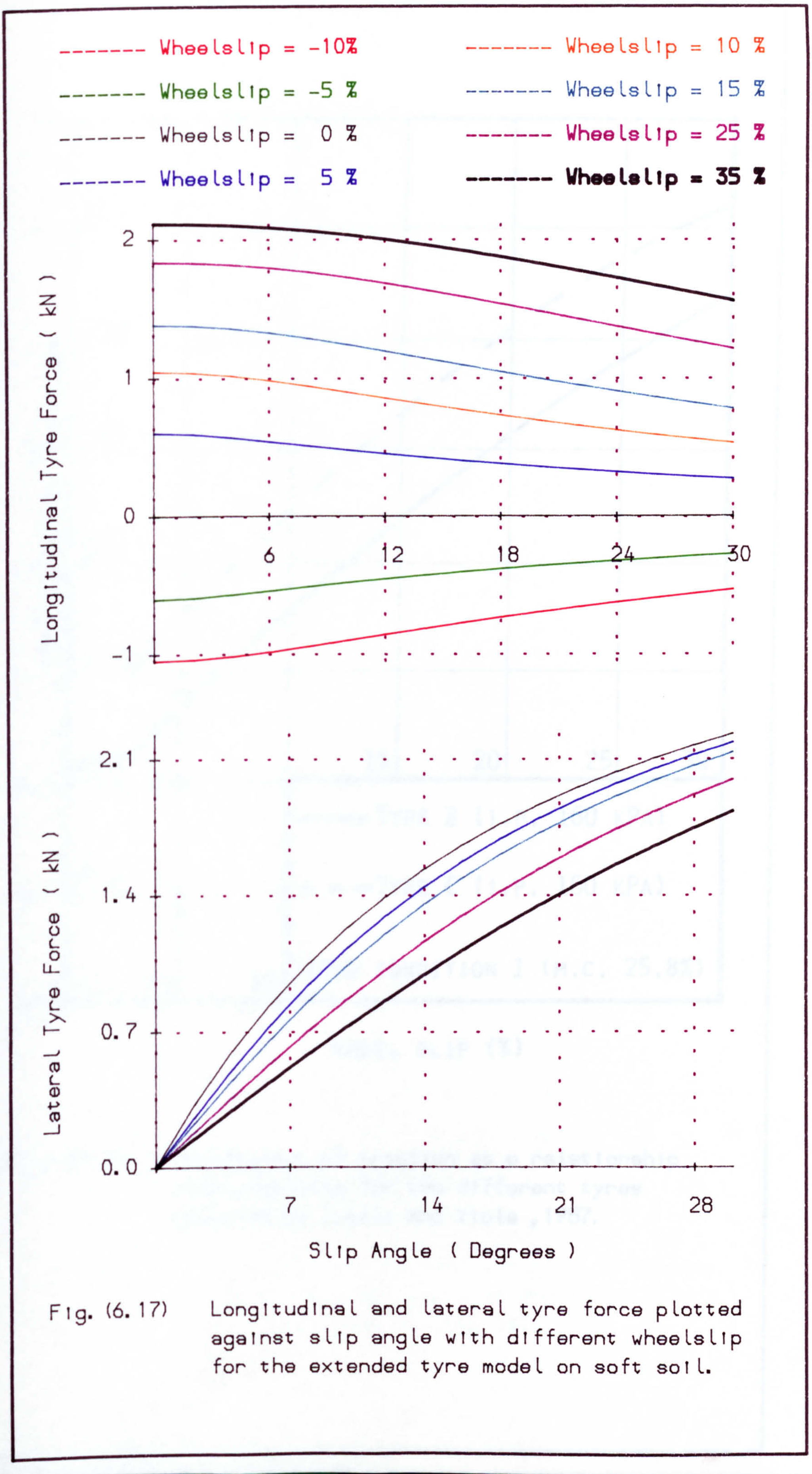

Fig. (6.17) Longitudinal and lateral tyre force plotted against slip angle with different wheelslip for the extended tyre model on soft soil.

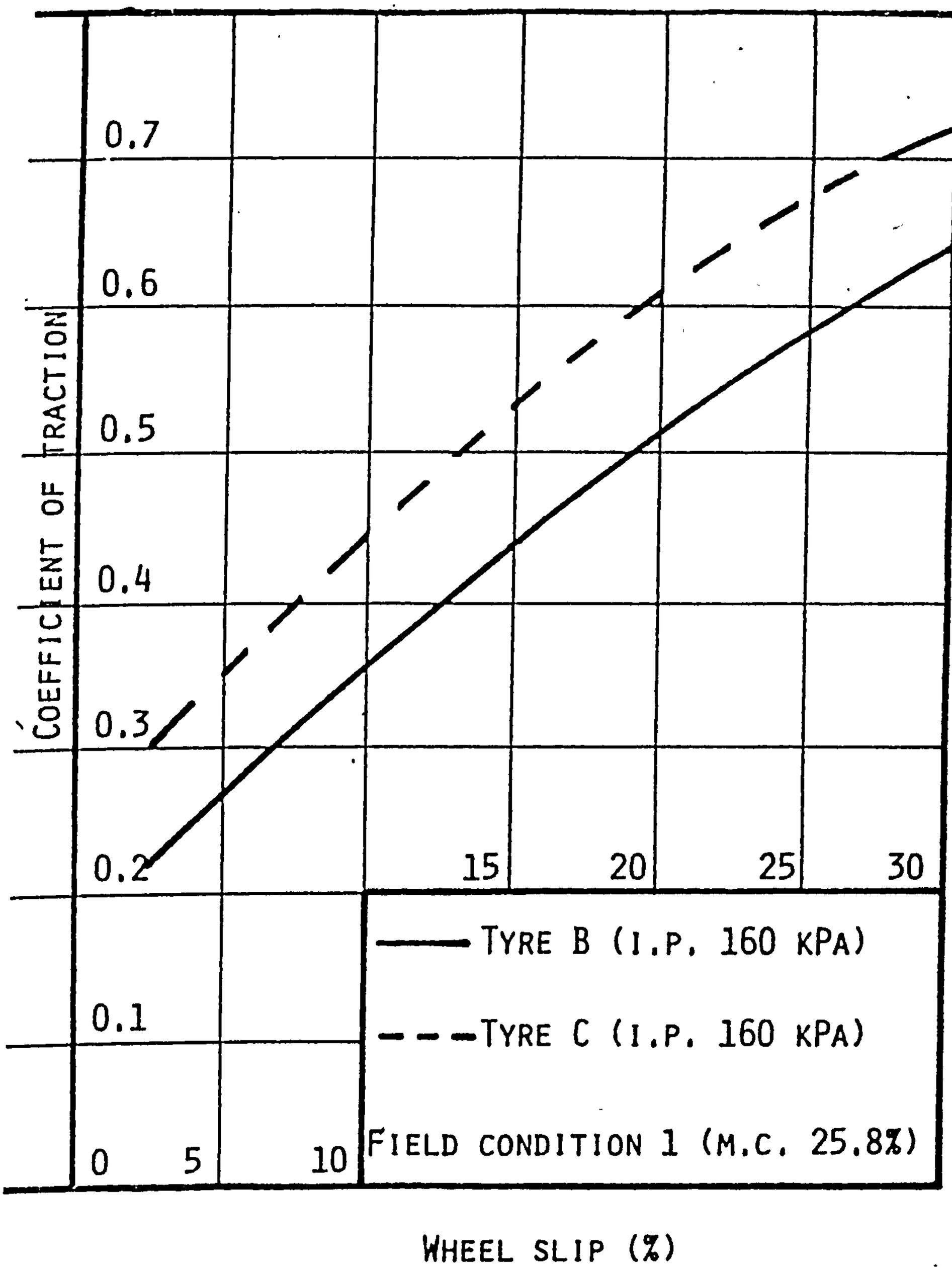

Fig. (6.18) Coefficient of traction as a relationship with wheelslip for two different tyres measured by Trolli and Viola, 1987.

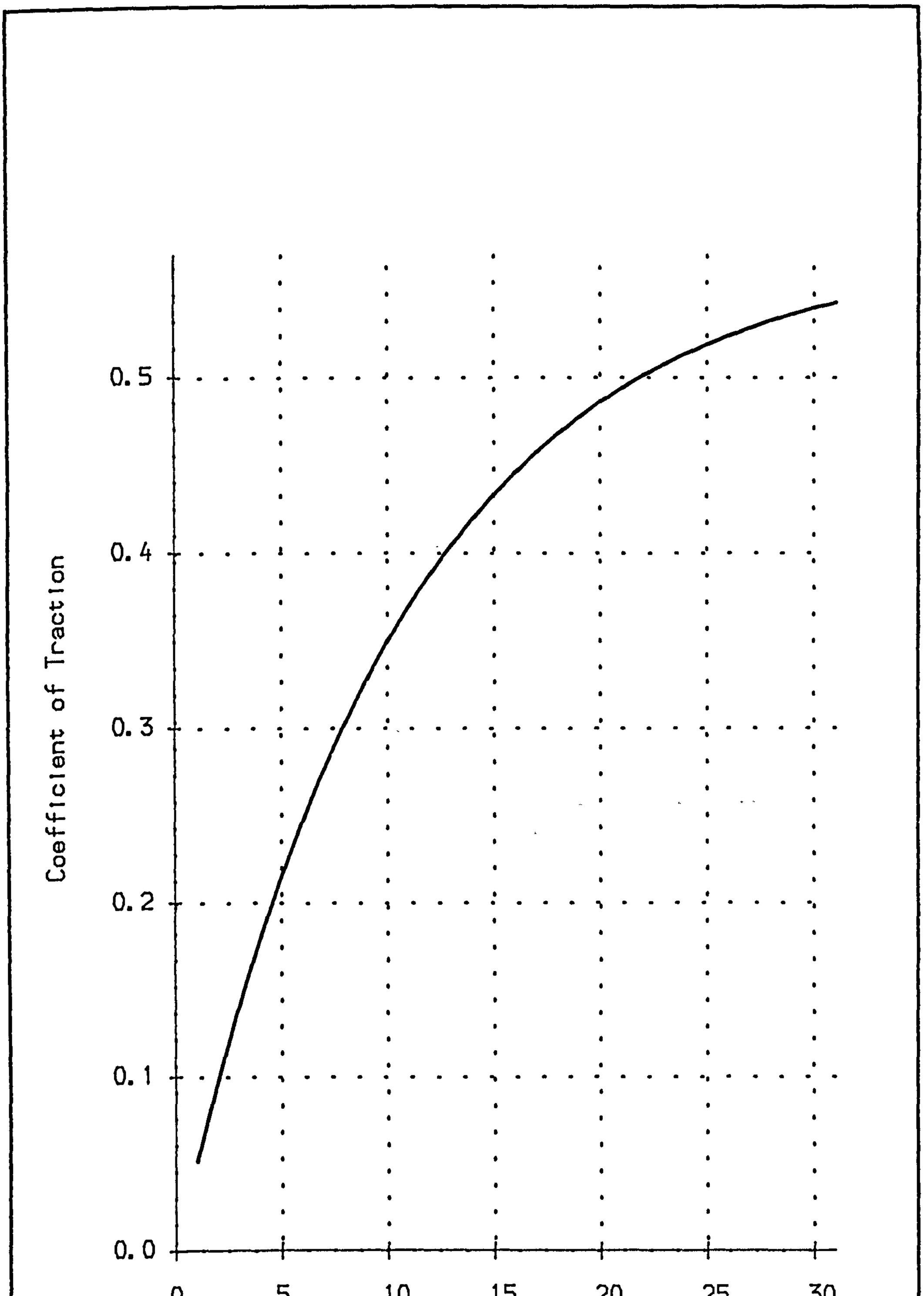

Fig. (6.19) Coefficient of traction plotted against wheelslip at zero slip angle for a tyre moving on sandy loam soil.

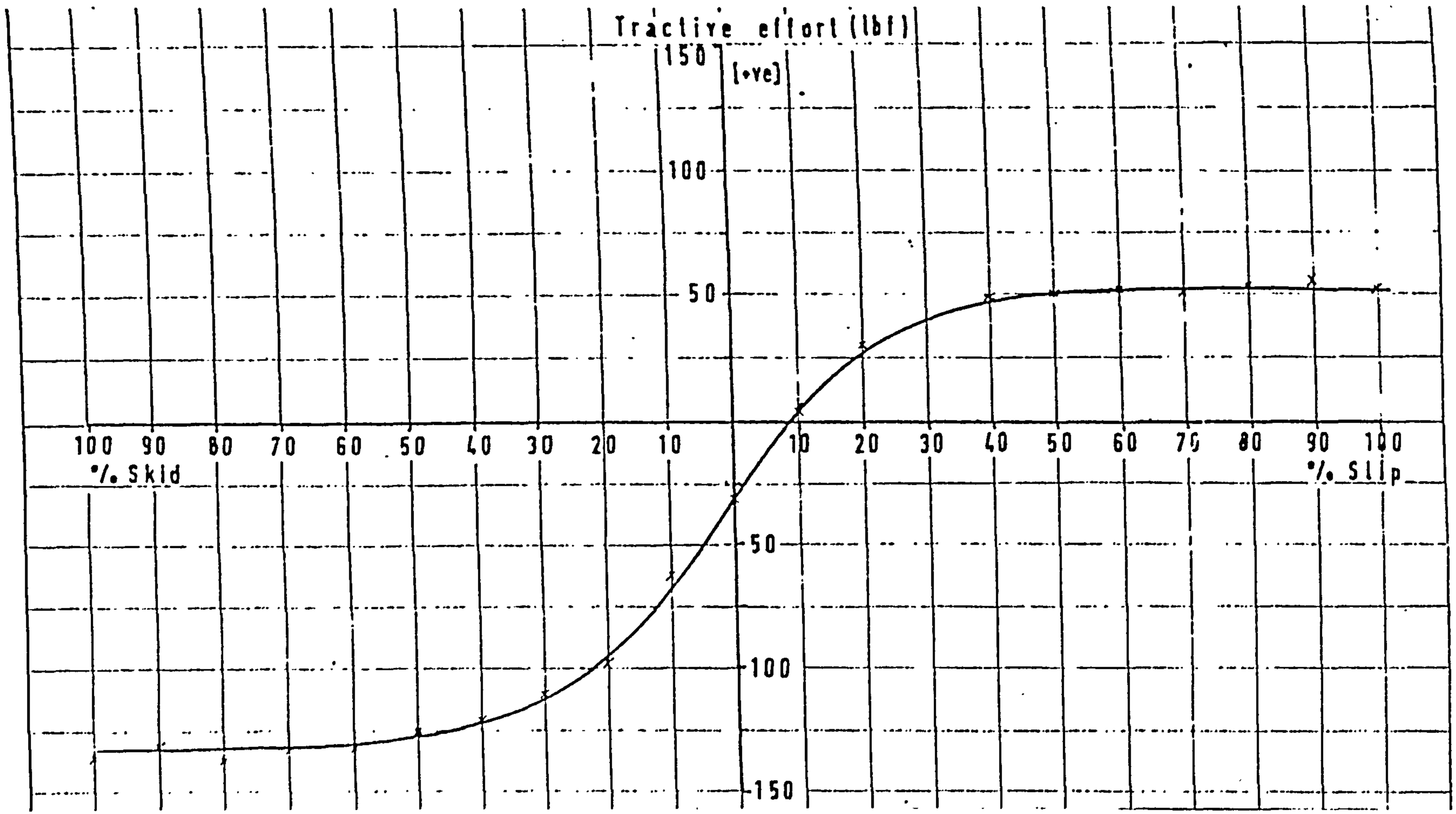

Fig. (6.20) Slip-pull curve for 6 x 12 tractor tyre at 10 p.s.i. in sand as measured by Riley, 1968.

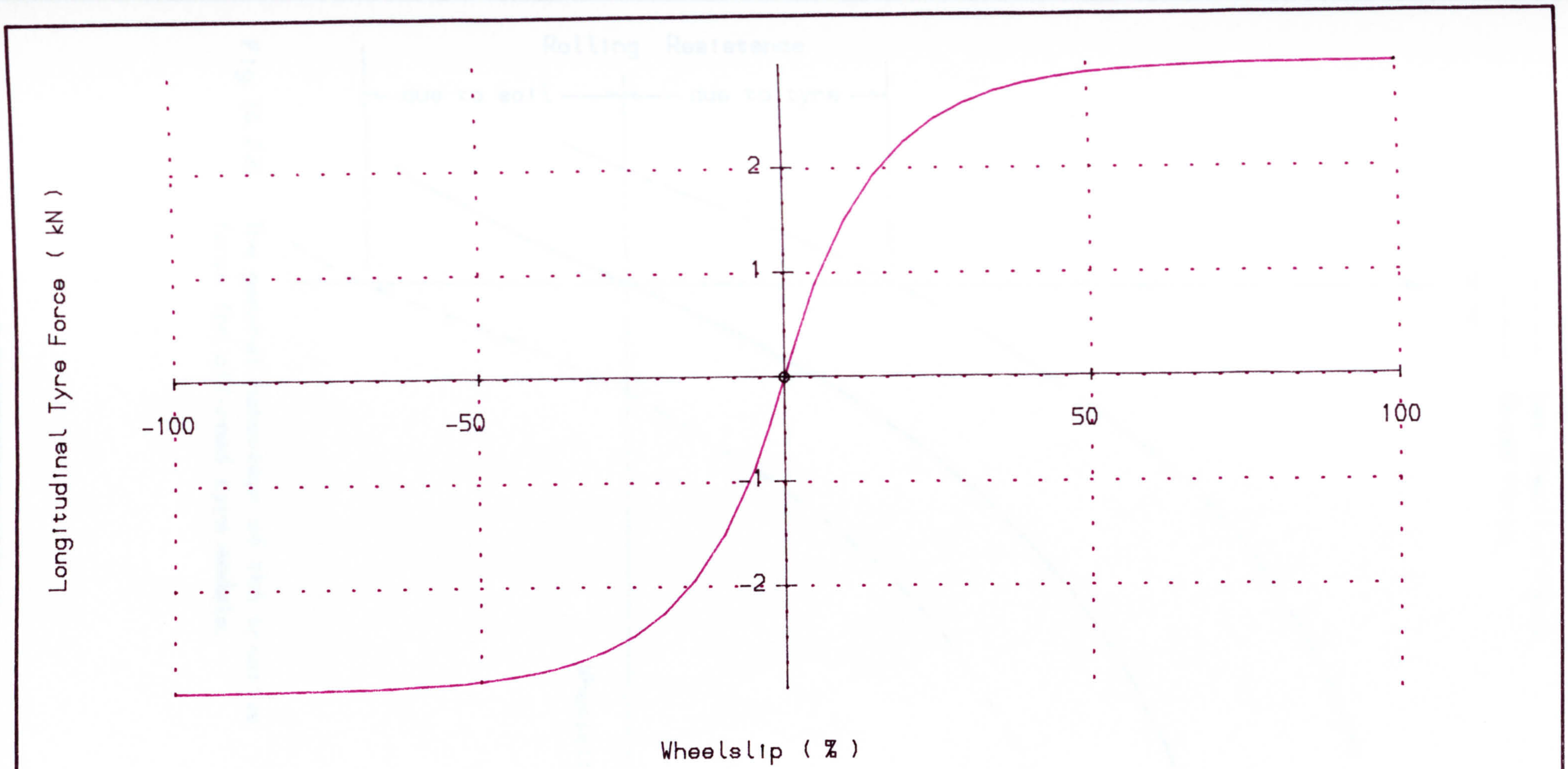

Fig. (6.21) Predicted longitudinal tyre force / wheelslip relationship at zero slip angle.

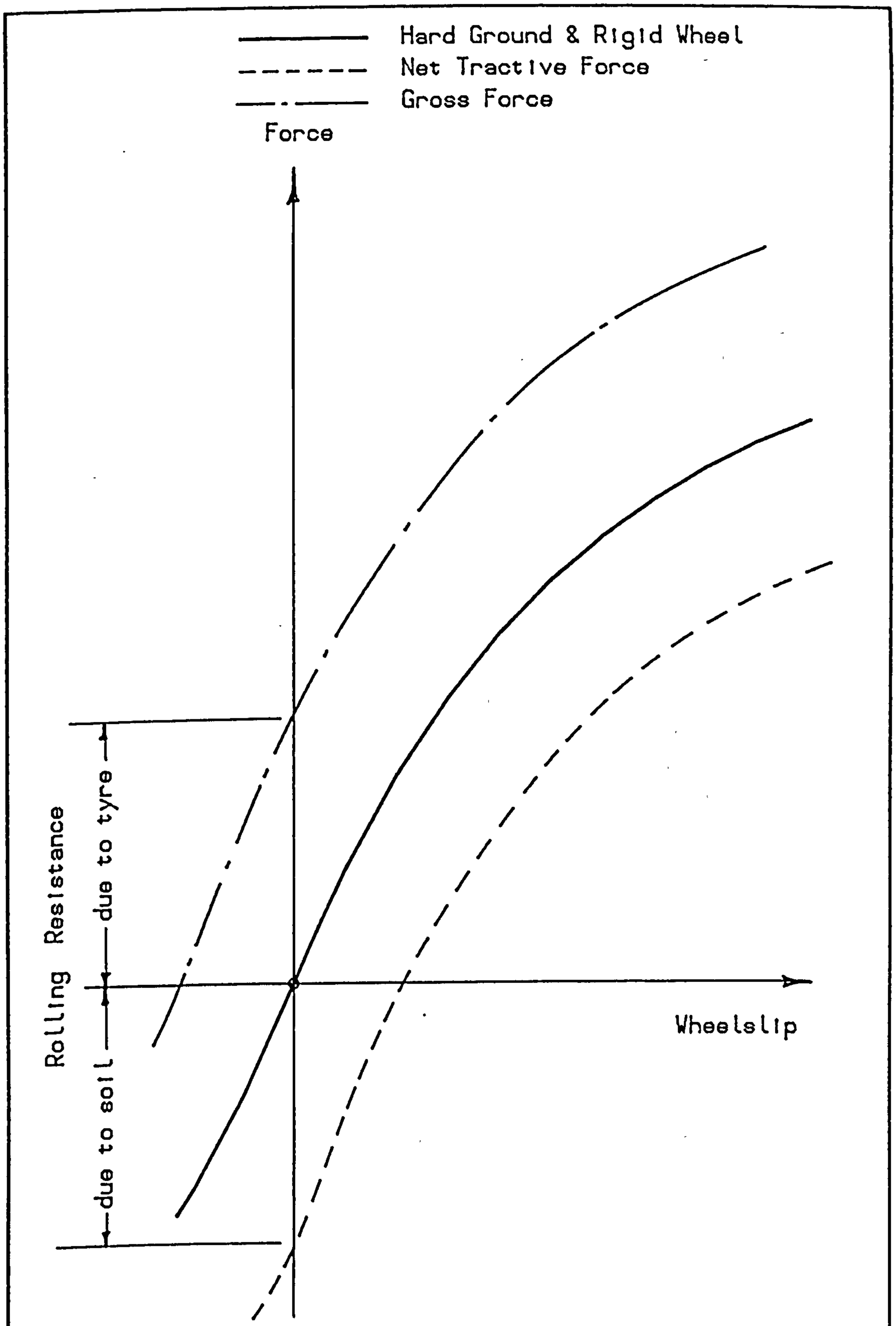

Fig. (6.22) The general behaviour of the tractive force for off-road tyre models.

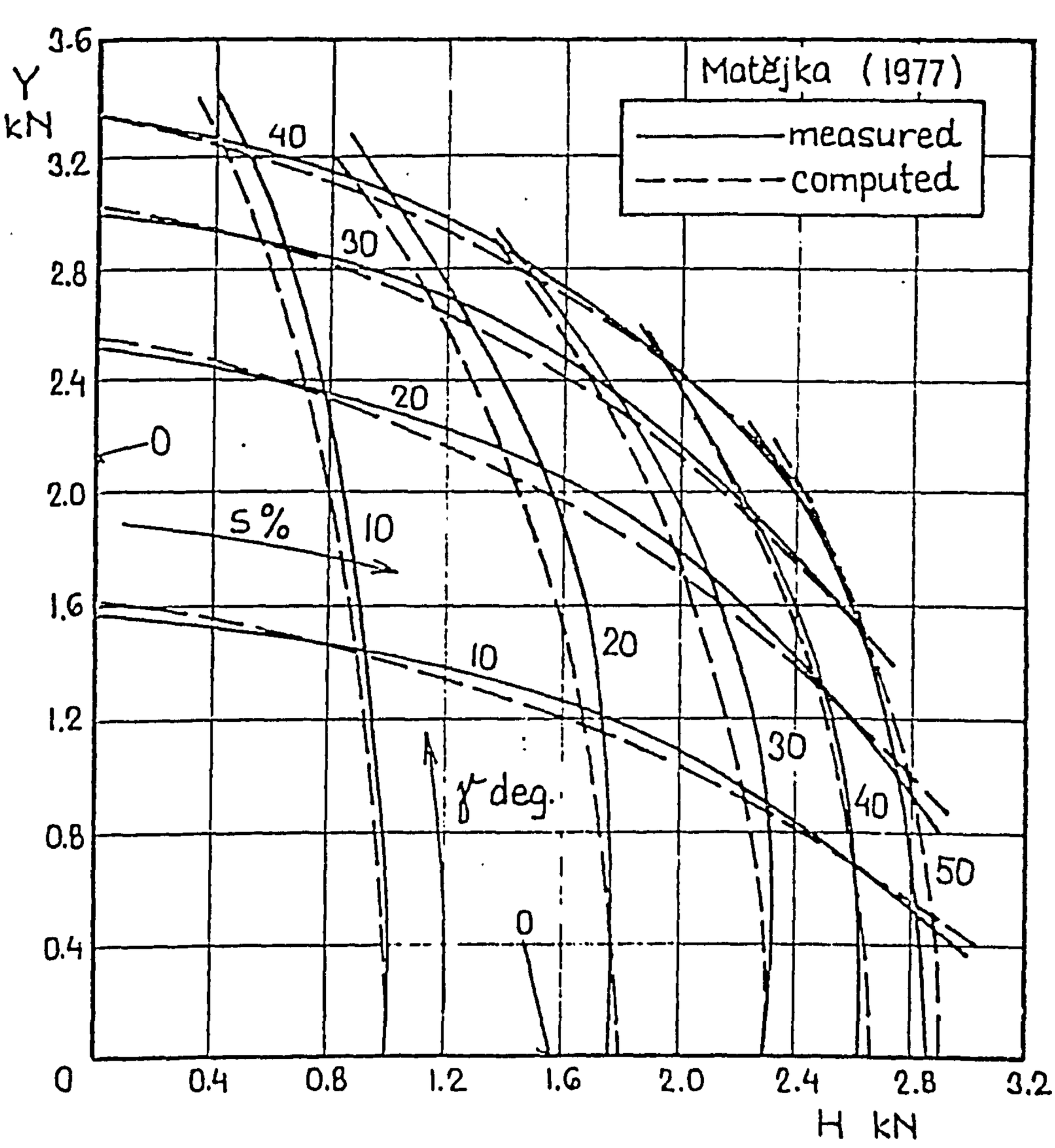

Fig. (6.23) Comparison between computed and measured lateral/longitudinal force relationships as obtained by Matejka, 1977.

Lines iso-slip angles

Slip angle = 0°

Slip angle = 10°

Slip angle = 20°

Slip angle = 30°

Slip angle = 40°

Tyre Load = 5.2 kN

Lines iso-wheelslip

Wheelslip = 0 %

Wheelslip = 10 %

Wheelslip = 20 %

Wheelslip = 30 %

Wheelslip = 40 %

Wheelslip = 50 %

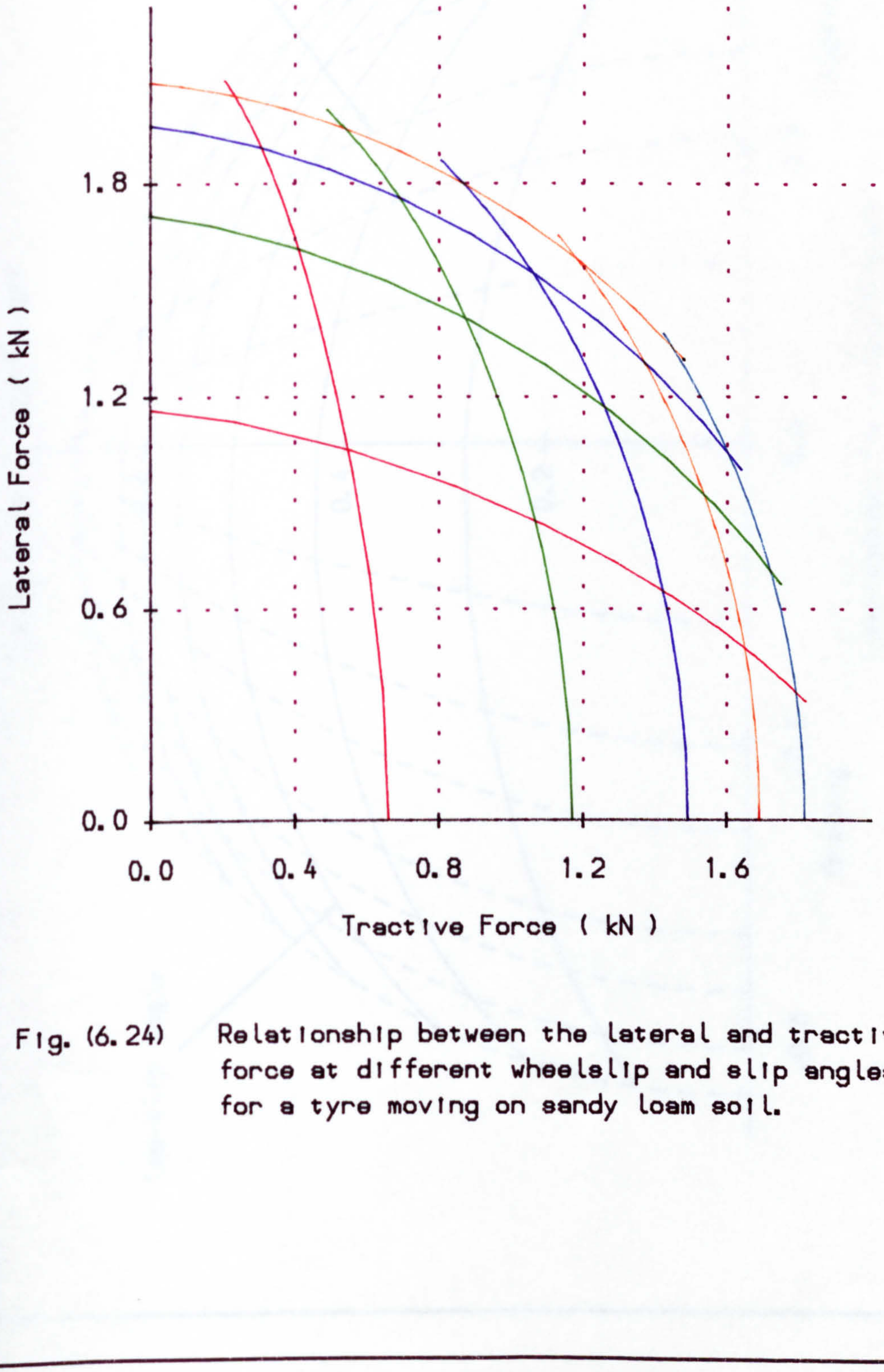

Fig. (6.24) Relationship between the lateral and tractive force at different wheelslip and slip angles for a tyre moving on sandy loam soil.

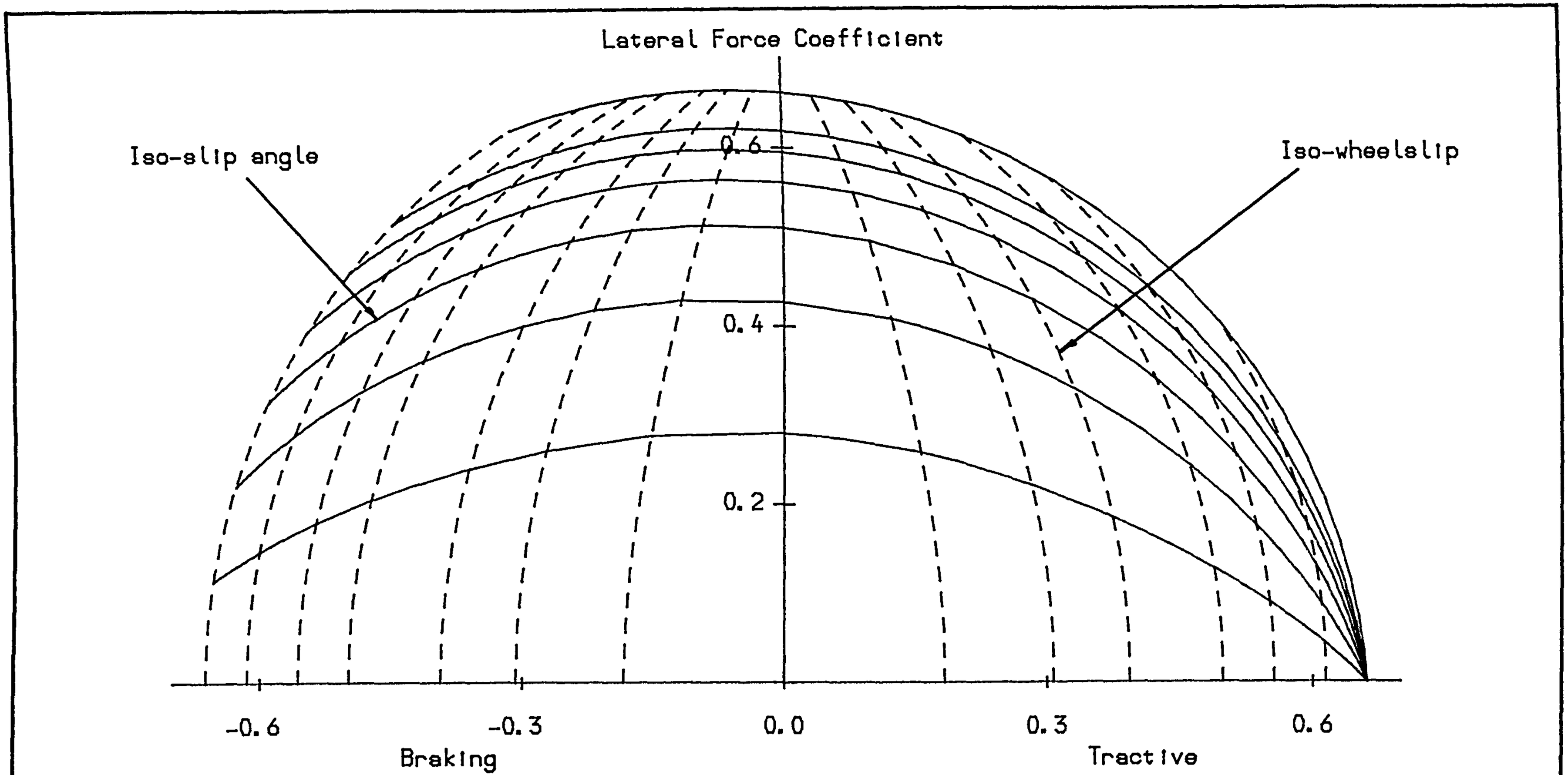

Fig (6.25) Tyre force characteristics predicted by Grecenko's model for a 7.50 x 18 tyre on sandy loam soil.

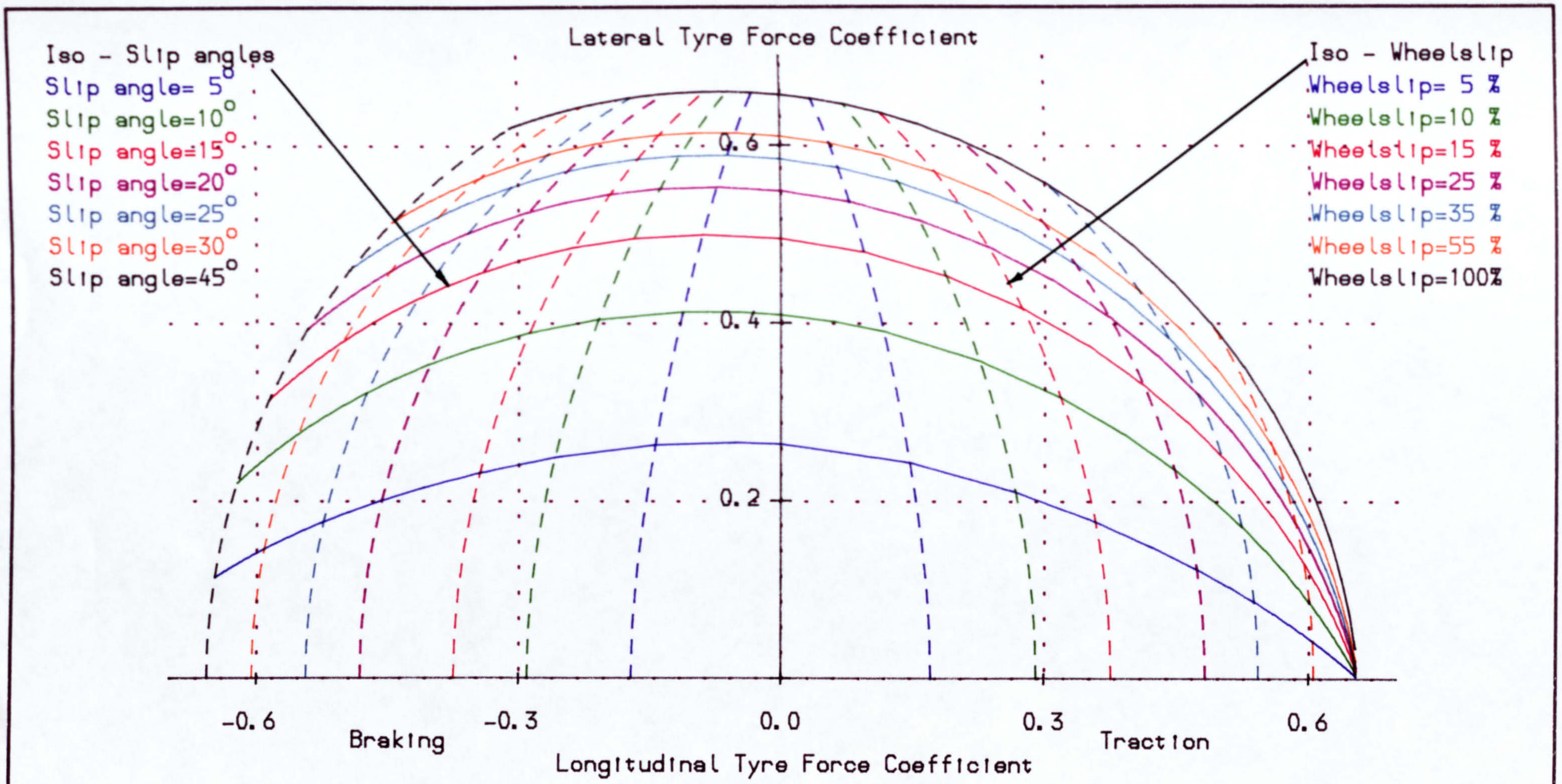

Fig. (6.26) Tyre force characteristics predicted by the modified model for a typical 7.50 x 18 tractor front tyre operating on sandy loam soil.

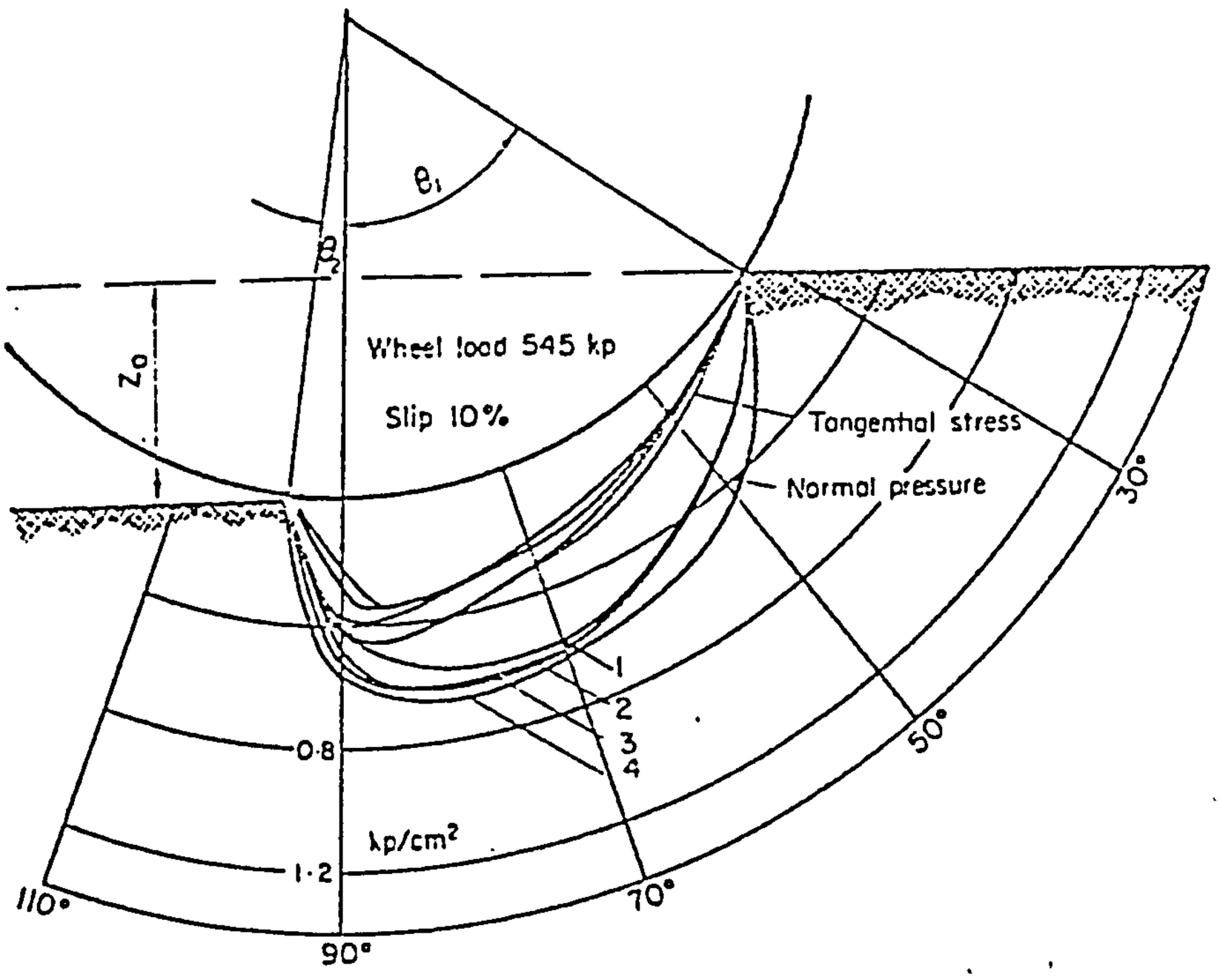

Fig. (6.27) Distributions of normal pressure and tangential stress measured by Krick, 1969.

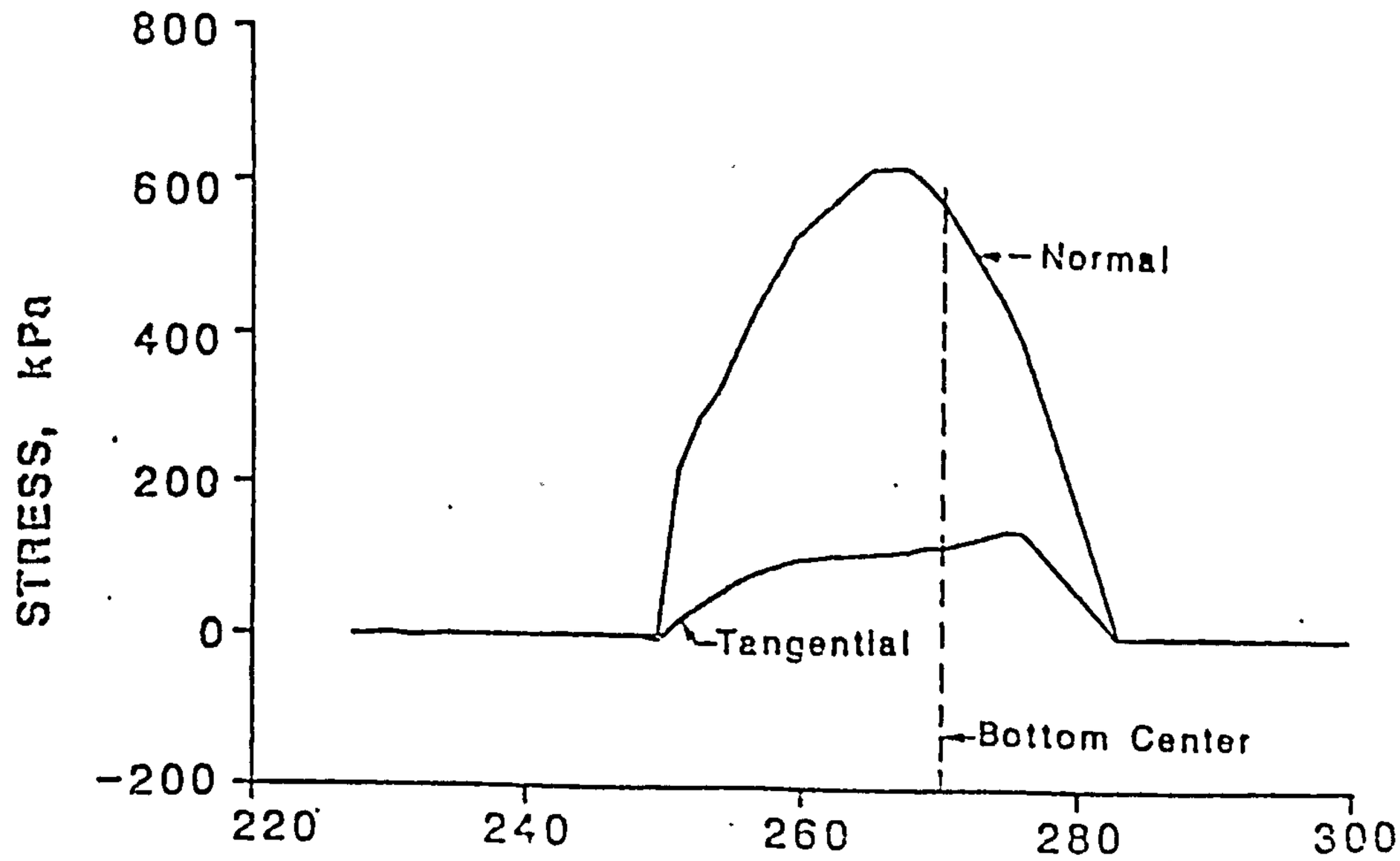

Fig. (6.28) Normal pressure and tangential stress distributions measured by Burt, 1987.

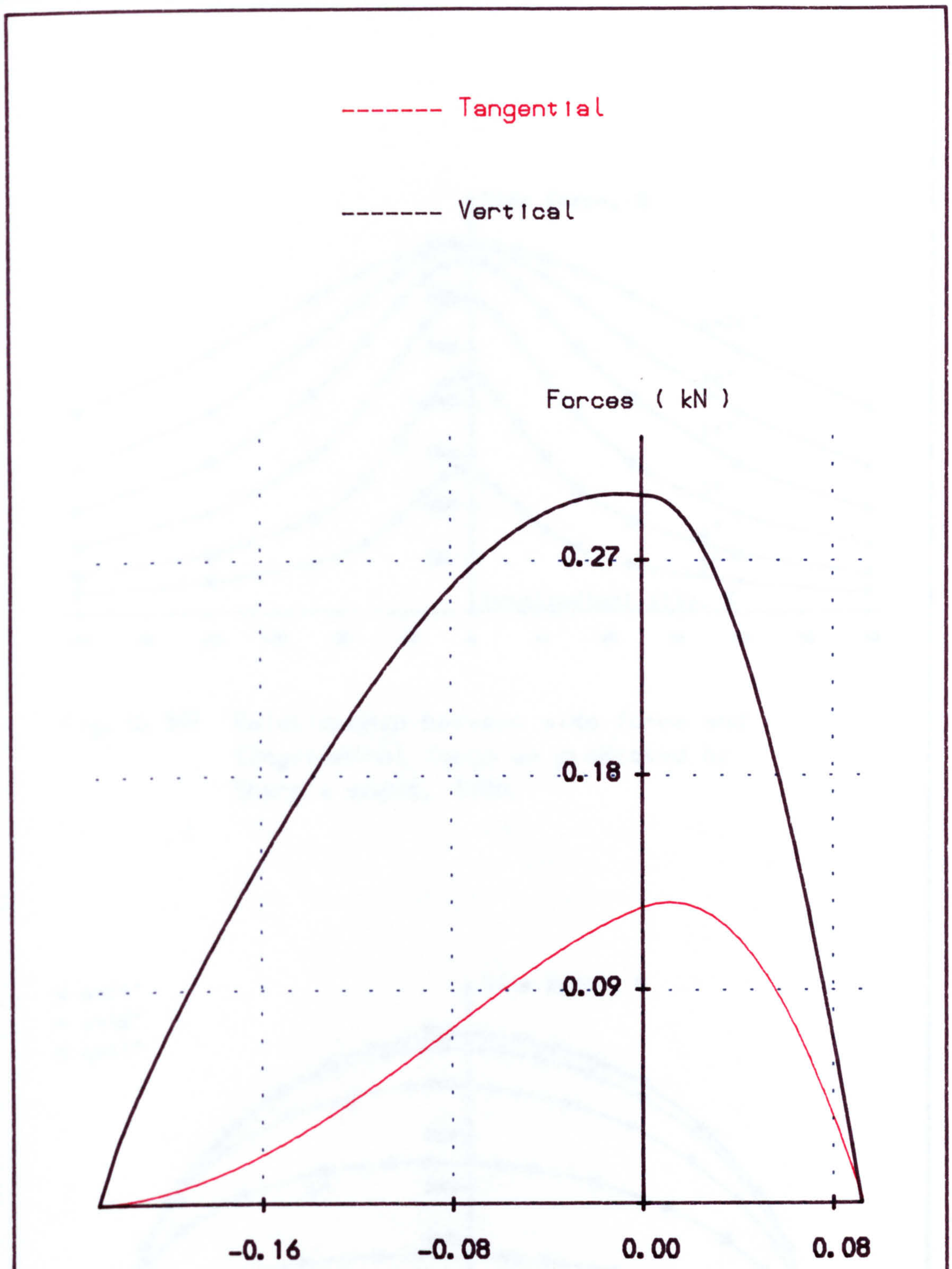

Fig. (6.29) Distributions of tyre forces along length of the contact region for a 7.50 x 18 tyre operating at 10% wheelslip, 10 deg. of slip angle and 5.2 kN tyre load.

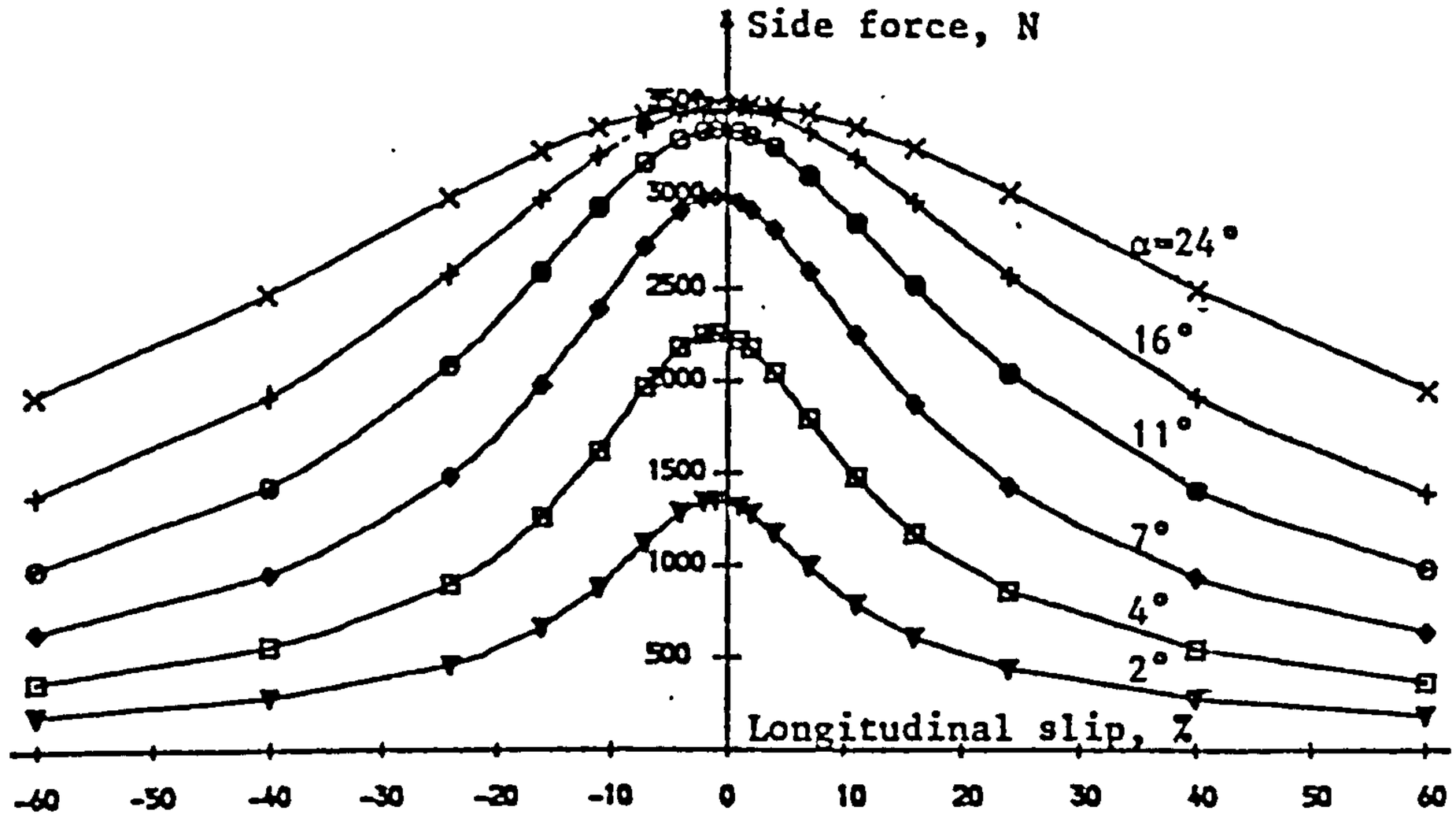

Fig. (6.30) Relationship between side force and longitudinal force as predicted by Sharp's model, 1986.

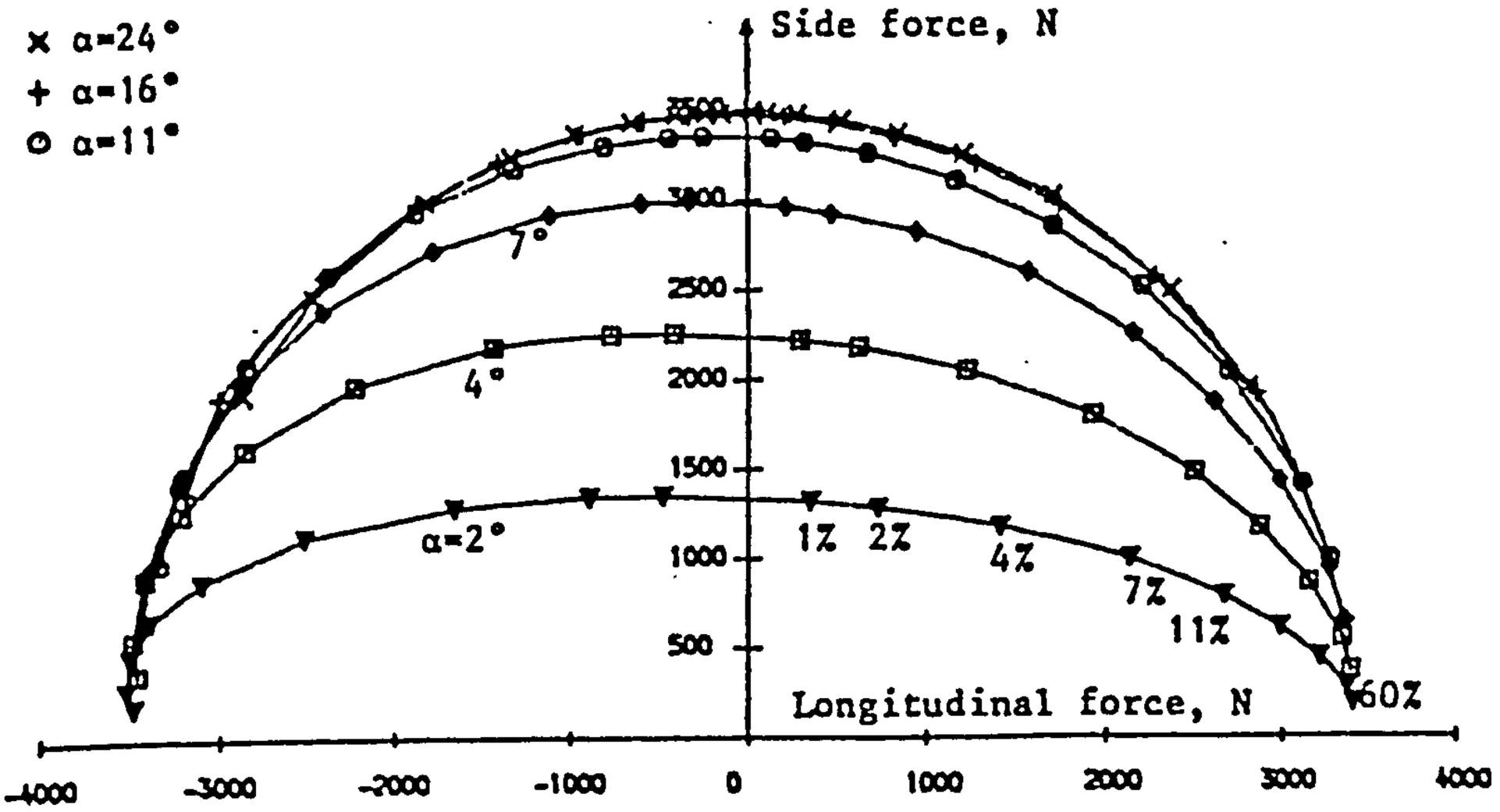

Fig. (6.31) Side force/longitudinal slip relationship with different slip angles as predicted by Sharp's model.

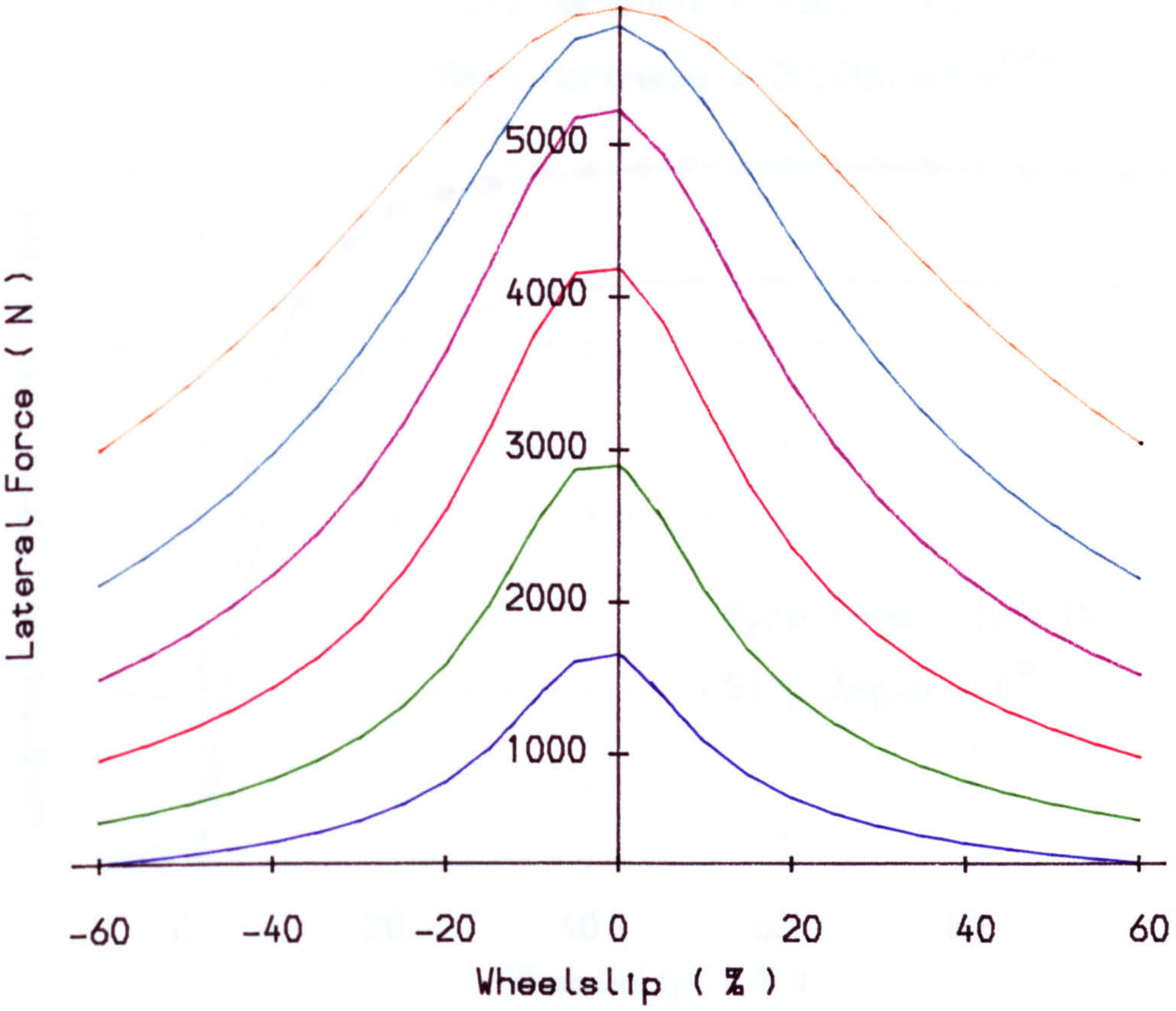

Fig. (6.32) Relationship between lateral force and wheelslip with different slip angles for a hard surface condition.

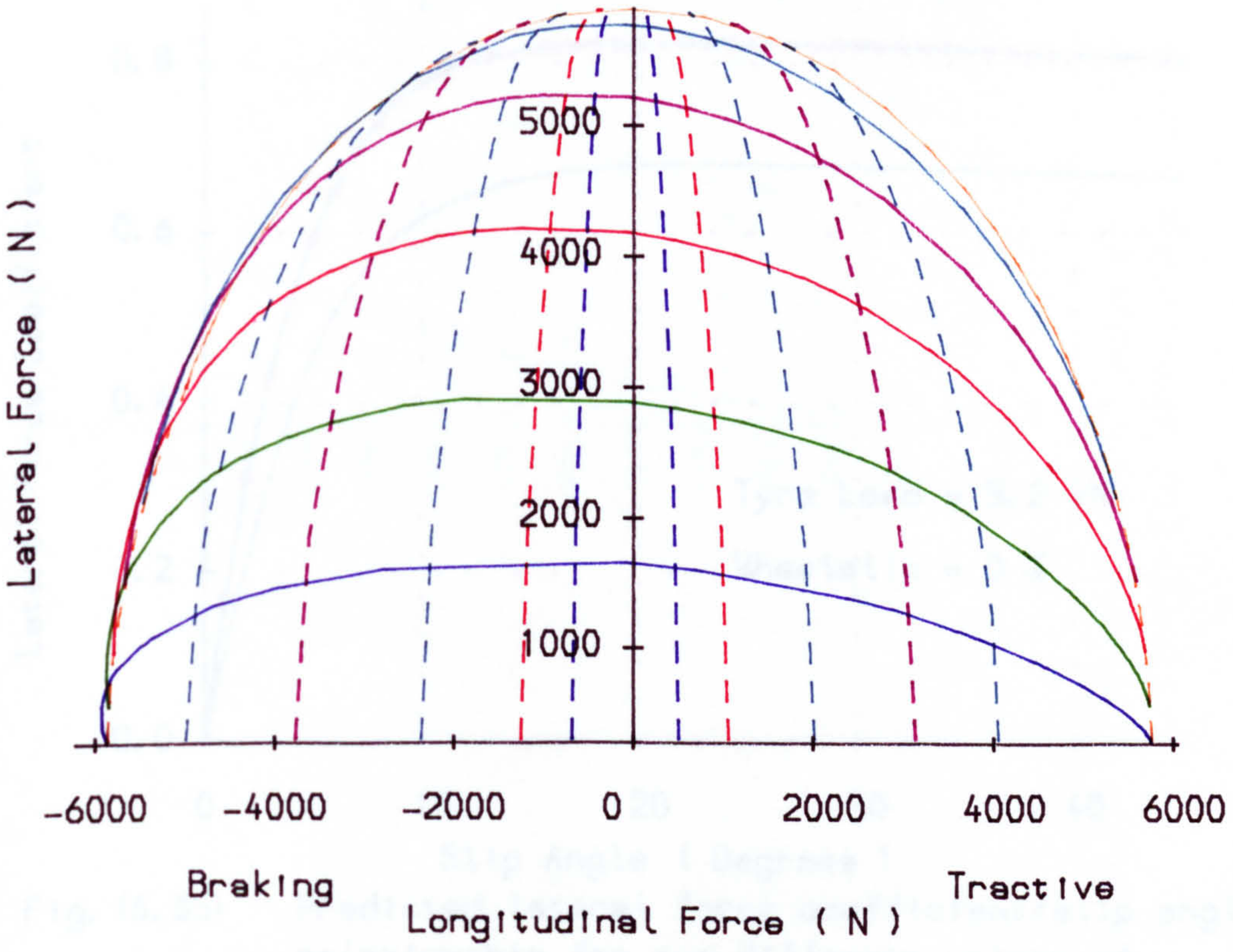

Fig (6.33) Spoke tyre model characteristics with a hard surface operating condition.

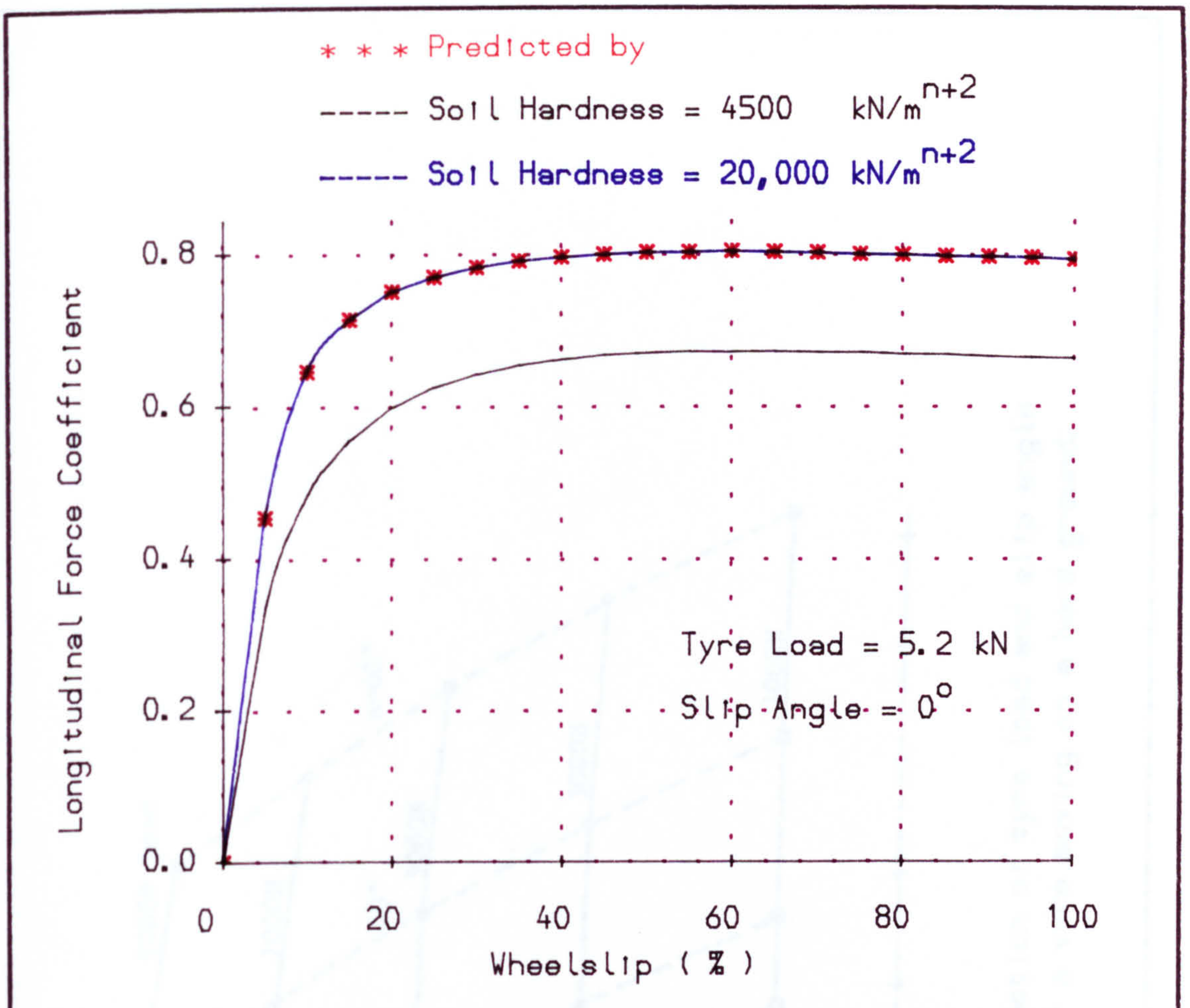

Fig. (6.34) Longitudinal force coefficient predicted by modified spoke tyre model for two different values of soil hardness compared with those predicted by Sharp's model.

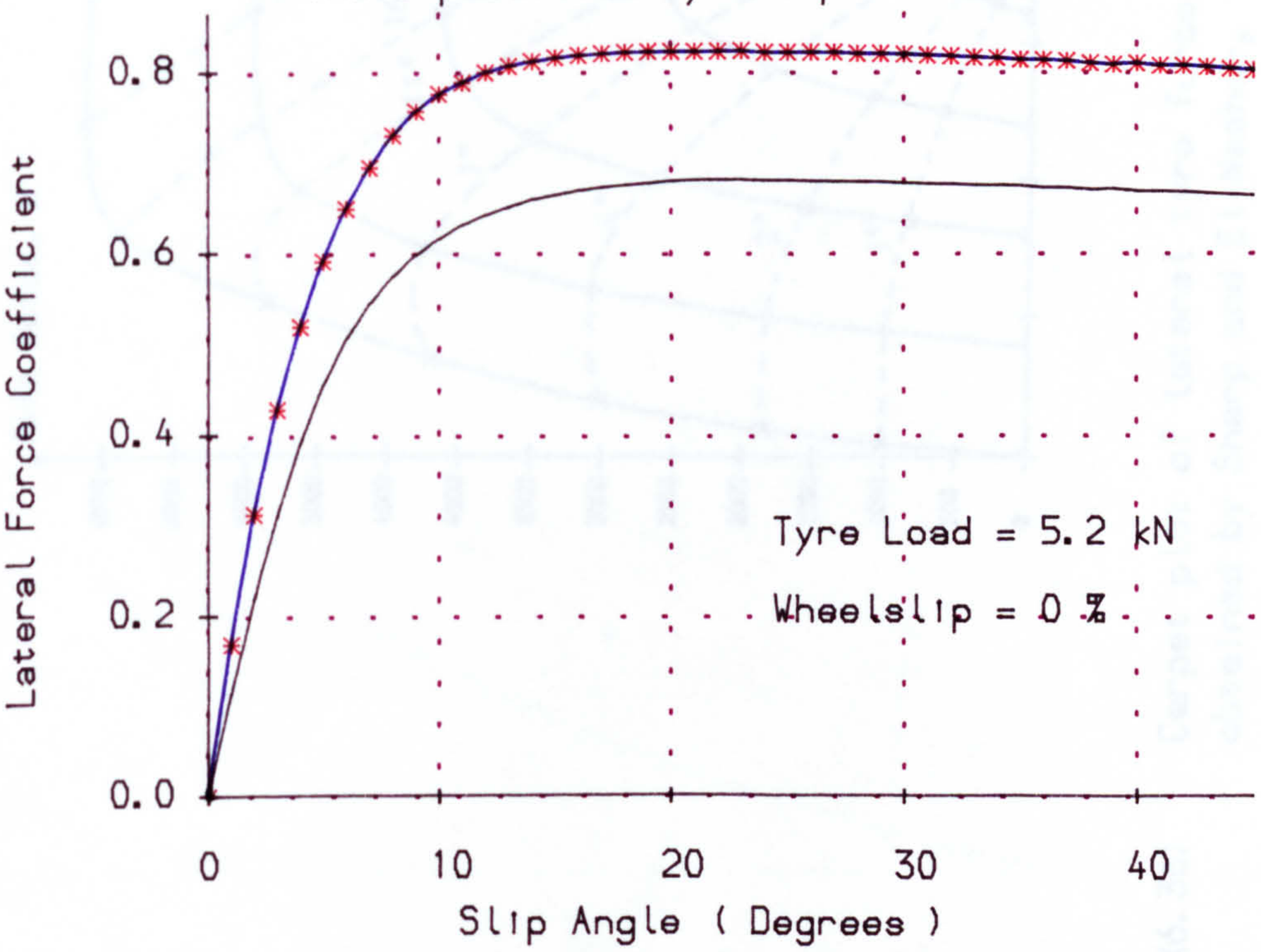

Fig. (6.35) Predicted lateral force coefficient/slip angle relationship for two different values of soil hardness compared with those predicted by Sharp's model.

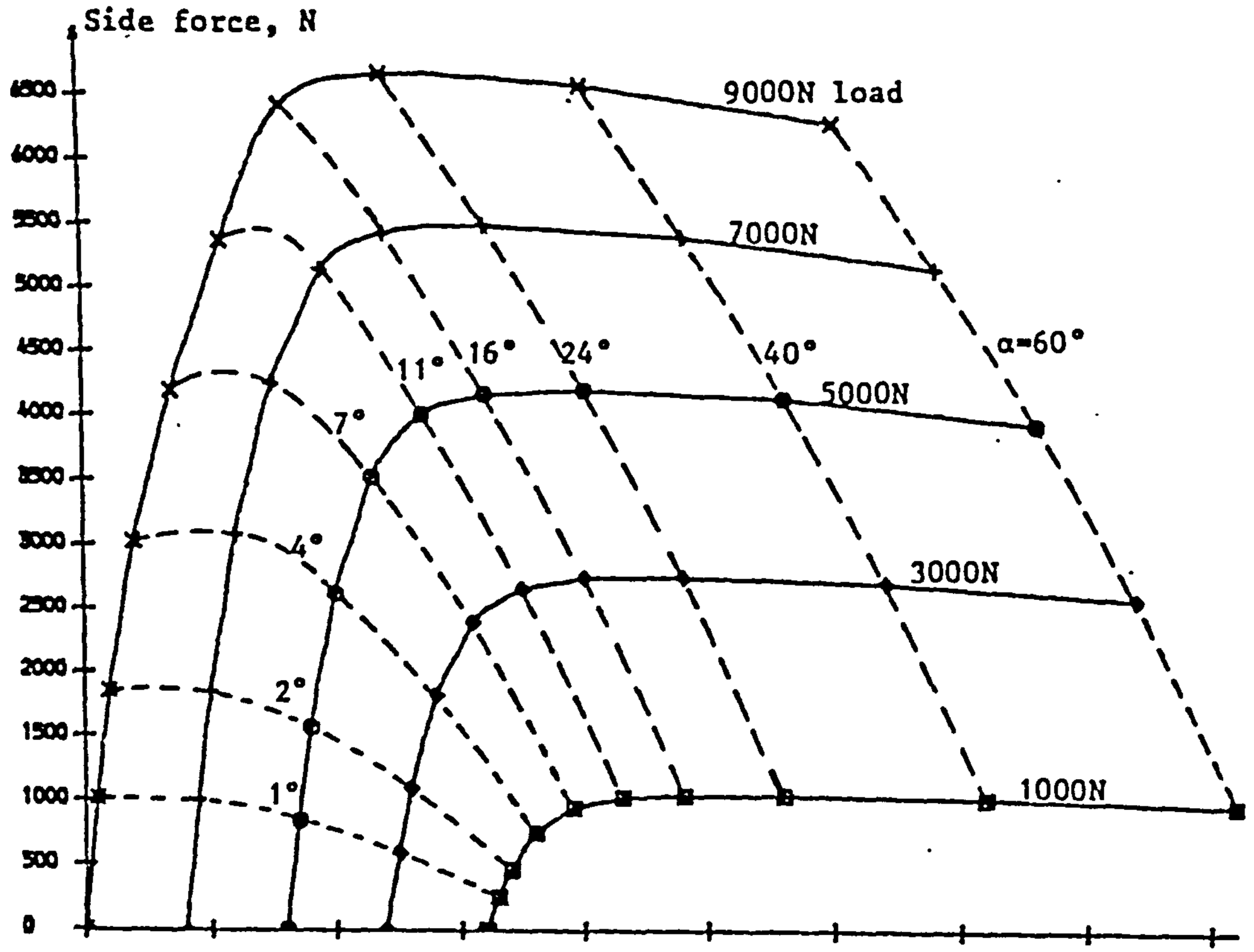

Fig. (6.36) Carpet plot of lateral tyre force as a function of tyre load and slip angle obtained by Sharp and El-Nashar, 1986 for a tyre moving on a hard ground.

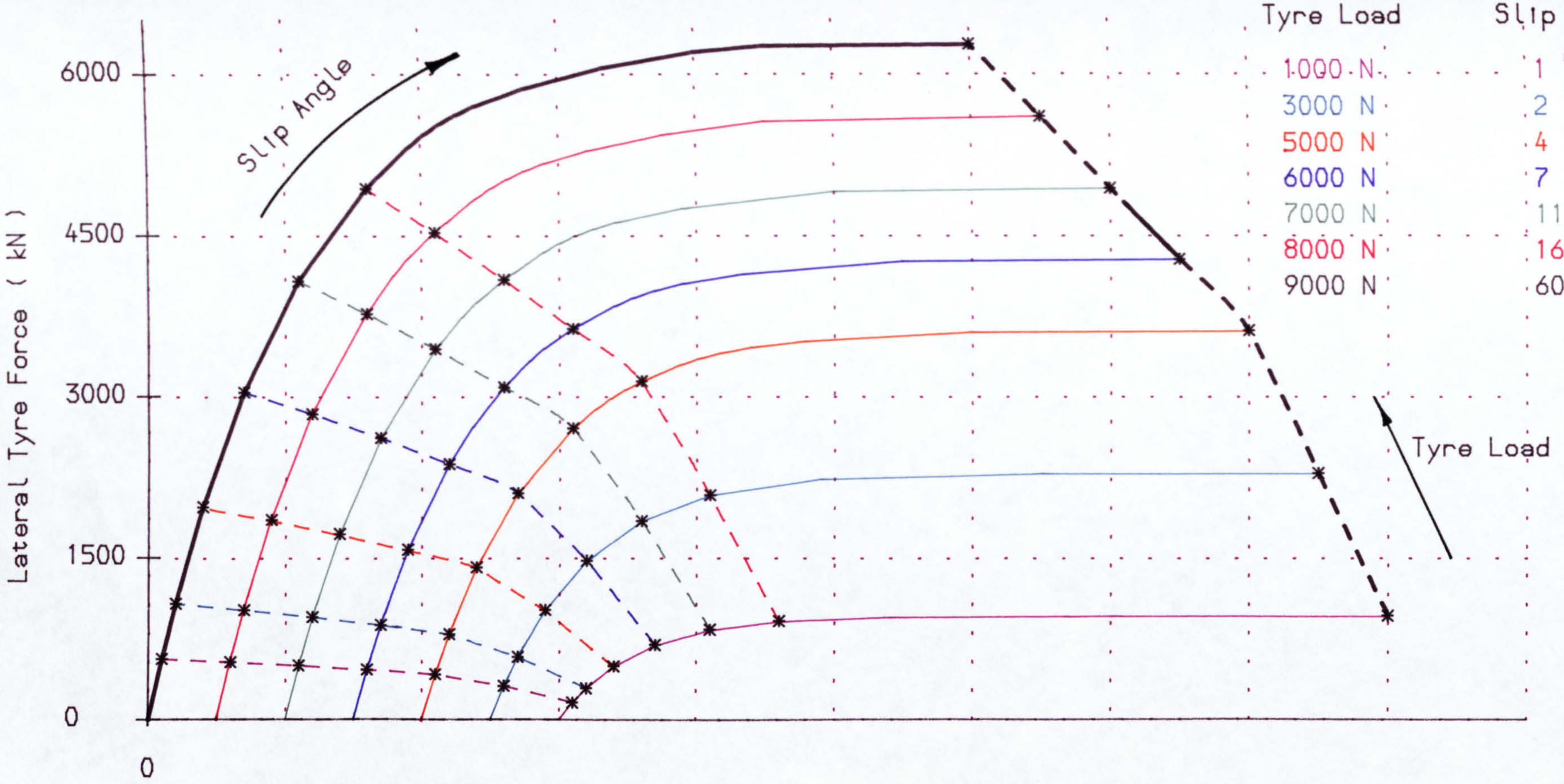

Fig. (6.37) Carpet plot of lateral tyre force as a function of tyre load and slip angle for a tyre moving on sandy loam soil.

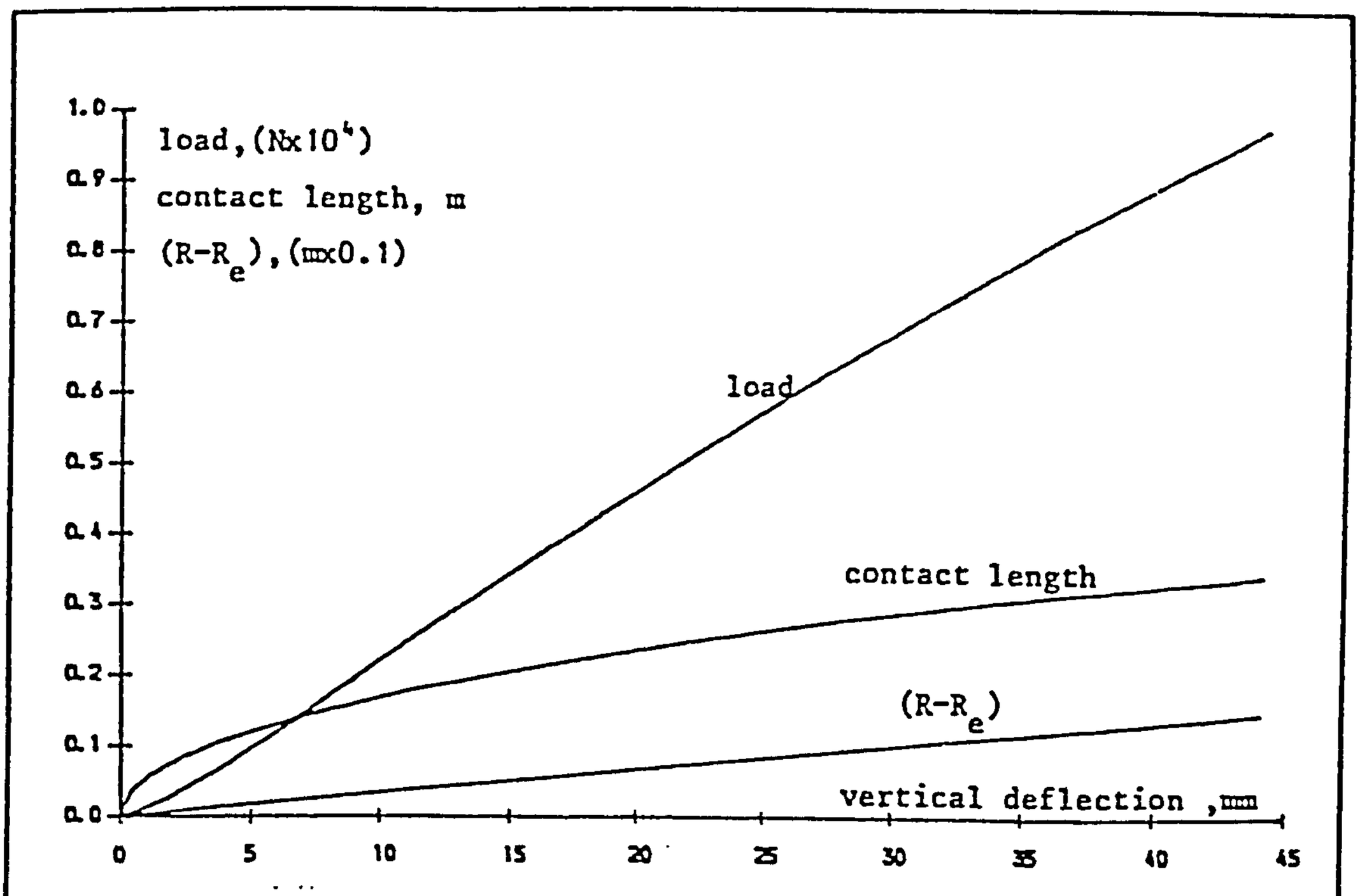

Fig. (6.38) Contact length change as a function of vertical deflection for the free rolling tyre as predicted by Sharp and El-Nashar, 1986.

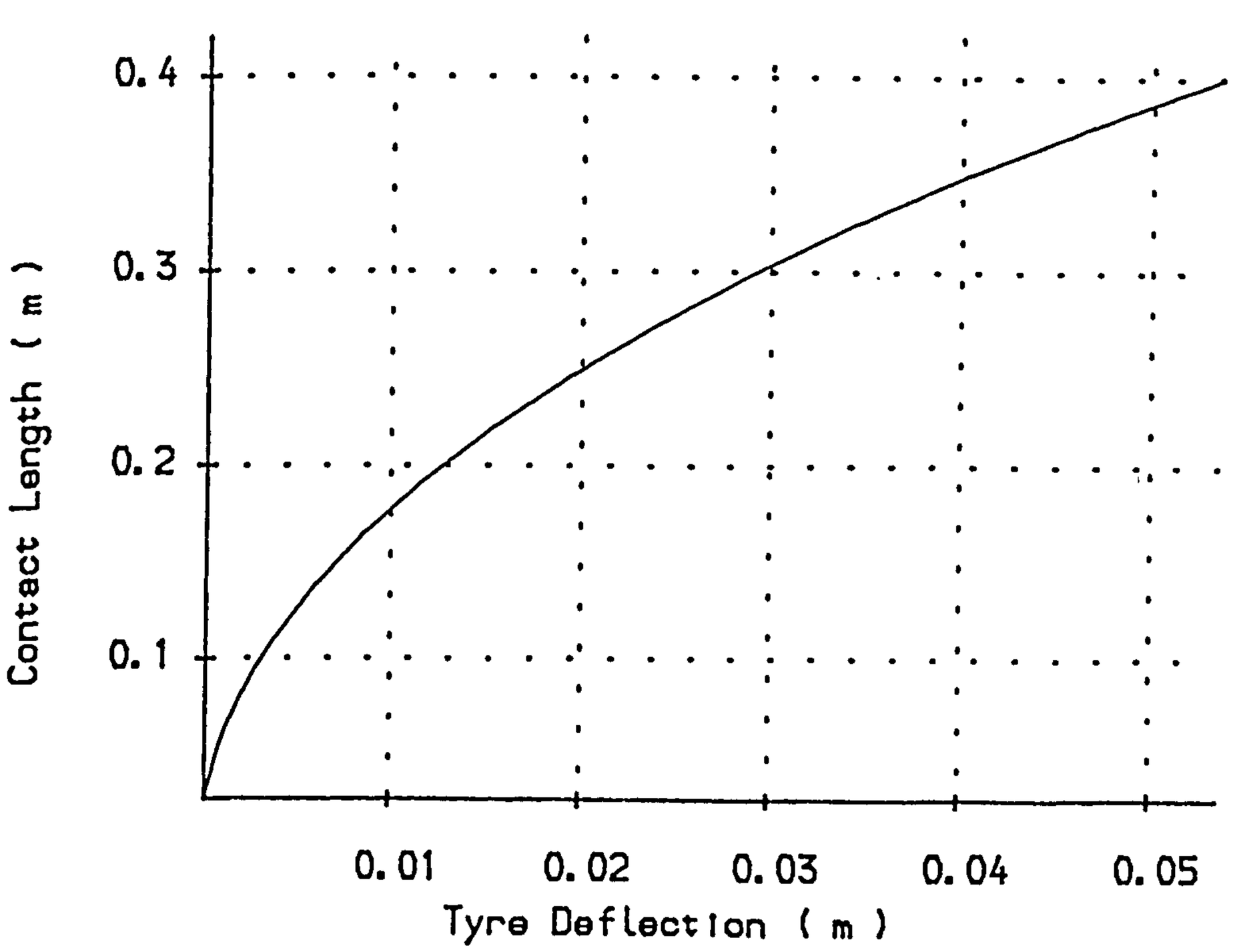

Fig. (6.39) Relationship between length of the contact region and tyre load predicted by the off-road tyre model.

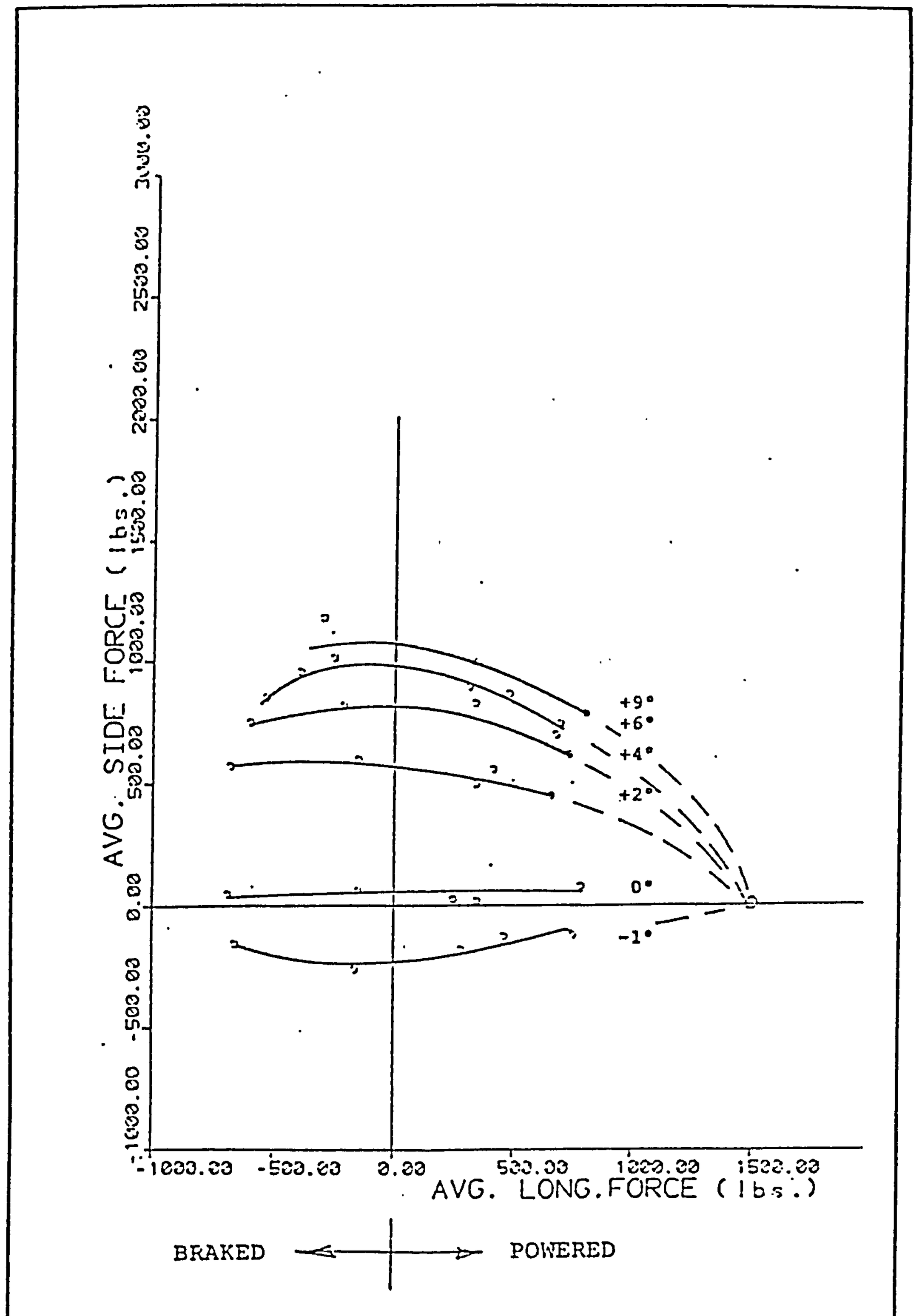

Fig. (6.40) Tyre side force as influenced by the application of the longitudinal force on soft soil as measured by Janosi, 1981.

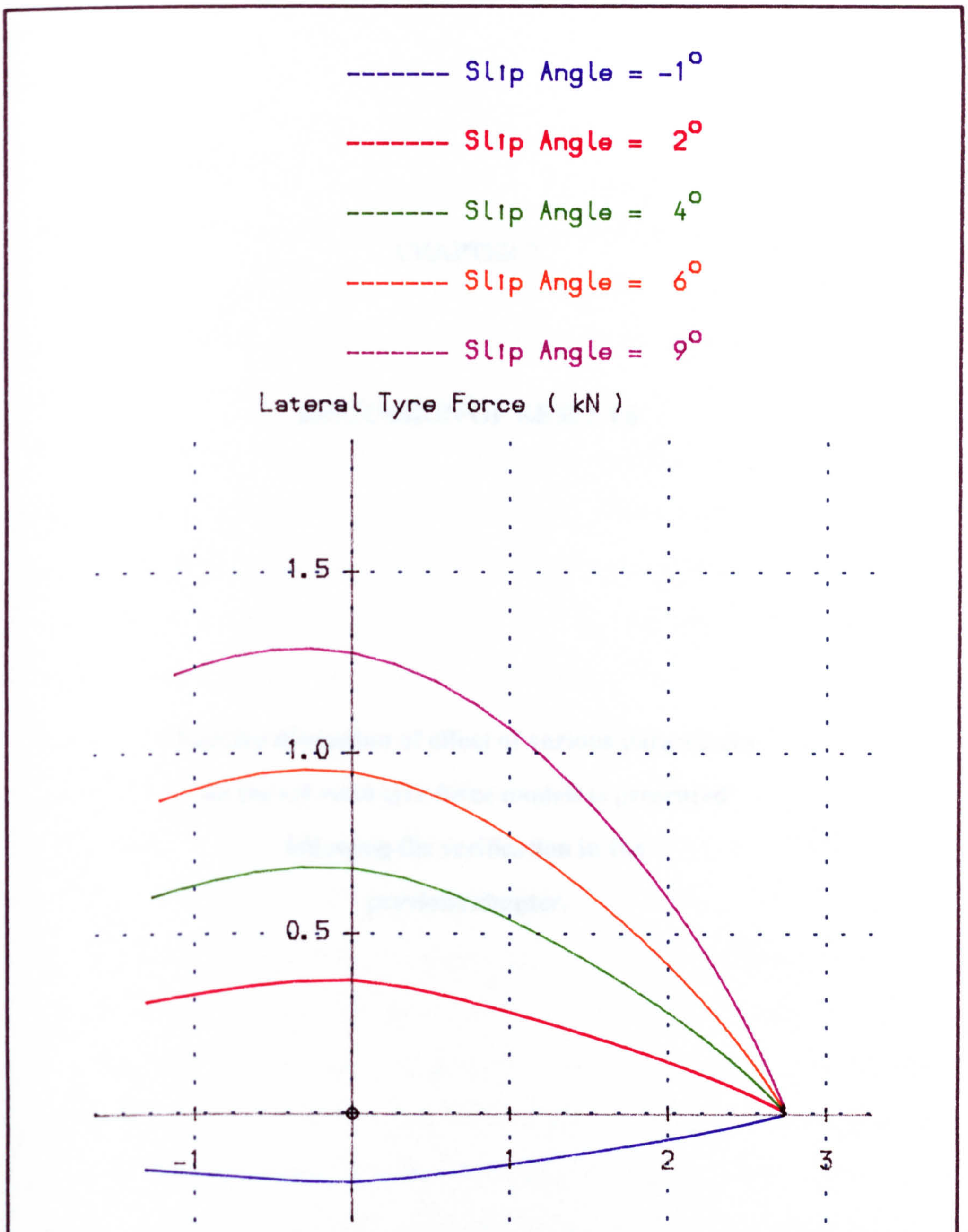

Fig. (6.41) Lateral tyre force characteristics as influenced by the longitudinal tyre force with different slip angles for a rolling tyre on sandy loam soil.

CHAPTER 7

DISCUSSION OF RESULTS

Further discussion of effect of various parameters on the off-road tyre force models is presented following the verification in the previous chapter.

7.1. INTRODUCTION

This chapter concerns the presentation of results obtained from the various off-road tyre models that have been developed to help investigate the handling and stability of off-road vehicles under specific operating conditions of wheelslip or wheelskid (traction or braking condition), slip angle and tyre load.

The predicted and measured results for various operating conditions have the same trends with slight differences in the magnitudes. This difference is expected as the data used in the models do not exactly match those used for the experiments usually because of insufficient data being provided in experimental papers or because it is presented in a form different from that used in the model.

General trends of the lateral force vs. slip angle relationship for a 7.50 x 18 front tractor tyre, for example are very close to those results obtained by Schwanghart [1968], Grecenko [1975], Matejka [1977] and Sharp and El-Nashar [1986] under similar operating conditions of slip angle, wheelslip and tyre loads.

With regard to Chapter 6, some insight into the general behavioural trends has been gained when comparing the results of off-road tyre force models with those obtained experimentally by a wide range of researchers. The factors affecting the behaviour of off-road tyre forces can be shown to have differing relative importance. These factors can be categorised into three main types. Firstly, the influence of the tyre load, second, the influence of the slip angle and finally the influence of wheelslip. The following results all refer to the spoke tyre model.

7.2. INFLUENCE OF TYRE LOAD

The radial tyre deflection and the soil sinkage are influenced by tyre load for a static tyre as shown in Fig.(7.1). The resulting tyre deflection and the soil sinkage noticeably increase with increasing tyre load. The maximum value of the soil sinkage and radial deflection occur at the centre of the wheel and decreases symmetrically till it reaches the minimum value at ends of the contact length. The effects of the tyre load

on the vertical and horizontal force distributions along the length of the contact region are shown in Fig.(7.2). The results show that the tyre forces generated from a static tyre on a deformable surface are significantly influenced by the tyre load.

The relationship between the lateral tyre force and tyre load is shown in Fig.(7.3). The curves representing this relationship are dependent on slip angle, the slope increasing with an increase in the slip angle. In general, lateral tyre force increases with the increasing tyre load with the shape of the relationship changing slightly as slip angle is increased from 5 to 30°.

The relationship between longitudinal tyre force and tyre load in Fig.(7.4) shows that the longitudinal tyre force increases significantly with increasing tyre load at constant wheelslip in an approximately linear manner over the range tested which represents approximately ±20% of the nominal tyre rated load.

7.3. INFLUENCE OF SLIP ANGLE

The influence of slip angle on lateral tyre force is shown in Fig.(7.5). The relationship between the lateral tyre force and slip angle with various wheelslip values indicates that the lateral tyre force increases with an increase in slip angle in an approximately exponential manner. This result confirms the measured results obtained by Schwanghart [1968]. Fig.(7.6) shows the influence of slip angle on longitudinal tyre force with different wheelslip ranged between 5% and 30%. Increasing slip angle produces decreases longitudinal tyre force.

Fig.(7.7) shows the influence of the slip angle on the lateral tyre force generated with various tyre loads. The tyre load is ranged from 2 up to 12 *kN* and slip angle from 0 to 45°. The general trend of lateral tyre force vs. slip angle at different tyre loads is very close to the results measured by Schwanghart [1968].

Lateral and longitudinal force coefficient distributions throughout the length of the contact region are shown in Fig.(7.8). As the slip angle increases the lateral force coefficient increases, while the longitudinal force coefficient decreases. In general, the

resultant of lateral and longitudinal force act at some distance behind the contact centre. This distance decreased with increasing slip angle in the case of the lateral force coefficient and it is this distance together with the force which controls the value of the aligning moment. The initial slope of the relationship between the aligning moment and slip angle is increased with tyre load increasing as shown in Fig.(7.9). As slip angle is then increased further, two things happen : the lateral force increases but the distance of its effective line of action relative to the tyre centreline decreases. Thus, the aligning moment reaches a maximum value and then drops to lower values. The way in which this trend is affected by tyre load is shown in detail in Fig.(7.9). Fig.(7.10) illustrates the relationships between the lateral tyre force and the aligning moment with different tyre load. The initial slope of this relationship is decreased with an increasing tyre load.

On other hand, in the case of the longitudinal force coefficient, both the force itself and the distance of the effective line of action of the resultant longitudinal force behaind the tyre centreline continue to decrease with increasing slip angle as more of the soil shear forces are used up in generating lateral force.

7.4. INFLUENCE OF WHEELSLIP

Wheelslip significantly influences lateral tyre force as shown in Fig.(7.11). For a specific slip angle, the lateral tyre force decreases as wheelslip increases as more of the soil forces are used to generate longitudinal force. the rate of increasing decreased with increase of the slip angle. Fig.(7.12) illustrates the relationship between the longitudinal tyre force and wheelslip at different slip angles. The slip angle significantly affects the shape of the important tractive force vs. wheelslip curve, and in marginal traction conditions it is clear that trying to manoeuvre a vehicle and thereby generating slip angles at the tyres could cause the vehicle to stall through insufficient traction force being available.

In Fig.(7.13) the longitudinal tyre force is plotted against wheelslip with various tyre loads. The slope of the relation between longitudinal tyre force and wheelslip

shows a significant increase as tyre load increases. The behaviour of lateral and longitudinal force coefficient distributions through the length of the contact region are shown in Fig.(7.14). At low values of wheelslip, most of the longitudinal force is generated at the rear of the contact area. However, as the wheelslip increases, more of the contact area is used to generate force and the shape of the curve changes.

The overall behaviour of the tyre as summarised in Fig.(7.15), gives a complete assessment of the influence of the main factors of the operating conditions. The forces available under any general conditions of slip angle, wheel slip or skid can be interpolated from these curves.

These relationships between lateral force, braking force, tractive force, wheelslip and slip angle, illustrated in the friction ellipse graph shown in Fig.(7.15), are for a 7.50 x 18 front tractor tyre in sandy loam soil with a tyre load of 5.2 kN. The longitudinal force (braking or tractive) significantly decreases with increasing lateral force as shown by lines of constant slip angle. On the other hand, there is a relatively sharp fall in lateral force with increasing tractive force at constant wheelslip, with a slow rising of the lateral force with braking force at constant wheelskid.

As a result, the relationships between the lateral and longitudinal forces are asymmetric. Of course, the distance that the tyre travels when subject to a tractive operating condition will be less than that in the free rolling case Whereas when a braking operating condition is applied, the distance will be greater than that in free rolling condition. However, the braking force gives a higher obtainable lateral force than when the tyre is producing a tractive force. The presence of the tractive force means that a higher slip angle is required to generate the same lateral force as in braking conditions.

7.5. CONCLUDING REMARKS

(1) The results from the tyre model presented in this chapter provide an understanding of the detailed behaviour at the soil-tyre interface of an off-road tyre operating on a deformable surface.

(2) The detailed distributions of the forces within the contact region have been shown and their relationships with the tyre's operating conditions have been presented.

(3) Finally, the overall behaviour of the tyre as summarised in the friction ellipse graph has been given.

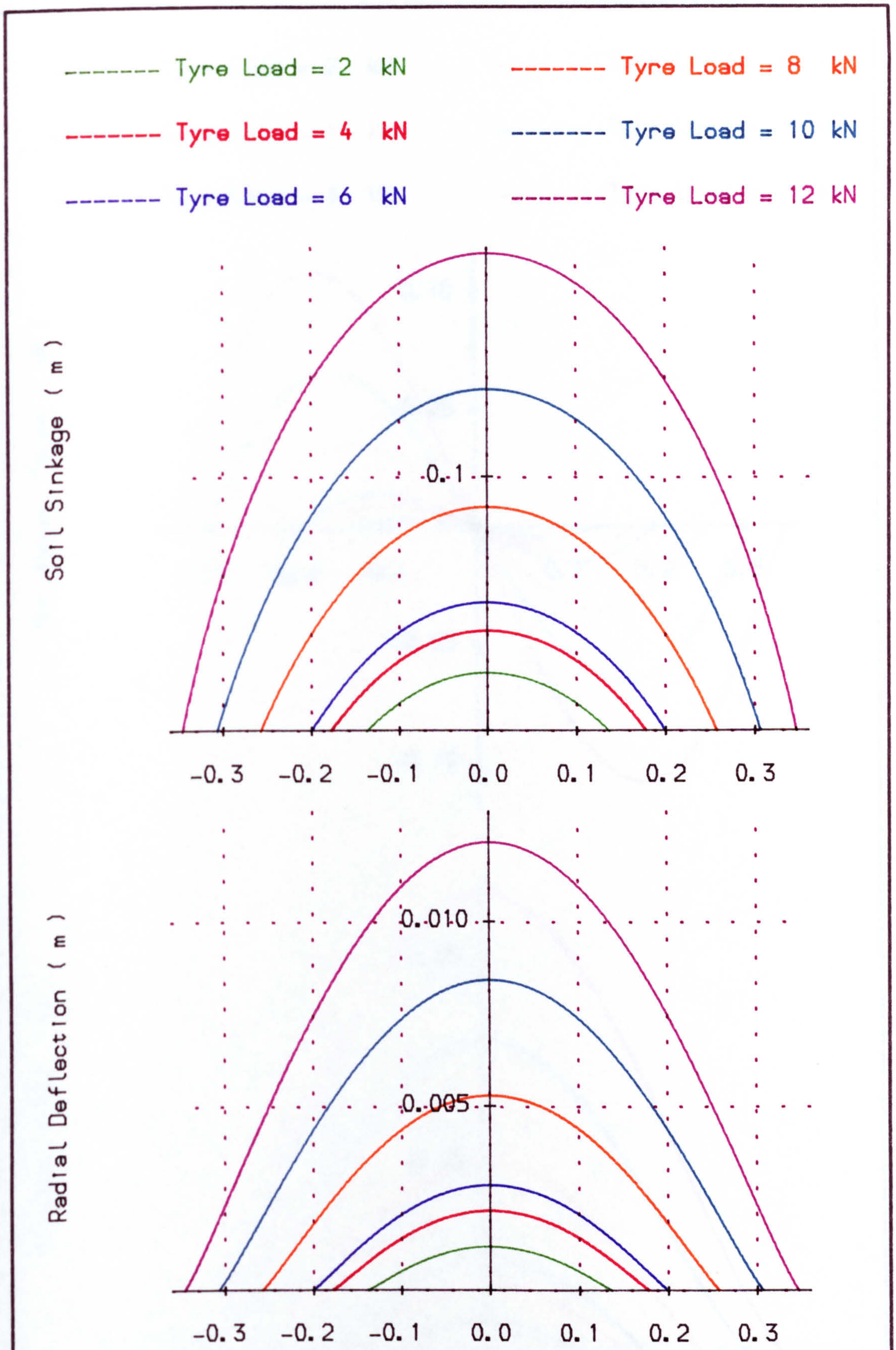

Fig. (7.1) Effect of tyre load on the radial deflection and soil sinkage for a static tyre on a deformable surface.

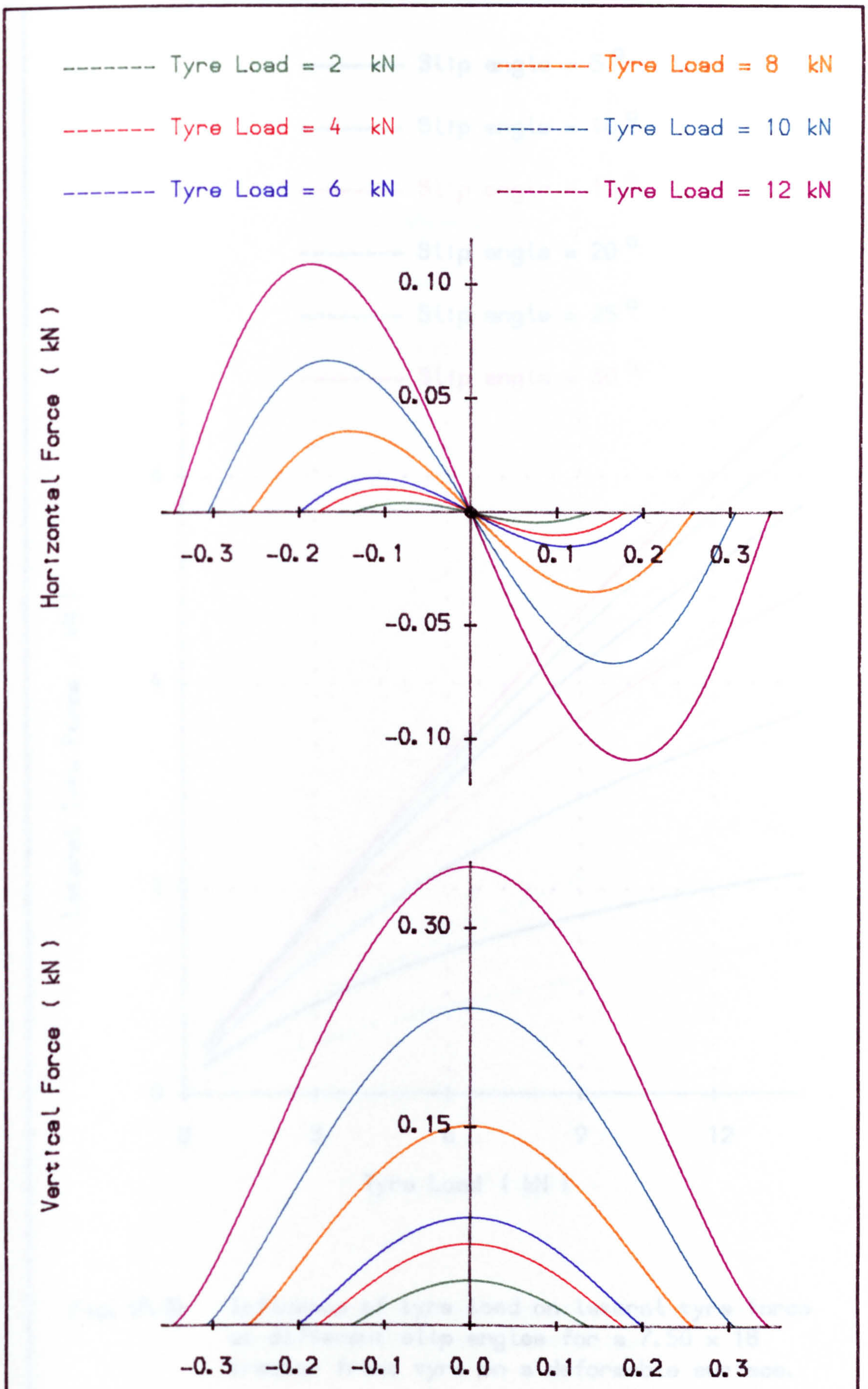

Fig. (7.2) Effect of tyre load on vertical and horizontal forces for static tyre on deformable soil.

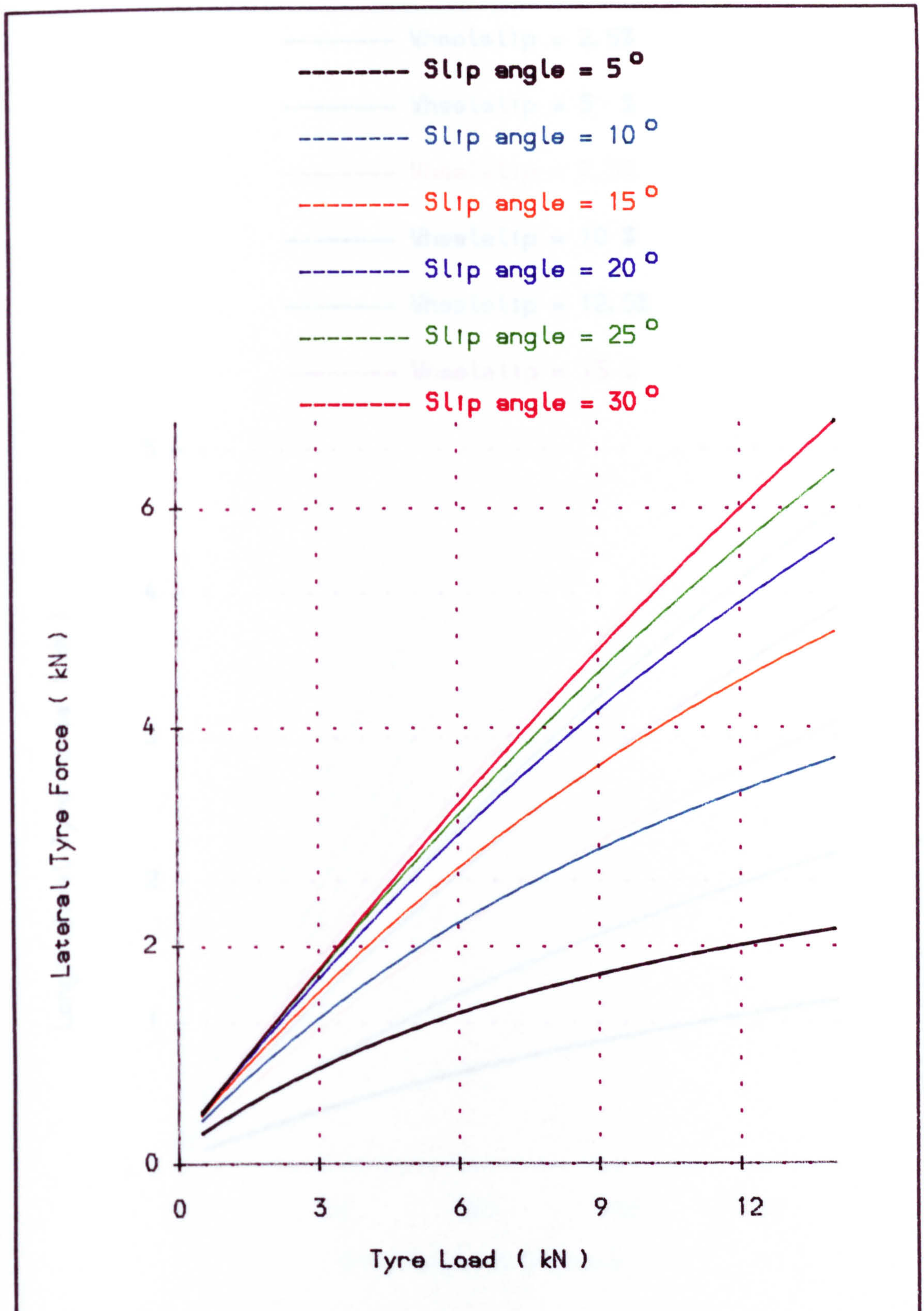

Fig. (7.3) Influence of tyre load on lateral tyre force at different slip angles for a 7.50 x 18 tractor front tyre on a deformable surface.

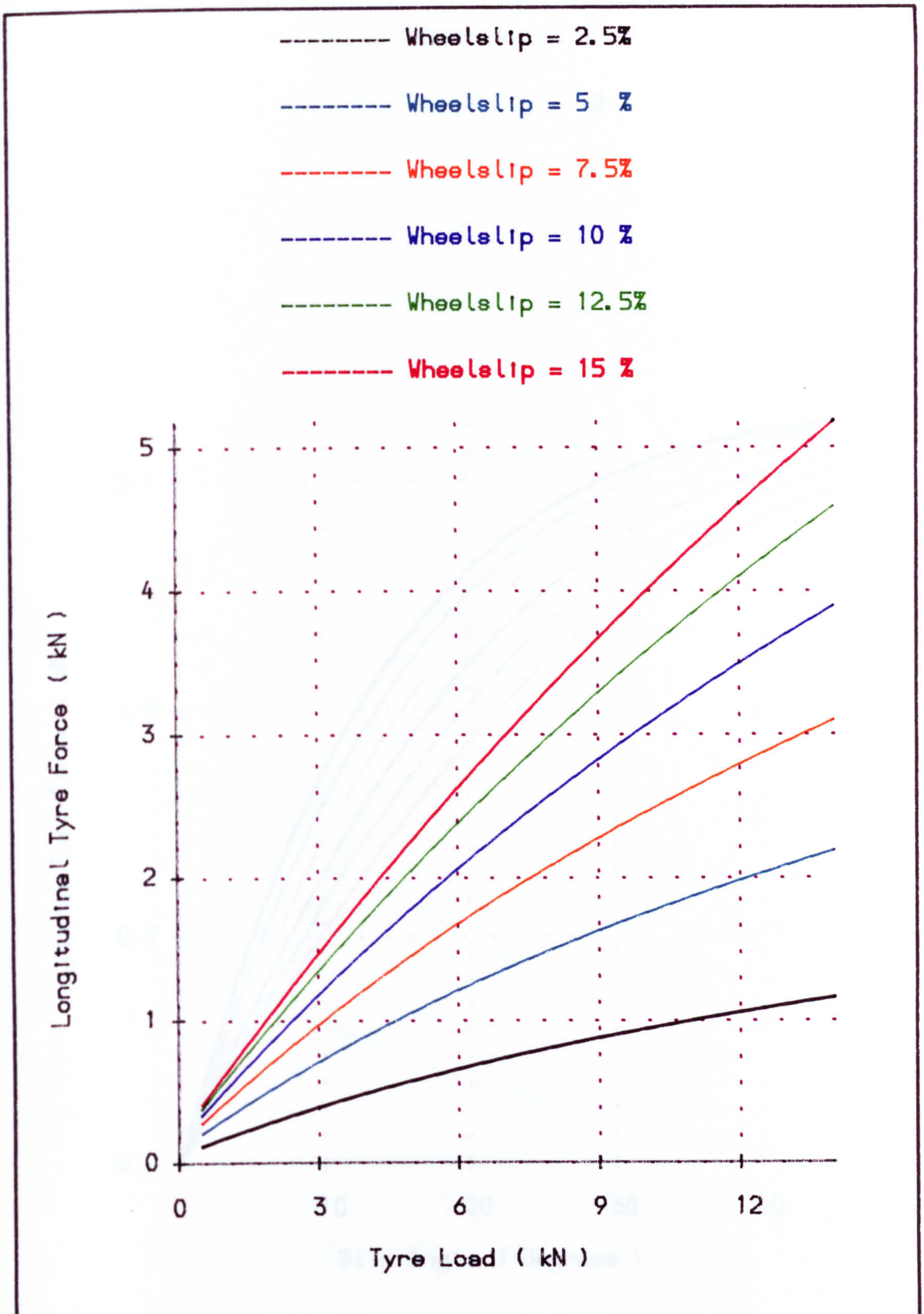

Fig. (7.4) Effect of the tyre load on longitudinal tyre force with different wheelslip.

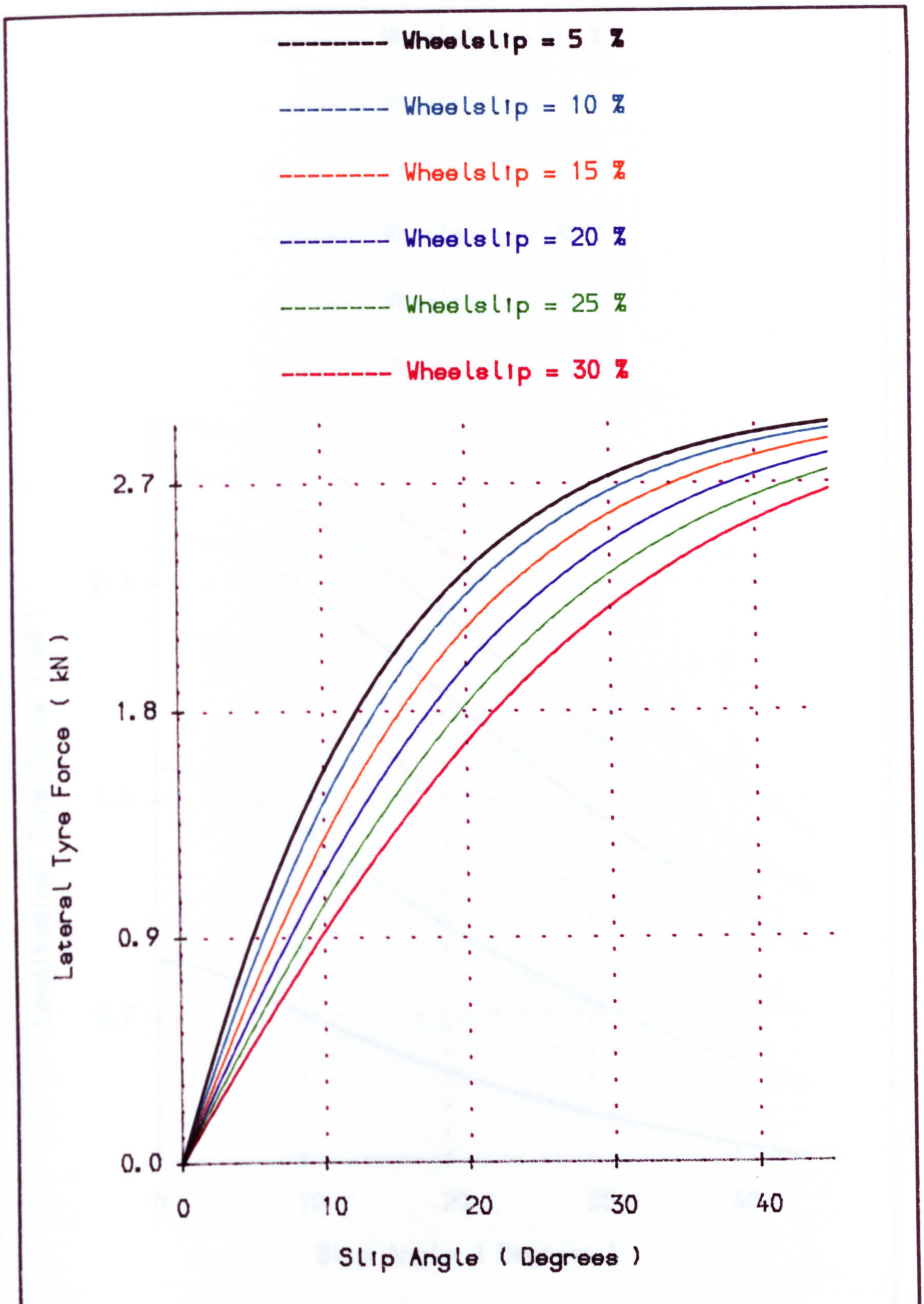

Fig. (7.5) The relationship between lateral tyre force and slip angle with different wheelslip.

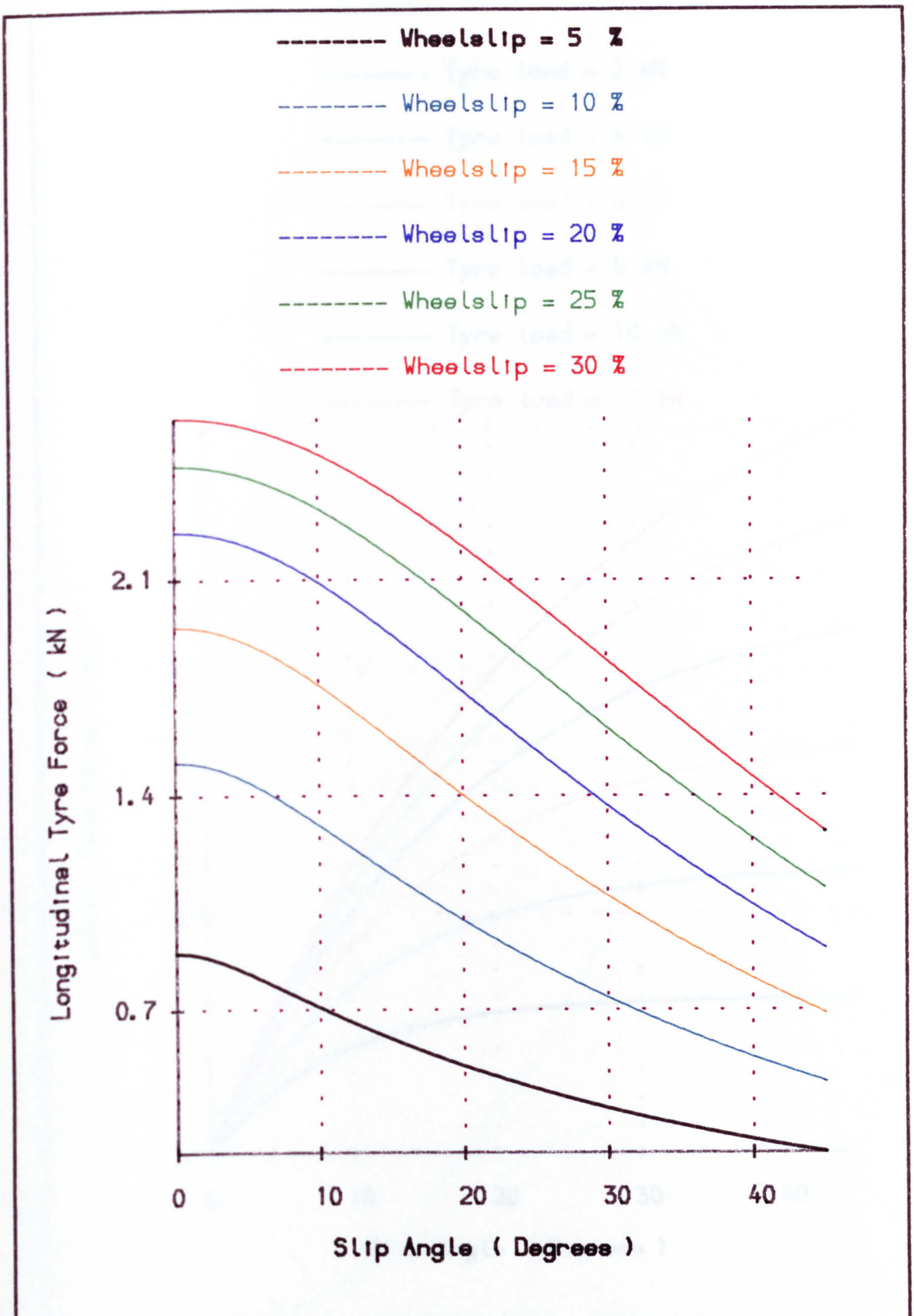

Fig. (7.6) Influence of wheelslip on longitudinal tyre force with various slip angles.

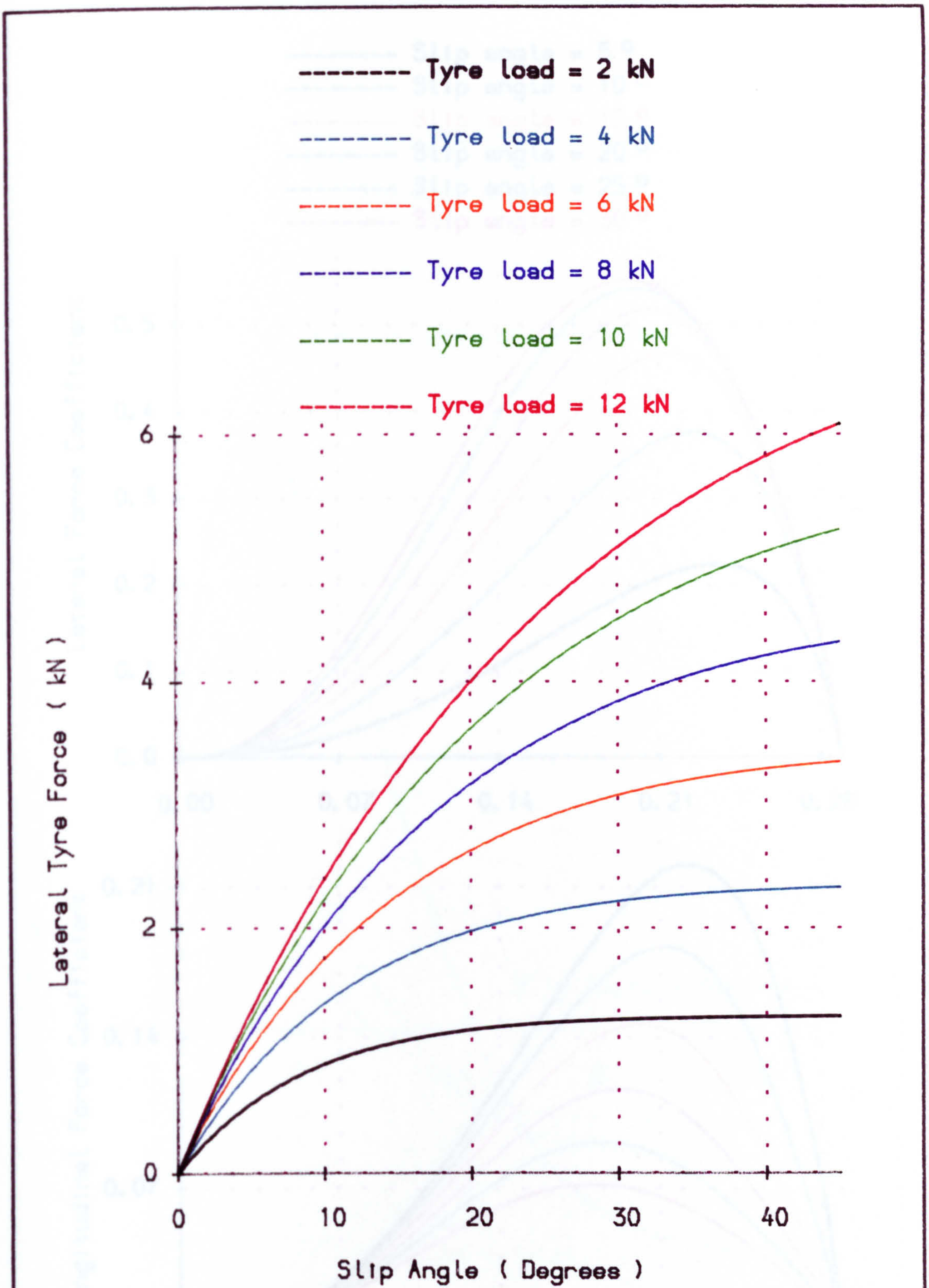

Fig. (7.7) Influence of slip angle on lateral tyre force with different tyre loads on a deformable surface.

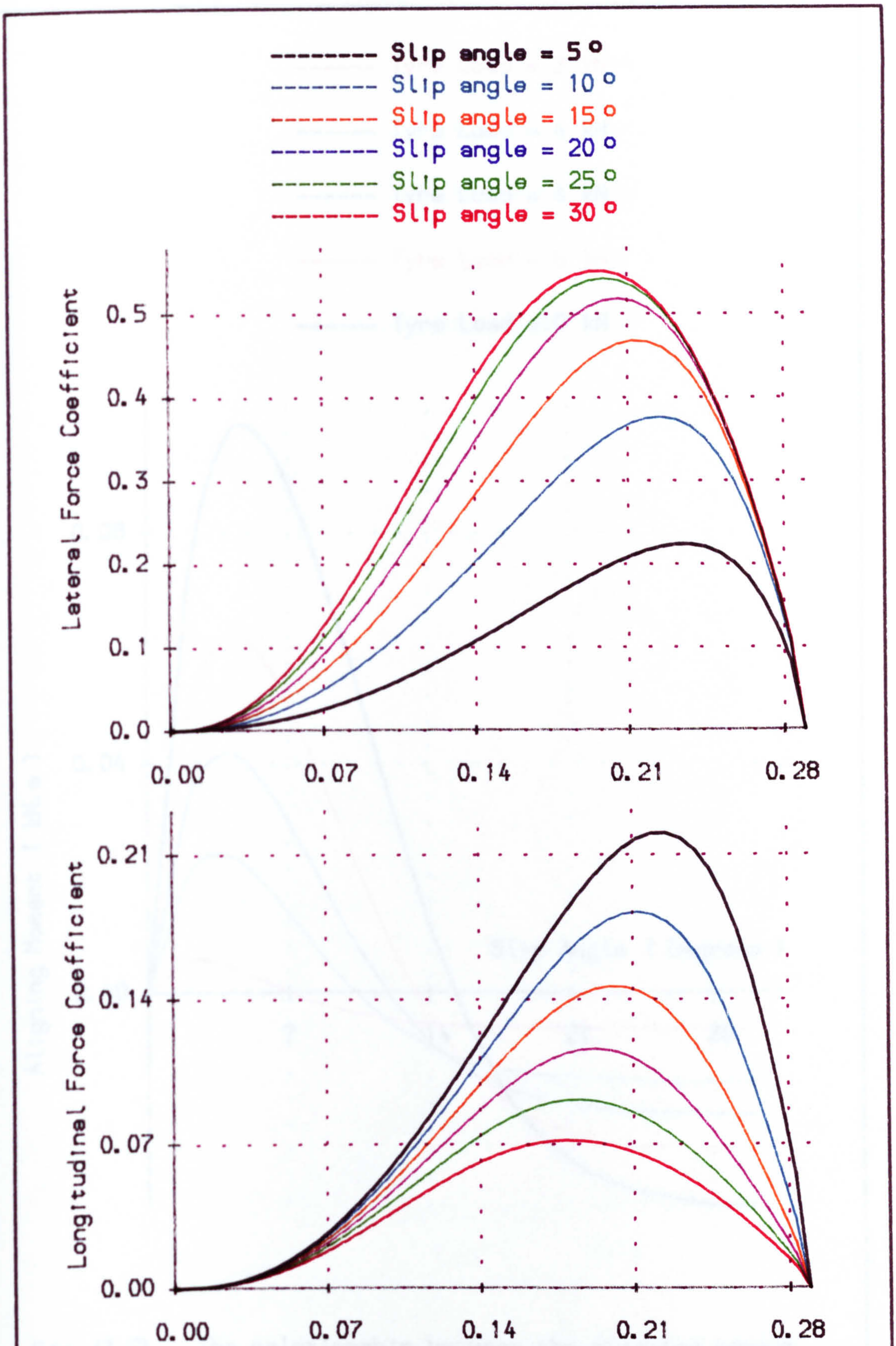

Fig. (7.8) Distributions of lateral and longitudinal force coefficient along the length of the contact region with different slip angles.

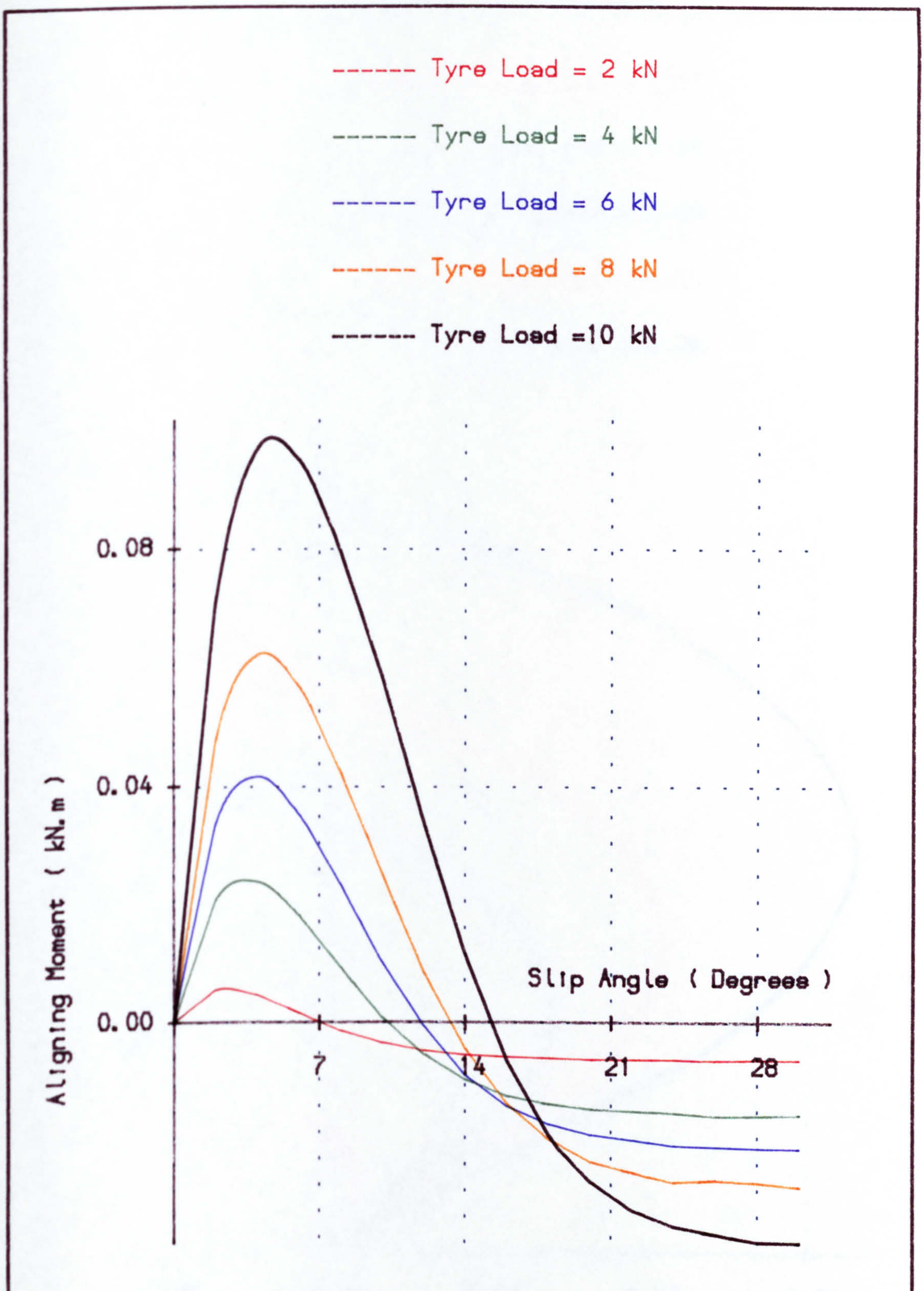

Fig. (7.9) The relationship between the aligning moment and slip angle with various tyre loads for a tyre moving on sandy loam soil.

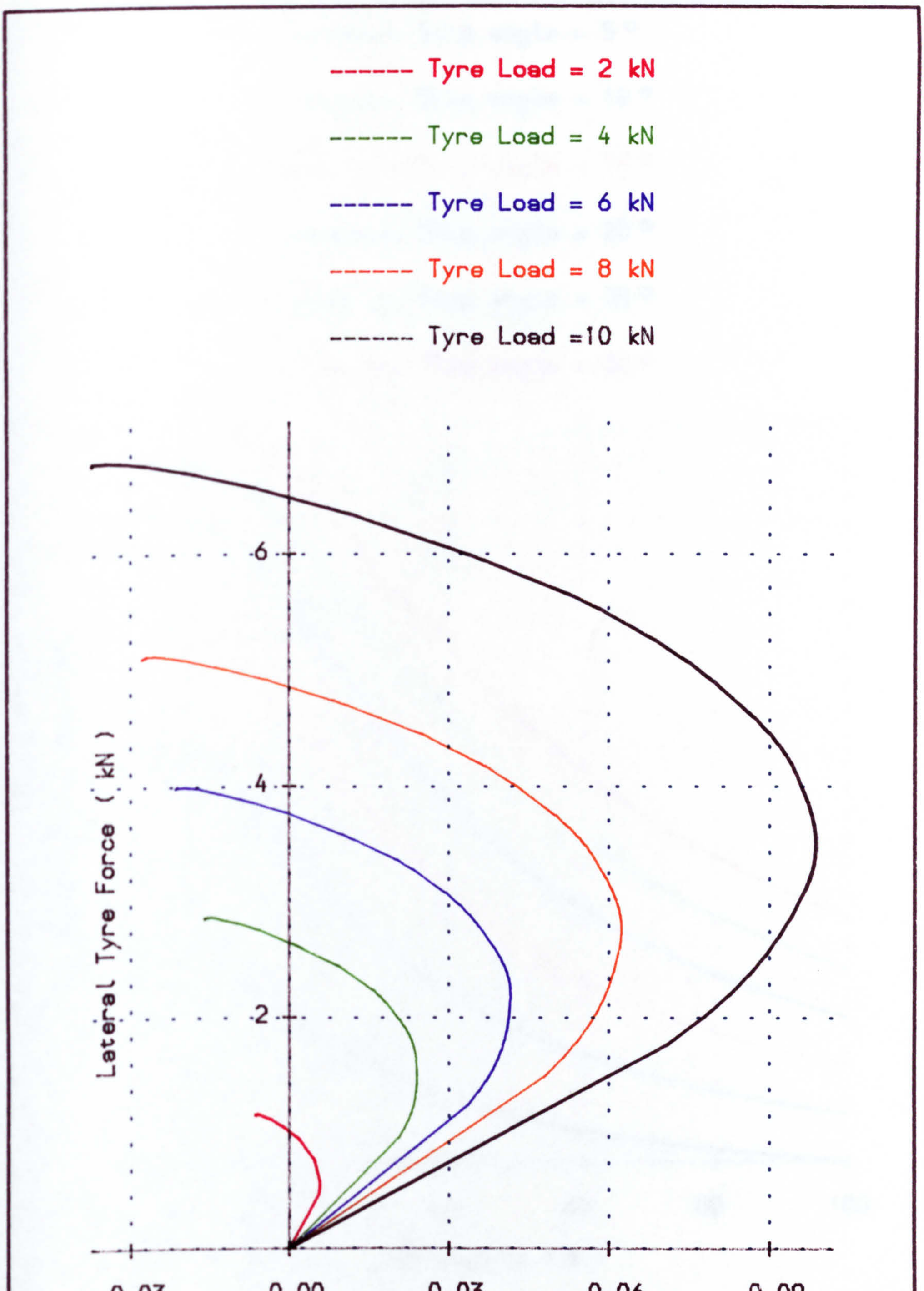

Fig. (7.10) Aligning moment as a function of the lateral tyre force and tyre load for a rolling tyre on sandy loam soil.

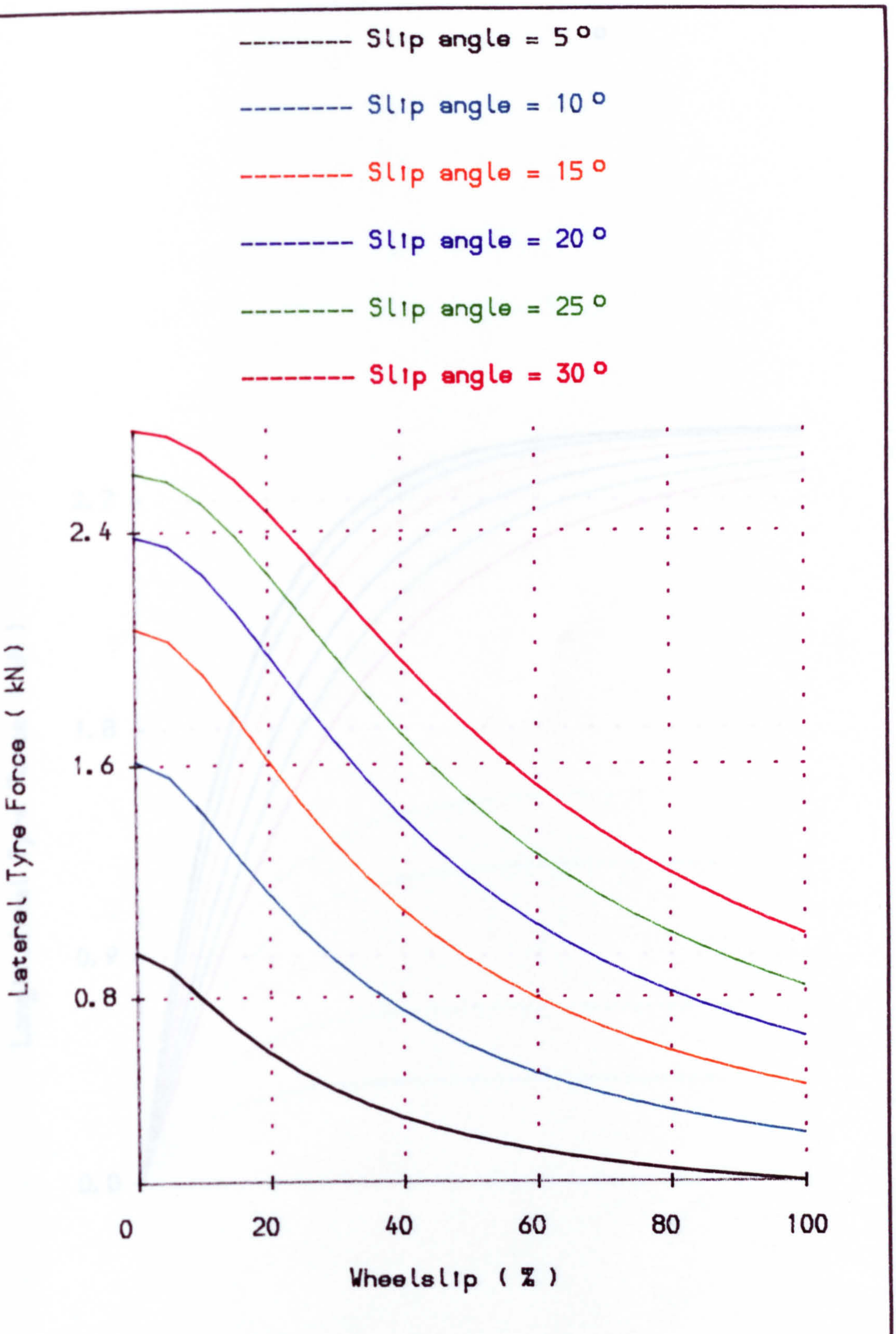

Fig. (7.11) Influence of wheelslip on lateral tyre force with different slip angle.

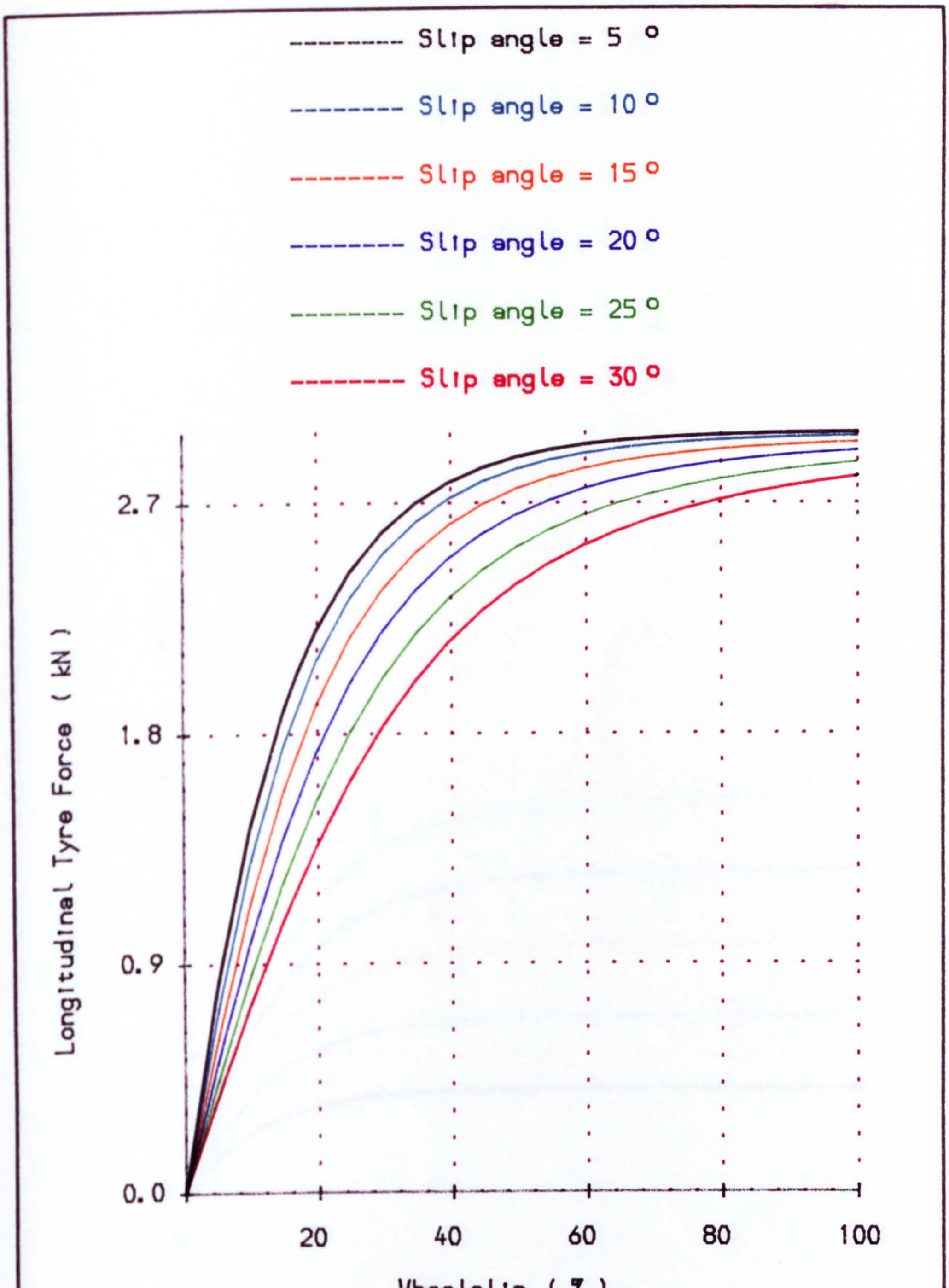

Fig. (7.12) The relationship between longitudinal tyre force and wheelslip with different slip angle.

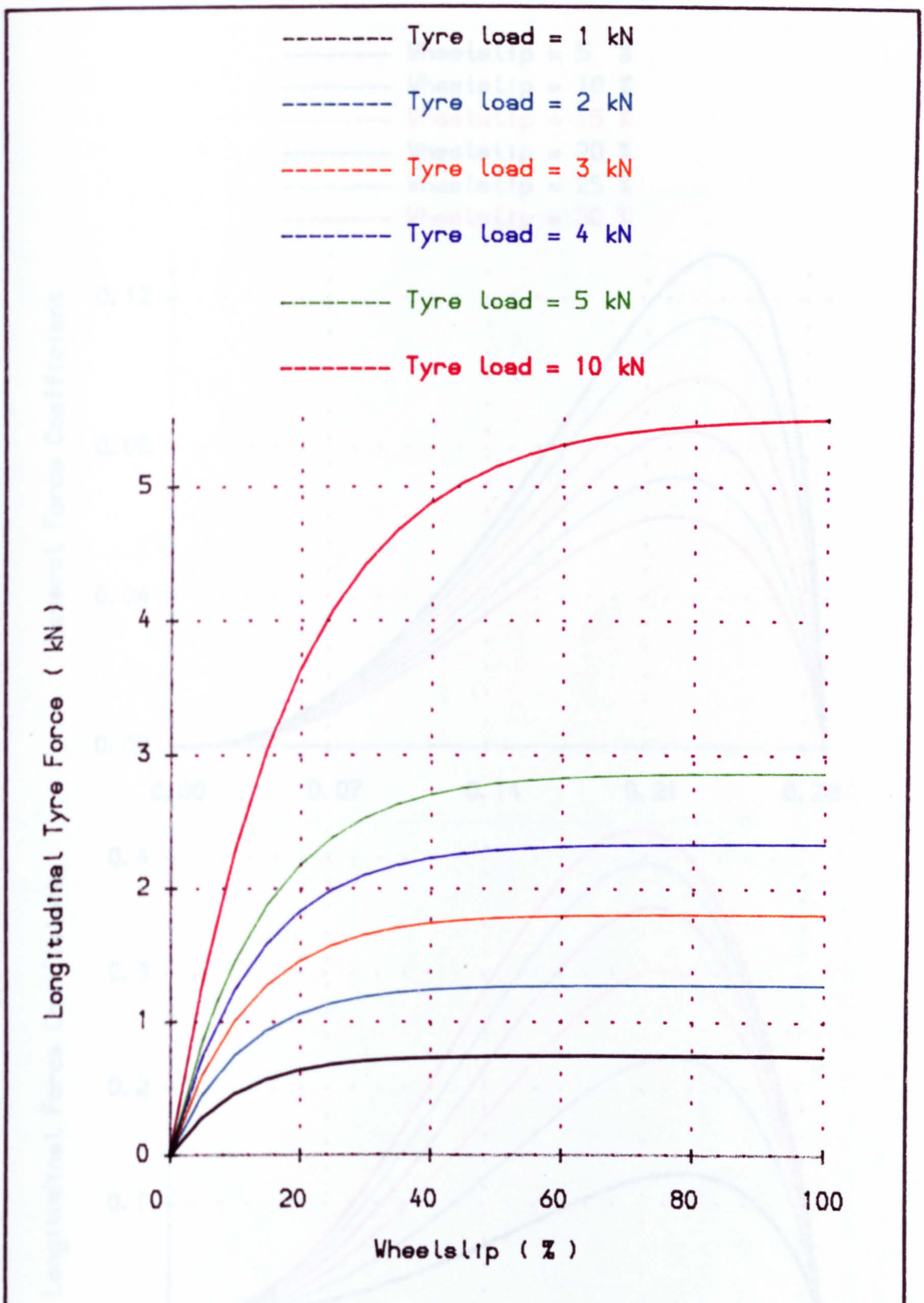

Fig. (7.13) Effect of wheelslip on longitudinal tyre force at different tyre loads.

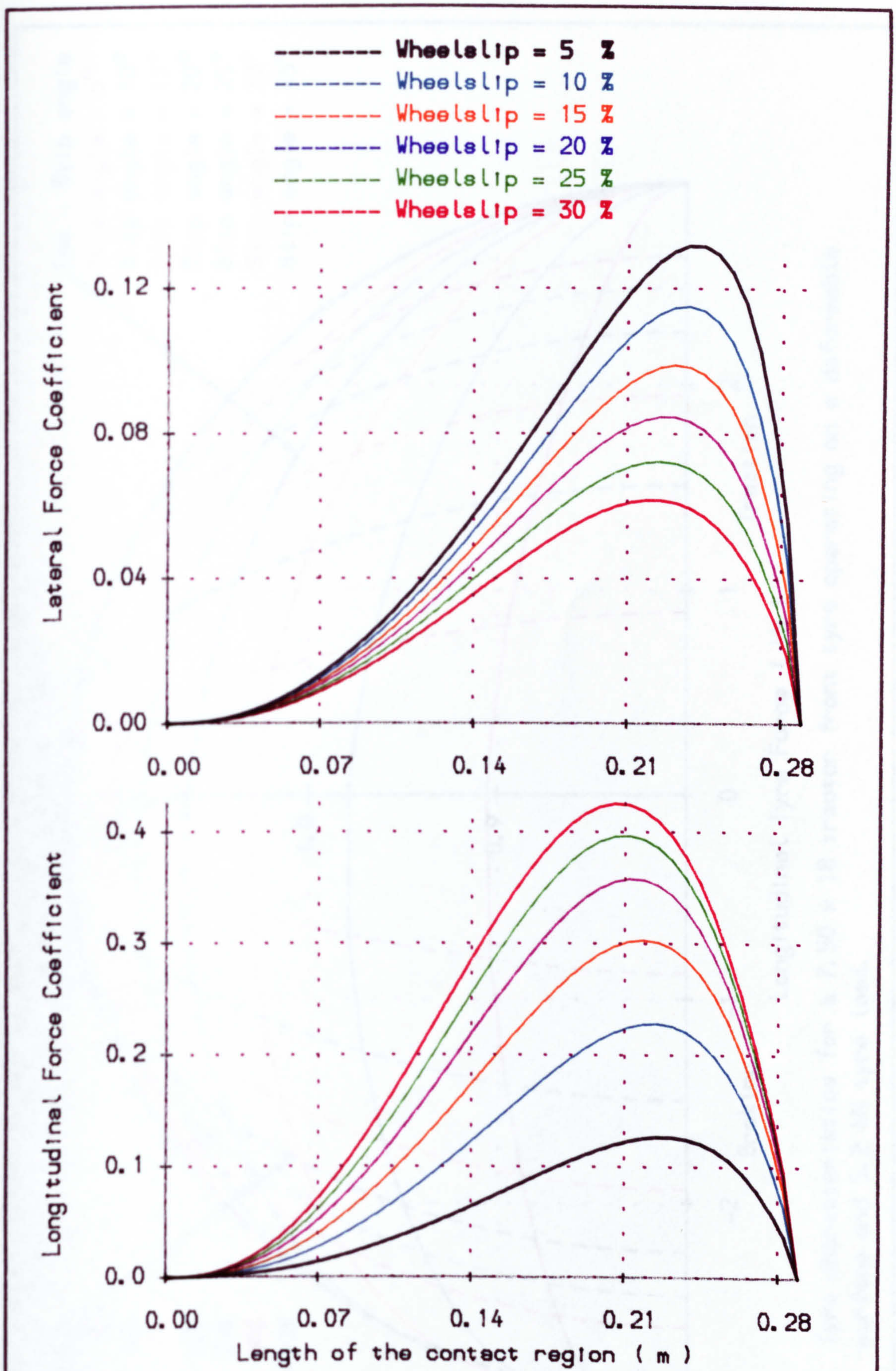

Fig. (7.14) Distributions of lateral and longitudinal force coefficient along the length of the contact region with different wheelslip.

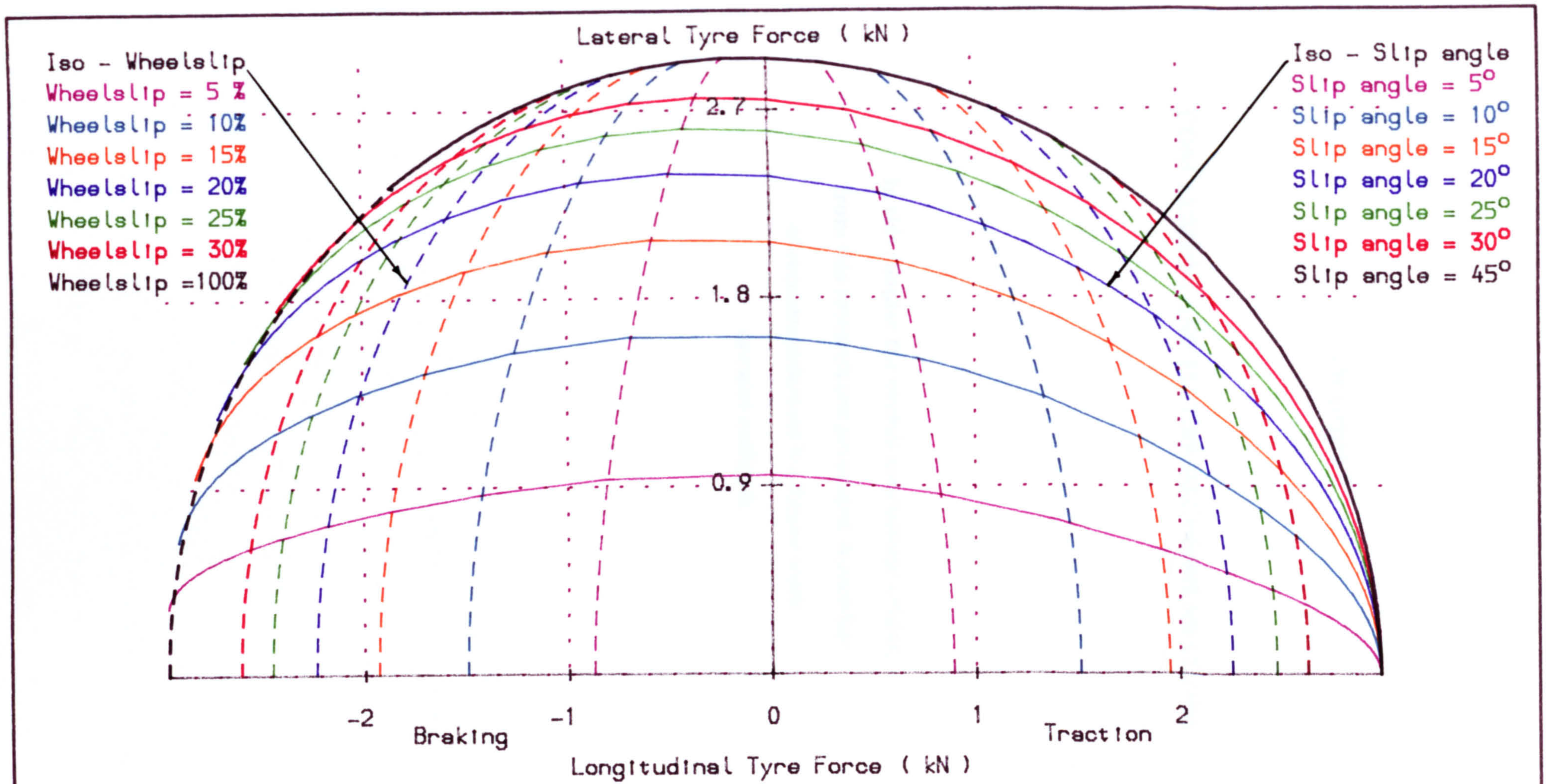

Fig. (7.15) Tyre characteristics for a 7.50 x 18 tractor front tyre operating on a deformable surface and 5.2 kN tyre load.

CHAPTER 8

CONCLUSIONS AND FUTURE RECOMMENDATIONS

In this chapter the overall conclusions arising from this research are presented. A number of recommendations for future work are also outlined.

8.1. CONCLUSIONS

The proposed spoke tyre model offers an improved qualitative description of behaviour in the tyre/soil contact region by incorporating both longitudinal and lateral tyre stiffness and by recognising that the soil forces necessary to sustain tyre deformations result, in general, in soil displacements throughout the contact region.

The resulting spoke model requires slightly more computation than previous models, but may conveniently be incorporated in off-road vehicle handling models to study combined steering and braking or traction manoeuvres. Although the model gives good qualitative agreement with previous measured data, further verification requires a more detailed set of measurements of tyre and soil deformations under a wide range of operation conditions.

It is believed that comparisons of the results obtained from the off-road tyre models with those results obtained from a wide range of work recorded in the literature presented, demonstrates the usefulness of an analysis using soil and tyre parameters. This is emphasised by the freedom to run the model under totally variable operating conditions and model parameters. The general conclusions to be made are as follows:-

1) A review of published work has established that there is a need for more study of lateral off-road tyre behaviour.

2) Various models for off-road tyres are proposed. One model is expressed in a simple form in terms of unspecified values for the operating conditions. The constraints are determined by solving a set of non-linear equations by using the simple optimization procedure.

3) A simple tyre model for off-road surface predicts forces in the vertical and longitudinal directions for a static and rolling tyre in steady state conditions.

4) The results from a simple tyre model are significantly in agreement in qualitative terms with the trends of the measured data obtained by a wide range of researchers. The quantitative agreement between the predicted and measured results has been also included and shown to be reasonable.

5) An extended model for combined lateral and longitudinal off-road tyre behaviour has been presented. It is based on the idea that in the tyre/ground contact region the forces due to soil shear must equal those due to tyre deflection at any point.

6) Predicted force relationships with slip angle and wheelslip using the extended model agree qualitatively with those obtained from measured data by a wide range of researchers.

7) The most important finding for the scope of the extended tyre model is that the model becomes the same as that proposed by Grecenko [1975] as the tyre stiffness is increased and it becomes the same as that proposed by Dugoff et al [1970] at U.M.T.R.I. as the soil strength increases. Additionally, the model is in a form which is suitable for inclusion in vehicle models to predict handling and steering behaviour.

8) The extended tyre model offers an improved qualitative description of behaviour in the tyre/soil contact region by incorporating both longitudinal and lateral tyre stiffness and by recognising that the soil forces necessary to obtain tyre deformations result, in general, in soil displacements throughout the contact region.

9) The resulting extended model requires slightly more computation than models previously proposed in the literature, but may conveniently be incorporated in off-road steering and braking or tractive modelling manoeuvres.

10) Although the extended model gives good qualitative agreement with previously measured data, further verification requires a more detailed set of measurements of tyre and soil deformations under combined longitudinal and lateral force conditions. A further research project at the University of Leeds is in progress to obtain such data.

11) The extended model represents a significant advance over previous models in that it is the first time that tyre/soil interaction has incorporated both the tyre flexibilities and soil deformation characteristics. At the extreme conditions of a very stiff tyre or very stiff soil, however, it reduces to models previously derived for off-road and on-road conditions respectively.

12) The multi-spoked tyre model on deformable soils is well suited to calculating the tyre forces in vehicle simulations because of its generality in that it can be used for on and off-road conditions, its reliance on readily available computing devices, and its mode of operation involving the specification of the motion and deduction of the forces.

13) The spoke tyre simulation represents a better understanding of the tyre behaviour in rapid manoeuvring and steering on off-road surface conditions. The method for modelling the tyre shows advantages over the extended tyre model because the forces obtained can be investigated in greater detail throughout the length of the contact region and the aligning moment as a function of the slip angle and tyre load is developed.

14) The predicted results show a significant qualitative agreement with measured data which have been collected from many sources and relate to a wide range of operating conditions. Quantitative agreement between the results and measured data is also shown although it is recognised that this comparison is often difficult because of the lack of soil and tyre data quoted in reports of measurements.

15) This application in this thesis of spoke tyre model, which was originally derived for road vehicle tyres, is novel in that it is the first attempt to model a flexible and deformable surface under the spoke tips. As the soil becomes infinitely stiff, the model reduces to that already proposed for a road tyre.

16) Each of the models is implemented in a computer programme suitable for inclusion in vehicle handling models, i.e. given the relevant data and operating conditions, the model produces the predicted tyre forces as outputs.

8.2. FUTURE RECOMMENDATIONS

From the work detailed and the conclusions drawn in this thesis it is apparent that several avenues for future work exist and these should be explored. In order to overcome the limitations described above, the recommendations for future research on off-road tyre models are summarised as follows : -

1) A detailed experimental study of the forces generated by off-road tyres model carefully controlled conditions eg. in a soil tank. The soil and tyre data should be measured and then the tyre forces measured over the entire range of operating conditions. This would provide a detailed and reliable data set against which to compare the model predictions.

2) Further extensions of these measurements would include various soil types, inflation pressures, tread pattern etc. In fact, such a programme of work is now in progress at the University of Leeds.

3) Development of off-road tyre models to include the real contact width which is expected to affect the tyre deflections and tyre forces.

LIST OF REFERENCES

Abeels, P.F.J. [1976] "Tire deflection and contact studies". J. of Terramechanics, Vol. 13 No. 3, pp (183-196).

Abeels, P.F.J. [1984] "Modeling of off-road tyres and soil for improved traction". Proceeding of 8th Int. Conf. of I.S.T.V.S., pp (16-31).

Abeels, P.F.J. [1987] "Off the road tyres". Proceedings of 9th Int. Conf. of I.S.T.V.S., Vol. I, pp (244-248).

Baker, C.J. and Collins, R.M. [1972] "A comparison of tractor rear tyres in their resistance to side slip". J. Agric. Engng. Res. 17s, 5 1, p 9.

Baladi, G.Y. and Rohani, B. [1984] "Development of a soil-wheel interaction model". Proceedings of 8th of Int. Conf. of I.S.T.V.S., pp (33-60).

Bekker, M.G. [1956] "Theory of Land Locomotion". University of Michigan Press, Ann Arbor, U.S.A.

Bekker, M.G. [1960] "Off-the-road locomotion". University of Michigan Press, Ann Arbor, U.S.A.

Bekker, M.G. and Janosi, Z.J. [1960] "Analysis of towed pneumatic tires moving in soft ground". U.S. Army O.T.A.C., Land Locomotion Laboratory Report RR-6.

Bekker, M.G. [1969] "Introduction to terrain-vehicle systems". The University of Michigan press, Ann Arbor, U.S.A.

Bekker, M.G. and Semonin, E.V. [1975] "Motion resistance of pneumatic tyres". J. of Automotive Engineering (J.A.E.), pp (6-10).

Bekker, M.G. [1985] "Parametric analyses of pneumatic tires update-samples of engineering problems and solutions in off-road locomotion". S.A.E. Transactions, Technical Series No 850536.

Bernard, J.E. ; Segel, L. and Wild, R.E. [1977] "Tire shear force generation during combined steering and braking maneuvers". S.A.E. Transactions, Paper No. 770852.

Bolling, I. [1981] "Distribution of vertical stresses in soil beneath wheels". Proceedings of 7th Int. Conf. of I.S.T.V.S., Vol. 2, pp (497-529).

Bolling, I. [1984] "Pressure tests in soil below tires of agricultural vehicles". Proceedings 8th Int. Conf. of I.S.T.V.S., pp (675-690).

Boonsinsuk, P. and Yong, R.N. [1984] "Soil compliance influence on tyre performance". Proceedings of 8th Int. Conf. of I.S.T.V.S., pp (61-80).

Burt, E.C. and Bailey, A.C. [1982] "Load and inflation pressure effects on tires". Transactions of the A.S.A.E., Vol. 25 No. 4, pp (881-884).

Burt, E.C. and Turner, J.L. [1983] "Soil mechanics in off-road vehicle design : A historical perspective". S.A.E., Paper No. 830805, pp (1-7).

Captain, K.M. ; Boghani, A.B. and Wormley, D.N. [1979] "Analytical tire models for dynamic vehicle simulation". Vehicle System Dynamics, Vol. 8, pp (1-32).

Clark, S.K. [1965] "The rolling tire under load". S.A.E. Transactions, pp(1-9), Paper No. 650493.

Clark, S.K. [1982] "Mechanics of pneumatic tyre". U.S. Dept. of Transportation, National Highway Traffic Safety Adminstration, Washington, U.S.A.

Crolla, D.A. and Hales, F.D. [1979] "The lateral stability of tractor and tractor trailer combinations". J. of Terramechanics, Vol. 16 No. 1, pp (1-22).

Crolla, D.A. and Horton, D.N.L. [1984] "Factors affecting the dynamic behaviour of higher speed agricultural vehicles". J. Agric. Engng. Res., Vol. 30, pp (277-288).

Crolla, D.A. and El-Razaz, A.S.A. [1987] "A review of the combined lateral and longitudinal force generation of tyres on deformable surfaces". J. of Terramechanics, Vol. 23, No 3, pp (199-225).

Crolla, D.A. ; El-Razaz, A.S.A. ; Alstead, C.J. and Hockley, C. [1987] "A model to predict the combined lateral and longitudinal forces on an off-road tyre". Proceedings of 9th Int. Conf. of I.S.T.V.S., Vol. 1, pp (362-372).

Chung, T.J. and Lee, J.K. [1975] "Dynamics of viscoelastoplastic soil under a driving wheel". J. of Terramechanics, Vol. 12, No. 1, pp (15-31).

Del Rosario, C.R. [1980] "Lateral force investigations on steered pneumatic tyres operating under soil conditions". Ph.D. Thesis, Silsoe College Cranfield Institute of Technology, England.

Dugoff, H. ; Fancher, P.S. and Segel, L. [1969] "Tire performance characteristics affecting vehicle response to steering and braking control inputs". Highway Safety Research Institute, University of Michigan, Report No. C5T-460, pp (897-00).

Dugoff, H. ; Fancher, P.S. and Segel, L. [1970] "An analysis of tire traction properties and their influence on vehicle dynamic performance". S.A.E. Transactions, Paper No. 700377, pp (341-366).

Dwyer, M.J. [1972] "Field measurement of agricultural tractor tyre performance at the National Institute of Agricultural Engineering". Proceedings of 4th I.S.T.V.S., Held Stockholm, pp (39-60).

Dwyer, M.J. ; Comely, D.R. and Evernden, D.W. [1974a] "The development of the N.I.A.E. handbook of agricultural tyre performance". N.I.A.E. Departmental Note DN/T/517/1415, pp (679-699).

Dwyer, M.J. ; Comely, D.R. and Evernden, D.W. [1974b] "The field performance of some tractor tyres related to soil mechanical properties". J. of Agric. Engng. Res., Vol. 19, pp (35-50).

El-Nashar, M.A. [1985] "The generation of shear forces by pneumatic tyres". Ph.D. Thesis University of Leeds, England.

Fancher, P.S. [1970] "Experimental studies of tire shear force mechanics". The University of Michigan, Ann Arbor Dot-HS-800-416. FH-11-6090, NBS CST 9285 18P.

Freeman, C.A. [1960] "Experimental determination of the effect of traction on cornering force". S.A.E. Transactions, Preprint Paper No 186B.

Freitag, D.R. [1965] "Wheels on soft soils, an analysis of existing data". Waterway Experiment Station, Technical Report No. 3-670.

Freitag, D.R. and Smith, M.E. [1966] "Center-line deflection of pneumatic tires moving in dry sand". J. of Terramechanics, Vol. 3 No. 1, pp (31-46).

Freitag, D.R. [1968] "Dimensional analysis of performance of pneumatic tires on sand". Transactions of the A.S.A.E., Vol. 2 No. 5, pp (669-672).

Freitag, D.R. ; Green, A.J. and Murphy, N.R. JR. [1975] "Normal stresses at the tyre-soil interface in yielding soils". U.S.Army Engineer Waterways Experiment Station, CE, Vicksburge pp (1-18).

Fujimoto, Y. [1977] "Performance of elastic wheels on yielding cohesive soils". J. of Terramechanics, Vol. 14 No 4, pp (191-210).

Gee-Clough, D. [1980] "Selection of tyre sizes for agricultural vehicles". J. of Agric. Engng. Res., Vol. 25, pp (261-278).

Gee-Clough, D. and Sommer, M.S. [1981] "Steering forces on undriven angled wheels". J. of Terramechanics, Vol. 18, No. 1, pp (25-49).

Gilfillan, G.; Spencer, H. B. and Rowe, F.P.H. [1976] "Some preliminary results from side force tests on a 7.50 x 16 tractor front tyre". Scottish Inst. of Agric. Engng. Departmental note SSN/203.

Gohich, H. [1984] "The development of tractors and other agricultural vehicles". J. of Engng. Res., Vol. 29 No. 1, pp (3-16).

Grecenko, A. [1967] "Binomic slip-thrust equation for tractors on predominantly frictional soil". J. of Terramechanics, Vol. 4 No. 4, pp (37-54).

Grecenko, A. [1969] "Slip and drift of the wheel with tyre on soft ground". Proc. 3rd I.S.T.V.S. Conf., Essen, Vol.II, pp (76-95).

Grecenko, A. [1975] "Some applications of the slip and drift theory of the wheel". 5th Int. Conf. of I.S.T.V.S. , Michigan, U.S.A.

Grecenko, A. [1984a] "Study of the motion of agricultural vehicles on steep grass-covered slopes". 8th Int. Conf. of I.S.T.V.S. ,Cambridge, England.

Grecenko, A. [1984b] "Operation on steep slopes : State-Of-The-Art Report". J. of Terramechanics, Vol. 21 No 2, pp (181-194).

Hettiaratchi, D.R.P. ; Witney, B.D. and Reece, A.R. [1966] "The calculation of passive pressure in two-dimensional soil failure". J. of Agric. Engng. Res., Vol. 11 No. 2, pp (89-107).

Hettiaratchi, D.R.P. [1969] "The calculation of passive earth pressure". Ph.D. Thesis, University of Newcastle-Upon-Tyne.

Horton, D.N.L. and Crolla, D.A. [1984] "The handling behaviour of off-road vehicles". Int. J. of Vehicle Design Vol. 5 Nos. 1/2, pp (197-218).

Ipek, I.S. [1959] "Forces and moments on a pneumatic tyre and their effect on the behaviour of pneumatic tyred vehicles on slopes". Thesis Tech. Hochsch. Brauschweig.

Iritanis, S. and Baba, T. [1964] "Forces on the contact patch of the tyre". Proceedings of 10th Int. Automobile Technical Congress, FISITA, pp (212-224).

Janosi, Z.J. [1962] "An analysis of pneumatic tire performance on deformable soils". Proceedings 1st Int. Conf. of Mechanics on Soil-Vehicle Systems, pp (737-762).

Janosi, Z.J. [1963] "Performance analysis of a driven non-deflecting tyre in soil". Land Locomotion Lab., Report No 8091.

Janosi, Z. J. ; Kamm, I.O. and Wray, G. [1981] "Tire turning forces under on-and off-road conditions". Proc. of the 7th Int. Conf. I.S.T.V.S., Calgary, late submission.

Jurkat, M.P. and Brady, P.M. [1981] "On a lateral force tire model for both highway and soft soil conditions". Proc. of the 7th Int. Conf. I.S.T.V.S., Calgary, late submission.

Karafiath, L.L. and Nowatzki, E.A. [1978] "Soil mechanics for off- road vehicle". Series on Rock and Soil Mechanics Vol. 2 No. 5 (1974/77), First Edition.

Knight, S.J. and Green, A.J. [1962] "Deflection of moving tire on firm to soft ground". Transactions of the A.S.A.E., Vol. 2, pp (116-120).

Kolobov, G.G. [1966] "Soil pressure measurements beneath tractor tyres". J. of Terramechanics, Vol. 3 Part 4, pp (9-15).

Komandi, G. [1976] "The determination of the deflection, contact area, dimensions, and load carrying capacity for driven pneumatic tires operating on concrete pavement" J. of Terramechanics, Vol. 13 No 1, pp (15-20).

Koolen, A.J. and Kuipers, H. [1983] "Agricultural Soil Mechanics". Springer-Verlag, Berlin Heidelberg New York Tokyo.

Kraft, D.C. and Phillips, N.S. [1975] "Turning forces developed by a pneumatic tire operating in soils, with application to vehicle design criteria". Proceedings of 5th Int. Conf. for Terrain-Vehicle Systems, Detroit, pp (473-792).

Krick, G. [1969] "Radial and shear stress distribution under rigid wheels and pneumatic tyres operating on yielding soils with consideration of tyre deformation". J. of Terramechanics, Vol. 6 No 3, pp (73-98).

Krick, G. [1973] "Behaviour of tyres driven in soft ground with side slip" J. of Terramechanics, Vol. 9 No 4, pp (9-30).

McAllister, M. [1979] "A rig for measuring the forces on a towed wheel". J. Agric. Engng. Res. Vol. 24, pp (259-265).

McAllister, M. ; Gee-Clough, D. and Evernden, G.W. [1981] "An investigation into forces on undriven angled wheels". N.I.A.E. Departmental note DN 1045.

McAllister, M. [1984] "Forces on undriven, angled wheels". Proceedings 8th Int. Conf. of I.S.T.V.S., pp (803-819).

Meyer, M. ; Marti, F. ; Schiess, J. and Schlapfer, H. [1978] "Performance of tractor rear tyres when operating across slopes". N.I.A.E. translation No 443, Silsoe, England, pp (1-13).

National Institute of Agricultural Engineering [1978] "Performance of tractor tyres". Project review PR/T/78/01002.

Nordeen, D.L. and Cortese, A.D. [1964] "Force and moment characteristics of rolling tires". S.A.E. Transactions, pp (1-13), Paper No. 713A (Preprint).

Nordeen, D.L. [1967] "Analysis of tire lateral forces and interpretation of experimental tire data". S.A.E. Transactions, Paper No. 670173.

Pacejka, H.B. [1981] "Analysis of tire properties". Chapter 9 of Mechanics of pneumatic tires S.K. Clark (ed.) N.B.S. Monograph 122 2nd ed.

Painter, D.J. [1981] "A simple deflection model for agricultural tyres". J. of Agric. Engng. Res., Vol. 26, pp (9-20).

Perdok, U.D. [1978] "A prediction model for the selection of tyres for towed vehicle on tilled soil". J. of Agric. Engng. Res., Vol. 23, pp (369-383).

Phillips, J.R. [1959] "Experimental determination of the forces on some towed drifting wheels". J. of Agric. Engng. Res., Vol. 4, pp (294-306).

Plackett, C.W. [1983] "Hard surface contact area measurement for agricultural tyres". Div. Note DN/1200, N.I.A.E., Silsoe, England.

Plackett, C.W. [1984] "The ground pressure of some agricultural tyres at low load and with zero sinkage". J. Agric. Engng. Res., Vol. 29, pp (159-166).

Plackett, C.W. [1985] "A review of force prediction methods for off-road wheels". J. Agric. Engng. Res. Vol. 31, pp (1-29).

Prettyman, C.E. [1981] "Computerised tyre footprint area measurements". A.S.E., Paper No. 810511, pp (1-5).

Reece, A.R. [1964] "Theory and practice of off-the-road locomotion". Presented at the Annual Conference, London 28th April, pp (82-90).

Reece, A.R. [1965] "The fundamental equation of earthmoving mechanics". I. Mech. E. Symposium on Earthmoving Equipment. Vol. 119, part 3F.

Riley, J.G. [1968] "The design of a single wheel tester". M.Sc. Thesis, University of Newcastle Upon Tyne.

Sakai, H. [1981] "Part 3 : Calculation of the six components force of a tyre". Int. J. of vehicle Design Vol. 2 No 3, pp (335-372).

Satake, M. and Mukai, T. [1972] "Traction and flotation characteristics of earthmover tires on soft soil". S.A.E. Transactions, Vol. 81, pp (2242-2250), Paper No.720743.

Savkoor, A.R. [1970] "The lateral flexibility of pneumatic tyre and its application to the lateral rolling contact problem". S.A.E. Transactions, pp (367-381), Paper No. 700378.

Schwanghart, H. [1968] "Lateral forces on steered tyres in loose soil". J. of Terramechanics, Vol. No. 5 No 1, pp (9-29).

Schwanghart, H. [1981] "Measurements of forces on steered towed wheels". Proc. of the 7th Int. Conf. I.S.T.V.S. Calgary, Vol. 1, pp (335-356).

Schwanghart, H. and Rott, K. [1984] "The influence of the tyre tread on the rolling resistance and steering forces on undriven wheels". 8th Int. Conf. of I.S.T.V.S. Cambridge, England, pp (872-888).

Segel, L. [1984] "Measuring and modeling mechanical properties of pneumatic tires". International Rubber Conference, Moscow.

Seitz, N. and Hussmann, A.W. [1971] "Forces and displacement in contact area of free rolling tires". S.A.E. Transactions, Vol. 80, pp (2323-2329), Paper No 710626.

Sharp, R.S. and El-Nashar, M.A. [1986] "A generally applicable digital computer based mathematical model for the generation of shear forces by pneumatic tyres." Vehicle System Dynamics, Vol. 15 No 4, PP (187-209).

Soane, B.D. ; Blackwell, P.S. ; Dickson, J.W. and Painter, D.J. [1981] "Computation by agricultural vehicles (A review in soil and wheel characteristics)". Soil and Tillage Research, Vol. 1, pp (207-237).

Soehne, W. [1953] "Distribution of pressure in the soil and soil deformation under tractor tyres". Grundl Landtech, Vol. 5, pp (49-63).

Taylor, P.A. and Birtwhistle, R. [1966] "Experimental studies of force systems on steered agricultural tyres". Proc. of the Inst. of Mech. Eng., Vol. 181 Part 24, pp (1-14).

Trolli, C. and Viola, L. [1987] "A new large base agricultural drive tyre : field tests on clay soil". Institute of Agricultural Engineering of the University of Milan Via Celoria, 2-20133 Milano, Italy.

Turnage, G.W. [1976] "In-soil tractive performance of selected radial and bias-ply tyres". Transactions of the A.S.A.E., paper No. 76-1520.

Vandenberg, G.E. and Gill, W.R. [1962] "Pressure distribution between a smooth tire and the soil". Transactions of the A.S.A.E., pp (105-107).

Wills, B.M.D. [1966] "The load sinkage equation in theory and practice". Proceedings of 2nd Int. Conf. of I.S.T.V.S., Held Quebec.

Wismer, R.D. and Luth, H.J. [1973] "Off-road traction prediction for wheeled vehicles". J. of Terramechanics, Vol. 10 No 2, pp (49-61).

Wong, J.Y. [1978] "Theory of ground vehicles". Carleton University, Ottawa, Ontario, U.S.A.

Yin, L. ; Wang, Z. ; Qiu, X. and Wang, Q. [1985] "Distribution of stresses beneath a drive pneumatic tyre and preduction of its tractive performance on sand". Proceedings of Int. Conf. on Soil Dynamics, Vol. 4, pp (738-755).

Yong, R.N. and Windish, E.J. [1970] "Determination of wheel contact stresses from measured instantaneous soil deformations". J. of Terramechanics, Vol. 7 Nos. 3/4, pp (57-67).

Yong, R.N. , Boonsinsuk, P. ,and Fattah, E.A. [1978a] "Prediction of tyre performance on soft soils relative to carcass stiffness and contact areas". J. of Terramechanics, Vol. 15 No 1, pp (643-675).

Yong, R.N. ; Fattah, E.A. and Boonsinsuk, P. [1978b] "Analysis and prediction of tyre-soil interaction and performance using finite elements". J. of Terramechanics, Vol. 15, No 1, pp (43-63).

Yong, R.N. ; Boonsinsuk, P. and Fattah, E.A. [1980] "Tyre flexibility and mobility on soft soils". J. of Terramechanics, Vol. 17, No 1, pp (43-58).